STRUCTURAL MODIFICATIONS OF MANGOSTIN WITH ENHANCED ANTIMYCOBACTERIAL AND ANTIVIRAL ACTIVITIES AND NEW SYNTHETIC STRATEGY FOR ANGIOGENESIS INHIBITOR, SEMAXANIB

A DISSERTATION

BY

PICHIT SUDTA

PRESENTED IN PARTIAL FULFILLMENT OF THE REQUIMENTS FOR THE DOCTOR OF PHILOSOPHY DEGREE IN APPLIED CHEMISTRY

AT SRINAKHARINWIROT UNIVERSITY

MARCH 2011

STRUCTURAL MODIFICATIONS OF MANGOSTIN WITH ENHANCED ANTIMYCOBACTERIAL AND ANTIVIRAL ACTIVITIES AND NEW SYNTHETIC STRATEGY FOR ANGIOGENESIS INHIBITOR, SEMAXANIB

A DISSERTATION

BY

PICHIT SUDTA

Presented in Partial Fulfillment of the Requirements for the

Doctor of Philosophy Degree in Applied Chemistry

at Srinakharinwirot University

March 2011

STRUCTURAL MODIFICATIONS OF MANGOSTIN WITH ENHANCED ANTIMYCOBACTERIAL AND ANTIVIRAL ACTIVITIES AND NEW SYNTHETIC STRATEGY FOR ANGIOGENESIS INHIBITOR, SEMAXANIB

AN ABSTRACT

BY

PICHIT SUDTA

Presented in Partial Fufillment of the Requirements for the

Doctor of Philosophy Degree in Applied Chemistry

at Srinakharinwirot University

March 2011

Pichit Sudta. (2011). *Structural modifications of mangostin with enhanced antimycobacterial and antiviral activities and new synthetic strategy for angiogenesis inhibitor, semaxanib*. Dissertation, Ph. D. (Applied Chemistry). Bangkok: Graduate School, Srinakharinwirot University. Advisor Committee: Assoc. Prof. Dr. Sunit Suksamrarn, Asst. Prof. Dr. Siritron Samosorn, Dr. Prasert Pattanaprateeb.

A series of mangostin analogues was designed and synthesized and their antimycobacterial activity against *Mycobacterium tuberculosis* and antiviral activity against *Herpes simplex* virus-1 (HSV-1) *in vitro* were evaluated. The antimycobacterial assay showed that a number of derivatives displayed good antituberculosis activity, in some cases higher than that of the reference drug kanamycin. In particular, 6-mono-*O*-methyltetrahydromangostin (**150**), 6-mono-*O*-ethyltetrahydromangostin (**152**) and 6-mono-*O*-allyltetrahydromangostin (**154**) exhibited potent antituberculosis activity with the identical MIC value of 0.78 μg/mL, which represent a novel class of promising leads for the development of novel anti-TB agents. The antiviral evaluation revealed that mangostin analogues **90**, **99, 120**, **140-141**, **144-146**, **148**, **154, 156-158** and **164** were new class of non-nucleoside antiviral agents which showed significant activity against HSV-1 with IC_{50} in the range of 1.10-8.60 μg/mL.

The development of synthetic strategy for the potent angiogenesis inhibitor, semaxanib, has been studied. Semaxanib (SU-5416, **82**) was successfully synthesized in high yield (81% yield) from reductive cylisation of the key intermediate (*Z*)-ethyl-3-(3,5-dimethyl-1*H*-pyrrole-2-yl)-2-(2-nitrophenyl)acrylate (**173**) by using zero-valent iron metal under ultrasonic irradiation.

การปรับเปลี่ยนโครงสร้างของสารแมงโกสตินกับฤทธิ์ต้านไมโคแบคทีเรียและไวรัสที่เพิ่มขึ้น และการสังเคราะห์วิธีใหม่สำหรับสารยับยั้งการสร้างหลอดเลือด เซแมกซานิบ

บทคัดย่อ

ของ

พิชิต สุดตา

เสนอต่อบัณฑิตวิทยาลัย มหาวิทยาลัยศรีนครินทรวิโรฒ เพื่อเป็นส่วนหนึ่งของการศึกษา
ตามหลักสูตรปรัชญาดุษฎีบัณฑิต สาขาเคมีประยุกต์
มีนาคม 2554

พิชิต สุดตา. (2554). *การปรับเปลี่ยนโครงสร้างของสารแมงโกสตินกับฤทธิ์ต้านไมโคแบคทีเรีย และไวรัสที่เพิ่มขึ้น และการสังเคราะห์วิธีใหม่สำหรับสารยับยั้งการสร้างหลอดเลือด เซแมกซานิบ*. ปริญญานิพนธ์ ปร.ด. (เคมีประยุกต์). กรุงเทพฯ: บัณฑิตวิทยาลัย มหาวิทยาลัยศรีนครินทรวิโรฒ. คณะกรรมการควบคุม: รองศาสตราจารย์ ดร. สุนิตย์ สุข สำราญ, ผู้ช่วยศาสตราจารย์ ดร. สิริธร สโมสร, ดร. ประเสริฐ พัฒนาประทีป

ได้ทำการออกแบบและสังเคราะห์สารอะนาลอกของสารแมงโกสติน และศึกษาฤทธิ์ทางชีวภาพในการต้านเชื้อวัณโรค (*Mycobacterial tuberculosis*) และการต้านเชื้อไวรัสเริม (Hepes simplex virus-1) จากการทดสอบฤทธิ์ในการต้านเชื้อวัณโรคของสารแมงโกสติน และสารอะนาลอกทั้งหมดที่สังเคราะห์ได้พบว่า สารอะนาลอกหลายชนิดแสดงฤทธิ์ดีในการต้านเชื้อวัณโรค โดยเฉพาะสาร 6-mono-*O*-methyltetrahydromangostin (**150**) สาร 6-mono-*O*-ethyltetrahydromangostin (**152**) และสาร 6-mono-*O*-allyltetrahydromangostin (**154**) ซึ่งแสดงฤทธิ์ต้านเชื้อวัณโรคที่สูง และดีกว่ายา kanamycin ด้วยค่า MIC เท่ากันที่ 0.78 μg/mL และพบว่าสารที่มีฤทธิ์ดีเหล่านี้เหมาะสำหรับการเป็นสารต้นแบบชนิดใหม่ในการพัฒนาไปเป็นยาต้านวัณโรค จากการทดสอบฤทธิ์ต้านเชื้อไวรัสพบว่าสารอะนาลอก **90**, **99, 120**, **140-141**, **144-146**, **148**, **154, 156-158** และสาร **164** เป็นสารต้านไวรัสประเภท non-nucleoside ชนิดใหม่ที่แสดงฤทธิ์ในการต้านเชื้อไวรัสเริมอย่างมีนัยสำคัญที่ค่า IC_{50} ในช่วง 1.10-8.60 μg/mL

นอกจากนี้ได้ทำการศึกษาและพัฒนาวิธีการสังเคราะห์สารเซแมกซานิบ (**82**) ซึ่งเป็นสารยับยั้งการสร้างหลอดเลือด พบว่าสาร เซแมกซานิบ (**82**) สามารถสังเคราะห์ได้ในปริมาณร้อยละผลที่ได้ที่สูงจากปฏิกิริยา reductive cyclisation ของสาร (*Z*)-ethyl-3-(3,5-dimethyl-1*H*-pyrrole-2-yl)-2-(2-nitrophenyl)acrylate (**173**) โดยใช้โลหะเหล็ก (Fe^0) ภายใต้สภาวะ ultrasonication

Acknowledgements

I would like to exprees my most sincere thank to my supervisor, Associate Professor Dr. Sunit Suksamrarn, for her kindness, invaluable guidance, supervision, excellent encouragement, every things she taught me throughout this study, teaching me so much along the way, especially providing me the fantastic opportunity to be a Ph.D. student.

I am grateful to Professor Dr. Apichart Suksamrarn, Department of Chemistry, Faculty of Science, Ramkhamhaeng University, for his invaluable suggestions, useful discussion and encouragement, especially providing me the opportunity to get research assistantship when I was a Master student.

This work was supported by the Royal Golden Jubilee Ph.D. Program of The Thailand Research Fund. I am grateful to the research team strengthening grant from the National Center for Genetic Engineering and Biotechnology (BIOTEC) for partially financial support and for antimycobacterial and antiviral bioassays.

I am grateful to Dr. Michael J. Kelso, School of Chemistry, University of Wollongong, Australia, for his valuable knowledge and helpful supervision during my work in Australia. I am also grateful to Asst. Prof. Dr. Siritron Samosorn and Asst. Prof. Dr. Apinya Chaivisuthangkura and Dr. Prasert Pattanaprateeb for their endless kindness, valuable guidance, valuable time and patient reading.

I am indebted to Dr. Wilford Lie, School of Chemistry, University of Wollongong, for recording the nuclear magnetic resonance spectra in some part of work. I am also indebted to Mr. Nitirat Chimnoi, Chulabhorn Research Institute, Thailand, and Asst. Prof. Dr. Boon-ek Yingyongnarongku and Mr. Widchaya Radchatawedchakoon, Department of Chemistry, Faculty of Science, Ramkhamheang University, for recording the mass spectra.

I am grateful to Mr. Samran Prabpai and Associate Professor Dr. Palangpon Kongsaeree, Department of Chemistry, Faculty of Science, Mahidol University for X-ray diffraction data.

I wish to express my appreciation to all of my teachers of the Department of Chemistry, Faculty of Science, Srinakharinwirot University, for their helps, teaching and discussion during I was a student here. It was a pleasure to have such polite and warm encouragement.

I am grateful to Mr. Payung Jiarawapi, Ms. Jannarin Nontakham, Ms. Natthakaln Lomchoey, Mr. Thongchai Khammee and Ms. Amornmart Jaratrungtawee, graduate students of The Department of Chemistry, Faculty of Science, Srinakharinwirot University for their encouragements, generosity and helpfulness. I would like to thank the staff of the Department of Chemistry, Faculty of Science, Srinakharinwirot University, for assistance.

I am indebted to my family for giving morale support and tolerating me. I owe much to my mother, my father and my grandma for their helps to overcome difficulties I have encountered.

Last but not least, my deepest appreciation is devoted to my close friends, Mr. Kyota Irei and Ms. Suthatip Kamkerd. I am grateful to them for their friendship and support everything for me to have such a beautiful life.

Pichit Sudta

TABLE OF CONTENTS

Chapter		Page
1	INTRODUCTION	
	Background……	1
	Some medicinal properties of genus *Garcinia*……	1
	Tuberculosis……...	15
	Herpes simplex……..	17
	Angiogenesis and cancer therapy……	19
	Objectives of the study……	24
	Scope of the study……...	24
2	REVIEW OF THE LITERATURE	
	Previous research on the synthesis of mangostin analogues and their biological activities……...	25
	Previous research on the synthesis of semaxanib (SU-5416)……	34
3	Experimental	
	General techniques……..	35
	Extraction of plant material and purification of α -mangostin (**1**)……	37
	General procedure for *O*-alkylated and *O*-acylated mangostin synthesis……	39
	Catalytic hydrogenation of **1**……...	54
	General procedure for *O*-alkylated and *O*-acylated tetrahydromangostin synthesis……...	55
	Demethylation of 3,6-di-*O*-methyltetrahydromangostin (**149**)……...	73
	Methylation of **166**……	76
	Bioassays……...	78
	Synthesis of semaxanib (SU-5416, **82**)……	83

TABLE OF CONTENTS (continued)

Chapter		**Page**
4	RESULTS AND DISCUSSION	
	Synthesis of α-mangostin (**1**) analogues.....	90
	Synthesis of tetrahydromangostin (**90**).....	102
	Synthesis of tetrahydromangostin analogues.....	104
	Antimycobacterial activity of mangostin and tetrahydromangostin analogues.....	119
	Effect of hydroxyl groups on mangostin core to antimycobacterial activity.....	123
	Antiviral activity of mangostin analogues.....	132
	Synthesis of semaxanib (SU-5416, **82**).....	137
5	CONCLUSION.....	150
	REFERENCES.....	153
	GLOSSARY.....	159
	CURRICULUM VITAE.....	162

LIST OF TABLES

Table		Page
1	Minimum inhibitory (μg/mL) against microorganism of compounds **1** and **89** and their hydrogenated derivatives **90** and **91**…….....	27
2	*In vitro* activity of α -mangostin (**1**) and its derivatives against *P. falciparum*……..	30
3	*In vitro* activity of ammonium salt mangostin derivatives against *P. fasiparum* compared with their parent amine compounds……	31
4	Cell proliferation inhibitory effects of mangostin derivatives (**92**, **95** and **123-128**)……	32
5	Antimycobacterial activity against *M. tuberculosis* of mangostin analogues……	79
6	Antimycobacterial activity against *M. tuberculosis* of *O*-methylated analogues **149** and **165-169**……	80
7	Antiviral activity against HSV-1 of **1** and its analogues……	82
8	Reaction conditions and percentage yield of the products obtained from the synthesis of mangostin analogues……..	100
9	Reaction conditions and the percentage isolated yield of the products from the synthesis of hydrogenated mangostin derivatives……..	117
10	MIC values (μ g/ mL) of mangostin analogues against *M. tuberculosis*...	121
11	Antimycobacterial activity against *M. tuberculosis* of mangostin analogues **90**, **149** -**150** and analogues **165**-**169**……..	130
12	IC_{50} values (μ g/ mL) of mangostin analogues against HSV-1……...	133
13	IC_{50} values of the active compounds against HSV-1……	134
14	Reduction conditions for produce SU-5416 (**82**)……	147

LIST OF FIGURES

Figure		Page
1	Xanthone basic skeleton……..	3
2	Structures of some isolated xanthones from *G. mangostana* L….....	3
3	Enzymatic hydrolysis of sphingomyelin with sphingomyelinase……..	8
4	Structure of anti-inflamatory drug sulindac (**62**)……..	11
5	The structure of stibogluconate, anti-leishmania drug……	13
6	Total synthesis of α -mangostin (**1**)……..	14
7	The first line antituberculosis drugs……	15
8	The mycobacterial cell wall……..	17
9	Icosahedrol capsid structure of herpes virus……	18
10	Antiviral drugs: acyclovir (**75**) and penciclovir (**76**)…….	19
11	The steps involved sprouting angiogenesis……..	20
12	Member of VEGF in mammals……	21
13	Some anti-angiogenic agents using for cancer treatment…….	23
14	Oxindole angiogenic VEGF-mediated agents……..	23
15	Synthesis of mangostin-3,6-*O*-diglucoside (**88**)……...	25
16	Catalytic hydrogenation of **1** and **89** to produce hydrogenated derivatives **90** and **91**.....	27
17	Synthesis of di-*O*-alkylmangostin derivatives (**92**-**98**) and di-*O*-acetylmangostin (**99**)……..	28
18	(a): Synthesis of halogenated mangostin derivatives (**129**-**132**), (b): oxidation of the mangostin derivative **133** ……..	33
19	Synthesis of SU-5416 (**82**) under Knoevenagel condensation…….	34
20	Synthesis of SU-5416 (**82**) by Tandem Horner-Wadsworth-Emmons/Heck procedure……..	34

LIST OF FIGURES (continued)

Figure		Page
21	The downfield shift of H-5 in ^{1}H-NMR spectrum (300 MHz, in $CDCl_3$) of **148** compared to that of parent compound **1**……	99
22	^{1}H-NMR spectrum (300 MHz, in $CDCl_3$) of product **90** (top) compared with compound **1** (bottom)……..	103
23	^{1}H-NMR spectra (300 MHz, in $CDCl_3$) of the products **149** and **150** from methylation reaction of **90**……..	105
24	^{13}C-NMR spectra (75 MHz, in $CDCl_3$) of the products **149** and **150** from methylation reaction **90**……..	106
25	The down field shift of H-4 and H-5 in ^{1}H-NMR spectrum (300 MHz, in $CDCl_3$) of compound **163** (a) and **164** (b)……..	116
26	The structure activity relationship (SAR) of mangostin analogues……..	122
27	Demethylation of **149** with aqueous morpholine…….	123
28	^{1}H-NMR spectra (300 MHz) of the products **165**, **166** and **167** from demethylation reaction of **149**……..	125
29	^{13}C-NMR spectra (75 MHz) of the products **165**, **166**, **167** from demethylation reaction of **149**……..	126
30	^{1}H-NMR spectra (300 MHz) of the products **166** and **167** from methylation reaction compared with starting **165**……	128
31	^{13}C-NMR spectrum (75 MHz) of the products **166** and **167** from methylation reaction compared with starting **165**……	129
32	Retrosynthetic analysis of semaxanib……	137
33	Synthesis of compound **172**……	139
34	Proposed mechanism for the formation of compounds **173** and **174**….	140
35	^{1}H-NMR spectrum (300 MHz, $CDCl_3$) of **173**……..	141
36	NOE correlation of H-8 and H-6 in NOESY spectrum (300 MHz, $CDCl_3$) of **173**……	27

LIST OF FIGURES (continued)

Figure		Page
37	Intramolecular hydrogen bonding (*Z*)-**173**.....	142
38	^{1}H-NMR spectrum (300 MHz, in $CDCl_3$) of (*E*)-**174**.....	143
39	The signal of non-equivalent methylene proton in ^{1}H-NMR spectrum and the proposed atropisomerism of (*E*)-**174**.....	144
40	Acid catalized isomerisation of (*E*)-**174**.....	145
41	The equilibrium between (*E*)-**174** and (*Z*)-**173** under acidic condition...	145
42	Reduction of **173** to produce of semaxanib (**82**).....	146
43	Intramolecular hydrogen bonding of semaxanib (**82**).....	148
44	Reductive cyclisation of **173** to produce **82**	149
45	Structure of the most active compounds against *M. tuberculosis*.....	151
46	The summarized new strategy for synthesis of semaxanib (SU-5416, **82**).....	152

CHAPTER 1
INTRODUCTION

Background

The current rapid technology development has resulted in that the world's population is survived in the toxic environment with hazard chemicals and pathogens resulting disease and death of the over young people. The cancer and infectious disease caused a critical problem associated with morbidity and mortality to mankind. Thus, new drugs are urgently required. Up to date, several investigations have demonstrated a diversity of sources and strategies for developing the new drugs including synthetic bioactive substances and natural occurring bioactive compounds.

1. Some medicinal properties of the genus *Garcinia*

In recent years, it becomes clear that a number of medicinal plants are more sources of interesting new drug candidates. Since ancient time people have been exploring nature, and in particular plants, in the search for new drugs. This has resulted in the use of a large number of medicinal plants to treat various diseases. Many of these plants have shown to be active, and quite a few drugs of Western medicine are based on the traditional use of medicinal plants (Joy; et al. 1998: 3). Both of the pure compounds from medicinal plants and their analogues are used as the drugs. One interesting point to be noticed that usually in plants are found a series of closely related compounds, rather than one single constituent. This is similar to the idea of combinatorial chemistry. Thus, the traditional uses of medicinal plants remain an important source for drug discovery.

Among the medicinal plants, the genus *Garcinia* (Clusiaceae) is a botanic source of the folk medicine and is the best known in Malaysia as a genus of fruit trees. The fruit of many species are edible and preserved or used as added ingredient in local dishes for example *G. atroviridis*, *G. cowa* and *G. hombroniana* (Nazre; et al. 2007: 31). *Garcinia* plants produce a yellow resin which is used in the making of varnish and in treatment of wounds. Many species are source of edible oils. The crude extract and the pure isolates of *Garcinia*

species have been exhibited significant various pharmacological activities. For example, *Garcinia dulcis* was mainly found in the Southeast Asia, and the seed and leaves have been used in traditional medicine against struma, parotitis, lymphatitis and other human diseases (Iinuma; et al. 1996: 472). *Garcinia subelliptica* has been cultivated as a windbreak in the Yaeyama islands of Japan and the isolated yellow pigment from its bark has been utilized as dye (Fukuyama; et al. 1998: 853). The pericarp of mangosteen fruit (*Garcinia mangostana* L.) has been used as a medicinal agent by Southeast Asians for centuries in the treatment of skin infections and wounds, and for the relief of diarrhea and amoebic dysentery (Mahabusarakam; et al. 1987: 474). In the Ayurvedic system of medicine, the fruit hull of this plant finds wide applications, mainly as an anti-inflammatory agent and in the treatment of diarrhea (Balasubramanian; & Rajagopalan. 1988: 1552). Mangosteen extracts and purified constituents have been subjected to a wide array of biological test germanes particularly to infectious diseases, cancer chemotherapy and cancer chemoprevention, diabetes and neurological conditions (Loo; et al. 2007: 9805).

1.1 Xanthones from *G. mangostana*

The "Mangosteen" tree is a tropical tree from India, Myanmar, Malasia, Philippines, Sri Lanka, and Thailand. The plant grows slowly to 7-12 m. high, and has straight trunk and dark brown bark. The fruit is dark purple or reddish which consist of 6-8 seeds, and have a white and juicy pulp. Mangosteen is known as the "queen of fruits" because it is one of the best tasting tropical fruits. *G. mangostana* has been shown to contain a variety of secondary metabolites especially oxygenated xanthones and prenylated xanthones. Xanthone is a class of the secondary metabolite which found in some higher plant families, fungi and lichens. The skeleton of xanthone is known as 9-xanthone or dibenzo-γ-pyrone, where two benzene moieties are linked through a carbonyl group and an oxygen atom (Figure 1). No free rotation of C-C bonds is possible as the ring are joined in fused formation. Various chemical groups may be attached to this backbone and these substituents define the particular functionalities or properties of the compound. The carbons skeleton could be numbered according to a biosynthetic convention. Carbons 1-4 are assigned to the acetate-derived ring A, and carbons 5-8 are assigned to the shikimate derived ring B (Bennett; & Lee. 1989: 967).

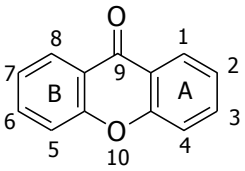

Figure 1 Xanthone basic skeleton

Xanthones have been classified in five groups: (a) simple oxygenated xanthone, (b) xanthone glycosides, (c) prenylated xanthones, (d) xanthonelignoids, and (e) miscellaneous xanthones (Sultonbawa; et al. 1980: 1465). To date, more more than eighty four xanthones have been isolated from the pericarp, trunk, branches of *G. mangostana*. Obolskiy et al reviewed the isolated xanthones obtained from the different parts of mangosteen which are summarized in Figure 2 (Obolskiy; et al. 2009: 1047).

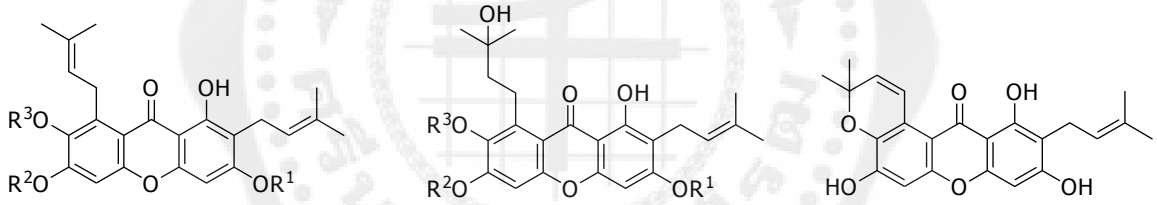

α-mangostin (**1**); $R^1 = R^2 = H$, $R^3 = Me$
β-mangostin (**2**); $R^1 = R^3 = Me$, $R^2 = H$
γ-mangostin (**3**); $R^1 = R^2 = R^3 = H$

garcinone C (**4**); $R^1 = R^2 = R^3 = H$
garcinone D (**5**); $R^1 = R^2 = H$, $R^3 = Me$

Figure 2 Structures of some isolated xanthones from *G. mangostana*

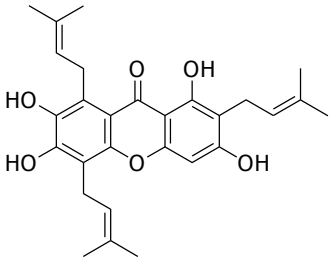

garcinone E (**7**)

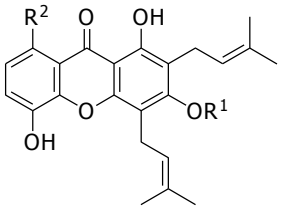

gartanin (**8**); $R^1 = H$, $R^2 = OH$
8-deoxygartanin (**9**); $R^1 = R^2 = H$
cudraxanthone G (**10**); $R^1 = Me$, $R^2 = H$
8-hydroxycudraxanthone (**12**); $R^1 = Me$, $R^2 = OH$

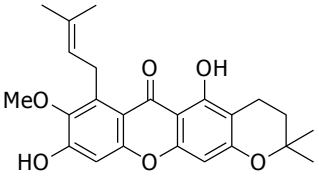

3-isomangostin (**11**)

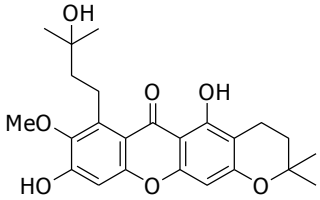

isomangostin hydrate (**13**)

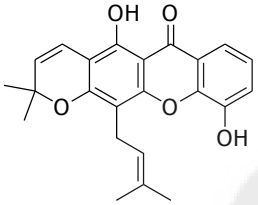

trapezifolixanthone (**14**)

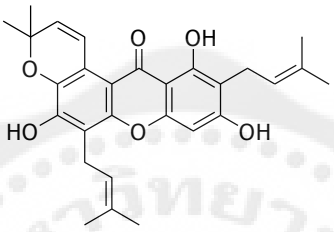

tovophyllin A (**15**)

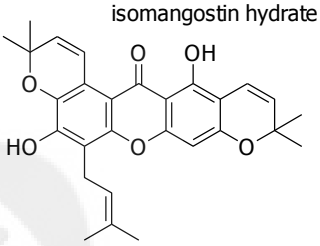

tovophyllin B (**16**)

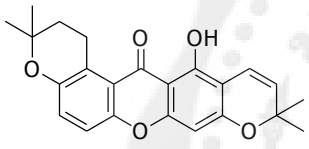

thwaitesixanthone (**17**)

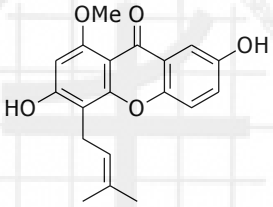

mangosharin (**18**)

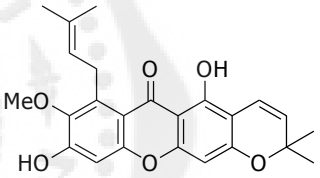

garciniafuran (**19**)

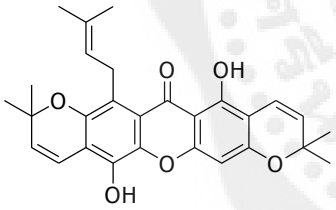

garcimangosone A (**20**)

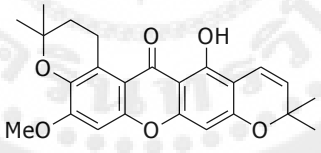

garcimangosone B (**21**)

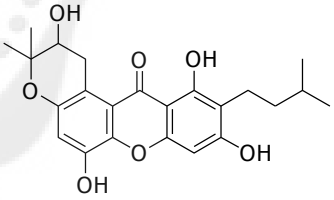

garcimangosone C (**22**)

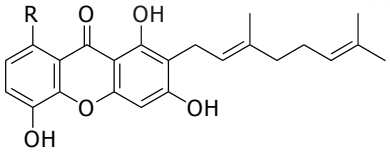

mangostinone (**23**); R = H
smeathxanthone A (**24**); R = O H

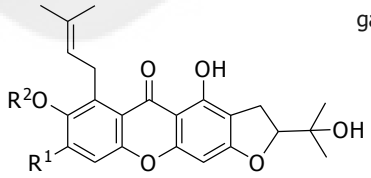

6-deoxy-7-demethylmangostanin (**25**); $R^1 = R^2 = H$
6-O-methylmangostanin (**26**); $R^1 = OMe$, $R^2 = Me$

Figure 2 (continued)

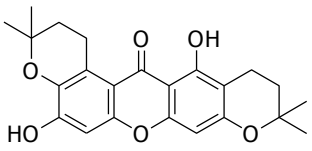

BR xanthone (**27**)

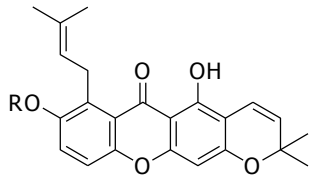

calabaxanthone (**28**); R = Me
demethylcalabaxanthone (**29**); R = H

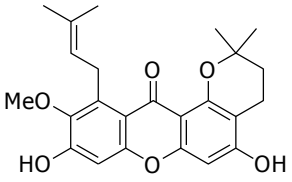

1-isomangostin (**30**)

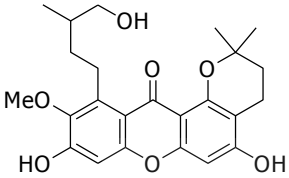

1-isomangostin hydrate (**31**)

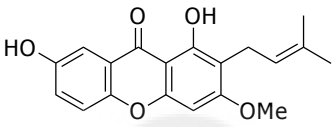

2-(3-methybut-2-enyl)-1,7-dihydroxy-
3-methoxyxanthone (**32**)

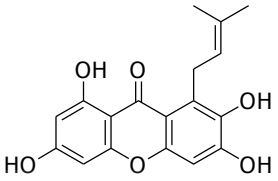

2,3,6,8-tetrahydroxy-1-
(3-methylbut-2-enyl)xanthone (**33**)

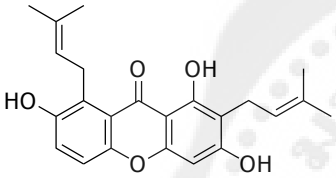

2,8-bis-(3-methylbut-2-enyl)
-1,3,7-trihydroxyxanthone (**34**)

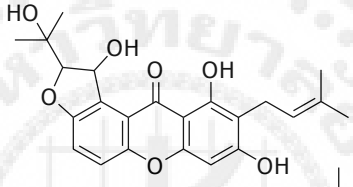

1,2-hihydro-1,8,10-trihydroxy-2-
(2-hydroxypropan-2-yl)-9-
(3-methylbut-2-enyl)
furo[3,2,a]xanthen-11-one (**37**)

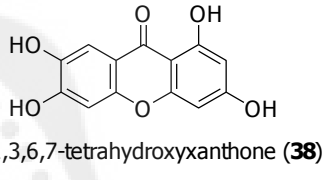

1,3,8-trihydroxy-4-methyl-2,7-
di (3-methylbut-2-enyl)xanthone (**39**)

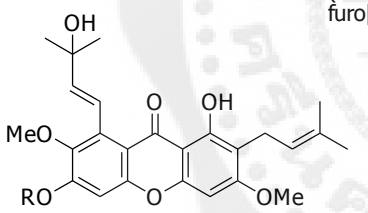

(16E)-1,6-dihydroxy-8-(3-hydroxy-3-methylbut-1-enyl)
-3,7-dimethoxy-2-(3-methylbut-2-enyl)xanthone (**35**); R = H

(16E)-1-hydroxy-8-(3-hydroxy-3-methylbut-1-enyl)
-3,6,7-trimethoxy-2-(3-methylbut-2-enyl)xanthone (**36**); R = Me

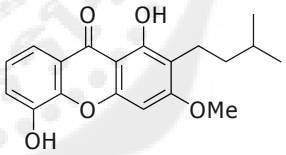

1,5-dihydroxy-2-(3-methylbut)-3-methoxyxanthone
(**42**)

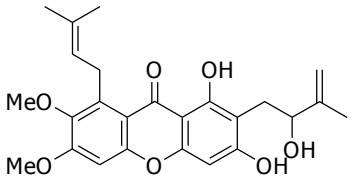

1,3-dihydroxy-2-(2-hydroxy-3-
methylbut-3-enyl)-6,7-dimethoxy-
8-(3-methylbut-2-enyl)xanthone (**40**)

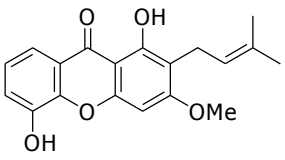

1,5-dihydroxy-3-methoxy-2-
(3-methylbut-2-enyl)xanthone (**41**)

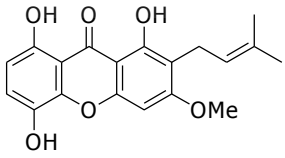

1,5,8-trihydroxy-3-methoxy-2-
(3-methylbut-2-enyl)xanthone (**43**)

Figure 2 (continued)

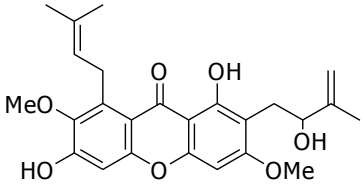

1,6-dihydroxy-2-(2-hydroxy-3-methylbut-3-enyl)-3,7-dimethoxy-8-(3-methylbut-2-enyl)xanthone (**44**)

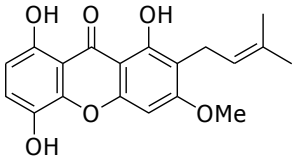

1,5,8-trihydroxy-3-methoxy-2-(3-methylbut-2-enyl)xanthone (**45**)

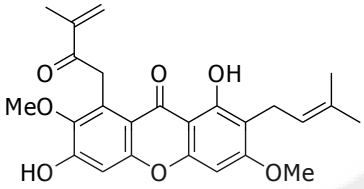

8-(2-carbonyl-3-methylbut-3-enyl)-1,6-dihydroxy-3,7-dimethoxy-2-(3-methylbut-2-enyl)xanthone (**46**)

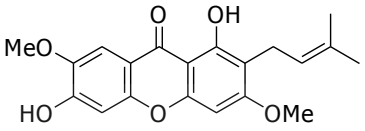

1,6-dihydroxy-3,7-dimethoxy-2-(3-methylbut-2-enyl)xanthone (**47**)

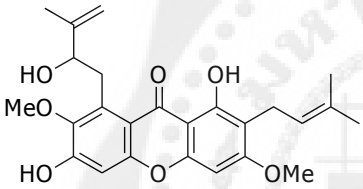

1,6-dihydroxy-8-(2-hydroxy-3-methylbut-3-enyl)-3,7-dimethoxy-2-(3-methylbut-2-enyl)xanthone (**48**)

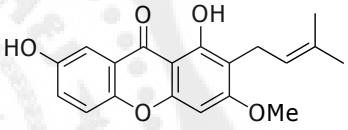

1,7-dihydroxy-2-(3-methylbut-2-enyl)-3-methoxyxanthone (**49**)

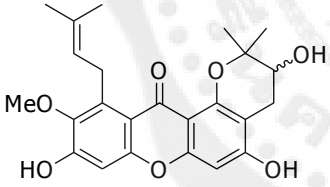

11-hydroxy-1-isomangostin (**50**)

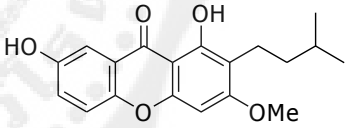

1,7-dihydroxy-2-isopentyl-3-methoxyxanthone (**51**)

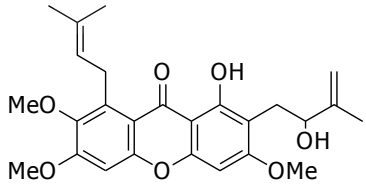

1,6-dihydroxy-2-(2-hydroxy-3-methylbut-3-enyl)-3,6,7-trimethoxy-8-(3-methylbut-2-enyl)xanthone (**52**)

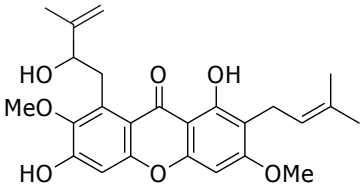

1,6-dihydroxy-8-(2-hydroxy-3-methylbut-3-enyl)-3,6,7-trimethoxy-2-(3-methylbut-2-enyl)xanthone (**53**)

Figure 2 (continued)

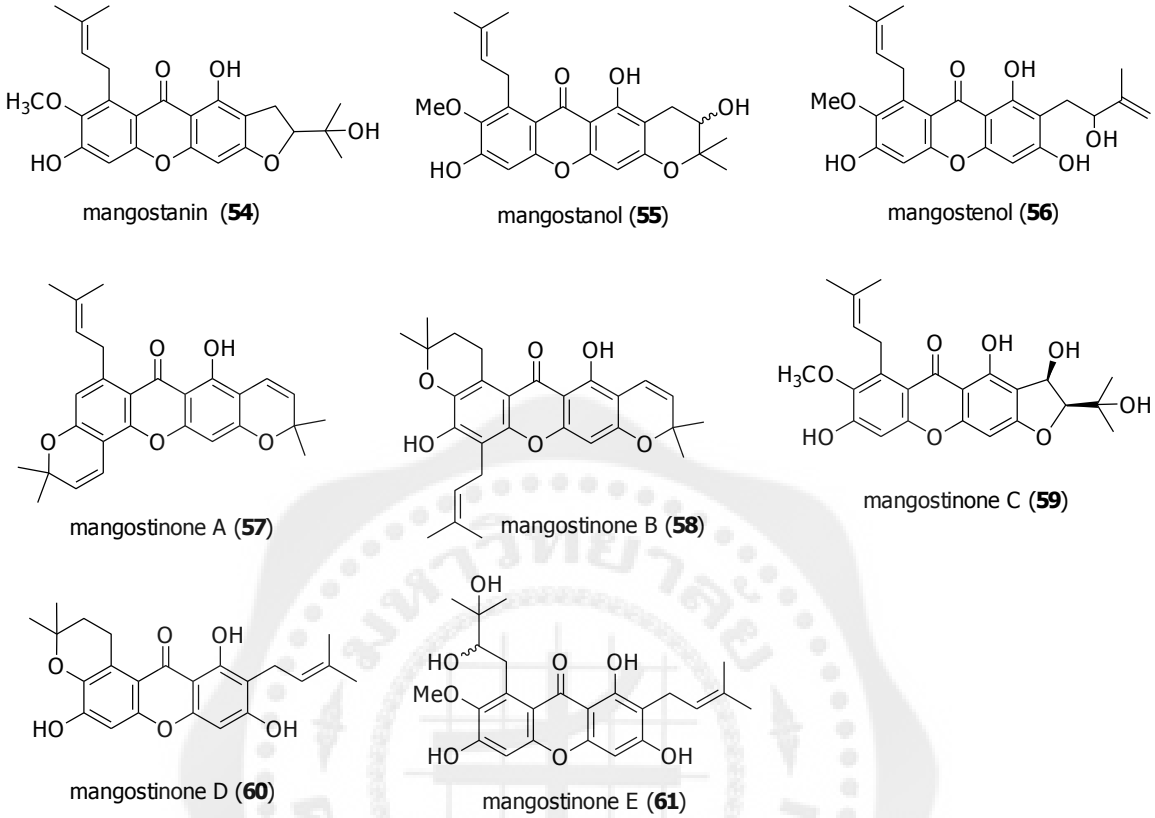

Figure 2 (continued)

Among the isolated xanthones of *G. mangostana*, α-mangostin (**1**) was the major coloring matter, and its structure was assigned as **1** by the research group of Yates long years ago (Yates; & Stout. 1958: 1691). α-Mangostin (**1**) is recognized as one of the major active mangosteen secondary metabolites, which exhibited various biological activities such as antioxidant (Jung; et al. 2006: 2077), anti-inflamatory (Chen; et al. 2008: 688), anti-HIV (Chen; et al. 1996: 381), antiplasmodial (Mahabusarakam; et al. 2006: 912) and anti-tuberculosis (Suksamrarn; et al. 2003: 857).

1.2 Some biological and medicinal properties of α-mangostin (**1**)

1.2.1 Anticancer-related targets properties

In 2003, Matsumoto et al. studied the induction of apoptosis in human leukemia cell lines (HL60) with α-Mangostin (**1**) and other five xanthones **2**, **3**, **6**, **23** and **8** (Figure 2). The *in vitro* cytotoxic effects of these xanthones were examined using Western Blot Analysis. The results revealed that after treatment at the concentrations from 5 to 40 μg of each xanthone for 72 h., all xanthones exhibited significant growth inhibition and compounds **1**-**3** were particularly effective even at the low dose of 10 μM. Compound **1** showed the strongest activity with the complete inhibition at IC_{50} 10 μM. Further investigation on the cell growth inhibitory activity against leukemia cell lines namely, K562, NB4, and U937 by **1** showed that no significant effect on the cell growth at the concentration lower than 2 μM, but remained inhibit against all cell lines at 5 μM. Among the cell lines tested, K562 cells seemed to be the most resistant to **1**. Thus, α-mangostin (**1**) appeared to preferentially inhibit leukemia cells (Matsumoto; et al. 2003: 1124). In the same year, Hamada et al. reported the activity of α-mangostin (**1**) against acidic sphingomyelinase. Sphingomyelinase are enzymes that catalyze the hydrolysis of sphingomyelin in to ceramides and phosphorylcholine and are involved in cell death, cell differentiation, and cell proliferation (Figure 3). In this study, compound **1** inhibited bovine brain-derived acidic sphingomyelinase (IC_{50} 5.15 μM) in a selective manner when compared with the neutral sphingomyelinase (IC_{50} 46.5 μM) (Hamada; et al. 2003: 3151).

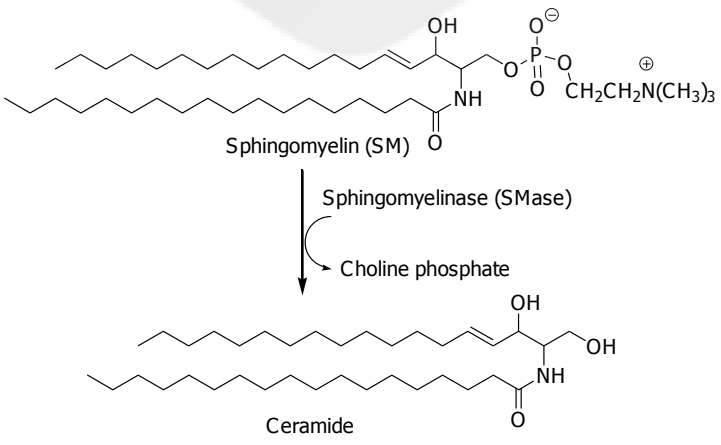

Figure 3 Enzymatic hydrolysis of sphingomyelin with sphingomyelinase

In the following year, Matsumoto et al. investigated the mechanism of cell death induced by α-mangostin (**1**) treatment in human leukemia cell line HL60. The study showed that **1** induced apoptosis in HL60 cell, of which was mediated by mitochondrial dysfunction in the early phase. Compound **1** induced caspases 9 and 3 activation, loss of mitochondrial membrane potential, and released of reactive oxygen species (ROS) and cytochrome C. These results indicated that mitochondria played a pivotal role in induction of apoptosis by **1** (Matsumoto; et al. 2004: 5799). Furthermore, Suksamrarn et al. reported the cytotoxicity of 19 xanthones which were isolated from mangosteen-fruit pericarp against three different human cancer cell lines: epidermoid carcinoma of mouth (KB), breast cancer (BC-1) and small cell lung cancer (NCI-H187). Among these xanthones, α-mangostin (**1**) displayed the most potent effect against BC-1 cell with an IC_{50} value of 0.92 μg/mL, an activity that was greater than the standard drug ellipticine (IC_{50} = 1.46 μg/mL). Moreover, **1** also had a cytotoxic activity against KB cell (IC_{50} = 2.08 μg/mL) (Sukamrarn; et al. 2006: 301).

1.2.2 Antibacterial properties

In 1996, Iinuma et al. examined 13 naturally occurring xanthones from *G. mangostana*, *G. subelliptica* Merr, *Calophyllum inophylum* L, *Harungana madagascariensis* Lam ex Poir and *G. dioica* Bl for their inhibitory effects against methicillin-resistant *Staphylococcus aureus* (MRSA). In this study, α-mangostin (**1**) exhibited anti-MRSA activity within the MIC (minimum inhibitory concentration) in the range 1.57-12.5 μg/mL, which was more active than the positive control, vancomycin (MIC= 3.13-6.25 μg/mL). Moreover, **1** in the presence of vancomycin exhibited increasing anti-MRSA activity which was not observed in the case of using other tested xanthones (Iinuma; et al. 1996a: 861). Suksamrarn et al. investigated the antituberculosis activity of prenylated xanthones which was obtained from mangosteen-fruit pericarp. Among them, compounds **1**, **2** and garcinone B (**6**) exhibited the most potent inhibitory effect against *Mycobacterium tuberculosis,* with the same MIC of 6.25 μg/mL; whereas trapezifolixanthone (**14**) and demethylcalabaxanthone (**29**) had an MIC value of 12.5 μg/mL and compounds **3**, **5**, **16**, **23** and mangostanin (**54**) had MIC values of 25 μg/mL. The mangostanol (**55**) and mangostenol (**56**) exhibited lowest antituberculosis potential with MIC values of 200 μg/mL and 100 μg/mL, respectively (Suksamrarn; et al. 2003: 857). The structures of these compounds are shown in Figure 2 The research group of Sakami reported that α-mangostin (**1**) had inhibitory activity against vancomycin resistant *Enterococci* (VRE) and MRSA with

MIC values of 6.25 and 12.5 μg/mL, respectively. The potent synergistic effects of **1** with gentamicin antibiotic against five strains of VRE and three strains of VSE (Vancomycin-sensitive *Enterococci*) were observed with the MICs range of 3.13-6.25 μg/mL. In addition, α- and β-mangostins (**1**-**2**) were extended to examine for their antibacterial activities against gram negative bacteria, such as *Escherichia coli* IFO 3972, *Proteus vulgaris* IFO 3988, *Serratia marcescens* IFO 12648, *E. coli* O157 (ATCC 43888), *Klebsiella pneumoniae* IFO 13277 and *Pseudomonas aeruginosa* IFO 13275**.** The results indicated that **1** and **2** were inactive against these gram negative bacteria (Sakagami; et al. 2005: 203).

1.2.3 Antimalarial property

Malaria remains one of the most serious tropical infectious diseases for human, and over 80% of cases in the world are caused mainly by *Plasmodium falciparum*. α-Mangostin (**1**) and β-mangostin (**2**) exhibited antimarial activity against *P. falciparum* with IC_{50} value of 5.1 and 7.0 μM, respectively (Riscoe; et al. 2005: 2539). In 2006, Azebaze et al. reported the antimalarial activity of **1** against FcM29-Cameroon (chloroquine resistant) and F32 (chloroquine sensitive) strains with IC_{50} in the range of 1.7-3.2 μg/mL (Azebaze; et al. 2006: 111). Moreover, the research group of Mahabusarakam found that α-mangostin (**1**) exhibited an IC_{50} value of 17 μM against *P. falciparum* (Mahabusarakam; et al. 2006: 912).

1.2.4 Anti-inflammatory property

Inflammation is defined as a localized reaction of tissue to irritation, injury, or infection. Symptom of inflammation include pain, swelling, red coloration to the area, and some time loss of movement or function. Inflammation are generated by two major classes of intracellular enzyme that are prostaglandins and leukotrienes. In prostaglandin pathway, inducible nitric oxide synthase (iNOS) and cyclooxygenase-2 (COX-2) are important enzymes playing a role in inflammation process. These enzymes could be activated by peroxynitrite ($ONOO^-$) which was produced from reaction of both nitric oxide (NO) and the superoxide anion (O_2^-) with each other in endothelial cells. Thus, the inhibition of NO production has become a simple approach to examine anti-inflammatory effect (Chen; et al. 2008: 688). Recently, Chen and colleagues investigated anti-inflammatory property of two xanthones, compounds **1** and **3** against the murine macroplage cell line, RAW 264.7. This investigation showed that both of **1** and **3**

significantly inhibited NO and PGE_2 production from lipopolysaccharide (LPS)-stimulated RAW 264.7 cells. The IC_{50} values for the inhibition of NO production by **1** and **3** were 12.4 and 10.1 μM, respectively. In addition, the effects of **1** and **3** on iNOS enzyme activity was examined compared with L-NAME, a specific inhibitor of NO synthase enzyme activity. The results suggested that **1** and **3** weakly inhibited iNOS activity in activated RAW 264.7 macrophages where as L-NAME significantly inhibited nitric accumulation by more than 50% at 200 μM. According to this observation, they summarized that neither **1** nor **3** exhibits a direct inhibitory effect on the enzyme activity of inducible NO synthase. Furthermore, the anti-inflammatory effects of **1** and **3** were evaluated by carrageenan-induced paw edema in mice that was used as an acute model of inflammation. The sulindac was used as reference drug in the testing. Both of **1** and sulindac treatment showed significant difference on paw edema inhibition when compared with control group. Compound **1** and sulindac displayed a potent inhibition on paw edema at 3 h and 5 h, respectively. Therefore, they suggested the on-set time of paw edema inhibition from **1** was more quickly than that of sulindac (**62**) (Figure 4). These data demonstrated that **1** has more potent anti-inflammatory activity than **3** *in vivo* (Chen; et al. 2008: 688).

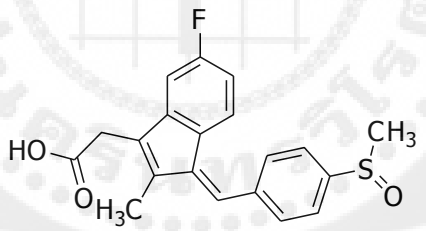

Figure 4 Structure of anti-inflammatory drug sulindac (**62**)

1.2.5 Antifungal property

The antifungal activity of **1** against *Candida albicans*, the most important microorganism implicated in oral candidiasis, was studied by Kaomongkolgit et al. The activity of **1** was conducted by comparison with positive control, clotrimazole and nystatin. The results revealed that compound **1** was effective against *C. albicans* with IC_{50} and minimum fungicidal concentration (MFC) at 1,000 and 2,000 μg/mL, respectively. Moreover, the *C. albicans* killing activity of **1** was also investigated by measuring the rate of fungicidal activity of the speed with which killing may occur at a given drug concentration.

For the time-kill assay, they compared the antifugal activity of **1** with that of clotrimazole and nystatin in order to find out a new natural inexpensive agent that might be used as adjunct therapy in the management of oral candidiasis. The results showed that the rate of *Candida* killing of **1** was more than the positive drugs, clotrimazole and nystatin. In addition, they reported that clotrimazole and nystatin showed a slight decrease in viable cell count in 30 minutes. This probably due to the onset of action of these agents, which was longer than 30 min. On the other hand, **1** exerts rapid antifungal activity against *C. albicans* within 20 min. This observation suggested that **1** seemed likely to be a promising new agent for treatment of oral candidiasis (Kaomongkolgit; et al. 2009: 401).

1.2.6 Anti-viral property

The research group of Chen reported the kinetic and inhibitory effects of compounds **1** and **3**, using proteolysis assay of the heptapeptide. The pepstatin A was used as positive control (IC_{50}= 76 $\pm$ 0.32 nM). The results showed that both compounds exhibited inhibitory activities on HIV protease with IC_{50} values of 5.12 $\pm$ 0.41 μM and 4.81 $\pm$ 0.32 μM, respectively. From the kinetic studies, the Ki (kinetic inhibitory constant) values of **1** and **3** were 10.7 $\pm$ 0.95 μM and 7.8 $\pm$ 0.40 μM, respectively. From this observation, it was concluded that the type of inhibition of both compounds was noncompetitive. From the IC_{50} and Ki values of **1** and **3** suggested that the structural difference between that compounds has very little effect on their anti-viral activity (Chen; et al. 1996: 381).

1.2.7 Anti-oxidant property

Jung et al. measured the peroxynitrite ($ONOO^-$) scavenging capacity of 13 xanthones by monitoring the oxidation of dihydrorhodamine 123 (DHR-123). $ONOO^-$ is the oxidant specie which is produced by the reaction between nitric oxide ($NO^{\cdot}$) and ($O_2^{\cdot-}$). The IC_{50} values for $ONOO^-$ scavenging was determined for several xanthones. Among them, α-mangostin (**1**) exhibited $ONOO^-$ scavenging with IC_{50} values of 12.2 μM, whereas compounds **3**, **5**, and 1-isomangostin (**30**) showed the activity with the IC_{50} 8.0, 26.0 and 19.2, respectively. These observation showed that the presence of hydroxyl group in molecule enhanced anti-oxidation potency of prenylated xanthone (Jung; et al. 2006: 2077).

1.2.8 Anti-Leishmanial property

Leishmaniasis is a complex of diseases spread throughout the tropical and subtropical world caused by haemoflagellate protozoan parasites. In humans, and other mammalian hosts, leishmania are obligate parasites of macrophages, surviving and multiplying in the phagolysomal compartment of these cells. The sodium stibogluconate (**63**, Figure 5) has been used as the first drug for treatment of both visceral leishmaniasis for over 50 years but they required long time to cure which had toxic effects and variable efficacy (Winter; et al. 2002: 8). In 2002, Winter et al. mentioned the antileismanial activity of **1** against *Leishmania* parasites in the amastigote stage of development. The result showed that, compound **1** was higher potency xanthone against leishmania parasite with the IC_{50} 0.00041 mg/mL than stibogluconate positive drug (IC_{50} = 0.1-1.0 mg/mL) (Winter; et al. 2002: 8).

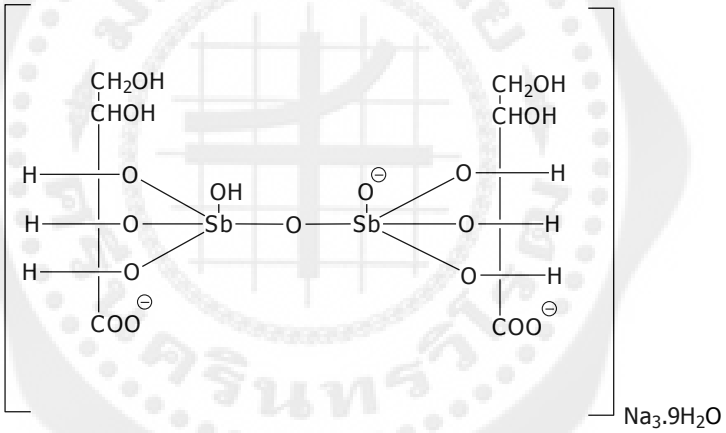

Stibogluconate [Sodium Antimony (V)Gluconate] (**63**)

Figure 5 The structure of stibogluconate, anti-leishmania drug

1.3 Sources of α-mangostin (**1**)

1.3.1 Plant sources containing α-mangostin (**1**)

α-Mangostin (**1**) is secondary metabolites commonly occurring in a number of higher plants such as *Cratoxylum cochinchinense* (Boonnak et al. 2009: 3003), *Cratoxylum formosum* spp *pruniflorum* (Duan; et al. 2010: 1283), *Allanblackia monticola*

STENER L.C. (Azebaze; et al. 2006: 111), *Garcinia cowa* (Panthong; et al. 2006: 999), and *G. mangostana* (Suksamrarn; et al. 2002: 761).

1.3.2 Synthetic α-mangostin (**1**)

Iikubo et al. reported the first direct synthesis of **1** (Figure 6). This direct synthetic method started with the synthesis of two key fragments (fragment **66** and **67**). The phenolic derivative **67** was obtained from 1,3,5-trihydroxybenzene, of which was subjected to several steps that were MOM protection, prenylation, TBS-protection, DIBAL-reduction and IBX oxidation. Another fragment **66** was constructed through the introduction of benzyl protecting group to 2,4-hydroxybenzaldehyde, followed by Baeyer Villiger oxidation and acid hydrolysis, and further bromination, allylation, and Lexieux-Johnson oxidation. A coupling step and cyclization reaction of both coupling partner using a PPh_3-CCl_4 protocol completed the total synthesis of **1** in total 43% yield (Iikubo; et al. 2002: 291).

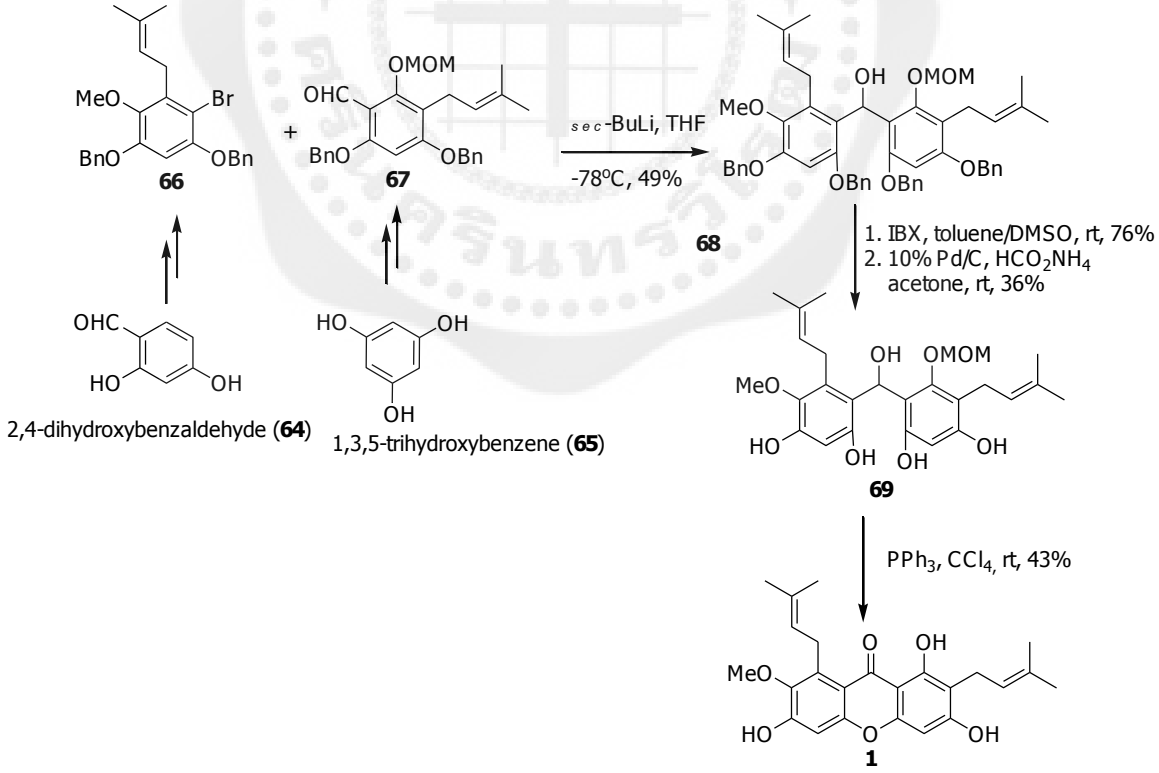

Figure 6 Total synthesis of α-mangostin (**1**)

2. Tuberculosis

Tuberculosis (TB) is the fundamental etiologic agent for human tuberculosis and is the biggest killer due to bacterial infection in the world today. Over one-third of the world's population is infected with TB with approximately 8 million new cases of infection every year (Dye; et al. 1999: 282). The number of cases worldwide is rapidly increasing due to the appearance of single drug-resistance (SDR) and multidrug-resistance (MDR) of strains of *Mycobacterium tuberculosis* which are insensitive to one or more the first-line anti-TB drugs isoniazid (INH, **70**), rifampin (**71**), ethambutol (**72**), streptomycin (**73**) and pyrazinamide (**74**)) (Figure 7) and also due to an increase in patients with immunodeficiency virus (HIV) infection (Tomioka. 2006: 4047).

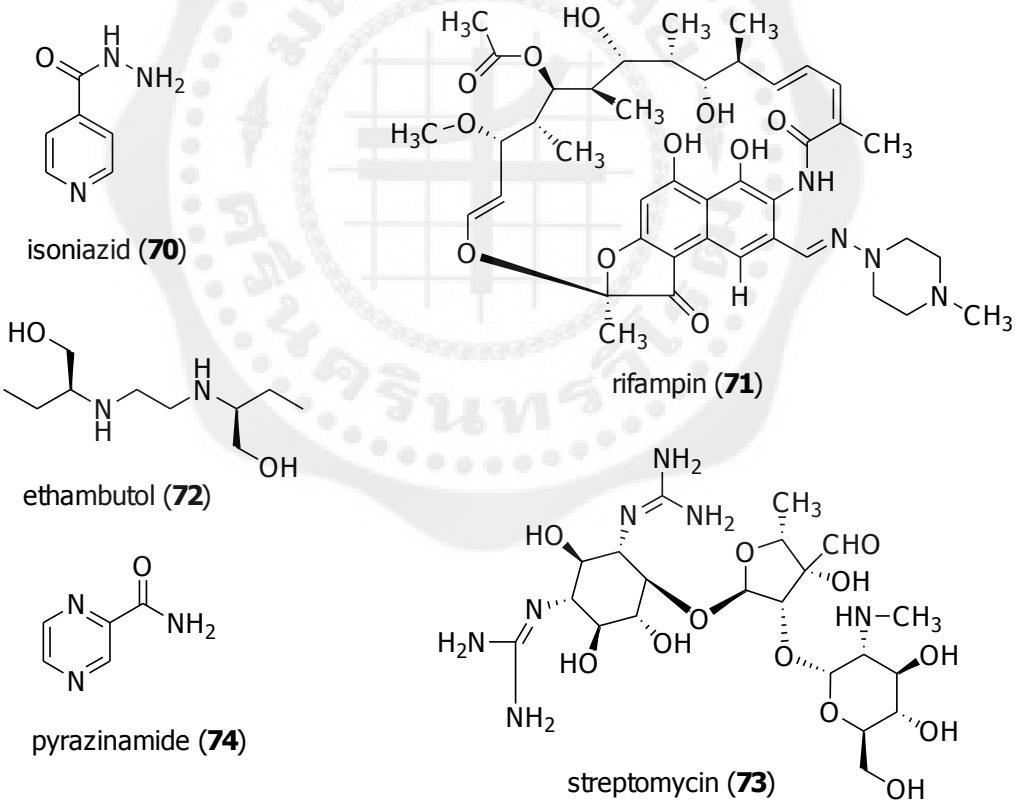

Figure 7 The first line tuberculosis drugs

2.1 *Mycobacterium tuberculosis*

M. tuberculosis is an intracellular obligate aerobic actinomycete about 2-6 μm long with a generation time of approximately 20-24 hours under optimal conditions. It forms tight, rope-like aggregates in liquid culture and creamy irregular raised colonies with condensed filaments in the center in solid media which grow up to 7 days or more (Cole; et al. 1998: 537). The mycobacterial protective outer lipid bilayer is the thickest biological membrane known, leading to mycobacteria naturally resistant to many antibiotics. The cell wall can be divided into two portions. As seen in Figure 8, the top of the cell membrane resides the peptigoglycan (PG), covalently attached to arabinogalactan (AG), which is in turn attached to mycolic acids. This insoluble section is known as the cell wall core. The outer leaflet consists of free lipids, interspersed with cell- wall proteins, phosphatidylinositol mannosides, the phthiocerol-containing lipids, lipomannan and lipoarabinomannan. These are the signaling and effector molecules in the disease process (Brennan; et al. 2003: 91).

2.2 Drug resistance of *Mycobacterium tuberculosis*

Drug resistance is a natural phenomenon and the mechanisms via which bacteria develop resistance are diverse and complex. *M. tuberculosis* resistance occurs due to its highly hydrophobic cell wall (Figure 8) that is impermeable to most drugs and the resistance determinates encoded by its genome (Tomioka. 2006: 4047). The example of the drug resistance of some first-line anti-TB drugs, the resistance to RIF is due to mutations in the rpoB gene which is responsible for producing the beta subunit of the DNA-dependent RNA polymerase. However, there is a small fraction of resistant bacteria that does not exhibit this mutation suggesting there are other mechanisms of RIF resistance. INH is inactivated by an enzyme called KatG and it inhibits an enzyme that is involved in fatty acid biosynthesis called InhA. ETH resistance is acquired via the mutations in the embB gene that encodes for the arabinosyl transferases that is inhibited by ETHb (Tomioka. 2006: 4047).

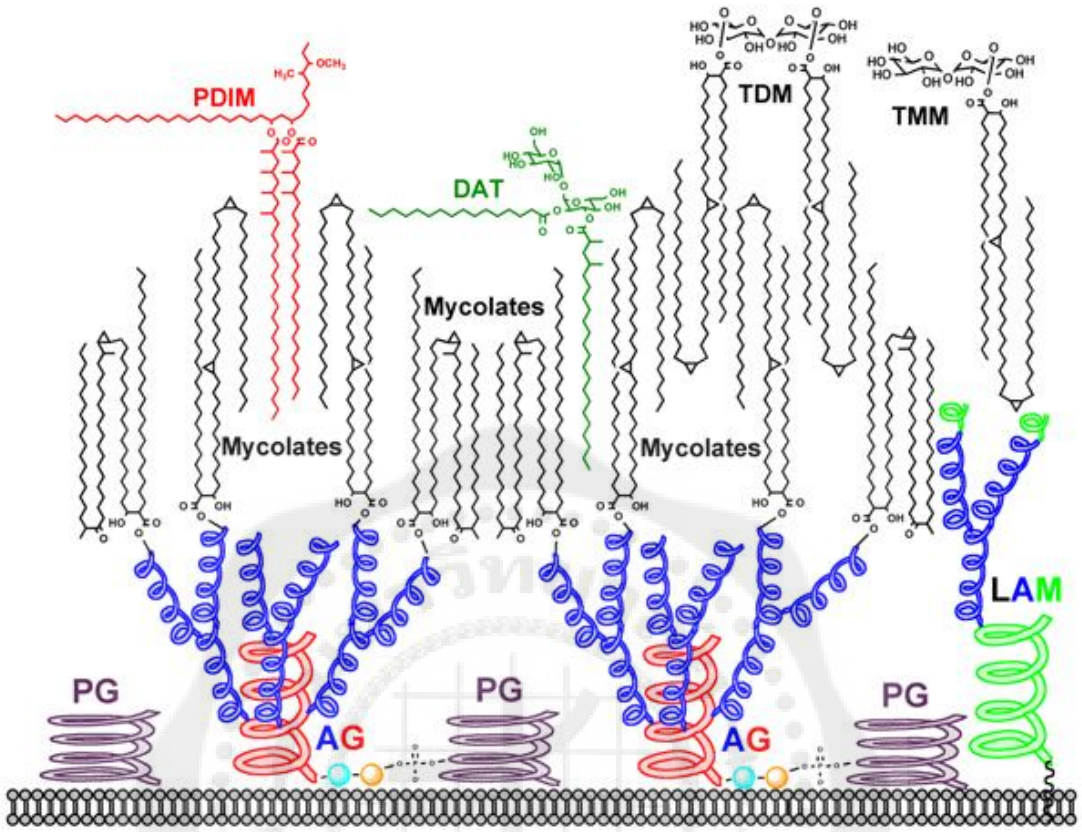

Figure 8 The mycobacterial cell wall (School of Bioscience. 2011: Online)

The emergence of strains of *M. tuberculosis* resistant to existent drugs has focused attention on the urgent need for discovery and development of new antimycobacterial agent.

3. Herpes simplex

3.1 Herpes virus: etiology and infection

The herpes simplex virus (HSV) is a double-strained DNA virus with an enveloped, icosahedral capsid (Figure 9). Herpes simplex is divided into two types: HSV type 1 (HSV-1) and HSV type 2 (HSV-2). HSV-1 primarily causes mouth, throat, face, eyes, and central nervous system infections, while HSV-2 primarily causes anogenital infections. However, each may cause infections in all areas (Chayavichitsilp; et al. 2009: 119). Herpes

simplex is most easily transmitted by direct contact with a lesion or the body fluid of an infected individual. Common infection of the skin or mucosa may affect the face and mouth (orofacial herpes), genitalia (genital herpes), or hands (herpes whitlow). More serious disorders occur when the virus infects and damages the eye (herpes keratitis), or spread to the central nervous system, damaging the brain (herpes encephalitis). The patients with immature or suppressed immune systems, such as newborns, transplant recipients, or AIDS are prone to severe complications from HSV infections (Dickerson; et al. 2003: 588).

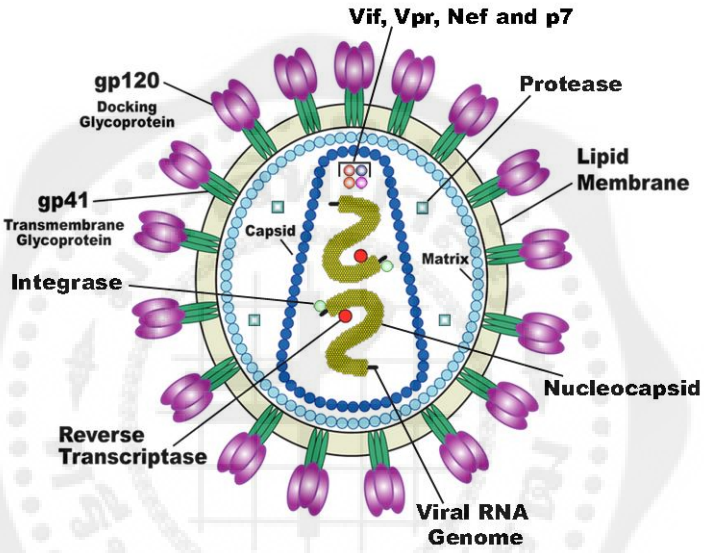

Figure 9 Icosahedrol capsid structure of herpes virus (Wikivisual. 2011: Online)

3.2 Chemotherapy of herpes simplex virus infections

Infection due to herpes viruses in humans have not proven amenable to control by immunization. Treatment usually involves general-purpose antiviral drugs for reducing the infection. Reducing the viral load can reduce the physical severity of outbreak-associated lesions and the number of infected cells shed by the body, thus lowering the chance of transmission to others. The antiviral drugs that are most commonly used are acyclovir (**75**) and penciclovir (**76**) (Figure 10). However, their increased and prolonged use has led to the emergence of a resistant virus (Bacon; et al. 2003: 114).

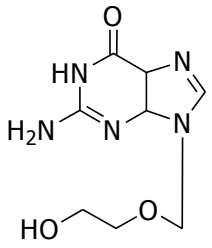

acyclovir (**75**)

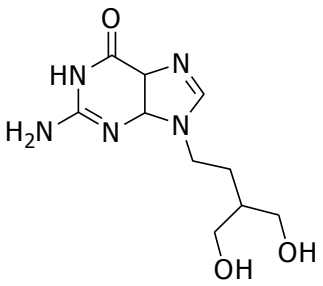

penciclovir (**76**)

Figure 10 Antiviral drugs: acyclovir (**75**) and penciclovir (**76**)

4. Angiogenesis and cancer therapy

Cancer is the most common cause of disease-related mortality in both men and women in the world. Despite initial responses to aggressive treatments the majority of patients will die as a result of their disease. Cancer development is a multistep process that requires genetic alterations to transform normal cell into tumor cells. Tumors can either be benign or malignant (Hanahan; et al. 2000: 57). In 2000, Hanahan and Weinberg suggested that a cell must acquire six traits to become malignant that were (a) self-sufficiency in growth signals, (b) insensitivity to growth-inhibitory (anti-growth) signal, (c) evasion of programmed cell death (apoptosis), (d) limitless replicative potential, (e) sustained angiogenesis, and (f) tissue invasion and metastasis (Hanahan; et al. 2000: 57). Each of these changes represents a potential target for cancer therapy since all of them are necessary for the progression of the disease. This has led to the search for more effective therapeutic strategies. One such strategy involves the ability of tumor to form new blood vessels (angiogenesis) which plays a pivotal role in tumor growth, invasion and metastasis.

4.1 Definition and the process of angiogenesis

Angiogenesis is the process of sprouting of capillaries from preexisting blood vessels, controlled by certain chemicals produced in the body. Some chemicals stimulate cells to repair damaged blood vessels or form new ones. It is the basic of several physiogical process, such as embryonic development, and placenta formation. Angiogenesis also occurs in adults, for example during the female reproduction cycle, repair

and regeneration of tissues and wound healing. After a primitive vascular formation in embryo, the blood vessels will start to remodel, undergo proliferation and regression, and branch and migrate into different regions of the embryo, the mechanism know as angiogenesis. The molecular characteristics of angiogenesis occur in stepwise progress (Figure 11). Sprouting angiogenesis is induced by hypoxia. The vessel starts to dilate in response to nitric oxide and become leaky in respond to vascular endothelial growth factor (VEGF). Pericytes are then removed from the branching vessel and the endothelial cells (EC) basement membrane and extracellular matrix (ECM) are degraded by specific enzyme such as matrix metalloproteinase (MMPs) (Figure 11B).

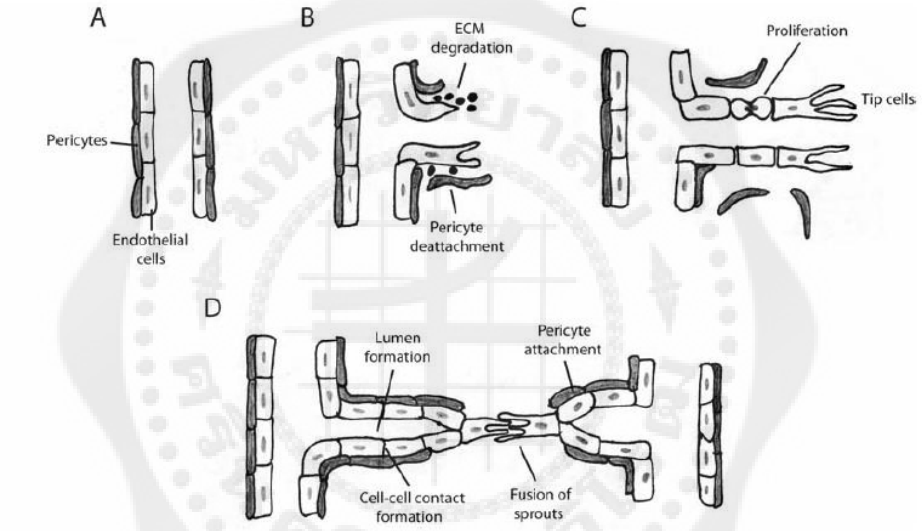

Figure 11 The steps involved sprouting angiogenesis (Ernkvist. 2008: 4)

The ECs was then started to sprout from the existing vessel, i.e. migrate and proliferate in response to VEGF and other endothelial cell mitogens until sufficient division have occurred (Figure 11C). The tip cells, non-proliferative, moves as a single cell in front of the stalk cells and, in contrast to the stalk cells. The tip cells were arrested and formed a tube-like structure after the ECs have reached their target (Figure 11D). The newly formed sprouts then anastomose to form vascular loops and networks (Bergers; et al. 2003: 401).

4.2 Vascular effectors for angiogenesis

The angiogenesis process is highly complex and dynamic process that is regulated by a number of growth factors. The essential factor for this process were ephrins, FGFs, Notch ligands, PDGFs, TGF- β and VEGFs. One of the major pathways involved promoting embryonic as well as tumor angiogenesis is the vascular endothelial growth factor (VEGF) family of proteins and receptors. In mammals, the VEGF consists of five members, VEGF-A, VEGF-B, VEGF-C, VEGF-D, and placenta growth factor (PlGF) (Figure 12). VEGF was originally discovered by its ability to induce permeability. The increase in permeability in tumors results in the leakage of several plasma proteins. VEGF act as a chemo attractant for ECs, which indicate that it plays a role in migration and invasion. It induces cell migration by activating factors such as focal adhesion kinase (FAK) and paxillin, leading to focal adhesion turnover and actin filament organization. VEGF also induces a variety of enzymes and proteins important in the degrading of the basement membrane, and helping the ECs to migrate and invade. VEGF appears to play a critical role in tumorigenesis and are therefore logical targets for novel anti-cancer therapies (Olsson; et al. 2006: 359).

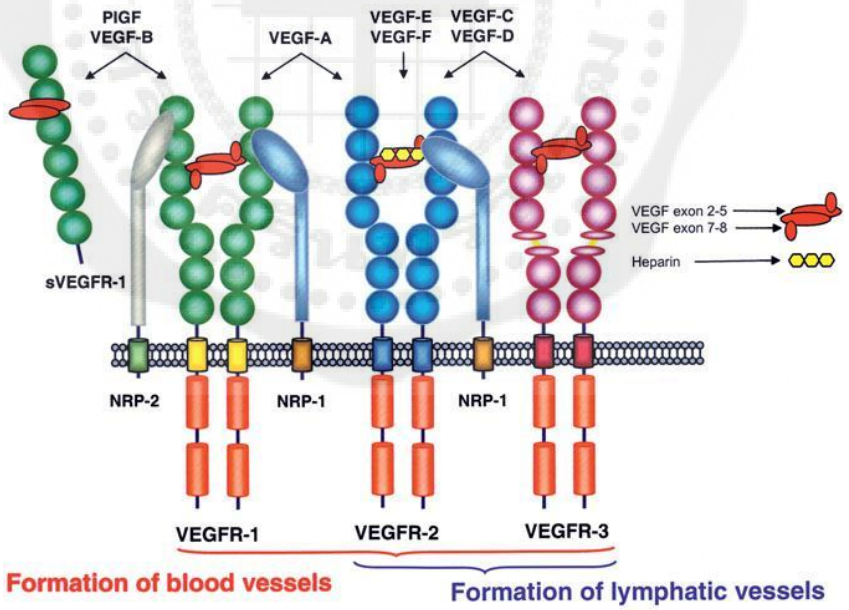

Figure 12 Member of VEGF in mammals (Rosenthallab. 2011: Online)

4.3 Angiogenesis inhibitors and cancer treatment

4.3.1 Inhibitor of angiogenesis as anti-cancer agents

Angiogenesis plays an more important role in the growth and spread of cancer. New blood vessels " feed " the cancer cell with oxygen and nutrients, allowing these cells to grow, invade nearby tissue, spread to other parts of the body, and form the new colonies of cancer cells. Because of cancer cannot grow or spread without the formation of new blood vessels, scientists are trying to find ways to stop angiogenesis. To stop angiogenesis requires treatment with anti-angiogenic factors, or drugs which reduce the production of proangiogenic factors, prevent them binding to their receptors or block their actions. The angiogenesis inhibitor or anti-angiogenic agents are the molecule that can prevent or slow down the growth of cancer by blocking the formation of new blood vessels. Recently, both of natural and synthetic angiogenesis inhibitors were designed and synthesized. Some angiogenesis inhibitors currently being used as drug for human cancer treatment such as thalidomide (**77**), squalamine (**78**), celecoxib (**79**), ZD6126 (**80**), and BMS 275291 (**81**) (Figure 13) for use with other drugs to treat lung cancer in clinical trial (Sridher; et al. 2003: 581).

4.3.2 Oxindole angiogenesis inhibitors

3-Alkenyl oxindoles are present in many compounds of angiogenesis inhibitor such as semaxanib (SU-5416, **82**), sunitinib (SU-11248, **83**), SU-9516 (**84**) and SU-6668 (**85**) (Figure 14). The structure of these angiogenic agents has an exocyclic alkenyl group and is capable of showing Z-E isomerism. In the solid state these compounds exists as the Z isomer, which is the stable form of this isomer. Among them, SU-5416 (**82**) is much current interest in the use in cancer therapy due to it is a potent and more selective inhibitor of the Flk-1/KDR receptor tyrosine kinase for the VEGF. Semaxanib (SU5416, **82**), the first in its class of anti-angiogenic agents, is small synthetic organic molecule that inhibits the growth of solid tumors by preventing the formation of blood vessels. SU-5416 (**82**) is a tyrosine kinase inhibitor best known as an inhibitor of the vascular endothelial growth factor receptor (VEGFR-2; Flk-1/KDR) and a suppressor of tumor vascularization, preventing the growth of multiple tumor types. In addition to inhibiting VEGFR-2 (IC_{50} = 1 μM), **82** also inhibits PDGFR (IC_{50} = 20 μM), c-Kit (IC_{50} = 30 nM), RET (IC_{50} = 170 nM), Flt-3 (IC_{50} = 160 nM), ABL (IC_{50} = 11 μ M), and ALK (IC_{50} = 1.2 μM). SU 5416 does not inhibit epidermal growth factor or fibroblast growth factor receptor

tyrosine kinases (IC_{50} > 100 μM) (Fong; et al. 1999: 99, Mologni; et al. 2006: 199, Litz; et al. 2004: 283). The structure of SU-5416 (**82**) is given in Figure 14.

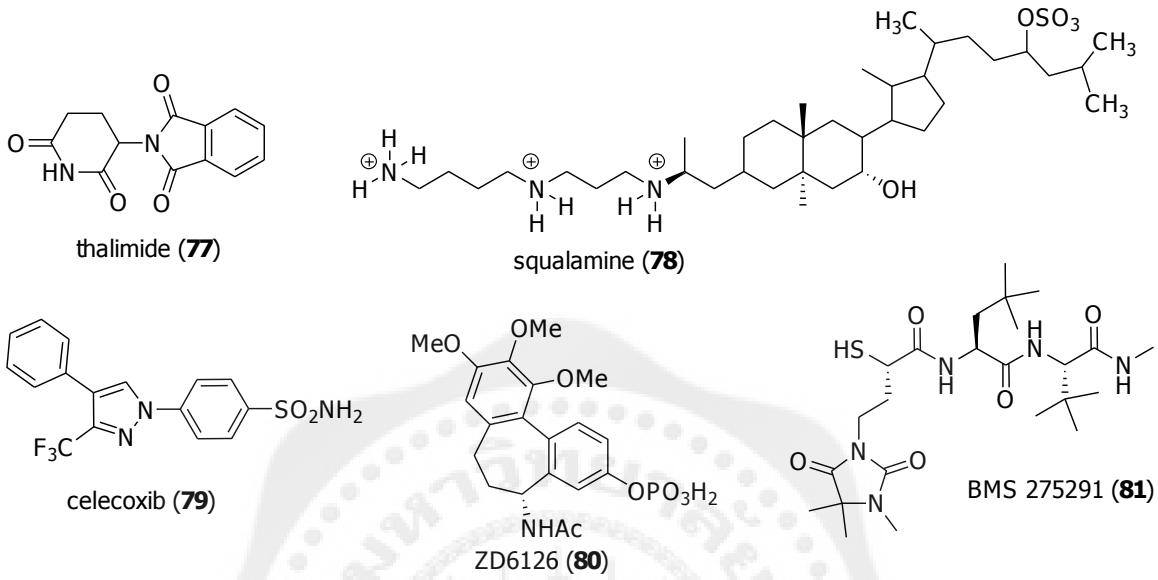

Figure 13 Some anti-angiogenic agents using for cancer treatment

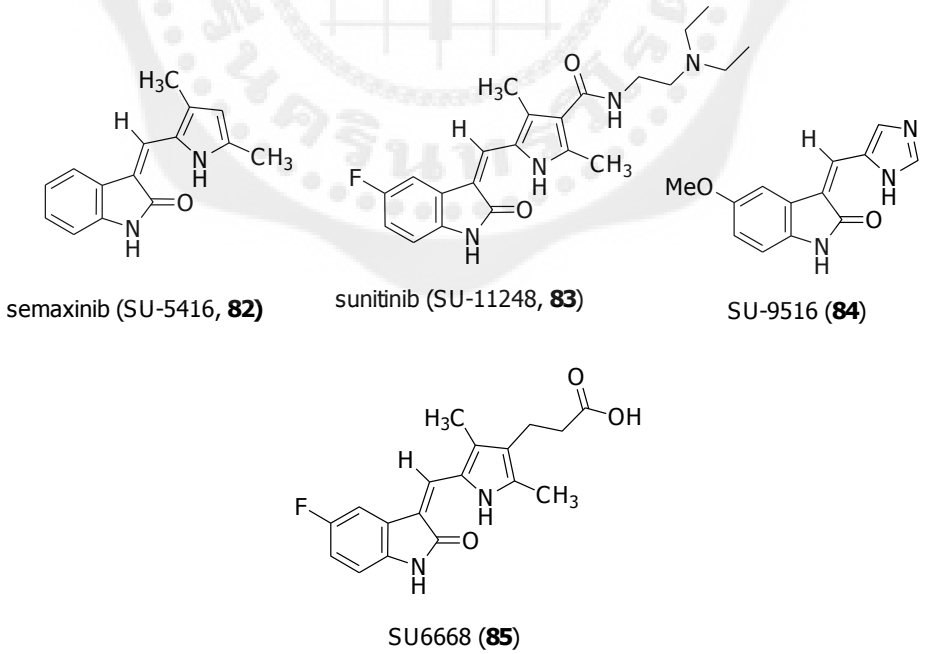

Figure 14 Oxindole angiogenic VEGF-mediated agents

Objectives of the study

With the natural abundance and broad range of activities of α-mangostin (**1**), this work focuses on the value added of natural product with increasing biological activities. Moreover, the approach for the facile and convenient synthesis of potent antiangiogenic agent SU-5416 (**82**) is urgently needed. Thus, the principal aims of this project are

1. To synthesize the structural analogues of the bioactive α-mangostin (**1**) with structural modification strategies

2. To examine anti-mycobacterial and anti-viral activities of the synthetic derivatives of **1**

3. To examine the structure activity relationship of the synthetic derivatives comparing with parent α-mangostin (**1**)

4. To develop the synthetic strategies for semaxanib (SU-5416, **82**)

Scopes of the study

1. The starting α-mangostin (**1**) was obtained from the isolation of dried fruit hull of *G. mangostana*

2. Structural modification strategies were employed with derivatization of 3-OH, 6-OH and both of prenyl groups at C-2 and C-8 by using simple chemical reactions such as alkylation, acylation, and catalytic hydrogenation

3. The synthetic analogues have been examined for some significant bioasays such as anti-tuberculosis or anti-Herpes simplex virus type 1 (HSV-1)

4. The developed Aldol-type condensation reaction was used for the synthesis of SU-5416 (**82**)

CHAPTER 2

REVIEW OF THE LITERATURE

1. Previous research on the synthesis of mangostin analogues and their biological activities

In 1979, Pai et al. synthesized mangostin-3,6-di-*O*-glucoside (**88**) and evaluated its pharmacological properties. They used α-mangostin (**1**) which was isolated from the fruit hull of *G. mangostana* (collected in Madras, India) as the starting compound. The mangostin-3,6-di-*O*-glucoside (**88**) was obtained from the *O*-alkylation reaction of **1** with α-bromoacetoglucose (**86**) followed by the hydrolysis of the diglucoside octa-acetate (**87**) by shaking with sodium methoxide in methanol (Figure 15).

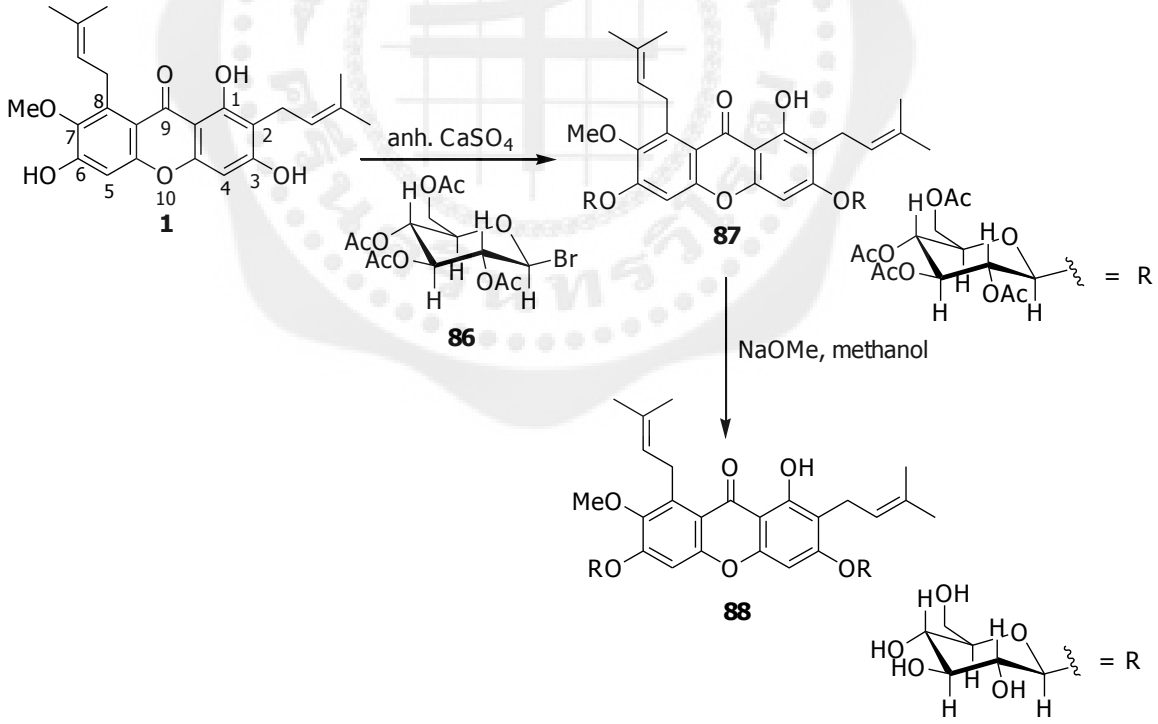

Figure 15 Synthesis of mangostin-3,6-*O*-diglucoside (**88**)

The pharmacological on the gross behavioral pattern in Swiss albino mice (20-30 g) and Wistar albino rats (100-150 g) of either sex of compound **88** was studied using modified S.M.A. counter to record spontaneous motor activity of animals. The effect of **88** on the spontaneous motor activity of mice was also compared with standard CNS depressants and CNS stimulants such as chloropromazine (5 mg/kg i.p.) and α - amphetamine (5 mg/kg i.p) and recorded on a smoked drum. The drug was administered to group of 5 mice each in doses of 50, 100, 200, and 300 mg/kg i.p. followed by gross behavioral recording at 15, 30, 60 and 120 minutes after drug administration. The result showed that, **88** produced definite signs of CNS depression in the gross behavioral investigation only at the does of 100 mg/kg i.p. and above. In addition, the pentobarbital sleeping time of the albino rats was studied. Compound **88** (100 mg/kg i.p) showed significant effect of the pentobarbital sleeping time. Rats pretreated with **88** slept for 119.2 $\pm$ 3.11 minutes as compared to 79.3 $\pm$ 3.19 minutes sleeping time in control groups (the gum acacia treated rats). The result suggested that, the percentage of the sleeping time of rats was increased in 53.81% after administration of **88** (Pai; et al. 1979: 361).

In 1996, Iinuma et al. reported the anti-MRSA activity of xanthones from Guttiferaeous plants. These xanthones showed intense antibacterial activity against both of MRSA and MSSA in the *in vitro* experiment. In addition, compound **1** and rubraxanthone (**89**) were converted to their hydrogenated derivatives, terahydromangostin (**90**) and octahydrorubraxanthone (**91**), respectively by catalytic hydrogenation reaction (figure 16). The anti-MRSA activity of **90** and **91** were evaluated, the activity was reduced, especially for **91** (Table 1). It was considered that double bounds on the alkyl chains are essential to the activity of a 1,3,6-trihydroxy-7-methoxyxanthone derivatives (Iinuma; et al. 1996: 861).

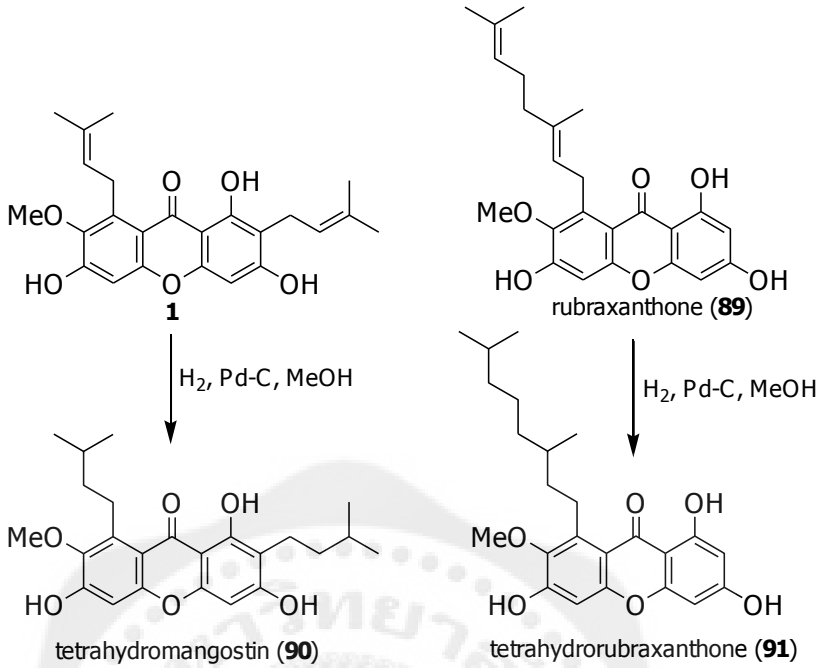

Figure 16 Catalytic hydrogenation of **1** and **89** to produce hydrogenated derivatives **90** and **91**

TABLE 1 Minimum inhibitory (μg/mL) against microorganism of compounds **1** and **89** and their hydrogenated derivatives **90** and **91**

Compound	MRSA strain			MSSA strain			*S. aureus* NIHJ 209p
	1-11	1-33	25-22	24-11	26-30	1-38	
1	6.25	1.57	12.50	3.13	1.57	6.25	1.57
89	12.50	12.50	0.80	12.50	3.13	3.13	0.313
90	12.5	12.5	0.80	12.5	3.13	3.13	1.57
91	>25.00	>25.00	12.50	>25.00	25.00	25.00	12.5

In 1997, Gopalakrisnan et al. reported the synthesis of di-*O*-alkylmangostin derivatives (**92-98**) and di-*O*-acetylmangostin (**99**) and their antifungal activities (Fgure 17). The mangostin derivatives **92-99** were tested for their antifungal activity against three phytopathogenic fungi, *Fusarium oxysporum vasinfectum*, *Alternaria tenuis*, and *Dreschlera oryzae*. These three fungi were selected because they are phytopathogens for agricultural importance. The results showed that, alkylating the C-3 and C-6 hydroxyls in **1** decrease the antifungal activity considerably by about half for methyl substitution, and replacement with alkyl groups of increasing chain length correlates with decreasing inhibitory activity. The results could be summarized that the free hydroxyls are important for optimal antifungal activity (Gopalakrisnan; et al. 1997: 519).

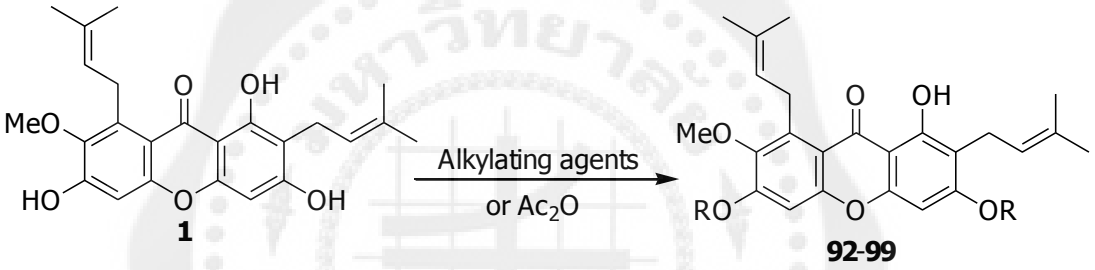

Reagent	Compound	R
Methyl iodide	**92**	CH_3
Diethylsulfate	**93**	CH_2CH_3
n-Propyl bromide	**94**	$CH_2CH_2CH_3$
n-Butyl iodide	**95**	$(CH_2)_3CH_3$
Isopropyl bromide	**96**	$CH(CH_3)_2$
Allyl bromide	**97**	$CH_2CH=CH_2$
Methallyl chloride	**98**	$CH_2C(CH_3)=CH_2$
Acetic anhydride	**99**	$COCH_3$

Figure 17 Synthesis of di-*O*-alkylmangostin derivatives (**92-98**) and di-*O*-acetylmangostin (**99**)

In 2006, Mahabusarakam et al. synthesized the derivatizatives of **1** to produce potential antiplasmodial substances. The mangostin analogues were conducted by functionalization of the reactive phenolic hydroxyl groups (3-OH and 6-OH) with acethylation and alkylation reaction. α-Mangostin (**1**) and its derivatives (**92**, **100**-**118**) were tested *in vitro* against *P. falciparum* strain k1 (chloroquine- and pyrimethamine-resistant). The activity of each compound was determined as the concentration required to inhibit malaria parasite growth by 50% (IC_{50}), and the results are shown in Table 2. The results showed that, analogues with a methoxyl group (compound **92)**, acyl group (compound **100**), and alkylcyano group (compounds **108** and **109**) at one or both hydroxyl groups showed a decrease in activity (IC_{50} > 17.00 μM). The derivatives containing two hydroxyl group (compounds **103** and **104**) did not have enhanced activity, whereas a mono substituted of dihydroxypropyl derivative (**94**) increased the activity (IC_{50} = 7.40 μM). The carbamide derivative (**97**) exhibited significant activity (IC_{50} 4.50 μM). The most potent antiplasmodial activity against *P. falciparum* were the alkylamine analogues (compounds **110**-**118**). In addition, some ammonium hydrochloride salt derivatives were also prepared to increase solubility and affinity with the heme carboxylate side chain of the plasmodial cells. Some amine compounds (**110**-**113**) were converted to their ammonium salts (**119**-**122**) by treating with hydrochloric acid in methanol. The ammonium derivatives **119**-**122** were also tested for antiplasmodial activity against *P. falciparum* strain k1. The comparison of IC_{50} of antiplasmodial activity of ammonium salts with the parent amine are shown in Table 3. The data showed that increasing the solubility of amine with ammonium salt formation did not significantly enhance antiplasmodial activity (Mahabusarakam; et al. 2006: 912).

TABLE 2 *In vitro* activity of α-mangostin (**1**) and its derivatives against *P. falciparum*

Compound	Substituent	IC_{50} (μM), Mean ± SD
	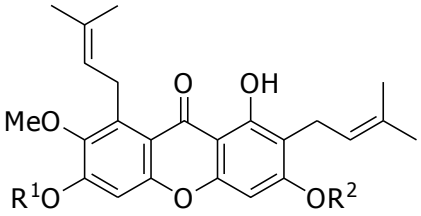	
1	$R^1 = R^2 = H$	17.00 ± 1.00
92	$R^1 = R^2 = CH_3$	> 20.00
100	$R^1 = H$, $R^2 = COCH_3$	> 20.00
101	$R^1 = CH_2CH_2CH_2OH$, $R^2 = H$	5.30 ±0.30
102	$R^1 = H$, $R^2 = CH_2CHOHCH_2OH$	7.40 ± 0.30
103	$R^1 = CH_2CHOHCH_2OH$, $R^2 = H$	16.00 ± 1.00
104	$R^1 = R^2 = CH_2CHOHCH_2OH$	> 18.00
105	$R^1 = H$, $R^2 = CH_2CONH_2$	4.50 ± 0.30
106	$R^1 = R^2 = CH_2CH(O)CH_2$	6.10 ± 0.30
107	$R^1 = CH_2CH(O)CH_2$, $R^2 = H$	13.00± 1.00
108	$R^1 = R^2 = CH_2CH_2CH_2C\equiv N$	18.00± 1.00
109	$R^1 = R^2 = CH_2CH_2CH_2C\equiv N$, $R^2 = H$	21.00 ± 2.00
110	$R^1 = CH_2CH_2N(CH_2CH_3)_2$, $R^2 = H$	0.30 ± 0.02
111	$R^1 = R^2 = CH_2CH_2N(CH_2CH_3)_2$	1.50 ± 0.10
112	$R^1 = CH_2CH_2N(CH_3)_2$, $R^2 = H$	0.60 ± 0.03
113	$R^1 = CH_2CH_2CH_2N(CH_3)_2$, $R^2 = H$	0.10 ± 0.01
114	$R^1 = CH_2CH(OH)CH_2N(CH_2CH_3)_2$, $R^2 = H$	0.05 ± 0.005
115	$R^1 = CH_2CH(OH)CH_2N(CH_3)_2$, $R^2 = H$	0.60 ± 0.03
116	$R^1 = R^2 = CH_2CH(OH)CH_2N(CH_3)_2$	0.60 ± 0.03
117	$R^1 = CH_2CH(OH)CH_2NHCH(CH_3)_2$, $R^2 = H$	0.60 ± 0.03
118	$R^1 = R^2 = CH_2CH(OH)CH_2NHCH(CH_3)_2$	0.70 ± 0.03

TABLE 3 *In vitro* activity of ammonium salt mangostin derivatives against *P. fasiparum* compared with their parent amine compounds

Compound	IC_{50}	Compound	IC_{50} [a]
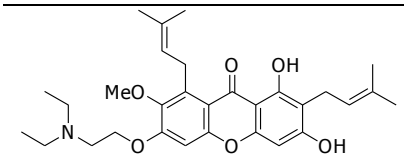 **110**	0.30 ± 0.02	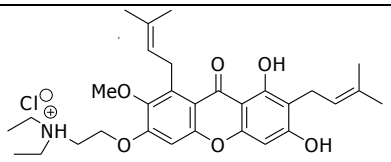 **119**	0.75 ± 0.03
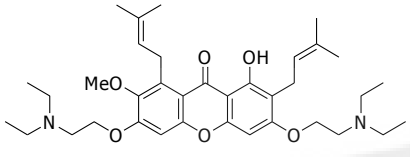 **111**	1.50 ± 0.10	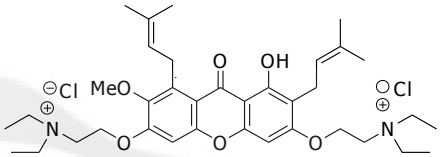 **120**	0.50 ± 0.02
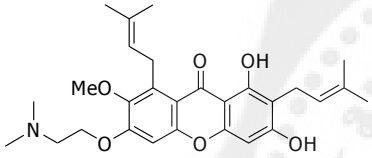 **112**	0.60 ± 0.03	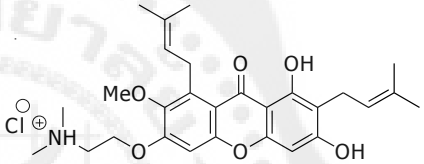 **121**	2.5 ± 0.10
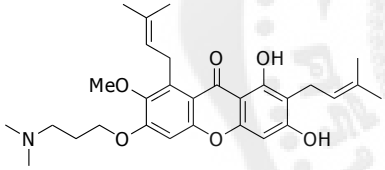 **113**	0.10 ± 0.01	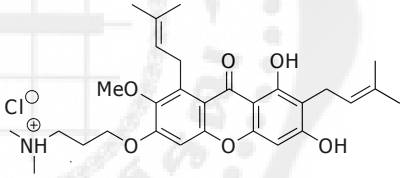 **122**	0.75 ± 0.03

[a] (μM), Mean ± SD

The research group of Ha prepared some derivatives of α-mangostin (**1**) by *O*-alkylation reaction of the reactive hydroxyl groups at C-3 and C-6. All derivatives were examined for cytotoxicity against MCF-7 (human breast cancer cells) and DLD-1 (human colon cancer cells). They summarized that α-mangostin (**1**) was the most active compound, the mono-*O*-allylmangostin (**128**) lead to more active than the di-*O*-alkylated compounds. These observations indicated that the hydroxyl groups at C-3 and C-6 are crucial for the cytotoxic activity (Ha; et al. 2009: 830).

TABLE 4 Cell proliferation inhibitory effects of mangostin derivatives (**92**, **95** and **123-128**)

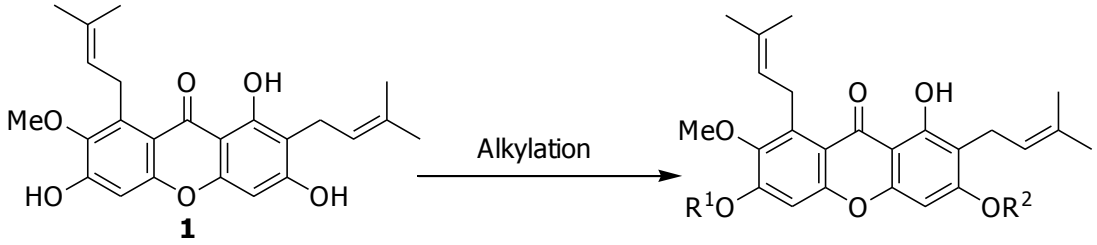

compound	R^1	R^2	Inhibition of cell proliferation[a]	
			48 h	72 h
1	H	H	87.1 ± 1.0	96.7 ± 0.4
92	CH_3	CH_3	22.2 ± 2.0[b)]	8.9 ± 0.7
95	$(CH_2)_3CH_3$	$(CH_2)_3CH_3$	18.7 ± 3.5	20.1 ± 2.3
123	$CH_2CH=C(CH_3)_2$	$CH_2CH=C(CH_3)_2$	27.4 ± 6.1	14.5 ± 1.4
124	$CH_2C_6H_4OCH_3$	$CH_2C_6H_4OCH_3$	23.6 ± 3.5	44.5 ± 4.5
125	$CH_2C_6H_5$	$CH_2C_6H_5$	12.3 ± 1.5	9.0 ± 2.2
126	$CH_2C_6H_4CH_3$	$CH_2C_6H_4CH_3$	4.4 ± 2.8	3.8 ± 1.7
127	$(CH_2)_4CH_3$	$(CH_2)_4CH_3$	9.0 ± 2.5	24.7 ± 6.2
128	$CH_2CH=CH_2$	H	37.1 ± 2.8	66.3 ± 3.2

[a] The inhibition of cell proliferation was estimated in DLD-1 cell using the MTT assay

[b] The data presented are mean of three experiments ± S.D.

In addition, α -mangostin (**1**) was modified as halogenated derivatives and evaluation inhibitory activity on PDGF-induced human aortic smooth cells proliferation by Nishihama and colleagues. Treatment of **1** with NBS or NCS effected selective halogenation at C-4 position to yield **129** and **130**, respectively. Both of halogenated **129** and **130** were then methylated with methyl iodide treatment in mild basic condition to give 3,6-di-*O*-methyl-4-bromomangostin (**131**) and 3,6-di-*O*-methyl-4-chloromangostin (**132**) in moderate yields (Figure 18a). Moreover, **1** was converted to stable xanthone **133** via two-step procedure of methylation and catalytic hydrogenation. Compound **133** was then oxidized with *m*CPBA to occur hydroxylated **134** and benzopyran derivative (**135**) in low yield (Figure 18b). The inhibitory activities of natural **1**, along with **129-135** against PDGF-induced HASMC proliferation were examined by the [^{3}H] thymidine incorporation procedure. The biological assay revealed that halogenated **129-132** showed weak to moderate

activities, compound **134** and **135** produced by *m*CPBA oxidation exhibited remarkable inhibitory activities at a concentration of 1 μM. The most active analogue was **134** which showed inhibitory activity at testing concentration of 0.1 μM. The reason why the hydroxyl function of **134** improved higher inhibitory activity than the Br-function of **135** remains unclear (Nishihama; et al. 2009: 759).

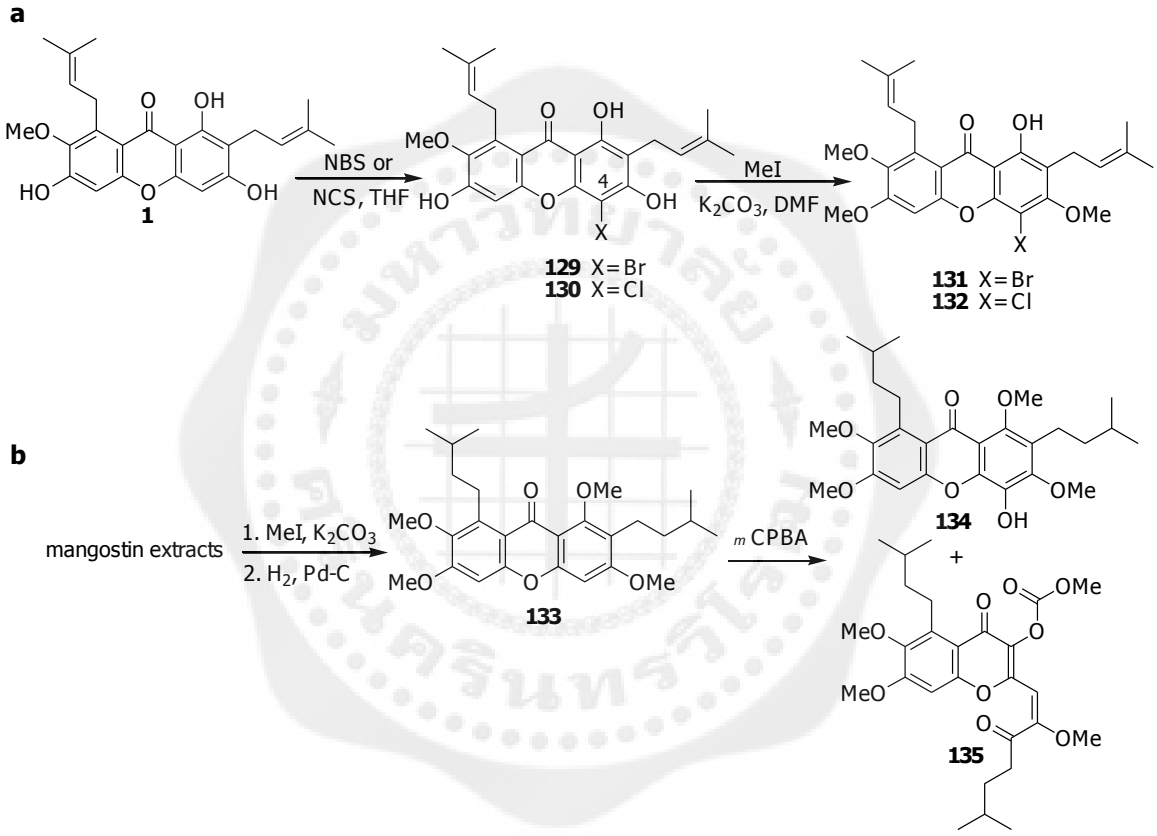

Figure 18 (a): Synthesis of halogenated mangostin derivatives (**129-132**), (b): oxidation of the mangostin derivative **133**

2. Previous research on the synthesis of semaxanib (SU-5416)

SU-5416 (**82**) has been synthesized from commercially available 3,5-dimethylpyrole-2-carboxaldehyde (**137**) by Knoevenagel condensation with indolin-2-one (**136**) in ethanol in the presence of piperidine (Sun; et al. 1998: 2588). Under the condensation reaction, compound **82** was obtained in 57% yield.

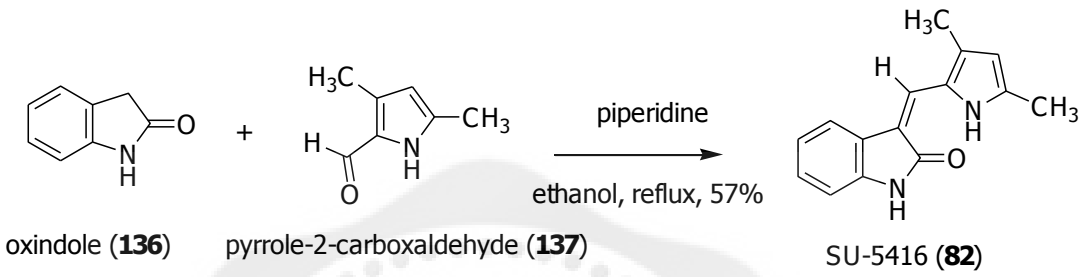

Figure 19 Synthesis of SU-5416 (**82**) under Knoevenagel condensation

Recently, SU-5416 was prepared from condensation of halophosphonate compound (**138** or **139**) by Tandem Horner-Wadsworth-Emmons/Heck procedure with **137** in the presence of tetrakis(triphenylphosephine)palladium as catalyst under microwave (Figure 20). The results indicated that iodophosphonate **139** often gave higher yields than the corresponding bromide **138** (Lubkoll; et al. 2010: 6606).

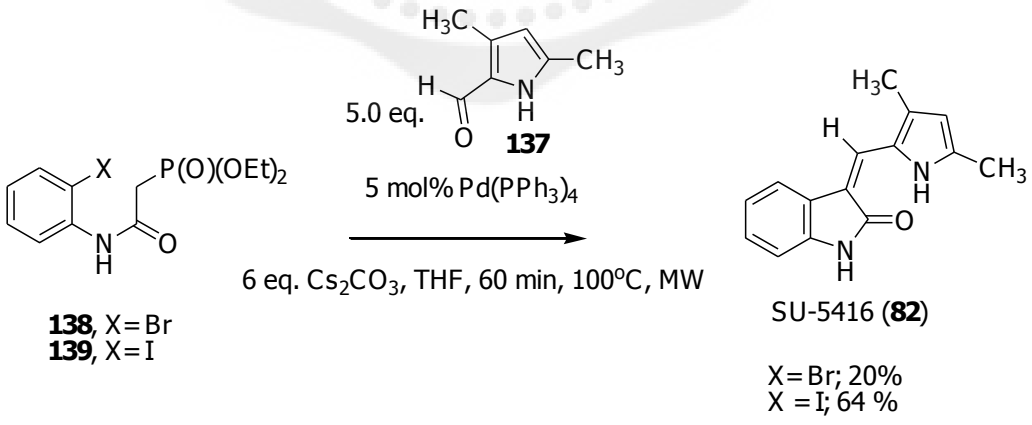

Figure 20 Synthesis of SU-5416 (**82**) by Tandem Horner-Wadsworth-Emmons/Heck procedure

CHAPTER 3

EXPERIMENTAL

General Techniques

1. Solvents and chemicals

The commercial grade organic solvents were distilled before used. All organic solvents employing in the reaction, were analytical grade, including anhydrous grade for dried condition. The term pet. spirit refers to petroleum spirit with boiling range 40-60^{o}C. The alkylating and acylating agents were analytical grade which were purchased from Fluka, Aldrich, and Acros Organic, Inc. Potassium hydride was supplied as a 30% dispersion in mineral oil. Solvent removal involved rotary evaporation under reduced pressure. α-Mangostin (**1**), the starting compound, was obtained from *Garcinia mangostana*.

2. Thin-Layer chromatography (TLC)

2.1 Adsorbent and detection

Qualitative thin-layer chromatography (TLC) was carried out on Macherey-Nagel aluminium sheets (Merck 1.05554), coated with a 1.25 mm layer of silica gel 60 F_{254} with a fluorescent indicator UV_{254}. After development, the plates were viewed under UV light at wavelengths 254 and 365 nm before being sprayed with anisaldehyde reagent or ammonium molybdate solution.

2.2 Anisaldehyde stain reagent

Thin-layer chromatograms were stained with an anisaldehyde solution mixed with 2.5% anisaldehyde, 3.4% sulphuric acid, 1.0% glacial acetic acid and absolute ethanol. The plates were subsequently heated with a hot plate at 100-120 ºC for 1-2 minutes in order to ensure the optimum development of color.

2.3 Ammonium molybdate solution

TLC detection for the synthesis of SU-5416, the TLC plates were developed with ammonium molybdate solution mixed with 5 g of $(NH_4)_6Mo_7O_{24}.4H_2O$ in 35 mL of semi-concentrated nitric acid and 65 mL water. The plates were subsequently heated with a hot plate at 60 ºC for 1-2 minutes.

3. Column chromatography (CC)

3.1. Adsorbent and packing

Silica gel 60 with particle size 0.040-0.063 mm (Merck 1.09375) and less than 0.063 mm (Merck 1.07729) were used throughout the experiments. Slurry packing was used as standard method.

3.2. Sample loading and elution

The sample will be dissolved in a small volume of suitable organic solvent. The solution will be mixed with silica gel particle size < 0.063 mm or 0.040-0.063 mm, depending on the type of silica gel in column. The sample solution will be evaporated under reduced pressure and added onto the top of column. After loading of sample onto the column, and appropriate solvent system will be used as a mobile phase in the isocratic or gradient systems.

4. Physical constants

Melting points were determined using a Griffin melting point apparatus. The temperature is given in degree Celsius.

5. Instrumentation

5.1. Infrared (IR) absorption spectra

IR spectra of sample in potassium bromide (KBr) pellets or film were recorded on Perkin Elmer FT-IR Spectrum BX spectrophotometer.

5.2. Nuclear magnetic resonance (NMR) spectra

^{1}H-NMR (300 MHz) and ^{13}C-NMR (75 MHz) spectra were recorded on a Bruker Avance 300 FT-NMR spectrometer (Department of Chemistry, Faculty of Science, Srinakharinwirot University). ^{1}H-NMR (500 MHz) and ^{13}C-NMR (126 MHz) spectra were recorded using a Varian Unity 500 Inova spectrometer (School of chemistry, University of Wollongong). ^{1}H-NMR and ^{13}C-NMR spectra were referenced to residual protonated solvent signals and deuterated solvent signals, respectively. Coupling constants were calculated in Hertz (Hz). The following abbreviation were used when describing the multiplicities of the peaks observed in the ^{1}H-NMR spectra : s (singlet), d (doublet), dt (doublet of triplets), t (triplet), q (quartet), m (multiplet), and br (broad). Proton and carbon assignments were derived from 2D NMR experiments including COSY, NOESY, HMQC, HSQC, and HMBC.

5.3. Mass Spectra

Electrospray ionization (ESI) mass spectra were obtained with a Finnigan LC-Q mass spectrometer (Department of chemistry, Faculty of Science, Rhamkhamhaeng University). Electrospray ionization-time-of-flight (ESI-TOF-MS) mass spectra (Bruker Daltonics GmbH, Bremen, Germany) were recorded with micrOTOF-Q II, an orthogonal acceleration quadrupole time-of-flight (Q-TOF) mass spectrometer equipped with electrospray interface (Archemica International Co, Ltd.). Fast atom bombardment (FAB) mass spectra were reccorded with a Finnigan MAT 90 mass spectrometer (Department of chemistry, Faculty of Science, Mahidol University).

6. Extraction of Plant Material and Purification of α-Mangostin (1)

The mangosteen fruit (*G mangostana*) was collected from Narathiwat province, South of Thailand. The fruit hull was left to air dry at room temperature. The dried fruit hull was mashed and extracted using ethyl acetate at room temperature. The plant material was removed by filtration and the solvent evaporated by using of rotary evaporator, to yield a brown solid of extract. The EtOAc extract (30.0 g) was subjected to isolate with quick column chromatography. The polarity of the solvent system was gradually increased during the progression of the column as follows: hexane, hexane-DCM, DCM, DCM-EtOAc, EtOAc, and EtOAc-MeOH. The column was finally washed with MeOH.

The fractions were collected *ca*. 100 mL. These were spotted on TLC plate which was eluted with hexane: acetone (1:2.5) solvent system and viewed under UV light followed by anisaldehyde reagent. The fractions were appropriately combined into five main fractions, namely 1 to 5. The fraction 2 which contained α-mangostin (**1**) as the major xanthone was further purified. Purification of fraction 2 (3.2 g) by column chromatography (silica gel, 0.040-0.063 mm) using a solvent system comprised of hexane, hexane-acetone (99:1 to 80:20) gave 9 subfractions. The subfractions 4 and 5 were the interesting fractions which contained **1** as the major xanthone when compared with authentic sample by TLC. These fractions were combined to obtain pure **1** (2.98 g, 10%). The isolated α-mangostin (**1**) was used as starting material for derivatization to produce various synthetic derivatives with the expected of novel bioactive compounds will be obtained.

α-mangostin (**1**) (**sss1556**)

Yellow solid, m.p. 177-178 º C (lit. m.p. 180-182 º C, Yate; et al. 1958: 1691)

IR (KBr) ν_{max} : 3421, 3268, 2925, 2963, 1645, 1609, 1580, 1465, 1281, 1185, 1077, 1050, 984, 849 and 1119 cm^{-1}.

^{1}H-NMR ($CDCl_3$, 300 MHz): δ_H 1.67 (s, 3H, H-14), 1.75 (s, 3H, H-19), 1.81 (s, 6H, H-15, H-20), 3.43 (d, 2H, *J*= 6.6 Hz, H-11), 3.78 (s, 3H, 7-OCH_3), 4.07 (d, 2H, *J*= 5.4 Hz, H-16), 5.25 (m, 2H, H-12, H-17), 6.16 (s, 1H, OH), 6.27 (s, 1H, H-4), 6.31 (s, 1H, OH), 6.81 (s, 1H, H-5) and 13.76 (s, 1H, 1-OH).

^{13}C-NMR ($CDCl_3$, 75 MHz): δ_C 17.5 (C-14), 17.9 (C-19), 21.2 (C-11), 25.5 (C-15), 25.6 (C-20), 26.1 (C-16), 60.9 (7-OCH_3), 92.6 (C-4), 101.6 (C-5), 103.0 (C-9a), 109.9 (C-2), 111.4 (C-8a), 122.2 (C-12), 123.3 (C-17), 131.4 (C-13), 131.8 (C-18), 137.2 (C-8), 142.9 (C-7), 155.3 (C-10a), 155.6 (C-6), 155.7 (C-4a), 160.1 (C-1), 161.7 (C-3) and 181.8 (C-9).

7. General procedure for *O*-alkylated and *O*-acyated mangostin synthesis

Appropriate akylating agents (0.50 - 1.81 mmol) or acylating agents (0.05 - 1.43 mmol) was added to a solution of 0.05 - 0.50 mmole of α-mangostin (**1**) in analytical grade acetone or ethanol containing anhydrous potassium carbonate (0.26 - 0.71 mmol). For some reactions, dry pyridine or potassium hydroxide were used as base instead of potassium carbonate. The mixture was stirred for 3 - 168 h, and the reaction progress was monitored by TLC. The mixture was then poured into cold water, and was extracted with ethyl acetate (3x15 mL). The organic phase was washed with water, dried over anhydrous Na_2SO_4 and concentrated *in vacuo*. The crude product was purified by gradient column chromatography using *n*-hexane and ethyl acetate as the eluting solvent.

8. *O*-Alkylation and *O*-acylation of α -mangostin (1)

8.1 Methylation of α-mangostin (**1**)

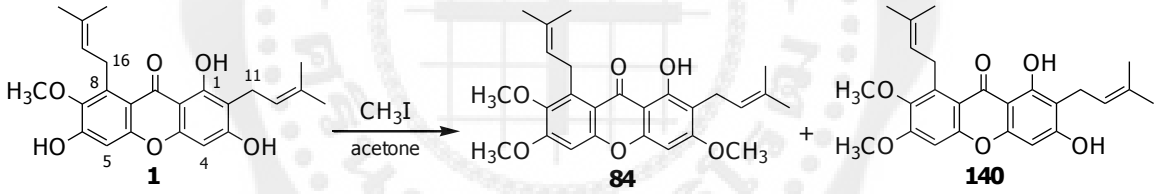

To a stirred solution of **1** (152.2 mg, 0.37 mmol) and K_2CO_3 (51.7 mg, 0.37 mmol) in acetone was added with iodomethane (200.2 mg, 1.41 mmol). The solution was left stirring at room temperature for 23 hours. The mixture was then poured into cold water, and was extracted with ethyl acetate (EtOAc) (3x15 mL). The combined ethyl acetate was washed with water, dried over anhydrous Na_2SO_4 and evaporated under reduced pressure to dryness. The product was purified by gradient column chromatography (silica gel < 0.0063 mm) using *n*-hexane to *n*-hexane: EtOAc (95:5) as eluting solvent to give 3,6-di-*O*-methylmangostin (**84**) (53.0 mg, 33%) and 6-mono-*O*-methylmangostin (**140**) (61.0 mg, 39%).

3,6-Di-*O*-methylmangostin (**84**) (**sss3564**)

Pale yellow solid, m.p. 93-95 ºC. (lit. m.p. 120-122 ºC, Gopalakrisnan; et al. 1997: 519, lit. m.p. 119-122 ºC, Ha; et al. 2009: 830).

R_f ($CHCl_3$): 0.61.

IR (KBr) ν_{max} : 3434, 2926, 1646, 1595, 1458, 1429, 1281, 1213, 1173 and 1119 cm^{-1}.

^{1}H-NMR ($CDCl_3$, 300 MHz): δ_H 1.67 (s, 6H, H-15, H-20), 1.79 (s, 3H, H-14), 1.84 (s, 3H, H-19), 3.34 (d, 2H, *J*= 6.9 Hz, H-11), 3.79 (s, 3H, 7-OCH_3), 3.89 (s, 3H, 3-OCH_3), 3.95 (s, 3H, 6-OCH_3), 4.12 (d, 2H, *J*= 6.3 Hz, H-16), 5.20 (br t, 1H, *J*= 6.9 Hz, H-12), 5.23 (br t, 1H, *J*= 6.3 Hz, H-17), 6.30 (s, 1H, H-4), 6.72 (s, 1H, H-5) and 13.48 (s, 1H, 1-OH).

^{13}C-NMR ($CDCl_3$, 75 MHz): δ_C 17.7 (C-14), 18.1 (C-19), 21.3 (C-11), 25.8 (C-15 and C-20), 26.1 (C-16), 55.7 (6-OCH_3), 55.9 (3-OCH_3), 60.9 (7-OCH_3), 88.6 (C-4), 98.1 (C-5), 103.7 (C-9a), 111.4 (C-2), 112.0 (C-8a), 122.3 (C-12), 123.2 (C-17), 131.7 (C-13 and C-18), 137.2 (C-8), 143.9 (C-7), 155.1 (C-4a and C-10a), 158.0 (C-6), 159.7 (C-1), 163.3 (C-3) and 181.9 (C-9).

ESMS (+ve) *m/z* (% rel. intensity): 439 $[M+H]^+$ (100).

6-Mono-*O*-methylmangostin (**140**) (**sss703**)

Pale yellow solid, m.p. 95-97 ºC. (lit. orange gum, Panthong; et al. 2006: 999).

R_f (CH_3Cl): 0.41.

IR (KBr) ν_{max} : 3412, 2915, 1649, 1610, 1462, 1382, 1278, 1213 and 1101 cm^{-1}.

^{1}H-NMR ($CDCl_3$, 300 MHz): δ_H 1.65 (s, 6H, H-15, H-20), 1.75 (s, 3H, H-15), 1.82 (s, 3H, H-14, H-19), 3.43 (d, 2H, *J*= 7.1 Hz, H-11), 3.77 (s, 3H, 7-OCH_3), 3.93 (s, 3H, 6-OCH_3), 4.10 (d, 2H, *J*= 6.4 Hz, H-16), 5.23 (m, 2H, H-12 and H-17), 6.22 (s, 1H, 3-OH), 6.26 (s, 1H, H-4), 6.72 (s, 1H, H-5) and 13.82 (s, 1H, 1-OH).

^{13}C-NMR ($CDCl_3$, 75 MHz): δ_C 17.8 (C-14), 18.1 (C-19), 21.4 (C-11), 25.8 (C-15 and C-20), 26.1 (C-16), 55.9 (6-OCH_3), 60.9 (7-OCH_3),

93.1 (C-4), 98.3 (C-5), 104.3 (C-9a), 108.4 (C-2), 111.9 (C-8a), 121.4 (C-12), 123.1 (C-17), 131.8 (C-18), 136.0 (C-13), 137.5 (C-8), 143.5 (C-7), 155.0 (C-4a), 155.4 (C-10a), 158.1 (C-6), 160.6 (C-1), 161.5 (C-3) and 182.0 (C-9).

ESMS (+ve) *m/z* (% rel. intensity): 447 $[M+Na]^+$ (100).

8.2 Ethylation of **1**

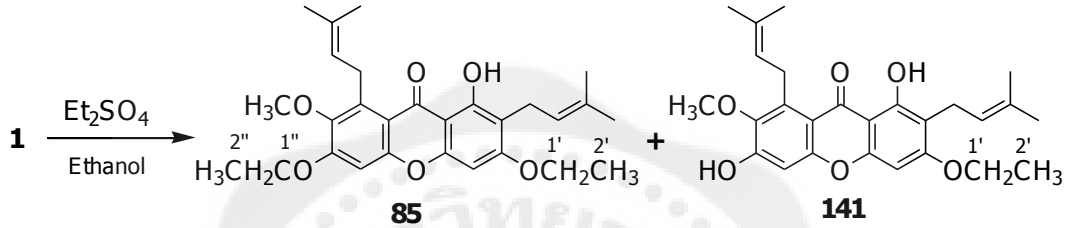

A solution of **1** (100.0 mg, 0.24 mmol) and potassium hydroxide (39.7 mg, 0.69 mmol, KOH in EtOH) in absolute ethanol was subjected to ethylation with diethyl sulphate (125.6 mg, 0.81 mmol). The mixture was stirred at room temperature for 4 hours and 30 minuts. The mixture was quenched with cold water followed by extraction with ethyl acetate (3x15 mL). The organic phase was combined, washed with water, dried over anhydrous Na_2SO_4 and concentrated *in vacuo* to dryness. The product was purified by gradient column chromatography (silica gel < 0.0063 mm) using *n*-hexane to *n*-hexane: EtOAc (95:5) as eluting solvent to give 3,6-di-*O*-ethylmangostin (**85**) (38.0 mg, 24%) and 3-mono-*O*-ethylmangostin (**141**) (7.0 mg, 6%).

3,6-Di-*O*-ethylmangostin (**85**) (**sss723**)

Pale yellow solid, m.p. 96-98 ºC. (lit. m.p. 112-114 ºC, Gopalakrisnan; et al. 1997: 519).

R_f ($CHCl_3$): 0.63.

IR (KBr) ν_{max} : 3448, 2918, 1642, 1596, 1467, 1433, 1387, 1279, 1204 and 1121 cm^{-1}.

^{1}H-NMR ($CDCl_3$, 300 MHz): δ_H 1.47 (br t, 3H, *J*= 7.0 Hz, H-2"), 1.53 (br t, 3H, *J*= 6.9 Hz, H-2'), 1.66 (s, 3H, H-15), 1.68 (s, 3H, H-20), 1.78 (s, 3H, H-14,), 1.82 (s, 3H, H-19), 3.36 (d, 2H, *J*= 7.1 Hz, H-11), 3.80 (s, 3H, 7-OCH_3), 4.12 (m, 6H, H-16, H-1', H-1"), 5.23 (br s, 1H, H-

12), 5.25 (br s, 1H, H-17), 6.27 (s, 1H, H-4), 6.69 (s, 1H, H-5) and 13.49 (s, 1H, 1-OH).

^{1}H-NMR ($CDCl_3$): δ_H 1.45 (t, 6H, 2xCH_3), 1.60 (t, 6H, 2xCH_3), 1.8 (s, 6H, 2xCH_3), 3.18 (s, 2H, H-11), 3.72 (s, 3H, OCH_3), 4.03 (m, 6H, H-16, H-1'and H-1''), 5.09 (m, 2H, H-12 and H-17), 5.95 (1H, s, H-4), 6.35 (s, 1H, H-5) and 13.25 (s, 1H, 1-OH) (Gopalakrisnan; et al. 1997: 519).

ESMS (+ve) *m/z* (% rel. intensity): 489 $[M+Na]^+$ (100).

3-Mono-*O*-ethylmangostin (**141**) (**sss1091**)

Yellow viscous.

R_f ($CHCl_3$): 0.44.

IR (KBr) ν_{max}: 3409, 2922, 1643, 1598, 1464, 1426, 1372, 1279, 1200 and 1111 cm^{-1}.

^{1}H-NMR ($CDCl_3$, 300 MHz): δ_H 1.45 (br t, 3H, *J*= 6.9 Hz, H-2'), 1.68 (s, 6H, H-15, H-20), 1.80 (s, 3H, H-14), 1.83 (s, 3H, H-19), 1.82 (s, 3H, H-19), 3.34 (d, 2H, *J*= 7.2 Hz, H-11), 3.78 (s, 3H, 7-OCH_3), 4.12 (q, 2H, *J*= 6.9 Hz, H-1'), 4.13 (d, 2H, *J*= 6.8 Hz, H-16), 5.23 (br s, 1H, H-12), 5.23 (m, 2H, H-12, H-17), 6.29 (s, 1H, H-4), 6.80 (s, 1H, H-5) and 13.39 (s, 1H, 1-OH).

^{13}C-NMR ($CDCl_3$, 75 MHz): δ_C 14.6 (C-2'), 17.8 (C-14), 18.2 (C-19), 21.4 (C-11), 25.8 (C-15 and C-20), 26.5 (C-16), 62.0 (7-OCH_3), 64.1 (C-1'), 89.4 (C-4), 101.4 (C-5), 103.7 (C-9a), 111.5 (C-2), 112.4 (C-8a), 122.3 (C-12), 123.2 (C-17), 131.3 (C-13), 132.0 (C-18), 137.0 (C-8), 142.5 (C-7), 154.3 (C-6), 155.1 (C-4a), 155.7 (C-10a), 159.7 (C-3), 162.8 (C-1), and 181.9 (C-9).

HRFAB-MS (+ve) *m/z* 439.2120 $[M+H]^+$ (calcd. for $C_{26}H_{29}O_6$ + H, 439.2121).

8.3 Allylation of **1**

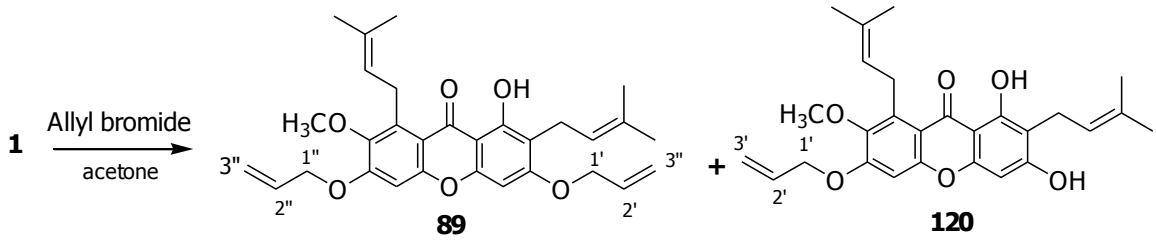

To a stirred solution of **1** (100.0 mg, 0.24 mmol) and K_2CO_3 (36.6 mg, 0.26 mmol) in acetone was added with allyl bromide (88.5 mg, 0.73 mmol). The solution was left stirring at room temperature for 52 hours. The mixture was then poured into cold water, and was extracted with ethyl acetate (EtOAc) (3x15 mL). The combined ethyl acetate was washed with water, dried over anhydrous Na_2SO_4 and evaporated under reduced pressure to dryness. The product was purified by gradient flash chromatography (silica gel < 0.0063 mm) using *n*-hexane to *n*-hexane: EtOAc (92:8) as eluting solvent to give 3,6-di-*O*-allylmangostin (**89**) (23.0 mg, 19%) and 6-mono-*O*-allylmangostin (**120**) (16.0 mg, 15%).

3,6-Di-*O*-allylmangostin (**89**) (**sss768**)

Yellow viscous. (lit. yellow solid, m.p. 78-80 ºC, Gopalakrisnan; et al. 1997: 519).

R_f (30% EtOAc: hexane): 0.46.

IR (KBr) ν_{max} : 3387, 2922, 1643, 1598, 1464, 1426, 1372, 1279, 1200, and 1111 cm^{-1}.

^{1}H-NMR ($CDCl_3$, 300 MHz): δ_H 1.65 (s, 6H, H-15, H-20), 1.77 (s, 3H, H-14), 1.82 (s, 3H, H-19), 3.38 (d, 2H, *J*= 7.0 Hz, H-11), 3.79 (s, 3H, 7-OCH_3), 4.09 (d, 2H, *J*= 7.3 Hz, H-16), 4.61 (d, 2H, *J*= 4.9 Hz, H-1'), 4.65 (d, 2H, *J*= 5.0 Hz, H-1''), 5.26 (m, 1H, H-12), 5.40 (m, 1H, H-17), 5.41 (m, 4H, H-3', H-3''), 6.08 (m, 2H, H-2', H-2''), 6.26 (s, 1H, H-4), 6.67 (s, 1H, H-5) and 13.47 (s, 1H, 1-OH).

^{13}C-NMR ($CDCl_3$, 75 MHz): δ_C 17.9 (C-14), 18.1 (C-19), 21.4 (C-11), 25.8 (C-15 and C-20), 26.1 (C-16), 60.8 (7-OCH_3), 69.0 (C-1'), 69.4 (C-1''), 89.5 (C-4), 99.2 (C-5), 104.0 (C-9a), 112.7 (C-2), 112.1 (C-8a), 117.7 (C-3'), 118.4 (C-3''), 122.3 (C-12), 123.2 (C-17), 131.5 (C-13),

131.7 (C-18), 131.9 (C-2'), 132.5 (C-2''), 137.4 (C-8), 144.1 (C-7), 155.0 (C-4a), 155.1 (C-10a), 156.8 (C-6), 159.9 (C-3), 162.2 (C-1) and 181.9 (C-9).

ESMS (+ve) *m/z* (% rel. intensity): 513 $[M+Na]^+$ (100).

6-Mono-*O*-allylmangostin (**120**) (**sss1287**)

Pale yellow solid, m.p. 82-84 ºC. (lit. yellow gum, Ha; et al. 2009: 830).

R_f (30% EtOAc: hexane): 0.22.

IR (KBr) ν_{max} : 3398, 2918, 1638, 1595, 1465, 1429, 1372, 1278, 1202, and 1116 cm^{-1}.

^{1}H-NMR ($CDCl_3$, 300 MHz): δ_H 1.60 (s, 3H, H-20), 1.74 (s, 3H, H-15), 1.82 (s, 6H, H-14, H-19), 3.43 (d, 2H, *J*= 7.2 Hz, H-11), 3.79 (s, 3H, 7-OCH_3), 4.09 (d, 2H, *J*= 7.1 Hz, H-16), 4.65 (d, 2H, *J*= 5.0 Hz, H-1'), 5.28 (m, 2H, H-12 and H-17), 5.33 (br d, 1H, *J*= 16.3 Hz, H-3′$_{trans}$), 5.46 (d, 1H, *J*= 11.4 Hz, H-3'$_{cis}$), 6.10 (m, 1H, H-2'), 6.26 (s, 1H, H-4), 6.28 (s, 1H, 3-OH), 6.70 (s, 1H, H-5) and 13.82 (s, 1H, 1-OH).

^{13}C-NMR ($CDCl_3$, 75 MHz): δ_C 17.9 (C-14), 18.1 (C-19), 21.4 (C-11), 25.8 (C-15 and C-20), 26.2 (C-16), 60.8 (7-OCH_3), 69.4 (C-1'), 93.1 (C-4), 97.9 (C-5), 103.7 (C-9a), 108.4 (C-2), 107.9 (C-8a), 118.4 (C-3'), 121.4 (C-12), 123.1 (C-17), 131.8 (C-13), 131.9 (C-2'), 135.6 (C-13), 137.4 (C-8 and C-18), 137.4 (C-8), 144.1 (C-7), 155.0 (C-4a), 155.2 (C-10a), 156.9 (C-6), 160.6 (C-3), 161.5 (C-1) and 182.0 (C-9).

HRFAB-MS (+ve) *m/z* 451.2120 $[M+H]^+$ (calcd. for $C_{27}H_{3o}O_6$ + H, 451.2118).

8.4 4-Bromobutylation of **1**

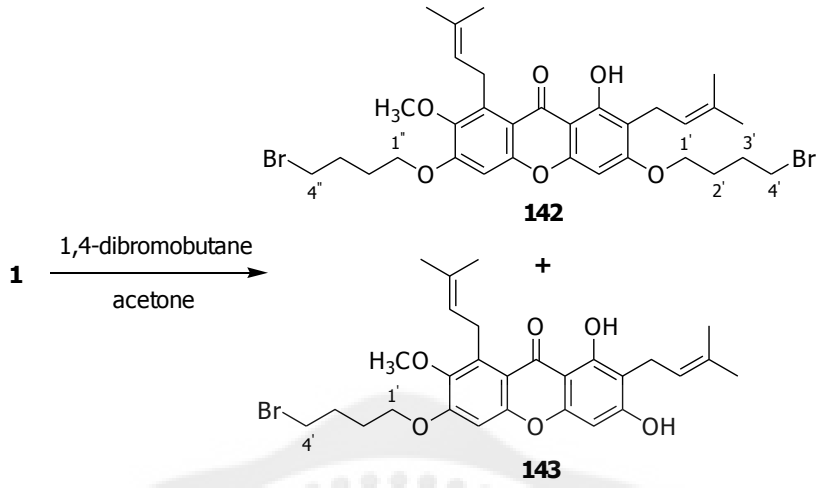

To a stirred solution of **1** (100.6 mg, 0.24 mmol) and K_2CO_3 (39.5 mg, 0.28 mmol) in acetone was added with 1,4-dibromobutane (106.5 mg, 0.50 mmol). The solution was left stirring at room temperature for 7 days. The mixture was then poured into cold water, and was extracted with ethyl acetate (EtOAc) (3x15 mL). The combined ethyl acetate was washed with water, dried over anhydrous Na_2SO_4 and evaporated under reduced pressure to dryness. The product was purified by gradient column chromatography (silica gel < 0.0063 mm) using *n*-hexane to *n*-hexane: EtOAc (92:8) as eluting solvent to give 3,6-di-*O*-(4-bromobutyl)mangostin (**142**) (52.0 mg, 31%) and 6-mono-*O*-(4-bromobutyl)mangostin (**143**) (22.0 mg, 16%).

3,6-Di-*O*-(4-bromobutyl)mangostin (**142**) (**sss1894**)

Yellow viscous.

R_f (30% EtOAc: hexane): 0.55.

IR (KBr) ν_{max} : 2927, 1642, 1597, 1497, 1469, 1279, 1205, 1113, 855, 821 and 787 cm^{-1}.

^{1}H-NMR ($CDCl_3$, 300 MHz): δ_H 1.66 (s, 6H, H-14, H-19), 1.77 (s, 3H, H-15), 1.82 (s, 3H, H-20), 2.08 (br s, 8H, H-2', H-2", H-3', H-3"), 3.33 (d, 2H, *J*= 6.3 Hz, H-11), 3.49 (br t, 4H, *J*= 6.3 Hz, H-4', H-4"), 3.79 (s, 3H, 7-OCH_3), 4.06 (br t, 4H, *J*= 5.4 Hz, H-1', H-1"), 4.10 (br s, 2H, H-16), 5.19 (br s, H-12), 5.21 (br s, 1H, H-17), 6.27 (s, 1H, H-4), 6.69 (s, 1H, H-5) and 13.47 (s, 1H, 1-OH).

^{13}C-NMR ($CDCl_3$, 75 MHz): δ_C 17.8 (C-14), 18.1 (C-19), 21.1 (C-11), 25.8 (C-20), 25.9 (C-15), 26.1 (C-16), 27.6 (C-3'), 27.7 (C-3''), 29.3 (C-2' and C-2''), 33.1 (C-4'), 33.2 (C-4''), 60.9 (6-OCH_3), 67.2 (C-1'), 67.8 (C-1''), 60.9 (7-OCH_3), 89.1 (C-4), 98.7 (C-5), 103.9 (C-9a), 111.5 (C-2), 112.1 (C-8a), 122.4 (C-12), 123.2 (C-17), 131.4 (C-13), 131.7 (C-18), 137.3 (C-8), 144.0 (C-7), 155.1 (C-4a), 155.2 (C-10a), 157.2 (C-6), 159.1 (C-1), 162.5 (C-3) and 181.9 (C-9).

ESMS (+ve) *m/z* (% rel. intensity): 679 $[M+H]^+$ (60).

6-Mono-*O*-(4-bromobutyl)mangostin (**143**) (**sss1895**)

Yellow viscous.

R_f (30% EtOAc: hexane): 0.40.

IR (KBr) ν_{max} : 3311, 2924, 1700, 1645, 1605, 1463, 1371, 1278, 1103, and 822 cm^{-1}.

^{1}H-NMR ($CDCl_3$, 300 MHz): δ_H 1.66 (s, 3H, H-19), 1.74 (s, 3H, H-14), 1.82 (s, 6H, H-15, H-20), 2.03 (m, 2H, H-3'), 2.08 (m, 2H, H-2'), 3.44 (d, 2H, *J*= 6.6 Hz, H-11), 3.51 (t, 2H, *J*= 6.3 Hz, H-4'), 3.77 (s, 3H, 7-OCH_3), 4.10 (br s, 4H, *J*= 5.4 Hz, H-1', H-16), 5.27 (br s, 1H, H-12), 6.29 (s, H-4), 6.69 (s, 1H, H-5), 6.71 (br s, 1H, H-17) and 13.79 (s, 1H, 1-OH).

^{13}C-NMR ($CDCl_3$, 75 MHz): δ_C 17.9 (C-14), 18.1 (C-19), 21.4 (C-11), 25.8 (C-15 and C-20), 26.2 (C-16), 27.6 (C-3'), 29.3 (C-2'), 33.0 (C-4'), 60.9 (6-OCH_3), 67.8 (C-1'), 60.9 (7-OCH_3), 93.1 (C-4), 98.8 (C-5), 104.0 (C-9a), 108.3 (C-2), 112.0 (C-8a), 121.4 (C-12), 123.1 (C-17), 131.8 (C-13), 135.9 (C-18), 137.3 (C-8), 144.0 (C-7), 155.3 (C-4a and C-10a), 157.0 (C-6), 160.6 (C-3), 161.5 (C-3) and 182.1 (C-9).

HR-FABMS (+ve) *m/z* 545.1513 $[M+H]^+$ (calcd. for $C_{28}H_{34}BrO_6$ + H, 545.1513).

8.5 Benzylation of **1**

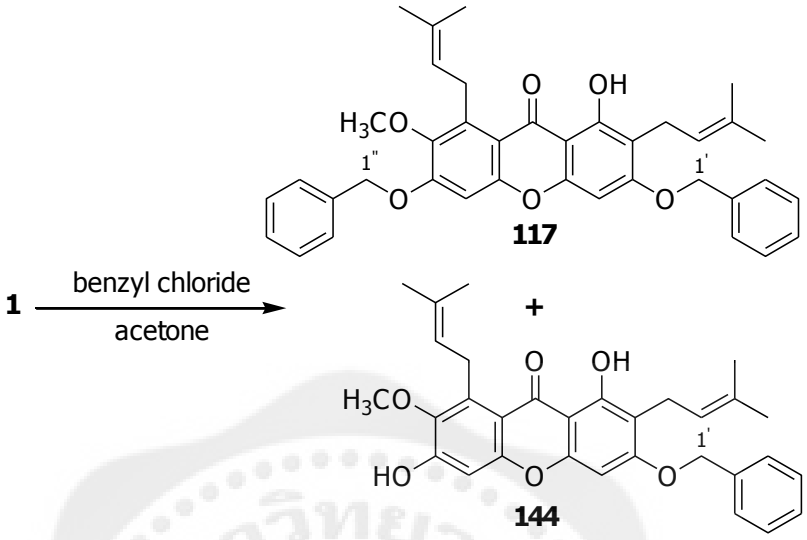

A solution of **1** (201.3 mg, 0.49 mmol) and K_2CO_3 (96.2 mg, 0.69 mmol) in acetone was subjected to benzylation with benzyl chloride (228.8 mg, 1.81 mmol). The mixture was stirred at room temperature for 4 days and 15 hours. The mixture was quenched with cold water followed by extraction with ethyl acetate (3x15 mL). The organic phase was combined, washed with water, dried over anhydrous Na_2SO_4 and concentrated *in vacuo* to dryness. The product was purified by gradient column chromatography (silica gel < 0.0063 mm) using *n*-hexane to *n*-hexane: EtOAc (95:5) as eluting solvent to give 3,6-di-*O*-benzylmangostin (**117**) (26.0 mg, 13%) and 3-mono-*O*-benzylmangostin (**144**) (48.0 mg, 24%).

3,6-Di-*O*-benzylmangostin (**117**) (**sss831**)

Pale yellow solid, m.p. 90-92 ºC. (lit. m.p. 109 -111 ºC, Ha; et al. 2009: 830).

R_f (30% EtOAc: hexane): 0.71.

IR (KBr) ν_{max} : 3420, 2918, 1743, 1642, 1599, 1462, 1375, 1278 and 1191 cm^{-1}.

^{1}H-NMR ($CDCl_3$, 300 MHz): δ_H 1.60 (s, 6H, H-15, H-20), 1.63 (s, 3H, H-14), 1.77 (s, 3H, H-19), 3.33 (d, 2H, *J*= 6.9 Hz, H-11), 3.75 (s, 3H, 7-OCH_3), 4.07 (d, 2H, *J*= 6.3 Hz, H-16), 5.08 (s, 2H, H-1'), 5.12 (s, 2H, H-

1''), 5.18 (br s, 2H, H-12, H-17), 6.27 (s, 1H, H-4), 6.70 (s, 1H, H-5), 7.34 (m, 10H, 2xPh) and 13.43 (s, 1H, 1-OH).

^{13}C-NMR ($CDCl_3$, 75 MHz): δ_C 17.0 (C-14), 17.8 (C-19), 21.4 (C-11), 25.8 (C-15 and C-20), 26.2 (C-16), 60.9 (7-OCH_3), 70.2 (C-1'), 70.7 (C-1''), 89.8 (C-4), 99.4 (C-5), 104.9 (C-9a), 109.9 (C-2), 111.8 (C-8a), 122.3 (C-12), 123.2 (C-17), 127.2 (C-3'), 127.3 (C-3''), 128.1 (C-5'), 128.4 (C-5''), 128.6 (C-4'), 128.8 (C-4''), 131.8 (C-13 and C-18), 135.7 (C-2'), 136.3 (C-2''), 137.4 (C-8), 144.5 (C-7), 155.1 (C-4a and C-10a), 157.0 (C-6), 160.0 (C-1), 162.4 (C-3) and 182.0 (C-9).

ESMS (+ve) *m/z* (% rel. intensity): 591 $[M+H]^+$(89).

3-Mono-*O*-benzylmangostin (**144**) (**sss844**)

Pale yellow solid, m.p. 140-141 ºC.

R_f (30% EtOAc: hexane): 0.49.

IR (KBr) ν_{max} : 3409, 2922, 1739, 1642, 1602, 1465, 1386, 1285 and 1180 cm^{-1}.

^{1}H-NMR ($CDCl_3$, 300 MHz): δ_H 1.60 (s, 3H, H-20), 1.69 (s, 3H, H-15), 1.71 (s, 3H, H-14), 1.83 (s, 3H, H-19), 3.40 (d, 2H, *J*= 6.9 Hz, H-11), 3.79 (s, 3H, 7-OCH_3), 4.08 (d, 2H, *J*= 6.3 Hz, H-16), 5.15 (s, 2H, H-1'), 5.24 (br s, 2H, H-12, H-17), 6.37 (s, 1H, H-4), 6.80 (s, 1H, H-5), 7.41 (m, 5H, Ph) and 13.43 (s, 1H, 1-OH).

^{13}C-NMR ($CDCl_3$, 75 MHz): δ_C 17.8 (C-14), 18.2 (C-19), 21.5 (C-11), 25.8 (C-15 and C-20), 26.5 (C-16), 62.1 (7-OCH_3), 70.3 (C-1'), 89.9 (C-4), 101.5 (C-5), 104.0 (C-9a), 111.5 (C-2), 111.8 (C-8a), 122.3 (C-12), 123.2 (C-17), 127.2 (C-3'), 128.1 (C-5'), 128.6 (C-4'), 131.5 (C-13) 132.0 (C-18), 136.0 (C-2'), 137.5 (C-8), 142.5 (C-7), 155.0 (C-4a), 155.4 (C-10a), 160.0 (C-1), 162.5 (C-3 and C-6) and 182.0 (C-9).

HRFAB-MS (+ve) *m/z* 501.2274 $[M+H]^+$ (calcd. for $C_{31}H_{31}O_6$ + H, 501.2277).

8.6 Acetylation of **1**

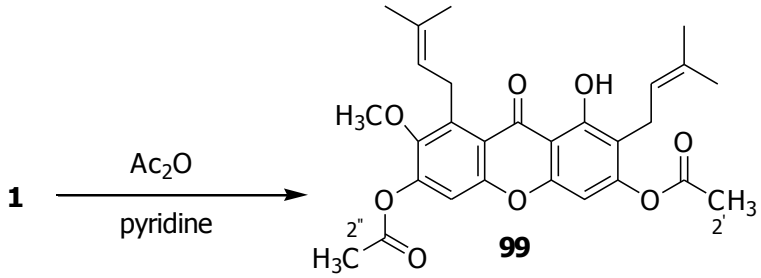

To a stirred solution of **1** (99.9 mg, 0.24 mmol) in pyridine was added with acetic anhydride (74.6 mg, 0.73 mmol). The solution was left stirring at room temperature for 24 hours. The mixture was then poured into cold water, and was extracted with ethyl acetate (EtOAc) (3x15 mL). The combined ethyl acetate was washed with water, dried over anhydrous Na_2SO_4 and evaporated under reduced pressure to dryness. The product was purified by gradient column chromatography (silica gel < 0.0063 mm) using *n*-hexane to *n*-hexane: EtOAc (90:10) as eluting solvent to give 3,6-di-*O*-methylcarboxymangostin (**99**) (81.0 mg, 68%).

3,6-Di-*O*-methylcarboxymangostin (**99**) (**sss2229**)

Pale yellow solid, m.p. 119-120 ºC. (lit. 113-114 ºC, Gopalakrisnan; et al. 1997: 519).

Rf (30% EtOAc: hexane): 0.49.

IR (KBr) ν_{max} : 3477, 2922, 1779, 1602, 1462, 1429, 1372, 1274 and 1184 cm^{-1}.

^{1}H-NMR ($CDCl_3$, 300 MHz): δ_H 1.60 (s, 6H, H-15, H-20), 1.75 (s, 3H, H-19), 1.81 (s, 3H, H-19), 2.32 (s, 3H, H-1'), 2.37 (s, 3H, H-1''), 3.29 (d, 2H, *J*= 6.7 Hz, H-11), 3.75 (s, 3H, 7-OCH_3), 4.12 (d, 2H, *J*= 5.8 Hz, H-16), 5.16 (br t, 2H, *J*= 5.8 Hz, H-12, H-17), 6.61 (s, 1H, H-4), 7.10 (s, 1H, H-5) and 13.40 (s, 1H, 1-OH).

^{13}C-NMR ($CDCl_3$, 75 MHz): δ_C 17.8 (C-14), 18.2 (C-19), 20.9 (C-2' and C-2''), 22.3 (C-11), 25.7 (C-20), 25.8 (C-15), 26.4 (C-16), 61.6 (7-OCH_3), 100.3 (C-4), 107.1 (C-9a), 110.5 (C-5), 116.2 (C-2), 116.8 (C-8a), 121.2 (C-12), 122.6 (C-17), 132.2 (C-13), 132.3 (C-18), 139.01 (C-8),

146.7 (C-7), 149.4 (C-10a), 153.6 (C-6), 154.0 (C-4a), 154.8 (C-3), 161.0 (C-1), 168.0 (C-1'), 168.4 (C-1'') and 182.8 (C-9).

ESMS (+ve) *m/z* (% rel. intensity): 495 $[M+H]^+$ (100).

8.7 Propionylation of **1**

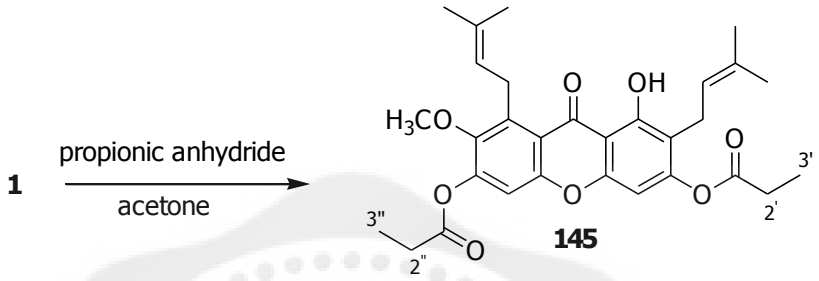

Compound **1** (20.6 mg, 0.05 mmol) was subjected to acylation with the same manner as described for the preparation of compound **99** from **1** by using propionic anhydride (6.53 mg, 0.05 mmol) as acylating instead of acetic anhydride and the reaction was stirred for 3 hours. The product was purified by gradient column chromatography (silica gel < 0.0063 mm) using *n*-hexane to *n*-hexane: EtOAc (90:10) as eluting solvent to give 3,6-di-*O*-ethylcarboxymangostin (**145**) (14.3 mg, 55%).

3,6-Di-*O*-ethylcarboxymangostin (**145**) (**sss1736**)

Yellow viscous.

Rf (30% EtOAc: hexane): 0.58.

IR (KBr) ν_{max} : 2925, 2854, 1768, 1621, 1462, 1377, 1275, 1172, 1122, 1085 and 896 cm^{-1}.

^{1}H-NMR ($CDCl_3$, 300 MHz): δ_H 1.27 (t, 3H, *J*= 7.5 Hz, H-3'), 1.30 (t, 3H, J= 7.5 Hz, H-3''), 1.66 (s, 6H, H-15, H-20), 1.74 (s, 3H, H-19), 1.81 (s, 3H, H-19), 2.61 (q, 2H, *J*= 7.5 Hz, H-2'), 2.66 (q, 2H, *J*= 7.5 Hz, H-2''), 3.28 (d, 2H, *J*= 6.7 Hz, H-11), 3.74 (s, 3H, 7-OCH_3), 4.11 (d, 2H, *J*= 5.9 Hz, H-16), 5.15 (br t, 1H, *J*= 6.7 Hz, H-12), 5.17 (br t, 1H, *J*= 5.9 Hz, H-17), 6.61 (s, 1H, H-4), 7.10 (s, 1H, H-5) and 13.40 (s, 1H, 1-OH).

^{13}C-NMR ($CDCl_3$, 75 MHz): δ_C 9.00 (C-3' and C-3''), 17.8 (C-14), 18.1 (C-19), 22.2 (C-11), 25.6 (C-20), 25.8 (C-15), 26.4 (C-16), 27.6 (C-2' and C-2''), 61.6 (7-OCH_3), 100.3 (C-4), 107.0 (C-9a), 110.6 (C-5), 116.2

(C-2), 116.8 (C-8a), 121.4 (C-12), 122.7 (C-17), 132.2 (C-13 and C-18), 139.0 (C-8), 146.7 (C-7), 149.5 (C-10a), 153.7 (C-6), 154.1 (C-4a), 155.0 (C-3), 161.0 (C-1), 171.5 (C-1'), 171.9 (C-1'') and 182.9 (C-9).

HR-TOFMS (ES^+): *m/z* 523.2332 $[M+H]^+$; calcd for $C_{30}H_{34}O_8$+H, 523.2336.

8.8 Butyrylation of **1**

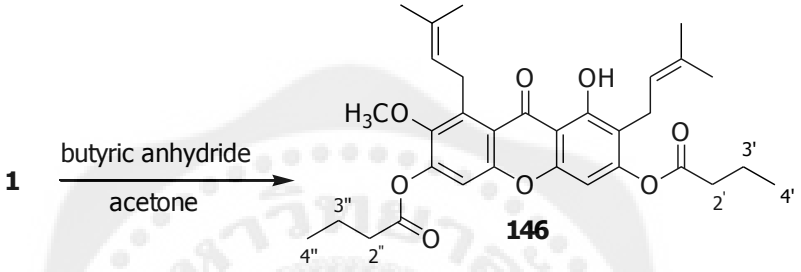

Compound **1** (100.3 mg, 0.24 mmol) was subjected to acylation with the same manner as described for the preparation of compound **99** from **1** by using butyric anhydride (47.5 mg, 0.25 mmol) as acylating instead of acetic anhydride and the reaction was stirred for 4 hours. The product was purified by gradient column chromatography (silica gel < 0.0063 mm) using *n*-hexane to *n*-hexane: EtOAc (92:8) as eluting solvent to give 3,6-di-*O*-propylcarboxymangostin (**146**) (95.0 mg, 70%).

3,6-Di-*O*-propylcarboxymangostin (**146**) (**sss1698**)

Pale yellow solid, m.p. 89-90 ºC.

Rf (30% EtOAc: hexane): 0.61.

IR (KBr) ν_{max} : 2967, 2934, 1767, 1619, 1606, 1460, 1425, 1274, 1172, 1133 and 1096 cm^{-1}.

^{1}H-NMR ($CDCl_3$, 300 MHz): δ_H 1.04 (t, 6H, *J*= 7.5 Hz, H-4', H-4''), 1.66 (s, 6H, H-15, H-20), 1.75 (s, 3H, H-14), 1.81 (br s, 7H, H-19, H-3', H-3''), 2.56 (t, 2H, *J*= 7.2 Hz, H-2'), 2.61 (t, 2H, *J*= 7.5 Hz, H-2''), 3.28 (d, 2H, *J*= 6.0 Hz, H-11), 3.74 (s, 3H, 7-OCH_3), 4.11 (d, 2H, *J*= 5.4 Hz, H-16), 5.13 (br t, 2H, *J*= 7.8 Hz, H-12, H-17), 6.60 (s, 1H, H-4), 7.09 (s, 1H, H-5) and 13.40 (s, 1H, 1-OH).

^{13}C-NMR ($CDCl_3$, 75 MHz): δ_C 13.6 (C-4' and C-4''), 17.3 (C-14), 18.1 (C-19), 18.3 (C-3' and C-3''), 22.2 (C-11), 25.6 (C-20), 25.7 (C-15), 26.4 (C-16), 36.0 (C-2''), 36.1 (C-2'), 61.7 (7-OCH_3), 100.2 (C-4), 107.0 (C-9a), 110.6 (C-5), 116.2 (C-2), 116.7 (C-8a), 121.3 (C-12 and C-17), 132.2 (C-13 and C-18), 139.0 (C-8), 146.7 (C-7), 149.5 (C-10a), 153.6 (C-6), 154.0 (C-4a), 154.9 (C-3), 160.9 (C-1), 170.6 (C-1'), 171.1 (C-1'') and 182.8 (C-9).

HR-TOFMS (ES^+): *m/z* 551.2639 $[M+H]^+$; calcd for $C_{32}H_{38}O_8$+H, 551.2639.

8.9 Benzoylation of **1**

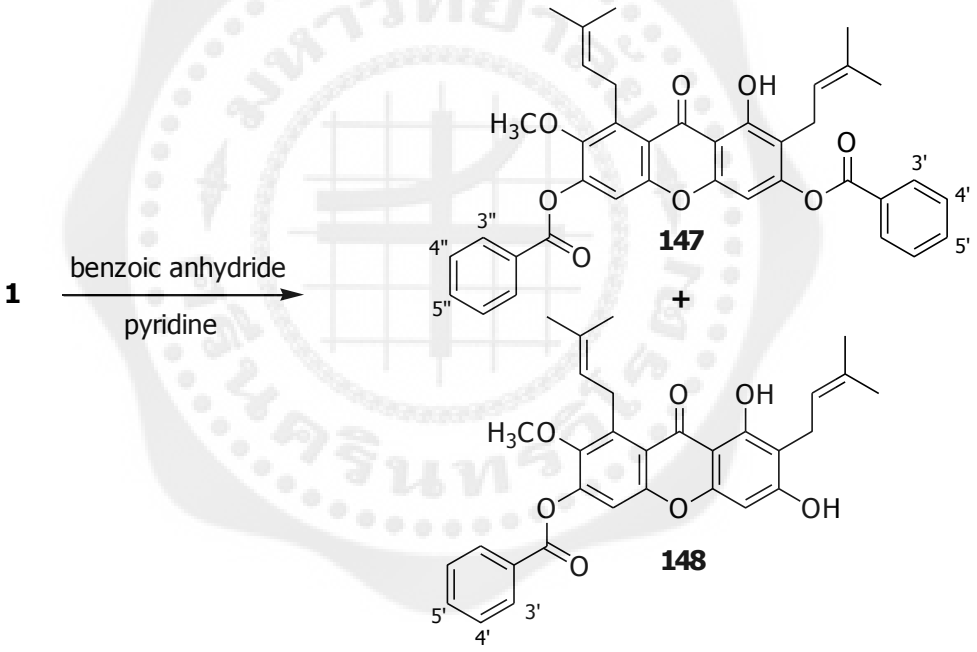

Compound **1** (205.1 mg, 0.50 mmol) was subjected to acylation by treatment with benzoic anhydride (322.4 mg, 1.43 mmol) and dry pyridine was used as base. The reaction was stirred at room temperaturefor 17 hours and 30 minuts. The product was purified by gradient column chromatography (silica gel < 0.0063 mm) using n-hexane to *n*-hexane: EtOAc (95:5) as eluting solvent to give 3,6-di-*O*-phenylcarboxymangostin (**147**, 81.6 mg, 13%) and 6-mono-*O*-phenylmangostin (**148**, 17.0 mg, 6%).

3,6-Di-*O*-phenylcarboxymangostin (**147**) (**sss994**)

Yellow solid, m.p. 85-86 ºC.

Rf (30% EtOAc: hexane): 0.61.

IR (KBr) ν_{max} : 3445, 2958, 1743, 1606, 1455, 1426, 1253, 1173, 1144, 1116 and 1096 cm^{-1}.

^{1}H-NMR ($CDCl_3$, 300 MHz): δ_H 1.71 (s, 6H, H-15, H-20), 1.84 (s, 6H, H-14, H-19), 3.39 (d, 2H, *J*= 6.7 Hz, H-11), 3.79 (s, 3H, 7-OCH_3), 4.19 (d, 2H, *J*= 6.0 Hz, H-16), 5.22 (br t, 2H, *J*= 6.0 Hz, H-12, H-17), 6.78 (s, 1H, H-4), 7.29 (s, 1H, H-5), 7.54 (m, 2H, H-4'), 7.55 (m, 2H, H-4''), 7.68 (m, 2H, H-5', H-5''), 8.23 (m, 4H, H-3', H-3'') and 13.49 (s, 1H, 1-OH).

^{13}C-NMR ($CDCl_3$, 75 MHz): δ_C 17.7 (C-14), 18.2 (C-19), 22.3 (C-11), 25.8 (C-15 and C-20), 26.5 (C-16), 61.9 (7-OCH_3), 100.5 (C-4), 107.2 (C-9a), 110.7 (C-5), 116.5 (C-2), 116.9 (C-8a), 121.4 (C-12), 122.6 (C-17), 128.6 (C-2'), 128.8 (C-2''), 128.9 (C-4' and C-4''), 130.3 (C-3' and C-3''), 132.3 (C-13 and C-18), 133.9 (C-5''), 134.1 (C-5'), 139.1 (C-8), 146.9 (C-7), 149.7 (C-6), 155.3 (C-1), 153.8 (C-4a), 154.1 (C-10a), 161.0 (C-3), 163.9 (C-1''), 164.2 (C-1') and 182.9 (C-9).

ESMS (+ve) *m/z* (% rel. intensity): 619 $[M+H]^+$ (100).

6-Mono-*O*-phenylcarboxymangostin (**148**) (**sss1106**)

Yellow solid, m.p. 188-190 ºC.

R_f (30% EtOAc: hexane): 0.41.

IR (KBr) ν_{max} : 3423, 2923, 1752, 1645, 1607, 1462, 1382, 1260, 1183 and 1149 cm^{-1}.

^{1}H-NMR ($CDCl_3$, 300 MHz): δ_H 1.67 (s, 6H, H-20), 1.75 (s, 3H, H-15), 1.81 (s, 3H, H-14), 1.82 (s, 3H, H-19), 3.44 (d, 2H, *J*= 6.9 Hz, H-11), 3.76 (s, 3H, 7-OCH_3), 4.15 (d, 2H, *J*= 6.0 Hz, H-16), 5.26 (br t, 2H, *J*= 6.0 Hz, H-12, H-17), 6.27 (s, 1H, H-4), 7.22 (s, 1H, H-5), 7.56 (br t, 2H, *J*= 7.4 Hz, H-4'), 7.70 (br t, 1H, *J*= 7.3 Hz, H-5'), 8.23 (d, 2H, *J*= 7.4 Hz) and 13.58 (s, 1H, 1-OH).

^{13}C-NMR ($CDCl_3$, 75 MHz): δ_C 17.9 (C-14), 18.2 (C-19), 21.4 (C-11), 25.8 (C-15 and C-20), 26.4 (C-16), 61.8 (7-OCH_3), 93.3 (C-4), 103.8 (C-9a), 108.8 (C-2), 110.5 (C-5), 116.9 (C-8a), 121.4 (C-12), 122.9

(C-17), 128.5 (C-2'), 128.8 (C-4'), 130.4 (C-3'), 132.1 (C-18), 134.1 (C-5'), 135.4 (C-13), 139.0 (C-8), 146.6 (C-7), 149.0 (C-6), 153.8 (C-10a), 154.9 (C-4a), 160.9 (C-1), 162.0 (C-3), 164.2 (C-1') and 182.1 (C-9).

HR-FABMS (+ve): *m/z* 515.2058 $[M+H]^+$; calcd for $C_{31}H_{29}O_7$ + H, 515.2070.

9. Catalytic hydrogenation of 1

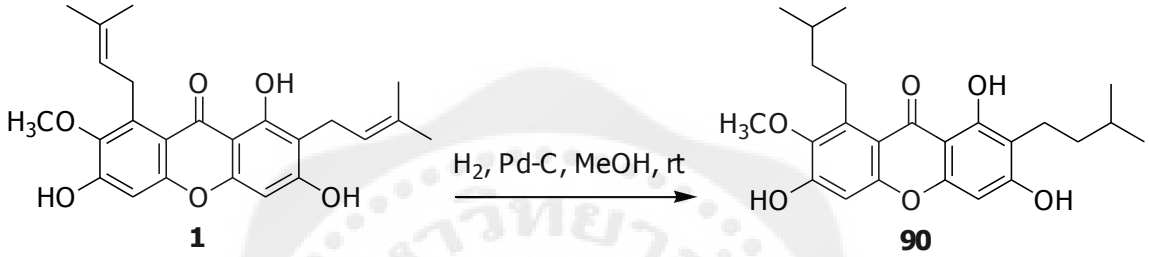

A mixture of α-mangostin (**1**) (5.00 g, 12.1 mmol) and Pd black (0.05%) in MeOH (10.0 mL) was vigorously stirred under H_2 atmosphere for 6 h with Parr hydrogenator, and the reaction progress was monitored by TLC. The reaction was completed when the green color was changed to red colour after spraying with anisaldehyde-H_2SO_4 reagent. The insoluble material was filtered off through a Celite pad, and the filtrate was concentrated *in vacuo*. A yellow viscous residue was obtained after evaporating off the solvent followed by crystallization from the mixture of solvent (acetone: hexane; 1:19) to give tetrahydromangostin (**90**) (4.86 g, 98%).

Tetrahydromangostin (**90**) (**sss3689**)

Pale yellow needles, m.p. 128-130 °C. (lit. yellow viscous oil, Iinuma; et al, 1996b: 861).

R_f (30% EtOAc: hexane): 0.34.

IR (KBr) ν_{max} : 3475, 3203, 2953, 1646, 1608, 1467, 1206, 1122, 1067, 980 and 820 cm^{-1}.

^{1}H-NMR ($CDCl_3$, 300 MHz): δ_H 0.95 (d, 6H, *J*= 6.8 Hz, H-14, H-15), 0.97 (d, 6H, *J*= 6.8 Hz, H-19, H-20), 1.40 (br q, 2H, *J*= 7.9 Hz, H-12), 1.45 (br q, 2H, *J*= 7.9 Hz, H-17), 1.62 (m, 1H, H-13), 1.73 (m, 1H, H-18), 2.63 (br t, 2H, *J*= 7.9 Hz, H-11), 3.30 (br t, 2H, *J*= 7.9 Hz, H-16), 3.81 (s,

3H, 7-OCH_3), 5.72 (br s, 1H, 3-OH), 6.22 (s, 1H, H-4), 6.34 (br s, 1H, 6-OH), 6.75 (s, 1H, H-5) and 13.84 (s, 1H, 1-OH).

^{13}C-NMR ($CDCl_3$, 75 MHz): δ_C 20.1 (C-11), 22.4 (2xCH_3), 22.5 (2xCH_3), 25.5 (C-16), 28.2 (C-13), 28.8 (C-18), 37.9 (C-12), 40.2 (C-17), 62.2 (7-OCH_3), 92.5 (C-4), 101.2 (C-5), 103.7 (C-9a), 110.9 (C-2), 112.2 (C-8a), 139.2 (C-8), 142.3 (C-7), 154.3 (C-4a), 154.5 (C-10a), 155.7 (C-6), 160.0 (C-3), 161.1 (C-1) and 181.9 (C-9).

HR-FABMS (+ve): *m/z* 415.2121; calcd for $C_{24}H_{30}O_6$ + H, 415.2120.

10. General procedure for *O*-alkyated and *O*-acylated tetrahydromangostin synthesis

Appropriate akylating agents (0.10 - 0.18 mmol) or acylating agents (0.14 – 0.25 mmol) was added to a solution of 0.06 – 0.19 mmole of tetrahydromangostin (**90**) in acetone containing potassium carbonate (0.07 – 0.28 mmol). The mixture was stirred for 1-72 h, and the reaction progress was monitored by TLC. The mixture was then poured into cold water, and was extracted with ethyl acetate (3x15 mL). The organic phase was washed with water, dried over anhydrous Na_2SO_4 and concentrated *in vacuo*. The crude product was purified by gradient column chromatography using *n*-hexane: acetone or *n*-hexane: ethyl acetate as the eluting solvent system.

11. *O*-Alkylation and *O*-acylation of tetrahydromangostin (90)

11.1 Methylation of tetrahydromangostin (**90**)

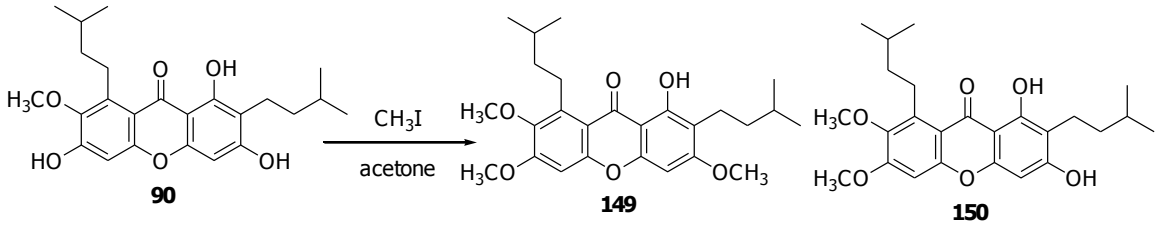

To a stirred solution of **90** (30.6 mg, 0.07 mmol) and K_2CO_3 (11.8 mg, 0.07 mmol) in acetone was added with iodomethane (21.5 mg, 0.15 mmol). The solution was left stirring at room temperature for 24 hours. The mixture was then poured into cold water, and was extracted with ethyl acetate (EtOAc) (3x15 mL). The combined ethyl acetate was washed with water, dried over anhydrous Na_2SO_4 and evaporated under reduced pressure to dryness. The product was purified by gradient column chromatography (silica gel < 0.0063 mm) using *n*-hexane to *n*-hexane: EtOAc (95:5) as eluting solvent to give 3,6-di-*O*-methyltetrahydromangostin (**149**) (9.6 mg, 30%) and 6-mono-*O*-methyltetrahydromangostin (**150**) (16 mg, 40%).

3,6-Di-*O*-methyltetrahydromangostin (**149**) (**sss1188**)

Pale yellow solid, m.p. 92-94 °C.

R_f (30% EtOAc: hexane): 0.50.

IR (KBr) ν_{max} : 3416, 2915, 1599, 1462, 1375, 1278, 1209 and 1141 cm^{-1}.

^{1}H-NMR ($CDCl_3$, 300 MHz): δ_H 0.93 (d, 6H, *J*= 6.5 Hz, H-14, H-15), 0.97 (d, 6H, *J*= 6.5 Hz, H-19, H-20), 1.38 (br q, 2H, *J*=7.7 Hz, H-12), 1.40 (br q, 2H, *J*= 7.9 Hz, H-17), 1.58 (m, 1H, H-13), 1.73 (m, 1H, H-18), 2.62 (br t, 2H, *J*= 7.7 Hz, H-11), 3.33 (br t, 2H, *J*= 7.9 Hz, H-16), 3.80 (s, 3H, 7-OCH_3), 3.87 (s, 3H, 3-OCH_3), 3.94 (s, 3H, 6-OCH_3), 6.29 (s, 1H, H-4), 6.70 (s, 1H, H-5) and 13.62 (s, 1H, 1-OH).

^{13}C-NMR ($CDCl_3$, 75 MHz): δ_C 20.1 (C-11), 22.5 (C-14 and C-19), 22.6 (C-15 and C-20), 25.0 (C-16), 28.2 (C-13), 28.8 (C-18), 38.0 (C-12), 40.2 (C-17), 55.7 (3-OCH_3), 55.9 (6-OCH_3), 61.1 (7-OCH_3), 88.3 (C-4), 97.8 (C-5), 103.8 (C-9a), 112.8 (C-2), 112.1 (C-8a), 139.4 (C-8), 143.7

(C-7), 154.9 (C-4a), 155.3 (C-10a), 157.8 (C-6), 163.4 (C-3), 159.9 (C-1) and 181.9 (C-9).

HR-TOFMS (ES^+): *m/z* 443.2429 $[M+H]^+$; calcd for $C_{26}H_{35}O_6$ + H, 443.2428.

6-Mono-*O*-methyltetrahydromangostin (**150**) (**sss2069**)

Pale yellow solid, m.p. 115-116 $^{\circ}C$.

R_f (30% EtOAc: hexane): 0.39.

IR (KBr) ν_{max} : 3476, 3200, 2953, 1613, 1470, 1368, 1266, 1193, 1121, 1067, 1034, 980 and 819 cm^{-1}.

^{1}H-NMR ($CDCl_3$, 300 MHz): δ_H 0.96 (d, 6H, *J*= 6.9 Hz, H-14, H-15), 0.98 (d, 6H, *J*= 7.0 Hz, H-19, H-20), 1.40 (br q, 2H, *J*= 7.6 Hz, H-12), 1.46 (br q, 2H, *J*= 7.6 Hz, H-17), 1.62 (m, 1H, H-13), 1.74 (m, 1H, H-18), 2.64 (br t, 2H, *J*= 7.6 Hz, H-11), 3.33 (br t, 2H, *J*= 7.6 Hz, H-16), 3.81 (s, 3H, 7-OCH_3), 3.95 (s, 3H, 6-OCH_3), 5.46 (br s, 1H, 3-OH), 6.24 (s, 1H, H-4), 6.71 (s, 1H, H-5) and 13.87 (s, 1H, 1-OH).

^{13}C-NMR ($CDCl_3$, 75 MHz): δ_C 20.1 (C-11), 22.5 (C-14 and C-15), 22.6 (C-19 and C-20), 25.0 (C-16), 28.2 (C-13), 28.8 (C-18), 37.9 (C-12), 40.2 (C-17), 55.9 (6-OCH_3), 61.2 (7-OCH_3), 92.4 (C-4), 97.9 (C-5), 103.8 (C-9a), 110.9 (C-2), 112.0 (C-8a), 139.4 (C-8), 143.7 (C-7), 154.5 (C-4a), 155.4 (C-10a), 157.9 (C-6), 159.9 (C-3), 161.0 (C-1) and 182.0 (C-9)

HR-TOFMS (ES^-): *m/z* 427.2124 $[M-H]^-$; calcd for $C_{25}H_{31}O_6$ - H, 427.2126.

11.2 Ethylation of **90**

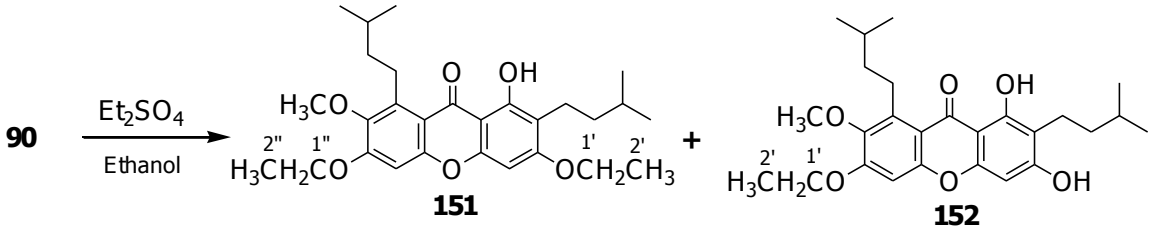

Compound **90** (58.3 mg, 0.14 mmol) was subjected to *O*-ethylation with the same manner as described for the preparation of compounds **149** and **150** from **90** by using diethyl sulphate (21.5 mg, 0.14 mmol) as alkylating agent instead of methyl iodide and the reaction was stirred for 22 hours. The product was purified by gradient column chromatography (silica gel < 0.0063 mm) using *n*-hexane to *n*-hexane: EtOAc (95:5) as eluting solvent to give 3,6-di-*O*-ethyltetrahydromangostin (**151**) (24.8 mg, 37%) and 6-mono-*O*-ethyltetrahydromangostin (**152**) (34.1 mg, 55%).

3,6-Di-*O*-ethyltetrahydromangostin (**151**) (**sss2286**)

Pale yellow solid, m.p. 75-76 °C.

R_f (30% EtOAc: hexane): 0.62.

IR (KBr) ν_{max} : 3452, 2948, 1638, 1600, 1466, 1384, 1364, 1285, 1202, 1140, 854 and 813 cm^{-1}.

^{1}H-NMR ($CDCl_3$, 300 MHz): δ_H 0.93 (d, 6H, *J*= 6.5 Hz, H-14, H-15), 0.97 (d, 6H, *J*= 6.5 Hz, H-19, H-20), 1.38 (m, 2H, H-12), 1.41 (m, 2H, H-17), 1.43 (t, 3H, *J*= 6.8 Hz, H-2'), 1.51 (t, 3H, *J*= 6.9 Hz, H-2''), 1.60 (m, 1H, H-13), 1.73 (m, 1H, H-18), 2.61 (br t, 2H, *J*= 7.7 Hz, H-11), 3.31 (br t, 2H, *J*= 7.9 Hz, H-16), 3.81 (s, 3H, 7-OCH_3), 4.04 (q, 2H, *J*= 6.8 Hz, H-1'), 4.12 (q, 2H, *J*= 6.9 Hz, H-1'') , 6.21 (s, 1H, H-4), 6.63 (s, 1H, H-5) and 13.63 (s, 1H, 1-OH).

^{13}C-NMR ($CDCl_3$, 75 MHz): δ_C 14.2 (C-2', C-2''), 20.1 (C-11), 22.5 (C-14 and C-15), 22.6 (C-19 and C-20), 25.1 (C-16), 28.2 (C-13), 28.7 (C-18), 38.0 (C-12), 40.2 (C-17), 61.1 (7-OCH_3), 63.9 (C-1'), 64.3 (C-1''), 89.0 (C-4), 98.3 (C-5), 103.7 (C-9a), 112.7 (C-2), 111.9 (C-8a), 139.2 (C-8), 143.7 (C-7), 154.9 (C-4a), 155.3 (C-10a), 157.0 (C-6), 162.7 (C-3), 159.9 (C-1) and 181.9 (C-9).

HR-FABMS (+ve): *m/z* 471.2746 $[M+H]^+$; calcd for $C_{28}H_{39}O_6$ + H, 471.2746.

6-Mono-*O*-ethyltetrahydromangostin (**152**) (**sss2285**)

Pale yellow solid, mp 129-130 ^{O}C.

R_f (30% EtOAc: hexane): 0.39.

IR (KBr) ν_{max} : 3303, 2956, 2870, 1634, 1605, 1587, 1456, 1286, 1195, 1129 and 820 cm^{-1}.

^{1}H-NMR ($CDCl_3$, 300 MHz): δ_H 0.95 (d, 6H, *J*= 6.5 Hz, H-14, H-15), 0.97 (d, 6H, *J*= 6.7 Hz, H-19, H-20), 1.41 (br q, 2H, *J*= 8.0 Hz, H-12), 1.42 (br q, 2H, *J*= 7.8 Hz, H-17), 1.54 (t, 3H, *J*= 6.9 Hz, H-2'), 1.62 (m, 1H, H-13), 1.74 (m, 1H, H-18), 2.63 (dt, 2H, *J*= 5.7, 8.0 Hz, H-11), 3.32 (dt, 2H, *J*= 5.2, 7.8 Hz, H-16), 3.81 (s, 3H, 7-OCH_3), 4.14 (q, 2H, *J*= 6.9 Hz, H-1'), 5.41 (br s, 1H, 3-OH), 6.29 (s, 1H, H-4), 6.67 (s, 1H, H-5) and 13.89 (s, 1H, 1-OH).

^{13}C-NMR ($CDCl_3$, 75 MHz): δ_C 14.5 (C-2'), 20.1 (C-11), 22.5 (C-14, C-15, C-19 and C-20), 25.1 (C-16), 28.2 (C-13), 28.8 (C-18), 37.9 (C-12), 40.2 (C-17), 61.1 (7-OCH_3), 64.4 (C-1'), 92.3 (C-4), 98.4 (C-5), 104.0 (C-9a), 110.7 (C-2), 112.0 (C-8a), 139.4 (C-8), 144.0 (C-7), 154.6 (C-4a), 155.1 (C-10a), 157.2 (C-6), 159.7 (C-3), 161.1 (C-1) and 182.0 (C-9).

HR-FABMS (+ve): *m/z* 443.2439 $[M+H]^+$; calcd for $C_{26}H_{35}O_6$ + H, 443.2433.

11.3 Allylation of **90**

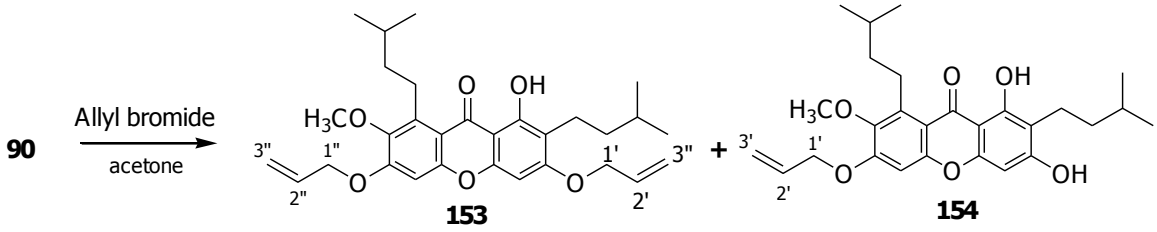

Compound **90** (40.6 mg, 0.10 mmol) was subjected to *O*-allylation with the same manner as described for the preparation of compounds **149** and **150** from **90** by using allyl bromide (12.0 mg, 0.10 mmol) as alkylating agent instead of methyl iodide and the reaction was stirred for 48 hours. The product was purified by gradient column chromatography (silica gel < 0.0063 mm) using *n*-hexane to *n*-hexane: EtOAc (95:5) as eluting solvent to give 3,6-di-*O*-allyltetrahydromangostin (**153**) (11.6 mg, 24%) and 6-mono-*O*-allyltetrahydromangostin (**154**) (26.3 mg, 59%).

3,6-Di-*O*-allyltetrahydromangostin (**153**) (**sss1985**)

Pale yellow solid, m.p. 78-79°C.

R_f (30% EtOAc: hexane): 0.75.

IR (KBr) ν_{max} : 3503, 2954, 2869, 1761, 1624, 1602, 1461, 1425, 1286, 1238, 1177, 1125, 1038 and 842 cm^{-1}.

^{1}H-NMR ($CDCl_3$, 300 MHz): δ_H 0.93 (d, 6H, *J*= 6.5 Hz, H-14, H-15), 0.98 (d, 6H, *J*= 6.6 Hz, H-19, H-20), 1.38 (br q, 2, *J*= 7.8 Hz, H-12), 1.40 (br q, 2H, *J*= 8.0 Hz, H-17), 1.59 (m, 1H, H-13), 1.72 (m, 1H, H-18), 2.66 (dt, 2H, *J*= 5.5, 7.8 Hz, H-11), 3.33 (dt, 2H, *J*= 5.7, 8.0 Hz, H-16), 3.82 (s, 3H, 7-OCH_3), 4.58 (dd, 2H, *J*= 1.4, 4.8 Hz, H-1'), 4.65 (dd, 2H, *J*= 1.3, 5.0 Hz, H-1'') 5.30 (dd, 1H, *J*= 1.4, 10.5 Hz, H-3a'), 5.34 (dd, 1H, *J*= 1.3, 9.2 Hz, H-3a''), 5.43 (dd, 1H, *J*= 1.4, 14.8 Hz, H-3b'), 5.49 (dd, 1H, *J*= 1.3, 10.0 Hz, H-3b''), 6.05 (m, 2H, H-2', H-2''), 6.26 (s, 1H, H-4), 6.68 (s, 1H, H-5) and 13.63 (s, 1H, 1-OH).

^{13}C-NMR ($CDCl_3$, 75 MHz): δ_C 20.2 (C-11), 22.5 (C-14 and C-15), 25.6 (C-19 and C-20), 25.1 (C-16), 28.3 (C-13), 28.8 (C-18), 38.0 (C-12), 40.2 (C-17), 61.1 (7-OCH_3), 68.8 (C-1'), 69.4 (C-1''), 89.4 (C-4), 98.9

(C-5), 103 (C-9a), 112.2 (C-8a), 113.0 (C-2), 132.0 (C-2''), 132.5 (C-2'), 139.5 (C-8), 143.9 (C-7), 154.8 (C-4a), 155.2 (C-10a), 156.7 (C-6), 160.1 (C-1) and 181.9 (C-9).

HR-TOFMS (ES^+): *m/z* 495.2750 $[M+H]^+$; calcd for $C_{30}H_{38}O_6$ + H, 495.2741.

6-Mono-*O*-allyltetrahydromangostin (**154**) (**sss1986**)

Pale yellow solid, m.p. 59 - 60 ^{o}C.

R_f (30% EtOAc: hexane): 0.50.

IR (KBr) ν_{max} : 3433, 2956, 1642, 1605, 1463, 1424, 1287, 1198, 1126, 1038 and 822 cm^{-1}.

^{1}H-NMR ($CDCl_3$, 300 MHz): δ_H 0.95 (d, 6H, *J*= 6.5 Hz, H-14, H-15), 0.98 (d, 6H, *J*= 6.6 Hz, H-19, H-20), 1.41 (m, 4H, H-12, H-17), 1.57 (m, 1H, H-13), 1.74 (m, 1H, H-18), 2.63 (br t, 2H, *J*= 7.8 Hz, H-11), 3.32 (br t, 2H, *J*= 7.8 Hz, H-16), 3.82 (s, 3H, 7-OCH_3), 4.64 (d, 2H, *J*= 4.2 Hz, H-1'), 5.42 (dd, 2H, *J*= 10.7, 16.8 Hz, H-3'), 6.06 (m, 1H, H-2'), 6.21 (s, 1H, H-4), 6.66 (s, 1H, H-5) and 13.86 (s, 1H, 1-OH).

^{13}C-NMR ($CDCl_3$, 75 MHz): δ_C 20.1 (C-11), 22.5 (C-14,C-15, C-19 and C-20), 25.1 (C-16), 28.2 (C-13), 28.8 (C-18), 37.9 (C-12), 40.2 (C-17), 61.4 (7-OCH_3), 69.4 (C-1'), 92.3 (C-4), 98.9 (C-5), 104.0 (C-9a), 112.1 (C-2, C-8a), 118.4 (C-3'), 131.9 (C-2'), 139.6 (C-8), 143.9 (C-7), 154.5 (C-4a), 156.7 (C-6), 159.8 (C-3), 161.1 (C-1) and 182.0 (C-9).

HR-TOFMS (ES^-): *m/z* 453.2273 $[M-H]^-$; calcd for $C_{27}H_{34}O_6$ -H, 453.2480.

11.4 4-Bromobutylation of **90**

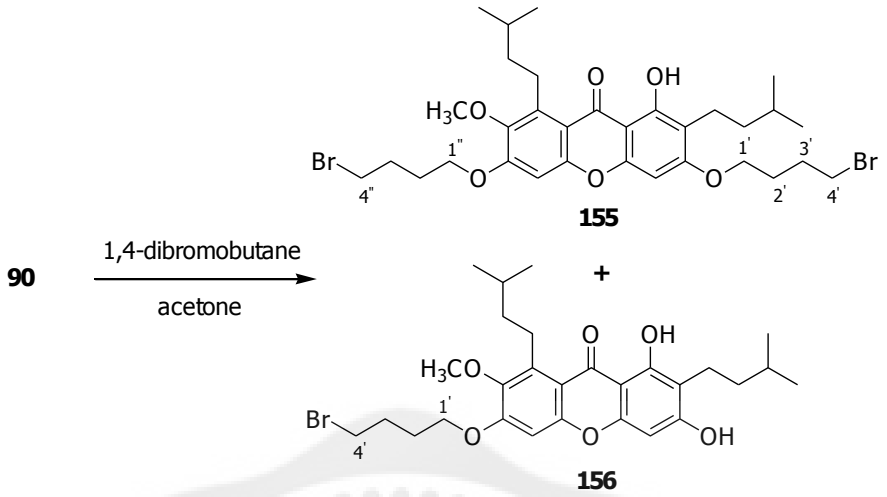

Compound **90** (25.8 mg, 0.06 mmol) was subjected to *O*-butylation with the same manner as described for the preparation of compounds **149** and **150** from **90** by using 1,4-dibromobutane (25.6 mg, 0.12 mmol) as alkylating agent instead of methyl iodide and the reaction was stirred for 24 hours. The product was purified by gradient column chromatography (silica gel < 0.0063 mm) using *n*-hexane to *n*-hexane: EtOAc (95:5) as eluting solvent to give 3,6-di-*O*-(4-bromobutyl)tetrahydromangostin (**155**) (8.7 mg, 21%) and 6-mono-*O*-(4-bromobutyl)tetrahydromangostin (**156**) (12.4 mg, 36%).

3,6-Di-*O*-(4-bromobutyl)tetrahydromangostin (**155**) (**sss2075**)

Pale yellow solid, m.p. 78-79 ^{o}C.

R_f (30% EtOAc: hexane): 0.70.

IR (KBr) ν_{max} : 3503, 2954, 2869, 1761, 1624, 1602, 1461, 1425, 1286, 1238, 1177, 1125, 1038 and 842 cm^{-1}.

^{1}H-NMR ($CDCl_3$, 300 MHz): δ_H 0.93 (d, 6H, *J*= 6.5 Hz, H-14, H-15), 0.97 (d, 6H, *J*= 6.6 Hz, H-19, H-20), 1.36 (br q, 2H, *J*= 7.4 Hz, H-12), 1.41 (br q, 2H, *J*= 8.2 Hz, H-17), 1.60 (m, 1H, H-13), 1.74 (m, 1H, H-18), 2.01 (m, 2H, H-3''), 2.08 (m, 2H, H-3'), 2.09 (m, 4H, H-2', H-2''), 2.62 (br t, 2H, *J*= 7.5 Hz, H-11), 3.32 (br t, 2H, *J*= 6.5 Hz, H-16), 3.49 (t, 3H, *J*= 6.4 Hz, H-4'), 3.51 (t, 3H, *J*= 5.8 Hz, H-4''), 3.80 (s, 3H, 7-OCH_3), 4.08 (t, 2H, *J*= 5.8 Hz, H-1'), 4.10 (t, 2H, *J*= 5.7 Hz, H-1'') 6.25 (s, 1H, H-4), 6.67 (s, 1H, H-5) and 13.62 (s, 1H, 1-OH).

^{13}C-NMR ($CDCl_3$, 75 MHz): δ_C 20.1 (C-11), 22.5 (C-14 and C-15), 22.6 (C-19 and C-20), 25.1 (C-16), 27.6 (C-3'), 27.7 (C-3''), 28.3 (C-13), 28.8 (C-18), 29.4, (C-2', C-2''), 33.1 (C-4', C-4''), 38.1 (C-12), 40.2 (C-17), 61.2 (7-OCH_3), 67.1 (C-1'), 67.7 (C-1''), 88.9 (C-4), 98.4 (C-5), 103.9 (C-9a), 112.2 (C-8a), 112.8 (C-2), 139.5 (C-8), 143.8 (C-7), 154.9 (C-4a), 155.2 (C-10a), 157.0 (C-6), 160.1 (C-1) and 181.9 (C-9).

HR-TOFMS (ES^-): *m/z* 683.1587 $[M-H]^-$; calcd for $C_{32}H_{44}Br_2O_6$ - H, 683.1577.

6-Mono-*O*-(4-bromobutyl)tetrahydromangostin (**156**) (**sss2076**)

Yellow viscous.

R_f (30% EtOAc: hexane): 0.50.

IR (KBr) ν_{max} : 3446, 2956, 1636, 1604, 1464, 1286, 1196 and 1124 cm^{-1}.

^{1}H-NMR ($CDCl_3$, 300 MHz): δ_H 0.95 (d, 6H, *J*= 6.6 Hz, H-14, H-15), 0.97 (d, 6H, *J*= 7.0 Hz, H-19, H-20), 1.21 (br q, 4H, *J*= 7.8 Hz, H-12, H-17), 1.60 (m, 1H, H-13), 1.73 (m, 1H, H-18), 2.08 (m, 4H, H-2',H-3'), 2.63 (br t, 2H, *J*= 7.7 Hz, H-11), 3.32 (t, 2H, *J*= 7.7 Hz, H-16), 3.51 (br t, 2H, *J*= 5.9 Hz, H-4'), 3.80 (s, 3H, 7-OCH_3), 4.10 (br s, 2H, H-1'), 6.22 (s, 1H, H-4), 6.67 (s, 1H, H-5) and 13.86 (s, 1H, 1-OH).

^{13}C-NMR ($CDCl_3$, 75 MHz): δ_C 20.1 (C-11), 22.5 (C-14, C-15, C-19 and C-20), 25.1 (C-16), 27.6 (C-2'), 28.2 (C-13), 28.8 (C-18), 29.3 (C-3'), 33.1 (C-4'), 37.9 (C-12), 40.2 (C-17), 61.2 (7-OCH_3), 67.7 (C-1'), 92.4 (C-4), 98.5 (C-5), 103.8 (C-9a), 110.8 (C-2), 112.0 (C-8a), 139.5 (C-8), 143.7 (C-7), 154.4 (C-4a), 155.3 (C-10a), 157.1 (C-6), 159.8 (C-3), 159.8 (C-1) and 182.0 (C-9).

HR-TOFMS (ES^+): *m/z* 549.1847 $[M+H]^+$; calcd for $C_{28}H_{37}BrO_6$ + H, 549.1846.

11.5 Benzylation of **90**

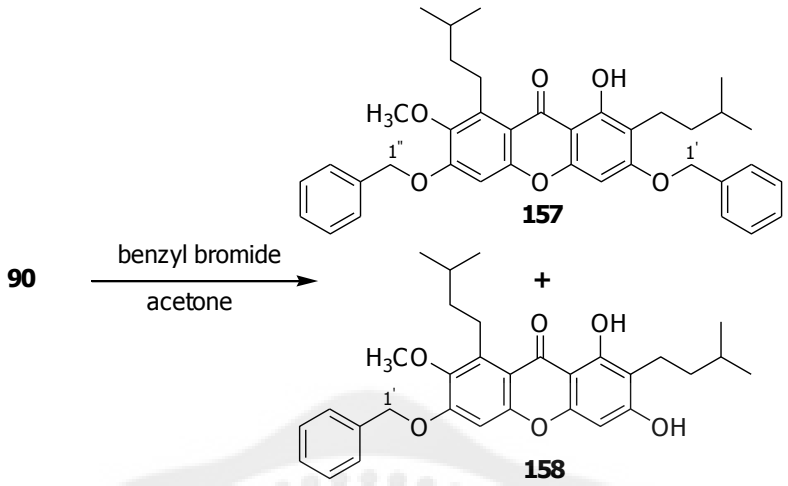

Compound **90** (38.4 mg, 0.09 mmol) was subjected to *O*-benzylation with the same manner as described for the preparation of compounds **149** and **150** from **90** by using benzyl bromide (30.7 mg, 0.18 mmol) as alkylating agent instead of methyl iodide and the reaction was stirred for 72 hours. The product was purified by gradient column chromatography (silica gel < 0.0063 mm) using *n*-hexane to *n*-hexane: EtOAc (95:5) as eluting solvent to give 3,6-di-*O*-benzyltetrahydromangostin (**157**) (13.9 mg, 25%) and 6-mono-*O*-benzyltetrahydromangostin (**158**) (19.7 mg, 42%).

3,6-Di-*O*-benzyltetrahydromangostin (**157**) (**sss1988**)

Pale yellow solid, m.p. 135-136 ^{o}C.

R_f (30% EtOAc: hexane): 0.72.

IR (KBr) ν_{max} : 3446, 2953, 1638, 1596, 1466, 1381, 1286, 1195, 1134, 1045, 976 and 876 cm^{-1}.

^{1}H-NMR ($CDCl_3$, 300 MHz): δ_H 0.91 (d, 6H, *J*= 6.6 Hz, H-14, H-15), 0.98 (d, 6H, *J*= 6.9 Hz, H-19, H-20), 1.41 (br q, 2H, *J*= 7.8 Hz, H-12), 1.46 (br q, 2H, *J*= 8.0 Hz, H-17), 1.62 (m, 1H, H-13), 1.75 (m, 1H, H-18), 2.69 (dt, 2H, *J*= 5.6, 7.8 Hz, H-11), 3.34 (dt, 2H, *J*= 5.3, 8.0 Hz, H-16), 3.80 (s, 3H, 7-OCH_3), 5.13 (s, 2H, H-1'), 5.17 (s, 2H, H-1") 6.33 (s, 1H, H-4), 6.74 (s, 1H, H-5), 7.40 (m, 10H, H-Ph) and 13.64 (s, 1H, 1-OH).

^{13}C-NMR ($CDCl_3$, 75 MHz): δ_C 20.5 (C-11), 22.5 (C-14 and C-15), 22.6 (C-19 and C-20), 25.1 (C-16), 28.3 (C-13), 28.8 (C-18), 38.1 (C-12), 40.2 (C-17), 61.2 (7-OCH_3), 70.1 (C-1'), 70.6 (C-1''), 89.6 (C-4), 99.1 (C-5), 104.3 (C-9a), 112.3 (C-8a), 113.1 (C-2), 126.9 (C-3'), 127.8 (C-3''), 128.0 (C-5'), 128.3 (C-5''), 128.5 (C-4'), 128.7 (C-4''), 135.7 (C-2'), 136.4 (C-2''), 139.6 (C-8), 144.0 (C-7), 154.8 (C-4a), 155.2 (C-10a), 156.8 (C-6), 160.1 (C-1) and 180.2 (C-9).

HR-TOFMS (ES^+): *m/z* 595.3038 $[M+H]^+$; calcd for $C_{38}H_{42}O_6$ + H, 595.3054.

6-Mono-*O*-benzyltetrahydromangostin (**158**) (**sss1990**)

Pale yellow solid, m.p. 109 -110 $^{\circ}$C.

R_f (30% EtOAc: hexane): 0.53.

IR (KBr) ν_{max} : 3384, 2953, 2866, 1644, 1608, 1465, 1382, 1365, 1289, 1194, 1122, 1041 and 819 cm^{-1}.

^{1}H-NMR ($CDCl_3$, 300 MHz): δ_H 0.95 (d, 6H, *J*= 6.5 Hz, H-14, H-15), 0.98 (d, 6H, *J*= 6.6 Hz, H-19, H-20), 1.40 (br q, 2H, *J*= 7.9 Hz, H-12), 1.44 (br q, 2H, *J*= 8.0 Hz, H-17), 1.59 (m, 1H, H-13), 1.74 (m, 1H, H-18), 2.63 (dt, 2H, *J*= 5.6, 7.9 Hz, H-11), 3.33 (dt, 2H, *J*= 5.3, 8.0 Hz, H-16), 3.83 (s, 3H, 7-OCH_3), 5.17 (s, 2H, H-1'), 6.21 (s, 1H, H-4), 6.74 (s, 1H, H-5), 7.38 (m, 5H, H-Ph) and 13.85 (s, 1H, 1-OH).

^{13}C-NMR ($CDCl_3$, 75 MHz): δ_C 20.1 (C-11), 22.5 (C-14, C-15, C-19 and C-20), 25.1 (C-16), 27.6 (C-2'), 28.2 (C-13), 28.8 (C-18), 37.9 (C-12), 40.2 (C-17), 61.2 (7-OCH_3), 70.6 (C-1'), 92.4 (C-4), 99.1 (C-5), 103.8 (C-9a), 110.9 (C-2), 112.2 (C-8a), 128.3 (C-5'), 128.7 (C-4'), 135.5 (C-2'), 139.6 (C-8), 143.9 (C-7), 154.5 (C-4a), 155.2 (C-10a), 156.8 (C-6), 160.6 (C-3), 161.1 (C-1) and 182.0 (C-9)

HR-TOFMS (ES^+): *m/z* 505.2590 $[M+H]^+$; calcd for $C_{31}H_{36}O_6$ + H, 505.2585.

11.6 Acetylation of **90**

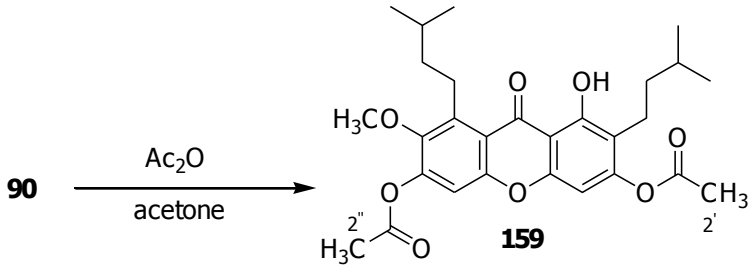

To a stirred solution of **90** (82.3 mg, 0.19 mmol) and K_2CO_3 (31.0 mg, 0.19 mmol) in acetone was added with acetic anhydride (19.4 mg, 0.19 mmol). The solution was left stirring at room temperature for 18 hours. The mixture was then poured into cold water, and was extracted with ethyl acetate (EtOAc) (3x15 mL). The combined ethyl acetate was washed with water, dried over anhydrous Na_2SO_4 and evaporated under reduced pressure to dryness. The product was purified by gradient column chromatography (silica gel < 0.0063 mm) using *n*-hexane to *n*-hexane: EtOAc (90:10) as eluting solvent to give 3,6-di-*O*-methylcarboxytetrahydromangostin (**159**) (69.3 mg, 70%).

3,6-Di-*O*-methylcarboxytetrahydromangostin (**159**) (**sss2223**)

Pale yellow solid, m.p. 118-120 $^{\circ}$C.

R_f (30% Acetone: hexane): 0.58.

IR (KBr) ν_{max} : 3438, 2954, 1757, 1635, 1602, 1458, 1433, 1375, 1285, 1195 and 1184 cm^{-1}.

^{1}H-NMR ($CDCl_3$, 300 MHz): δ_H 0.93 (d, 6H, J= 6.6 Hz, H-14, H-15), 0.98 (d, 6H, *J*= 6.6 Hz, H-19, H-20), 1.40 (br q, 2H, *J*= 8.0 Hz, H-12), 1.43 (br q, 2H, *J*= 8.2 Hz, H-17), 1.59 (m, 1H, H-13), 1.75 (m, 1H, H-18), 2.33 (s, 3H, H-2'), 2.37 (s, 3H, H-2''), 2.56 (dt, 2H, *J*= 5.5, 8.0 Hz, H-11), 3.31 (dt, 2H, *J*= 5.1, 8.2 Hz, H-16), 3.80 (s, 3H, 7-OCH_3), 6.60 (s, 1H, H-4), 7.08 (s, 1H, H-5) and 13.53 (s, 1H, 1-OH).

^{13}C-NMR ($CDCl_3$, 75 MHz): δ_C 20.9 (C-2', C-2''), 21.2 (C-11), 22.4 (C-14, C-15, C-19 and C-20), 25.4 (C-16), 28.2 (C-13), 28.9 (C-18), 37.8 (C-12), 40.1 (C-17), 61.9 (7-OCH_3), 100.1 (C-4), 107.0 (C-9a), 110.2 (C-5), 116.7 (C-8a), 117.5 (C-2), 141.1 (C-8), 146.5 (C-7), 149.4 (C-10a),

153.5 (C-4a), 154.8 (C-4a), 154.1 (C-6), 154,7 (C-3), 161.1 (C-1), 167.9 (C-1'), 168.5 (C-1''), 160.1 (C-1) and 182.9 (C-9).

HR-FABMS (+ve): *m/z* 499.2335 $[M+H]^+$; calcd for $C_{28}H_{34}O_8$ + H, 499.2331.

11.7 Propionylation of **90**

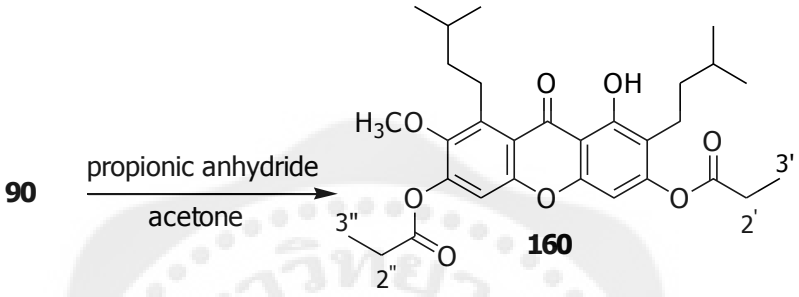

Compound **90** (50.7 mg, 0.12 mmol) was subjected to acylation with the same manner as described for the preparation of compounds **159** from **90** by using propionic anhydride (30.7 mg, 0.18 mmol) as acylating agent instead of acetic anhydride and the reaction was stirred for 4 hours. The product was purified by gradient column chromatography (silica gel < 0.0063 mm) using *n*-hexane to *n*-hexane: EtOAc (95:5) as eluting solvent to give 3,6-di-*O*-ethylcarboxytetrahydromangostin (**160**) (52.9 mg, 82%).

3,6-Di-*O*-ethylcarboxytetrahydromangostin (**160**) (**sss1963**)

Pale yellow solid, m.p. 82-83°C.

Rf (30% EtOAc: hexane): 0.62.

IR (KBr) ν_{max} : 3438, 2954, 1757, 1635, 1602, 1458, 1433, 1375, 1285, 1195 and 1184 cm^{-1}.

^{1}H-NMR ($CDCl_3$, 300 MHz): δ_H 0.95 (d, 6H, *J*= 6.6 Hz, H-14, H-15), 0.98 (d, 6H, *J*= 6.3 Hz, H-19, H-20), 1.29 (t, 3H, *J*= 7.5 Hz, H-3'), 1.30 (t, 3H, *J*= 7.5 Hz, H-3''), 1.39 (m, 2H, H-12), 1.42 (m, 2H, H-17), 1.59 (m, 1H, H-13), 1.75 (m, 1H, H-18), 2.55 (br t, 2H, *J*= 8.4 Hz, H-11), 2.62 (q, 2H, *J*= 7.5 Hz, H-2'), 2.69 (t, 2H, *J*= 7.5 Hz, H-2''), 3.33 (br t, 2H, *J*= 7.8 Hz, H-16), 3.78 (s, 3H, 7-OCH_3), 6.59 (s, 1H, H-4), 7.07 (s, 1H, H-5) and 13.54 (s, 1H, 1-OH).

^{13}C-NMR ($CDCl_3$, 75 MHz): δ_C 9.0 (C-3'), 9.1 (C-3''), 21.2 (C-11), 22.4 (4xCH_3), 25.4 (C-16), 27.6 (C-2'), 27.7 (C-2''), 28.2 (C-13), 28.9 (C-18), 37.9 (C-12), 40.1 (C-17), 61.9 (7-OCH_3), 100.1 (C-4), 107.0 (C-9a), 110.2 (C-5), 116.7 (C-8a), 117.5 (C-2), 141.1 (C-8), 146.5 (C-7), 149.4 (C-10a), 153.5 (C-4a), 154.1 (C-6), 154.8 (C-3), 161.1 (C-1), 171.5 (C-1'), 172.0 (C-1'') and 182.9 (C-9).

HR-TOFMS (ES^+): *m/z* 527.2644 $[M+H]^+$; calcd for $C_{30}H_{37}O_8$ + H, 527.2639.

11.8 Butyrylation of **90**

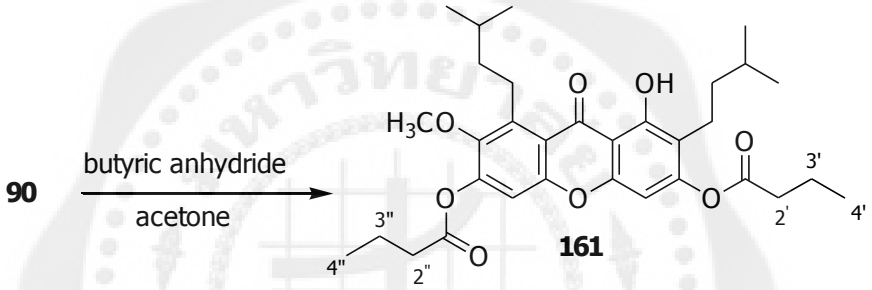

90 (25.8 mg, 0.07 mmol) was subjected to acylation with the same manner as described for the preparation of compounds **159** from **90** by using butyric anhydride (18.2 mg, 0.14 mmol) as acylating agent instead of acetic anhydride and the reaction was stirred for 30 min. The product was purified by gradient column chromatography (silica gel < 0.0063 mm) using *n*-hexane to *n*-hexane: EtOAc (95:5) as eluting solvent to give 3,6-di-*O*-propylcarboxytetrahydromangostin (**161**) (32.6 mg, 97%).

3,6-Di-*O*-propylcarboxytetrahydromangostin (**161**) (**sss2092**)

Pale yellow solid, m.p. 142-144 $^{\circ}$C.

R_f (30% EtOAc: hexane): 0.68.

IR (KBr) ν_{max} : 3383, 2955, 2869, 1735, 1644, 1611, 1464, 1287, 1168, 1125, 1036 and 827 cm^{-1}.

^{1}H-NMR ($CDCl_3$, 300 MHz): δ_H 0.93 (d, 6H, *J*= 6.4 Hz, H-14, H-15), 0.98 (d, 6H, *J*= 6.5 Hz, H-19, H-20), 1.05 (t, 3H, *J*= 6.9 Hz, H-4'), 1.06 (t, 3H, *J*= 7.1 Hz, H-4''), 1.38 (m, 2H, H-12), 1.40 (m, 2H, H-17), 1.55 (m, 1H, H-13), 1.79 (m, 1H, H-18), 1.81 (m, 4H, H-3', H-3''), 2.55 (br t, 4H, *J*=

7.7 Hz, H-11, H-2'), 2.61 (t, 2H, *J*= 7.3 Hz, H-2''), 3.33 (br t, 2H, *J*= 7.8 Hz, H-16), 3.78 (s, 3H, 7-OCH_3), 6.58 (s, 1H, H-4), 7.06 (s, 1H, H-5) and 13.55 (s, 1H, 1-OH).

^{13}C-NMR ($CDCl_3$, 75 MHz): δ_C 13.6 (C-4'), 13.7 (C-4''), 18.3 (C-3'), 18.4 (C-3''), 21.2 (C-11), 22.4 (C-14, C-15, C-19 and C-20), 25.4 (C-16), 27.6 (C-2'), 28.3 (C-13), 28.9 (C-18), 36.1 (C-2''), 36.2 (C-2'), 37.9 (C-12), 40.1 (C-17), 61.9 (7-OCH_3), 100.0 (C-4), 106.9 (C-9a), 110.2 (C-5), 116.7 (C-8a), 117.5 (C-2), 141.2 (C-8), 146.5 (C-7), 149.3 (C-10a), 153.5 (C-4a), 154.1 (C-6), 154.8 (C-3), 161.1 (C-1), 170.7 (C-1'), 171.2 (C-1'') and 182.9 (C-9).

HR-TOFMS (ES^+): *m/z* 555.2962 $[M+H]^+$; calcd for $C_{32}H_{43}O_8$ + H, 555.2952.

11.9 Benzoylation of **90**

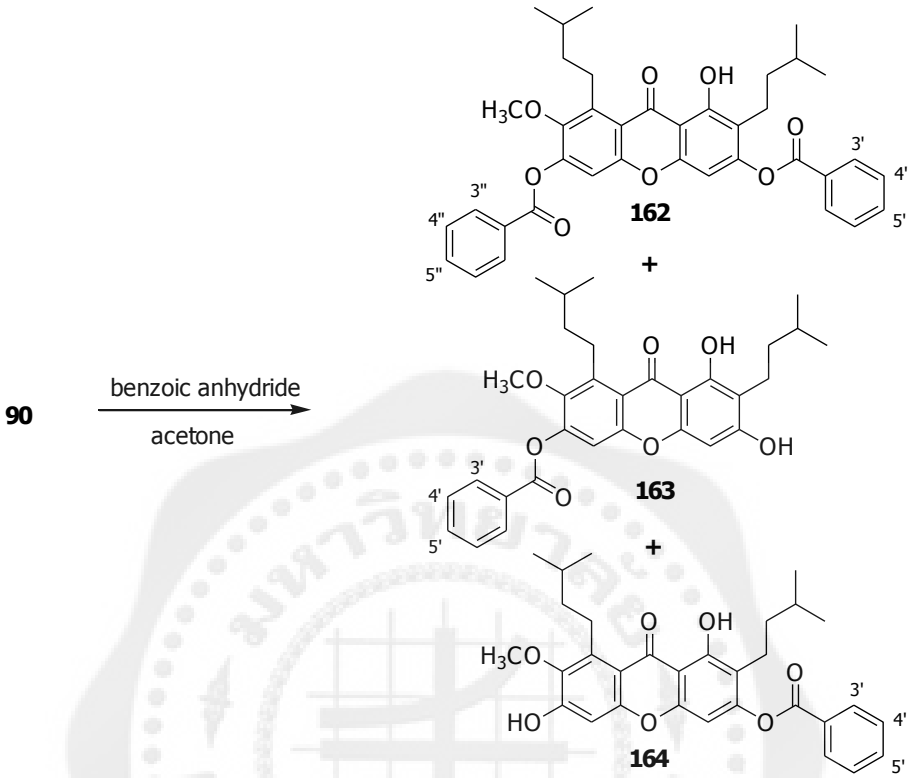

Compound **90** (60.5 mg, 0.14 mmol) was subjected to acylation with the same manner as described for the preparation of compounds **159** from **90** by using benzoic anhydride (13.9 mg, 0.14 mmol) as acylating agent instead of acetic anhydride and the reaction was stirred for 24 hours. The product was purified by gradient column chromatography (silica gel < 0.0063 mm) using *n*-hexane to *n*-hexane: EtOAc (95:5) as eluting solvent to give 3,6-di-*O*-phenylcarboxytetrahydromangostin (**162**) (8.9 mg, 5%), 6-mono-*O*-phenylcarboxytetrahydromangostin (**163**) (21.2 mg, 47%) and 3-mono-*O*-phenylcarboxytetrahydromangostin (**164**) (5.6 mg, 13%).

3,6-Di-*O*-phenylcarboxytetrahydromangostin (**162**) (**sss2060**)

Pale yellow solid, m.p. 58-60°C.

R_f (30% EtOAc : hexane): 0.73.

IR (KBr) ν_{max}: 3409, 2955, 2863, 1747, 1638, 1620, 1601, 1457, 1428, 1244, 1175, 1148, 1119, 1057 and 704 cm^{-1}.

^{1}H-NMR ($CDCl_3$, 300 MHz): δ_H 0.86 (d, 6H, *J*= 6.4 Hz, H-14, H-15), 1.00 (d, 6H, *J*= 6.5 Hz, H-19, H-20), 1.42 (br q, 2H, *J*= 8.0 Hz, H-12), 1.46 (br q, 2H, *J*= 8.3 Hz, H-17), 1.44 (m, 2H, H-17), 1.57 (m, 1H, H-13), 1.78 (m, 1H), 2.64 (br t, 2H, *J*= 8.0 Hz, H-11), 3.39 (br t, 2H, *J*= 8.3 Hz, H-16), 3.81 (s, 3H, 7-OCH_3), 6.76 (s, 1H, H-4), 7.24 (s, 1H, H-5) 7.53 (t, 4H, *J*= 7.4 Hz, H-4' and H-4''), 7.66 (br t, 1H, *J*= 7.4 Hz, H-5''), 7.67 (br t, 1H, *J*= 7.4 Hz, H-5'), 8.22 (br t, 4H, *J*= 7.4 Hz, H-3' and H-3'') and 13.61 (s, 1H, 1-OH).

^{13}C-NMR ($CDCl_3$, 75 MHz): δ_C 21.3 (C-11), 22.4 (C-14, C-15, C-19 and C-20), 25.5 (C-16), 28.2 (C-13), 28.9 (C-18), 38.0 (C-12), 40.1 (C-17), 62.1 (7-OCH_3), 100.3 (C-4), 110.4 (C-5), 107.1 (C-9a), 117.7 (C-2), 116.9 (C-8a), 128.7 (C-2' and C-4'), 128.8 (C-2'' and C-4''), 130.2 (C-3' and C-5'), 130.4 (C-3''), 134.1 (C-5''), 141.2 (C-8), 146.7 (C-7), 149.5 (C-10a), 153.6 (C-4a), 154.2 (C-6), 155.1 (C-3), 161.2 (C-1), 163.8 (C-1''), 164.3 (C-1') and 183.0 (C-9).

HR-TOFMS (ES^+): *m/z* 623.2622 $[M+H]^+$; calcd for $C_{38}H_{38}O_8$ + H, 623.2639.

6-Mono-*O*-phenylcarbonyloxytetrahydromangostin (**163**) (**sss2061**)

Pale yellow solid, m.p. 171-172 °C.

R_f (30% EtOAc: hexane): 0.67.

IR (KBr) ν_{max} : 3392, 2961, 2929, 2863, 1735, 1615, 1468, 1433, 1375, 1308, 1174, 1113 and 844 cm^{-1}.

^{1}H-NMR ($CDCl_3$, 300 MHz): δ_H 0.96 (d, 6H, *J*= 6.9 Hz, H-14, H-15), 0.99 (d, 6H, *J*= 7.0 Hz, H-19, H-20), 1.42 (m, 4H, *J*= H-12, H-17), 1.58 (m, 1H, H-13), 1.76 (m, 1H, H-18), 2.62 (br t, 2H, *J*= 7.6 Hz, H-11), 3.28 (br t, 2H, *J*= 7.6 Hz, H-16), 3.79 (s, 3H, 7-OCH_3), 5.89 (br s, 1H, 3-OH), 6.16 (s, 1H, H-4), 7.17 (s, 1H, H-5), 7.55 (t, 2H, *J*= 7.4 Hz, H-4'), 7.69 (t,

1H, *J*= 7.4 Hz, H-5'), 8.24 (d, 2H, *J*= 7.4 Hz, H-3') and 13.57 (s, 1H, 1-OH).

^{13}C-NMR ($CDCl_3$, 75 MHz): δ_C 20.1 (C-11), 22.4 (C-14 and C-15), 22.5 (C-19 and C-20), 25.4 (C-16), 28.2 (C-13), 28.9 (C-18), 37.8 (C-12), 40.1 (C-17), 62.1 (7-OCH_3), 92.6 (C-4), 110.1 (C-5), 103.8 (C-9a), 111.2 (C-2), 117.0 (C-8a), 128.6 (C-2'), 128.8 (2xC-4'), 130.4 (2xC-3'), 134.2 (C-5'), 142.2 (C-8), 146.4 (C-7), 148.8 (C-10a), 153.9 (C-6), 154.5 (C-4a), 160.5 (C-3), 161.1 (C-1), 164.3 (C-1') and 181.9 (C-9).

HR-TOFMS (ES^+): *m/z* 519.2382 $[M+H]^+$; calcd for $C_{31}H_{34}O_7$ + H, 519.2377.

3-Mono-*O*-phenylcarbonyloxytetrahydromangostin (**164**) (**sss2062**)

Pale yellow solid, m.p. 173-174 °C.

R_f (30% EtOAc: hexane): 0.60.

IR (KBr) ν_{max} : 3438, 2952, 2868, 1726, 1609, 1576, 1468, 1432, 1281, 1167, 1125 and 703 cm^{-1}.

^{1}H-NMR ($CDCl_3$, 300 MHz): δ_H 0.84 (d, 6H, *J*= 6.4 Hz, H-14, H-15), 0.99 (d, 6H, *J*= 6.6 Hz, H-19, H-20), 1.44 (br q, 2H, *J*= 8.3 Hz, H-12), 1.46 (br q, 2H, *J*= 8.2 Hz, H-17), 1.56 (m, 1H, H-13), 1.72 (m, 1H, H-18), 2.61 (dt, 2H, *J*= 5.5, 8.3 Hz, H-11), 3.28 (dt, 2H, *J*= 5.2, 8.2 Hz, H-16), 3.82 (s, 3H, 7-OCH_3), 6.41 (s, 1H, 6-OH), 6.70 (s, 1H, H-4), 6.78 (s, 1H, H-5), 7.52 (t, 2H, *J*= 7.4 Hz, H-4'), 7.66 (t, 1H, *J*= 7.4 Hz, H-5'), 8.19 (d, 2H, J= 7.4 Hz, H-3') and 13.81 (s, 1H, 1-OH).

^{13}C-NMR ($CDCl_3$, 75 MHz): δ_C 21.3 (C-11), 22.4 (C-14, C-15, C-19 and C-20), 25.5 (C-16), 28.2 (C-13), 28.8 (C-18), 38.1 (C-12), 40.1 (C-17), 62.2 (7-OCH_3), 100.1 (C-4), 101.3 (C-5), 106.9 (C-9a), 112.2 (C-8a), 117.4 (C-2), 128.7 (2xC-3'), 129.0 (C-2'), 130.2 (2xC-4'), 133.9 (C-5'), 139.4 (C-8), 142.6 (C-7), 153.5 (C-4a), 154.5 (C-3), 154.9 (C-10a), 156.1 (C-6), 161.1 (C-1), 164.5 (C-1') and 182.6 (C-9).

HR-TOFMS (ES^-): *m/z* 517.2703 $[M-H]^-$; calcd for $C_{31}H_{34}O_7$ - H, 517.2701.

12. Demethylation of 3,6-di-*O*-methyltetrahydromangostin (149)

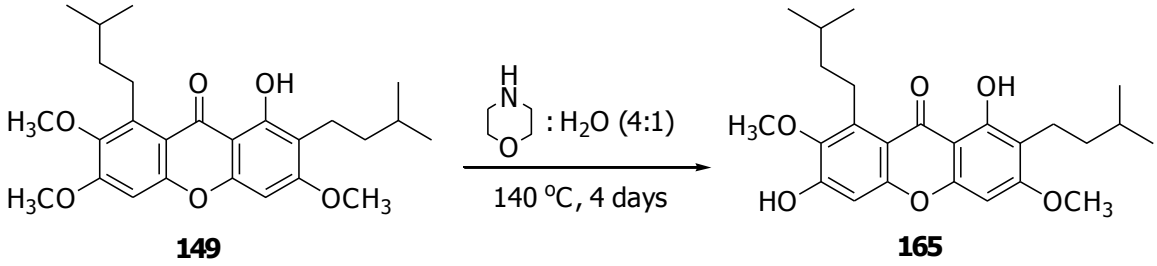

Compound **149** was subjected to demethylation by modification of the literature procedure (Bennett; et al. 1990: 1463). Thus, compound **149** (580.0 mg, 1.31 mmol), morpholine (8.0 mL), and water (2.0 mL) were placed in sealed tube (45 mL, capacity) and the mixture was purged with nitrogen gas. The reaction was heated at 140 ºC for 4 days. The morpholine was removed with ice-cold dilute HCl and extracted with ethyl acetate. A yellow viscous was obtained after evaporating off the solvent followed by purification with column chromatography eluting with 8.5:1.5 v/v of hexane-acetone to afford the demethylated product **165** in 10% yield (55.10 mg).

1,6-Dihydroxy-3,7-dimethoxy-2,8-di-(3-methylbutyl)xanthone (**165**)

(**sss2888**)

Pale yellow solid, m.p. 179-180 $^{\circ}$C.

R_f (30% EtOAc: hexane): 0.54.

IR (KBr) ν_{max} : 3419, 2954, 2867, 1651, 1598, 1462, 1289, 1202, 1141, 1090 and 846 cm^{-1}.

^{1}H-NMR ($CDCl_3$, 300 MHz): δ_H 0.93 (d, 6H, *J*= 6.5 Hz, H-14, H-15), 0.98 (d, 6H, *J*= 6.4 Hz, H-19, H-20), 1.38 (br q, 2H, *J*= 7.5 Hz, H-12), 1.45 (br q, 2H, *J* =7.5 Hz, H-17), 1.57 (m, 1H, H-13), 1.73 (m, 1H, H-18), 2.62 (br t, 2H, *J*= 7.5 Hz, H-11), 3.31 (br t, 2H, *J*= 7.5 Hz, H-16), 3.82 (s, 3H, 7-OCH_3), 3.87 (s, 3H, 3-OCH_3), 6.31 (s, 1H, H-4), 6.79 (s, 1H, H-5) and 13.56 (s, 1H, 1-OH).

^{13}C-NMR ($CDCl_3$, 75 MHz): δ_C 20.1 (C-11), 22.4 (C-14 and C-15), 22.6 (C-19 and C-20), 25.5 (C-16), 28.2 (C-13), 28.8 (C-18), 38.0 (C-

12), 40.2 (C-17), 55.7 (3-OCH_3), 62.2 (7-OCH_3), 88.6 (C-4), 101.1 (C-5), 103.7 (C-9a), 112.4 (C-8a), 112.8 (C-2), 139.2 (C-8), 142.4 (C-7), 154.2 (C-4a), 155.0 (C-6), 155.8 (C-10a), 159.9 (C-1), 163.6 (C-3) and 181.9 (C-9).

HR-TOFMS (ES^-): *m/z* 427.2124 $[M-H]^-$; calcd for $C_{25}H_{33}O_6$ - H, 427.2126.

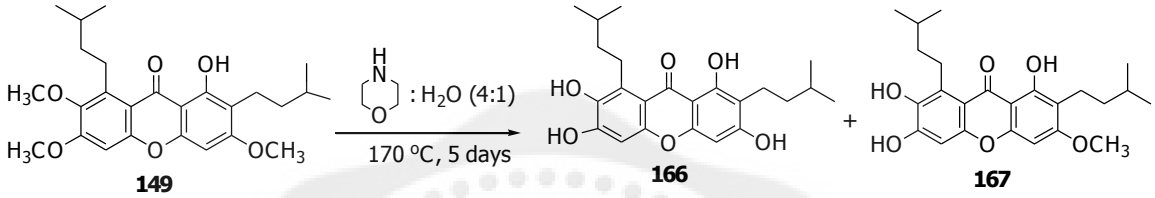

Compound **149** (1.45 g, 3.26 mmol), morpholine (8.0 mL), and water (2.0 mL) were placed in sealed tube (45 mL, capacity) and the mixture was purged with nitrogen gas. The reaction was heated at 170 ºC for 5 days. The morpholine was removed with ice-cold dilute HCl and extracted with ethyl acetate. A yellow viscous was obtained after evaporating off the solvent followed by purification with column chromatography eluting with 8.5:1.5 v/v hexane-acetone to afford the demethylated products **166** (245.0 mg) and **167** (180.0 mg) in 19 and 13% yields, respectively.

1,3,6,7-Tetrahydroxy-2,8-di-(3-methylbutyl)xanthone (**166**) (**sss3038**)

Pale yellow solid, m.p. 180-182^{O}C.

R_f (30% EtOAc: hexane): 0.34.

IR (KBr) ν_{max} : 3592, 3548, 3160, 2953, 1619, 1462, 1297, 1203, 1120 and 842 cm^{-1}.

^{1}H-NMR ($CDCl_3$, 300 MHz): δ_H 0.83 (d, 6H, *J*= 6.5 Hz, H-14, H-15), 0.97 (d, 6H, *J*= 6.6 Hz, H-19, H-20), 1.42 (m, 4H, H-12, H-17), 1.60 (m, 1H, H-13), 1.71 (m, 1H, H-18), 2.60 (br t, 2H, *J*= 7.5 Hz, H-11), 3.13 (br t, 2H, *J*= 7.7 Hz, H-16), 6.16 (s, 1H, H-4), 6.61 (s, 1H, H-5) and 13.87 (s, 1H, 1-OH).

^{13}C-NMR ($CDCl_3$, 75 MHz): δ_C 20.2 (C-11), 22.5 (C-14 and C-15), 22.6 (C-19 and C-20), 24.8 (C-16), 28.2 (C-13), 28.7 (C-18), 38.0 (C-

12), 38.7 (C-17), 92.8 (C-4), 100.0 (C-5), 103.5 (C-9a), 110.9 (C-2), 111.8 (C-8a), 130.3 (C-8), 139.1 (C-7), 149.9 (C-6), 152.9 (C-10a), 154.6 (C-4a), 160.5 (C-1, C-3) and 182.3 (C-9).

HR-TOFMS (ES^-): *m/z* 399.1813 $[M-H]^-$; calcd for $C_{23}H_{29}O_6$ - H, 399.1801.

1,6,7-Trihydroxy-3-methoxy-2,8-di-(3-methylbutyl)xanthone (**167**) (**sss3110**)

Pale yellow solid, m.p. 179-180°C.

R_f (30% EtOAc: hexane): 0.49.

IR (KBr) ν_{max} : 3492, 3236, 2953, 1646, 1616, 1484, 1289, 1213, 1138 and 841 cm^{-1}.

^{1}H-NMR ($CDCl_3$, 300 MHz): δ_H 0.89 (d, 6H, *J*= 6.5 Hz, H-14, H-15), 0.94 (d, 6H, *J*= 6.6 Hz, H-19, H-20), 1.32 (br q, 2H, *J*= 7.7 Hz, H-12), 1.42 (br q, 2H, *J*= 8.1 Hz, H-17), 1.54 (m, 1H, H-13), 1.69 (m, 1H, H-18), 2.58 (dt, 2H, *J*= 5.6, 7.7 Hz, H-11), 3.32 (dt, 2H, *J*= 5.2, 8.1 Hz, H-16), 3.82 (s, 3H, 3-OCH_3), 5.91 (br s, 1H, 7-OH), 6.23 (s, 1H, H-4), 6.71 (s, 1H, H-5), 8.83 (br s, 1H, 6-OH) and 13.70 (s, 1H, 1-OH).

^{13}C-NMR ($CDCl_3$, 75 MHz): δ_C 20.0 (C-11), 22.5 (C-14 and C-15), 22.6 (C-19 and 20), 24.7 (C-16), 28.1 (C-13), 28.6 (C-18), 38.0 (C-12), 39.0 (C-17), 55.6 (3-OCH_3), 88.3 (C-4), 100.1 (C-5), 103.7 (C-9a), 111.9 (C-8a), 112.3 (C-2), 130.3 (C-8), 139.3 (C-7), 149.9 (C-6), 152.9 (C-10a), 155.0 (C-4a), 159.8 (C-1), 163.2 (C-3) and 182.3 (C-9).

HR-TOFMS (ES^-): *m/z* 413.1972 $[M-H]^-$; calcd for $C_{24}H_{30}O_6$ - H, 413.1970.

13. Methylation of 166

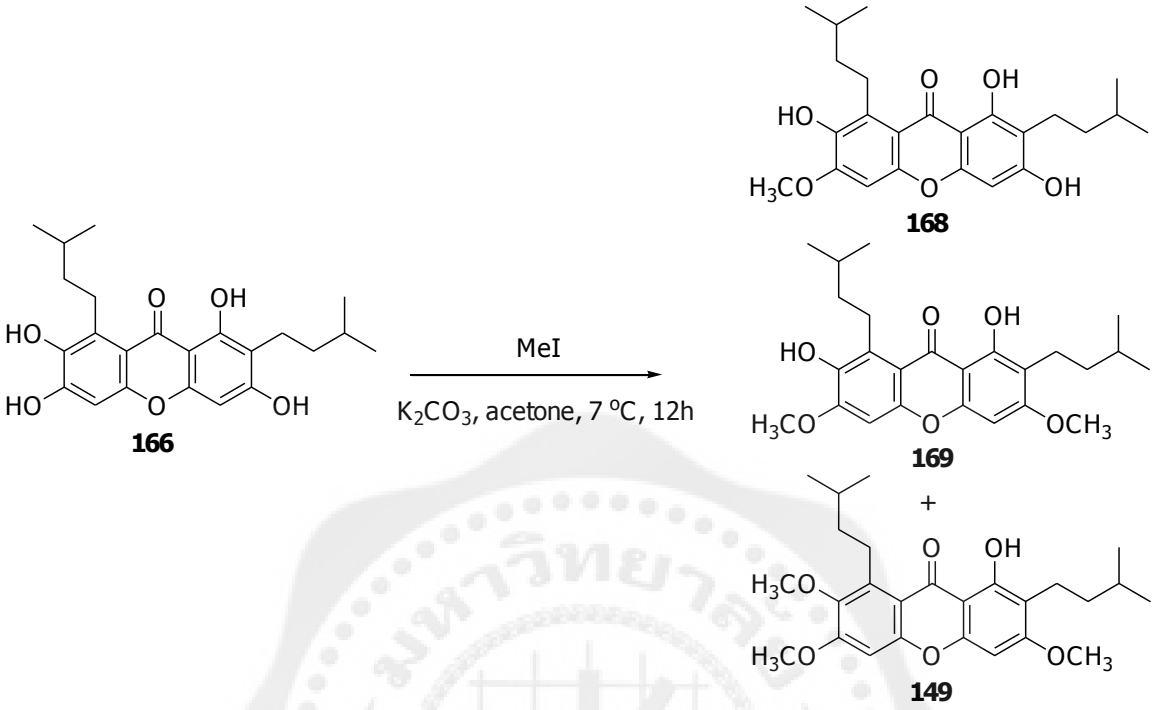

Iodomethane (19.8 mg, 0.14 mmol) was added to a solution of **166** (30.1 mg, 0.07 mmol) in acetone (1.5 mL) and K_2CO_3 (9.6 mg, 0.07 mmol). After stirring for 12 hours at 7°C, the reaction mixture was quenched with ethyl acetate and water, then extracted with ethyl acetate (3x100 mL). The combined organic phase was washed with water, dried over anhydrous sodium sulfate, filtered and concentrated *in vacuo*. The residue was purified by column chromatography eluting with 9.2: 0.8 v/v hexane-acetone to afford product **168** (3.5 mg), **169** (13.7 mg) along with **149** (5.4 mg) in 12 and 47 and 12% yields, respectively.

1,3,7-Trihydroxy-3-methoxy-2,8-di-(3-methylbutyl)xanthone (**168**)

(**sss3087**)

Pale yellow solid, m.p. 176-178^{O}C.

R_f (30% EtOAc: hexane): 0.37.

IR (KBr) ν_{max} : 3446, 2954, 2870, 1642, 1614, 1461, 1283, 1209, 1122 and 821 cm^{-1}.

^{1}H-NMR ($CDCl_3$, 300 MHz): δ_H 0.95 (d, 6H, *J*= 6.9 Hz, H-14, H-15), 0.97 (d, 6H, *J*= 7.0 Hz, H-19, H-20), 1.42 (br q, 2H, *J*= 8.0 Hz, H-12),

1.46 (br q, 2H, *J*= 8.0 Hz, H-17), 1.64 (m, 1H, H-13), 1.71 (m, 2H, H-18), 2.63 (dt, 2H, *J*= 5.7, 8.0 Hz, H-11), 3.36 (dt, 2H, *J*= 5.3, 8.3 Hz, H-16), 3.98 (s, 3H, 6-OCH_3), 6.22 (s, 1H, H-4), 6.68 (s, 1H, H-5) and 13.56 (s, 1H, 1-OH).

^{13}C-NMR ($CDCl_3$, 75 MHz): δ_C 20.1 (C-11), 22.6 (C-14, C-15, C-19 and C-20), 24.5 (C-16), 28.2 (C-13), 28.7 (C-18), 37.9 (C-12), 39.0 (C-17), 56.2 (6-OCH_3), 92.2 (C-4), 96.6 (C-5), 103.9 (C-9a), 110.6 (C-2), 112.4 (C-8a), 129.6 (C-8), 140.0 (C-7), 154.6 (C-4a), 151.1 (C-6), 152.7 (C-10a), 159.7 (C-3), 161.1 (C-1), 163.6 (C-3) and 182.4 (C-9).

HR-TOFMS (ES^-): *m/z* 413.1961 $[M-H]^-$; calcd for $C_{24}H_{30}O_6$ - H, 413.1970.

1,7-Dihydroxy-3,6-dimehoxy2,8-di-(3-methylbutyl)xanthone (**169**) (**sss3086**)

Pale yellow solid, m.p. 172-173°C.

R_f (30% EtOAc: hexane): 0.50.

IR (KBr) ν_{max}: 3491, 3357, 2968, 2922, 1649, 1601, 1462, 1286, 1177, 1119, 824 and 708 cm^{-1}.

^{1}H-NMR ($CDCl_3$, 300 MHz): δ_H 0.93 (d, 6H, *J*= 6.5 Hz, H-14, H-15), 0.98 (d, 6H, *J*= 6.5 Hz, H-19, H-20), 1.36 (br q, 2H, *J*= 7.8 Hz, H-12), 1.44 (br q, 2H, *J*= 8.0 Hz, H-17), 1.54 (m, 1H, H-13), 1.72 (m, 2H, H-18), 2.62 (dt, 2H, *J*= 5.7, 7.8 Hz, H-11), 3.36 (dt, 2H, *J*= 5.3, 8.0 Hz, H-16), 3.87 (s, 3H, 3-OCH_3), 3.98 (s, 3H, 6-OCH_3), 6.27 (s, 1H, H-4) and 6.69 (s, 1H, H-5).

^{13}C-NMR ($CDCl_3$, 75 MHz): δ_C 20.1 (C-11), 22.6 (C-14, C-15, C-19 and C-20), 24.5 (C-16), 28.2 (C-13), 28.7 (C-18), 38.0 (C-12), 39.0 (C-17), 55.7 (3-OCH_3), 56.2 (6-OCH_3), 88.3 (C-4), 99.3 (C-5), 103.9 (C-9a), 112.6 (C-2, C-8a), 129.6 (C-8), 140.0 (C-7), 155.0 (C-4a), 151.2 (C-6), 152.7 (C-10a), 159.9 (C-1), 163.3 (C-3) and 182.3 (C-9).

HR-TOFMS (ES^-): *m/z* 427.2122 $[M-H]^-$; calcd for $C_{25}H_{32}O_6$ - H, 427.2126.

14. Bioassays

14.1 Antimycobacterial Assay

The antimycobacterial activity was assessed against *Mycobacterium tuberculosis* H37Ra using the Microplate Alamar Blue Assay (MABA) (Collins; et al. 1997:1004-9). Briefly, initial candidate compound dilutions were prepared in dimethylsulfoxide (and subsequent twofold dilutions were performed in 0.1 mL of 7H9GC medium in the microculture plates. 100 µL of 5x104 CFU/mL of *M. tuberculosis* in 7H9GC-Tween was added to each well of 96 well microculture plates containing of test compound. Plates at 37ºC for 7 days. To three control wells which contained drug and medium, bacteria and medium, and medium only, the Alarmar Blue dye solution (20 µL of Alarmar Blue solution and 12.5 µL of 20% Tween) was added daily until a color change from blue to pink occurred, at which time the results were recorded at 24 hours post-dye addition. Fluorescence was measured in a Cytofluoro series 4000 Fluorescence Multi-Well Plate Reader (Per-septive Biosystems, Framingham, MA, U.S.A.) in bottom-reading mode with excitation at 530 nm and emission at 590 nm. Percent inhibition was defined 1-(test well FU of triplicate control wells) x100. The lowest drug concentration effecting an inhibition of 90% was considered the MIC. NIH, RMP and EMB were used as standard drugs (Table 5 and Table 6).

TABLE 5 Antimycobacterial activity against *M. tuberculosis* of mangostin analogues (MIC μg/mL)

Compounds	MIC	Compounds	MIC
α -Mangostin (**1**)	6.25	Tetrahydromangostin (**90**)	1.56
3,6-Di-*O*-methylmangostin (**84**)	inactive	3,6-Di-*O*-methyltetrahydromangostin (**149**)	inactive
6-Mono-*O*-methylmangostin (**140**)	6.25	6-Mono-*O*-methyltetrahydromangostin (**150**)	0.78
3,6-Di-*O*-ethylmangostin (**85**)	inactive	3,6-Di-*O*-ethyltetrahydromangostin (**151**)	inactive
3-Mono-*O*-ethylmangostin (**141**)	6.25	6-Mono-*O*-ethyltetrahydromangostin (**152**)	0.78
3,6-Di-*O*-allylmangostin (**89**)	inactive	3,6-Di-*O*-allyltetrahydromangostin (**153**)	inactive
6-Mono-*O*-allylmangostin (**120**)	3.125	6-Mono-*O*-allyltetrahydromangostin (**154**)	0.78
3,6-Di-*O*-(4-bromobutyl)-mangostin (**142**)	inactive	3,6-Di-*O*-(4-bromobutyl)-tetrahydromangostin (**155**)	inactive
6-Mono-*O*-(4-bromobutyl)-mangostin (**143**)	12.5	6-Mono-*O*-(4-bromobutyl)-tetrahydromangostin (**156**)	12.5
3,6-Di-*O*-benzylmangostin (**117**)	inactive	3,6-Di-*O*-benzyltetrahydromangostin (**157**)	12.5
3-Mono-*O*-benzylmangostin (**144**)	inactive	6-Mono-*O*-benzyltetrahydromangostin (**158**)	6.25
3,6-Di-*O*-methylcarboxymangostin (**99**)	12.5	3,6-Di-*O*-methylcarboxy--tetrahydromangostin (**159**)	3.13
3,6-Di-*O*-ethylcarboxymangostin (**145**)	50	3,6-Di-*O*-ethylcarboxy--tetrahydromangostin (**160**)	1.56
3,6-Di-*O*-propylcarboxymangostin (**146**)	50	3,6-Di-*O*-propylcarboxy--tetrahydromangostin (**161**)	25
3,6-Di-*O*-phenylmangostin (**147**)	inactive	3,6-Di-*O*-phenylcarboxy-tetrahydromangostin (**162**)	12.5
6-Mono-*O*-phenylmangostin (**148**)	12.5	6-Mono-*O*-phenylcarboxy-tetrahydromangostin (**163**)	3.125
		3-Mono-*O*-phenylcarboxy-tetrahydromangostin (**164**)	12.5

1) Inactive at MIC > 200 μg/mL

2) Standards : kanamycin as positive control; MIC = 1.25-2.5 μg/mL, isoniazid MIC = 0.05-0.1 μg/mL, rifampin MIC = 0.0023-0.0047 μg/mL

TABLE 6 Antimycobacterial activity against *M. tuberculosis* of *O*-methylated analogues **149** and **165-169** (MIC μg/mL)

Compounds	MIC	Compounds	MIC
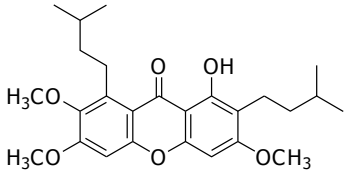 **149**	inactive	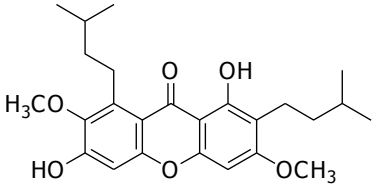 **165**	12.5
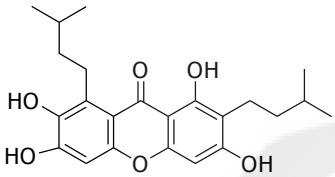 **166**	6.25	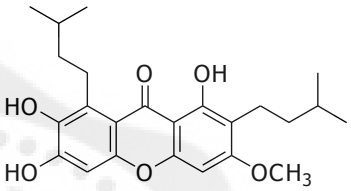 **167**	25
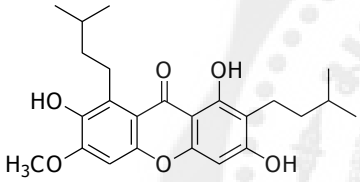 **168**	3.13	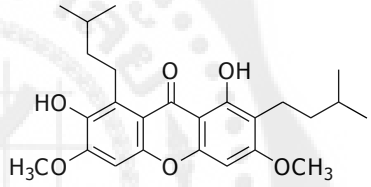 **169**	inactive

1) Inactive at MIC > 200 μg/mL

2) Standards: kanamycin as positive control; MIC = 1.25-2.5 μg/mL, isoniazid MIC = 0.05-0.1 μg/mL, rifampin MIC = 0.0023-0.0047 μg/mL

14.2 Anti-viral assay

Antiviral activity was evaluated against the *Herpes simplex* virus-type 1 employing a modified plaque reduction assay (Aou-Karum; et al. 1990: 340) and the colorimetric method described by Skehan et al (Skehan; et al. 1990: 1107). Briefly, microtiter trays with confluent monolayer cultures of Vero cells were inverted, and the medium was shaken out and replaced with serial dilutions of drugs in triplicate in 100 μL medium followed by tittered virus in 100 μL medium containing 10% calf serum in each well. In each tray the last row of well was reserved for controls that were not treated with the drugs. The tray were cultured for 66 h with care being taken not to disturb the cultures during incubation. The trays were inverted onto a pad of paper towels, and the remaining cells were rinsed carefully with medium and fixed with 3.7% formaldehyde in saline for at least 20 min. The fixed cells were rinsed with H_2O, strained with 0.5% crystal violet in 20% aqueous EtOH for 30 min, rinsed with H_2O, and examined visually. Antiviral activity is identified as confluent, relatively unaltered monolayer of stained Vero cells treated with HSV-1.

TABLE 7 Antiviral activity against HSV-1 of **1** and its analogues (IC_{50} , μg/mL)
(standard: acyclovir as positive control; IC_{50} = 2.0 μg/mL)

Compounds	IC_{50}	Compounds	IC_{50}
α -Mangostin (**1**)	mod act	Tetrahydromangostin (**90**)	1.10
3,6-Di-*O*-methylmangostin (**84**)	inactive	3,6-Di-*O*-methyltetrahydromangostin (**149**)	mod act
6-Mono-*O*-methylmangostin (**140**)	1.39	6-Mono-*O*-methyltetrahydromangostin (**150**)	mod act
3,6-Di-*O*-ethylmangostin (**85**)	inactive	3,6-Di-*O*-ethyltetrahydromangostin (**151**)	weak
3-Mono-*O*-ethylmangostin (**141**)	2.30	6-Mono-*O*-ethyltetrahydromangostin (**152**)	weak
3,6-Di-*O*-allylmangostin (**89**)	weak	3,6-Di-*O*-allyltetrahydromangostin (**153**)	inactive
6-Mono-*O*-allylmangostin (**120**)	1.70	6-Mono-*O*-allyltetrahydromangostin (**154**)	3.10
3,6-Di-*O*-(4-bromobutyl)mangostin (**142**)	inactive	3,6-Di-*O*-(4-bromobutyl)-tetrahydromangostin (**155**)	mod act
6-Mono-*O*-(4-bromobutyl)mangostin (**143**)	mod act	6-Mono-*O*-(4-bromobutyl)-tetrahydromangostin (**156**)	3.30
3,6-Di-*O*-benzylmangostin (**117**)	inactive	3,6-Di-*O*-benzyltetrahydromangostin (**157**)	6.54
3-Mono-*O*-benzylmangostin (**144**)	3.60	6-Mono-*O*-benzyltetrahydromangostin (**158**)	5.80
3,6-Di-*O*-methylcarboxymangostin (**99**)	1.50	3,6-Di-*O*-methylcarboxy-tetrahydromangostin (**159**)	mod act
3,6-Di-*O*-ethylcarboxymangostin (**145**)	1.60	3,6-Di-*O*-ethylcarboxy-tetrahydromangostin (**160**)	weak
3,6-Di-*O*-propylcarboxymangostin (**146**)	7.70	3,6-Di-*O*-propylcarboxy-tetrahydromangostin (**161**)	inactive
3,6-Di-*O*-phenylmangostin (**147**)	inactive	3,6-Di-*O*-phenylcarboxy-tetrahydromangostin (**162**)	nt
6-Mono-*O*-phenylmangostin (**148**)	8.60	6-Mono-*O*-phenylcarboxy-tetrahydromangostin (**163**)	mod act
		3-Mono-*O*-phenylcarboxy-tetrahydromangostin (**164**)	6.40

1) nt = not tested

2) mod act = moderately active

15. Synthesis of semaxanib (SU-5416, 82)

15.1 Synthesis of ethyl-2-(2-nitrophenyl) acetate (**171**)

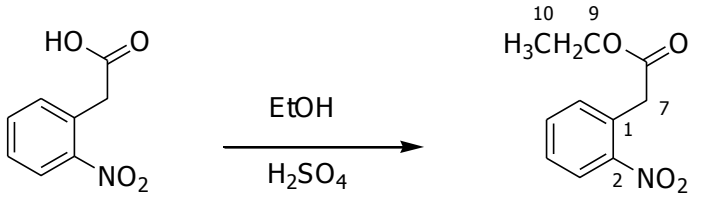

2-nitrophenyl acetic acid (**170**) ethyl-2-(2-nitrophenyl)-acetate (**171**)

To a solution of 2-nitrophenylacetic acid **170** (3.144 g, 17.3 mmol) in ethanol (35 mL) was added 5 drops of concentrated sulfuric acid. The reaction was stirred under refluxing for 2 hours. The reaction was monitored by TLC (70:30; petroleum spirit : acetone). After TLC showed no starting material, the reaction was allowed to cool and the excess ethanol was removed by evaporation. The crude mixture was diluted with diethyl ether (100 mL) and added to a separating funnel. The resulting organic layer was washed with water (3x25 mL), followed by saturated sodium bicarbonate (50 mL) and saturated sodium chloride (50 mL). The resulting organic layer was dried over anhydrous magnesium sulphate and concentrated *in vacuo* to dryness. The solid product was recrystalized with the mixture solvent of acetone in petroleum spirit (5 : 95) to give **171** as pale yellow solid (3.52 g, 97%).

Ethyl-2-(2-nitrophenyl)acetate (**171**) (Anthony; et al. 2007: 1-56)

White solid.

^{1}H-NMR ($CDCl_3$, 500 MHz): δ_H 1.16 (t, 3H, *J*= 7.0 Hz, H-10), 3.93 (s, 2H, H-7), 4.07 (q, 2H, *J*= 7.0 Hz, H-9), 7.28 (d, 1H, *J*= 7.5 Hz, H-6), 7.38 (t, 1H, *J*= 8.0 Hz, H-5), 7.50 (t, 1H, *J*= 7.5 Hz, H-4), 7.99 (d, 1H, *J*= 8.5 Hz, H-3).

ESMS (+ve) *m/z* (% rel. intensity): 210 $[M+H]^+$ (100).

15.2 Synthesis of 2-formyl-3,5-dimethyl-1*H*-pyrrole-1-methylcarboxylate (**172**)

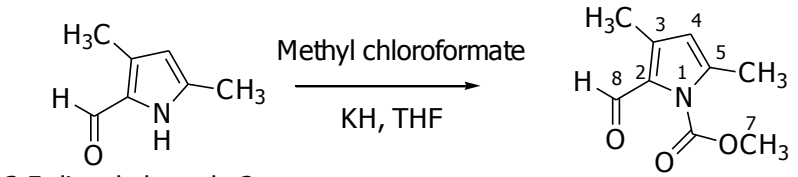

3,5-dimethylpyrrole-2-carboxaldehyde **(137)**

172

To a dry round bottom flask under an inert atmosphere (N_2) was added potassium hydride (0.41 g, 9.1 mmol) in dry THF (50 mL) and stirred and allowed to cool to 0 ºC. 3,5-Dimethylpyrrole-2-carboxaldehyde (**137**) (1.47 mg, 8.12 mmol) was diluted in dry THF (10 mL) and added dropwise to the stirred solution over ten minutes. The mixture was then allowed to stir at 0 ºC for a further 30 minutes. Methyl chloroformate (1.918 mg, 20.3 mmol) was diluted in dry THF (10 mL) and added dropwise to the stirring mixture over ten minutes. The reaction mixture was allowed to stir for a further 2 hours at room temperature. The reaction was followed by TLC (70:30; petroleum spirit : acetone). After TLC showed no starting material, the reaction was quenched with cooled ice-water (30 mL) and allowed to stir for fifteen minutes. The crude mixture was then extracted with ethyl acetate (3x25 mL) and concentrated *in vacuo*. The crude product was purified by gradient flash chromatography using 100% petroleum spirit to 95:5 (pet spirit: acetone) and concentrated *in vacuo* to give 2-formyl-3,5-dimethyl-1*H*-pyrrole-1-carboxylate (**172**) (1.83 g, 86%).

2-Formyl-3,5-dimethyl-1*H*-pyrrole-1-methylcarboxylate (**172**) (Anthony; et al. 2007: 1-56).

Light brown solid, m.p. 173-174 $^{\circ}$C.

^{1}H-NMR ($CDCl_3$, 500 MHz): δ_H 2.34 (s, 3H, 3-CH_3), 2.42 (s, 3H, 5-CH_3), 4.00 (s, 3H, H-7), 5.93 (s, 1H, H-4), 10.03 (s, 1H, H-8).

ESMS (+ve) *m/z* (% rel. intensity): 182 $[M+H]^+$ (100).

.

15.3 Synthesis of (Z)-ethyl-3-(3,5-dimethyl-1*H*-pyrrole-2-yl)-2-(2-nitrophenyl) acrylate (**173**) and (*E*)-ethyl-3-(3,5-dimethyl-1*H*-pyrrole-2-yl)-2-(2-nitrophenyl) acrylate (**174**)

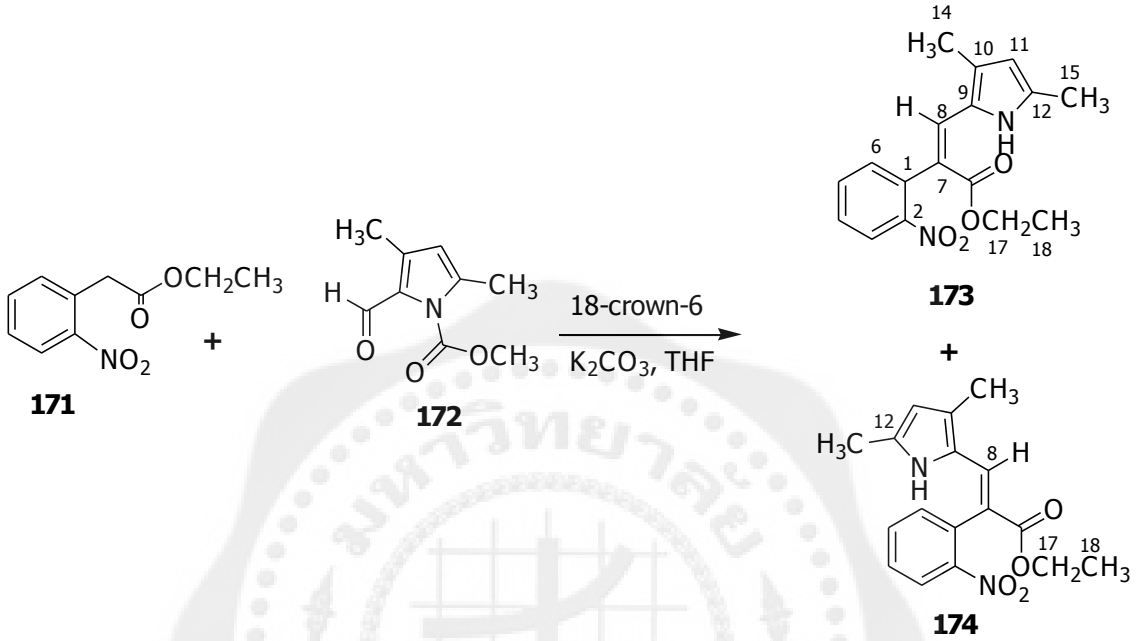

To a dry round bottom flask under an innert atmosphere was added anhydrous potassium carbonate 0.152 g, 1.106 mmol) in dry THF (15 mL) followed by addition of 18-crown-6 (0.082 g, 0.284 mmol). The mixture was stirred at room temperature for 10 minutes followed by addition of the solution of ethyl-2-(2-nitrophenyl) acetate (**171**) (0.115 g, 0.553 mmol) in dry THF (5 mL). The mixture was then heated at reflux for 3.0 hours. Methyl-2-formyl-3,5-dimethyl-pyrrole-1-carboxylate (**172**) (0.081 g, 0.477 mmol) was diluted in dry THF (5 mL) and added drop wise over 15 minutes to the stirring solution. The mixture was then heated at reflux for 18 hours. The mixture was quenched with water (30 mL), transferred to a separating funnel and extracted with ethyl acetate (3x35 mL). The organic layer was washed with saturated sodium bicarbonate (100 mL) and saturated sodium chloride (100 mL), then dried over magnesium sulphate and concentrated *in vacuo*. The crude product was purified by column chromatography using a gradient from petroleum spirit to 95:5 (pet spirit: acetone) to give **173** in 42% yield (0.0743 g) and **174** in 35 % yield (0.0555 g).

(*Z*)-Ethyl-3-(3,5-dimethyl-1*H*-pyrrole-2-yl)-2-(2-nitrophenyl)acrylate (**173**)

Red solid, m.p.143-146 º C.

R_f (30% acetone: pet spirit): 0.57.

IR (KBr) ν_{max} : 3280 (N-H), 1684 (C=O), 1579 and 1544 (C=C), 1519 (N-O Asymmetric stretching), 1338 (N-O Symmetric stretching) and 1200 (C-O) cm^{-1}.

^{1}H-NMR ($CDCl_3$, 500 MHz): δ_H 1.13 (t, 3H, *J*= 7.0 Hz, H-18), 2.17 (s, 3H, H-14), 2.35 (s, 3H, H-15), 4.12 (q, 2H, *J*= 7.0 Hz, H-17), 5.90 (s, 1H, H-11), 6.82 (s, 1H, H-8), 7.43 (m, 1H, H-6), 7.62 (t, 2H, *J*= 8.0 Hz, H-4, H-5), 8.02 (d, 1H, *J*= 8.0 Hz, H-3), 11.89 (br s, 1H, NH).

^{13}C-NMR ($CDCl_3$, 126 MHz): δ_C 13.7 (C-14), 14.1 (C-15), 29.9 (C-18), 62.1 (C-17), 111.5 (C-11), 112.7 (C-8), 124.1 (C-10), 124.6 (C-3), 127.8 (C-6), 129.9 (C-12), 131.5 (C-5), 132.5 (C-1), 133.5 (C-9), 134.3 (C-4), 137.5 (C-7), 148.5 (C-2), 161.1 (C-16).

ESMS (+ve) *m/z* (% rel. intensity): 314 $[M]^+$ (100).

(*E*)-Ethyl-3-(3,5-dimethyl-1*H*-pyrrole-2-yl)-2-(2-nitrophenyl)acrylate (**174**)

Red solid, m.p. 186-189 º C.

R_f (30% acetone: pet spirit): 0.32.

IR (KBr) ν_{max} : 3420 (N-H) 1701 (C=O), 1621 and 1565 (C=C), 1519 (N-O Asymmetric stretching), 1338 (N-O Symmetric stretching) and 1235 (C-O) cm^{-1}.

^{1}H-NMR ($CDCl_3$, 500 MHz): δ_H 1.19 (t, 3H, *J*= 7.0 Hz, H-18), 1.95 (s, 3H, H-14), 2.19 (s, 3H, H-15), 4.10 (dq, 1H, *J*= 4.0, 7.0 Hz, H-17), 4.23 (dq, 1H, *J*= 3.7, 7.0 Hz, H-17), 5.74 (s, 1H, H-11), 6.80 (s, 1H, NH), 7.49 (t, 1H, *J*= 7.5 Hz, H-4), 7.59 (t, 1H, *J*= 7.5 Hz, H-5), 7.67 (d, 1H, *J*= 7.5 Hz, H-6), 7.75 (s, 1H, H-8), 8.19 (t, 1H, *J*= 7.5 Hz, H-3).

^{13}C-NMR ($CDCl_3$, 126 MHz): δ_C 11.3 (C-15), 13.2 (C-14), 14.1 (C-18), 60.8 (C-17), 110.7 (C-11), 116.6 (C-7), 123.4 (C-10), 125.6 (C-3), 127.2 (C-8), 129.2 (C-4), 130. (C-9), 132.5 (C-1), 133.3 (C-6), 133.4 (C-5), 133.7 (C-12), 149.2 (C-2), 166.6 (C-16).

HR-TOFMS (ES^+): *m/z* 315.1237 $[M+H]^+$; calcd for $C_{17}H_{17}N_2O_4$ + H, 315.1723.

15.4 Acid catalized isomerisation of (*E*)-ethyl-3-(3,5-dimethyl-1*H*-pyrrol-2-yl)-2-(2-nitrophenyl) acrylate (**174**)

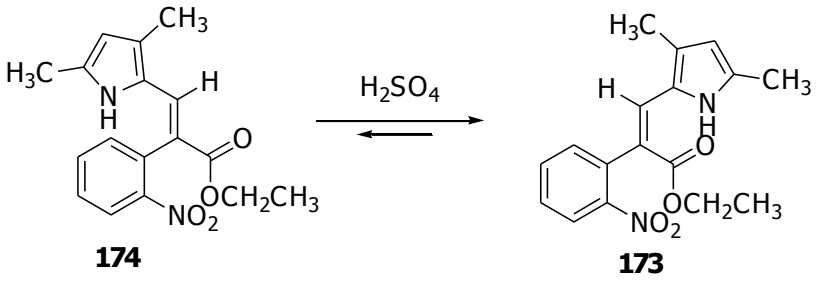

174 **173**

To a round bottom flask was added compound **174** (0.0555 g, 0.176 mmol) in THF (5.0 mL) followed by addition of concentrated sulfuric acid 3 drops. The mixture was then stirred at room temperature for 16 hours. The reaction was quenched with ice-water (100 mL) and transferred to a separating funnel and extracted with ethyl acetate (3x35 mL), washed the combined ether layers with saturated sodium bicarbonate (100 mL), then dried over magnesium sulphate and concentrated *in vacuo*. The crude product was purified by column chromatography using a gradient from petroleum spirit to 95:5 (pet spirit : acetone) to give **173** as red solid (0.0326 g, 58%) along with starting **174** as red brown solid (0.0093 g, 17%).

15.5 Reductive cyclisation of (*Z*)-ethyl-3-(3,5-dimethyl-1*H*-pyrrol-2-yl)-2-(2-nitrophenyl) acrylate (**173**) to produce semaxanib (SU5416**, 82**)

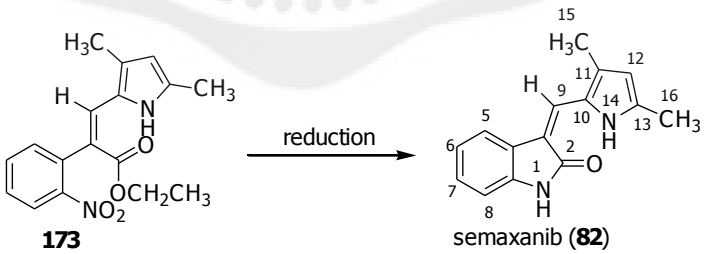

173 semaxanib (**82**)

15.5.1 Reduction using ammonium formate/Pd-C (Pogorelic'; et al. 2007: 202)

To a stirred suspension of nitro ethyl ester (**173**) (0.0507 g, 0.1603 mmol), and 10% Pd-C (0.02-0.03 g) in methanol (5 mL), ammonium formate was added (0.0397 g, 0.652 mmol) in a single portion. The resulting reaction

mixture was stirred at room temperature for 24 hours under nitrogen atmosphere. TLC (70:30; pet spirit: acetone) showed that the product was not observed.

15.5.2 Reduction using Fe (0) in CH_3COOH (Gamble; et al. 2007: 2777)

Compound **173** (0.0508 g, 0.161 mmol) was dissolved in a mixture of glacial acetic acid (2 mL), ethanol (3 ml) and water (2 mL). Reduced iron powder (0.085g, 1.51 mmol) was added and the reaction subjected to ultrasonic irradiation for 1 hour at 30 $^{\circ}C$. TLC (70:30; pet spirit: acetone) showed no starting material. The reaction mixture was filtered through a celite and washed with ethanol (20 mL). The filtrate was evaporated to dryness and was then extracted with diethyl ether (3x 15 mL) and water. The organic layer was wash with saturated sodium bicarbonate (30 mL), water (30 mL), and sodium chrolide (30 mL). The organic layer was dried over magnesium sulphate and concentrated *in vacuo*. The crude product was purified by column chromatography using a gradient from 100% petroleum spirit to 85:15 (pet spirit: acetone) to afford SU5416 (**82**) in 81% yield (0.0309 g).

15.5.3 Reduction using $NaBH_4$/Pd-C (Pogorelic'; et al. 2007: 202)

To a stirred suspension of an (Z)-alkene ethyl ester (**173**) (0.052 g, 0.166 mmol), Pd-C (0.01-0.05 g) in mixture solvent of CH_3OH and water (2:1, 5 mL), sodium borohydride was added (0.0126 g, 0.332 mmol). The resulting reaction mixture was stirred at room temperature for 30 minutes, the catalyst was removed through a celite pad and washed with methanol (20 mL). The filtrates was evaporated *in vacuo*. The resulting residue was triturated with water (20 mL), extracted with diethyl ether (15x3 mL) and dried over anhydrous Na_2SO_4. The crude product was purified by column chromatography using a gradient from 100% petroleum spirit to 85:15 (pet spirit: acetone) to give semaxanib (**82**) in 72 % yield (0.027 g).

15.5.4 Catalytic hydrogenation reaction (Pogorelic'; et al. 2007: 202)

A mixture of **173** (0.0507 g, 0.161 mmol) and Pd black in ethanol (5 mL) was vigorously stirred under hydrogen atmosphere (balloon) for 3 hours. The insoluble material were filtered off through a celite pad, and the filtrate was concentrated *in vacuo*. The crud product was purified by column chromatography with mixture solvent (petroleum spirit: acetone: 5:95), to afford **82** in 36% yield (0.0135 g) along with the decomposed product.

(*Z*)-3-[(2,4-Dimethylpyrrole-5-yl)methylidenyl]indolin-2-one (semaxanib, **82**)

Yellow solid, m.p. 217-220 ºC. (lit. 220-222 ºC, Lubkol; et al. 2010: 6606)

IR (KBr) ν_{max}: 3170, 1762, 1556, 1464, 1340, 1289, 784 and 734 cm^{-1}.

^{1}H-NMR (DMSO-d_6, 500 MHz): δ_H 2.28 (s, 3H, H-15), 2.30 (s, 2H, H-16), 5.99 (s, 1H, H-12), 6.83 (d, 1H, *J*= 7.4 Hz, H-5), 6.95 (t, 1H, *J*= 7.4 Hz, H-6), 7.08 (t, 1H, *J*= 7.4 Hz, H-7), 7.54 (s, 1H, H-9), 7.69 (d, 1H, *J*= 7.4 Hz, H-8), 10.78 (br s, 1H, H-1), 13.34 (br s, 1H, H-14).

^{13}C-NMR (DMSO-d_6, 126 MHz): δ_C 11.3 (C-15), 13.5 (C-16), 109.2 (C-5), 112.5 (C-12), 118.0 (C-8), 120.8 (C-7), 123.3 (C-9), 125.7 (C-2), 125.8 (C-4), 126.6 (C-6), 131.6 (C-10), 135.6 (C-13), 138.1 (C-8a), 169.4 (C-2).

ESMS (+ve) *m/z* (% rel. intensity): 238 $[M+H]^+$ (100).

CHAPTER 4

RESULTS AND DISCUSSTION

1. Synthesis of α-mangostin (1) analogues

α-Mangostin (**1**) has successfully been modified as *O*-alkylated and *O*-acylated analogues including its hydrogenated derivatives by using *O*-alkylation, *O*-acylation and catalytic hydrogenation reactions. 1D- and 2D NMR experiments allowed the assignments for proton and carbon chemical shifts of all synthetic products. Reaction conditions and percentage yields of the corresponding products are summarized in Table 8.

1.1 Synthesis of 3,6-di-*O*-methylmangostin (**84**) and 6-mono-*O* methylmangostin (**140**)

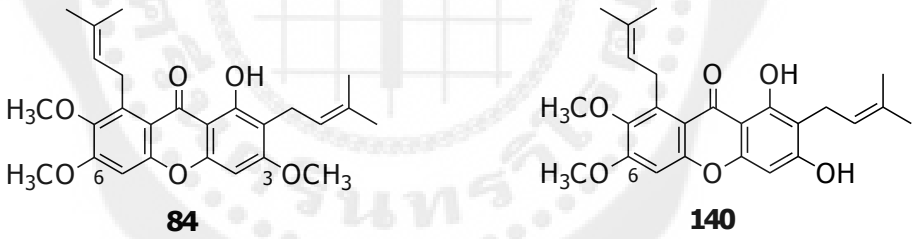

84 **140**

Compounds **84** and **140** were obtained in 33 and 39% yields respectively (Table 8), by treatment of α-mangostin (**1**) with methyl iodide in acetone solution in the presence of K_2CO_3 at room temperature. The NMR spectrum of compound **84** was identical to that of starting compound **1** except for the presence of two extra methoxyl signals at δ_H 3.89, δ_c 55. (3-OCH_3) and δ_H 3.95, δ_c 55.8 (6-OCH_3), meaning that **84** was the di-*O*-methylated derivative. The protonated molecular ion peak at *m/z* 439 $[M+H]^+$ was observed from the ESMS. The NMR data for compound **84** combined with its ESMS indicated that compound **84** was 3,6-di-*O*-methylmangostin. Compound **84** has been synthesized to evaluate antifungal activity and cytotoxicity by the research group of Gopalakrisnan

(Gopalakrishnan; et al. 1997: 519) and Ha (Ha; et al. 2009: 830), respectively. In addition, compound **84** is known as naturally occurring fuscaxanthone C (Panthong; et al. 2006: 999).

The ESMS of compound **140** exhibited the sodiated molecular ion peak at *m/z* 447 $[M+Na]^+$. The NMR spectrum of compound **140** showed only one extra singlet signal at δ_H 3.93 (δ_c 55.9) with integration for three protons, when compared with the ^{1}H-NMR spectrum of **1** (δ_H 3.96) , extra singlet signal indicating that the product **142** was the mono-methylated analogue of **1**. The HMBC experiment revealed the ^{13}C-^{1}H correlation between H-5 (δ_H 6.74) and proton of O-CH_3 with C-6 (δ_C 158.0) which indicated that the new one methoxyl group was located at C-6 position. Thus, compound **142** was indeed 6-mono-*O*-methylmangostin. In addition, ^{1}H and ^{13}C-NMR data of **142** was very similar to that of cowaxanthone B, a natural xanthone isolated from *Garcinia cowa* (Panthong; et al. 2006: 999). Therefore the structure of **142** was proved to be 6-*O*-monomethylmangostin.

1.2 Synthesis of 3,6-di-*O*-ethylmangostin (**85**) and 3-mono-*O*-ethylmangostin (**141**)

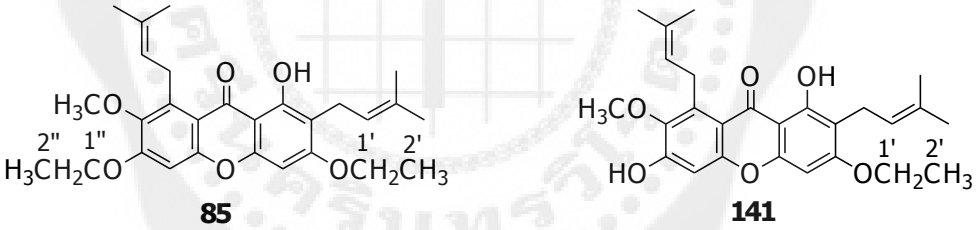

85 **141**

Compounds **85** and **141** were prepared from the *O*-ethylation reaction of **1** by the treatment with diethyl sulfate in the presence of potassium carbonate in acetone. Compound **85** was isolated as the major product in 24% yield (Table 8) and ESMS indicated the sodiated molecular ion peak at *m/z* 489 $[M+Na]^+$. The ^{1}H-NMR spectrum of compound **85** showed the signal of hydrogen bonded hydroxyl group at δ_H 13.49 (s, 1-OH) and the presence of the overlapping signal *O*-methylene proton at δ_H 4.12 (m, 4H) which was assigned to be H-1' and H-1". The two triplet signals of extra methyl proton appeared at δ_H 1.47 (*J*= 7.0 Hz) and 1.53 (*J*= 6.9 Hz) assignable to H-2" and H-2', respectively. The NMR data for compound **85** combined with its mass spectrum indicated

that compound **85** was a 3,6-di-*O*-ethylmangostin. Compound **85** has been also synthesized by Gopalakrishnan and coworker (Gopalakrishnan; et al. 1997: 519).

Compounds **141** was isolated as minor product (6%, Table 8) from the same reaction with the formation of **85**. Its HR-FABMS indicated a pseudo-molecular ion peak at *m/z* 439.2120 $[M+H]^+$ which was compatible with the molecular formular $C_{26}H_{30}O_6$. The ^{1}H-NMR displayed the signal of hydrogen bonded hydroxyl proton at δ_H 13.39 (s, 1H, 1-OH) and the presence of the extra ethyl ether group at δ_H 4.12 (q, 2H, *J*= 6.9 Hz) and δ_H 1.43 (br t, 3H, *J*= 6.9 Hz) when compared with the parent compound **1**. The HMBC experiment of compound **141** showed ^{1}H-^{13}C correlation of singlet aromatic proton at δ_H 6.29 (H-4) and the *O*-methylene proton (H-1') at δ_H 4.12 (δ_c 64.1) to the same aromatic quarternary carbon at δ_C 159.7 (C-3). This observation confirmed that compound **141** was 3-mono-*O*-ethylmangostin which was obtained from the *O*-ethylation reaction at the more sterically hindered 3-OH.

1.3 Synthesis of 3,6-di-*O*-allylmangostin (**89**) and 6-mono-*O*-allylmangostin (**120**)

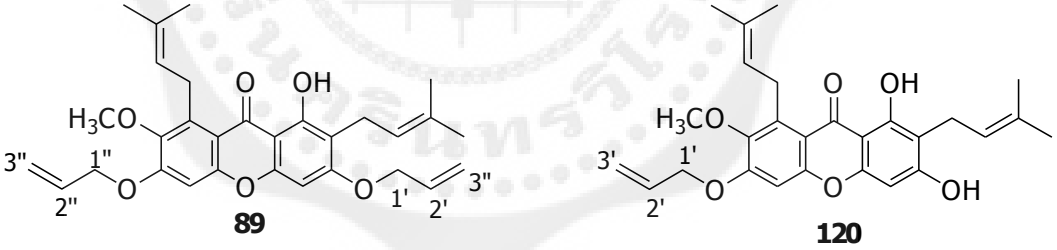

Compounds **89** and **120** were obtained by treatment of α-mangostin (**1**) with allyl bromide in acetone solution in the presence of K_2CO_3 at room temperature (Table 8). Compound **89** was isolated from this *O*-allylation reaction as major product in only 19% yield. The ESMS of compound **89** exhibited the $[M+Na]^+$ ion at *m/z* 513. The comparison of ^{1}H-NMR spectrum of compound **89** with parent **1** showed that **89** was identical to the spectrum of **1** except for the presence of two doublet signals at δ_H 4.61 (2H, *J* = 4.9 Hz, H-1'), δ_H 4.65 (2H, *J* = 5.0 Hz, H-1'') and for the presence of olefinic proton as multiplet signals at δ_H 5.41 (4H, H-3', H-3'') and δ_H 6.08 (2H, H-2', H-2''), indicating the presence of two allyl groups in the core structure. The ^{13}C-NMR spectrum

also indicated the presence of two *O*-allyl groups at δ_c 69.0 (C-1'), 69.4 (C-1''), 117.7 (C-3'), 118.4 (C-3''), 131.9 (C-2') and 132.5 (C-2''). The presence of 1-OH proton signal at δ_H 13.47 (s, 1H) in ^{1}H-NMR spectrum of **89** combined with its ^{13}C-NMR and mass data confirmed that compound **89** was 3,6-di-O-allylmangostin. In addition, compound **89** has been successfully synthesized to evaluate antifungal activity against phytopatogenic fungi by the research group of Gopalakrishnan (Gopalakrisnan; et al. 1997: 519).

The ^{1}H-NMR spectrum of compound **120** exhibited the 1-OH signal as singlet at δ_H 13.82 and one extra *O*-methylene proton signal at δ_H 4.65 (2H, *J*= 5.0 Hz), which was assigned to be H-1'. In addition, ^{1}H-NMR spectrum of **120** also showed new olefinic proton signals at δ_H 5.33 (br d, 1H, *J*= 16.3 Hz), δ_H 5.46 (d, 1H, *J*= 10.5 Hz) and δ_H 6.10 (m, 1H,) assignable to H-3'$_{trans}$, H-3'$_{cis}$ and H-2', respectively. The signals at δ_c 69.4, 118.4 and 131.9 in ^{13}C-NMR spectrum of **120** were assigned as C-1', C-3' and C-2', respectively. The HR-FABMS of compound **120** exhibited the pseudomolecular ion peak at *m/z* 451.2120 $[M+H]^+$ which was compatible with the molecular formular $C_{27}H_{31}O_6$. HMBC experiment of compound **120** showed ^{1}H-^{13}C correlation of doublet signal proton at δ_H 4.65 (H-1') and singlet signal of aromatic proton at δ_H 4.26 (H-1') to the same oxygenated quarternary carbons at δc 156.9 (C-6). Combining the spectroscopic information described above, we concluded that compound **120** was 6-mono-*O*-allylmangostin. Compound **120** has been prepared by Ha and coworker to evaluate for its cytotoxic activity (Ha; et al. 2009: 830).

1.4 Synthesis of 3,6-di-*O*-(4-bromobutyl)mangostin (**142**) and 6-mono-*O*-(4-bromobutyl)mangostin (**143**)

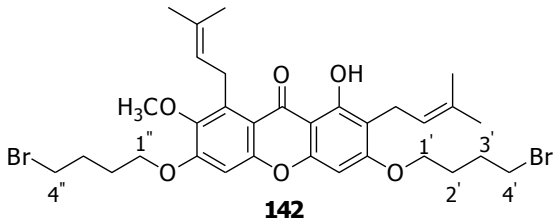

142

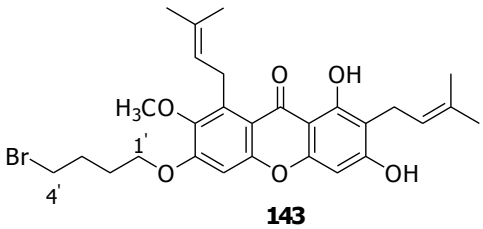

143

Compounds **142** and **143** were obtained by treatment of **1** with 1,4-dibromobutane in acetone solution in the presence of potassium carbonate in 31 (52.0 mg) and 16 % (22.0 mg) yields, respectively. The ESMS spectrum of compound **142**

displayed the pseudomolecular ion peak at *m/z* 679 $[M+H]^+$. The ^{1}H-NMR signals at δ_H 13.47 (br s, 1H, 1-OH), 2.08 (br s, 8H, H-2', H-2", H-3' and H-3"), 3.49 (br t, 4H, *J*= 6.3 Hz, H-4' and H-4"), and 4.06 (br t, 4H, *J*= 5.4 Hz, H-1' and H-1") suggested the presence of two 4-bromobutyl substituents in core structure. The ^{13}C-NMR of **142** also indicated the presence of two 4-bromobutyl groups at δ_c 27.6, 27.7, 33.1, 33.2, 67.2 and 67.8 assigned to C-3', C-3", C-4', C-4", C-1', C-1", respectively and overlapping signal at δ_c 29.3 assigned to C-2' and C-2". Combining the spectroscopic data described above we concluded that the structure of **142** was 3,6-di-*O*-(4-bromobutyl)mangostin.

The ^{1}H-NMR spectrum of compound **143** revealed the presence of only one 4-bromobutyl group at δ_H 2.03 (m 2H, H-3'), 2.08 (m, 2H, H-2'), 3.51 (t, 2H, *J*= 6.3 Hz, H-4') and 4.10 (br s, 2H, H-1') when compared to that of compound **1**. The ^{13}C-NMR spectrum also confirmed the presence of one new substituent at δ_c 27.6 (C-3'), 29.3 (C-2'), 33.0 (C-4') and 67.8 (C-1'). The broad singlet at δ_H 4.10 correlates to the quaternary carbon resonating at δc 157.0 (C-6) in its HMBC spectrum, indicated that the mono-substitution occurred at C-6. The ESMS of compound **143** exhibited the pseudomolecular ion peak at *m/z* 545 $[M-H]^-$. The NMR data for compound **143** combined with its mass data indicated that compound **143** was 6-mono-*O*-(4-bromobutyl)mangostin.

1.5 Synthesis of 3,6-di-*O*-benzylmangostin (**117**) and 3-mono-*O*-benzylmangostin (**144**)

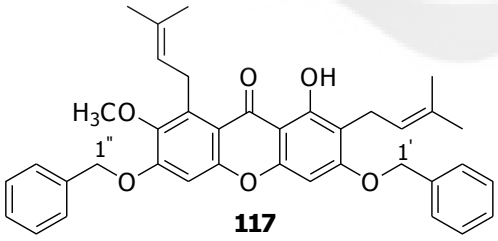

117

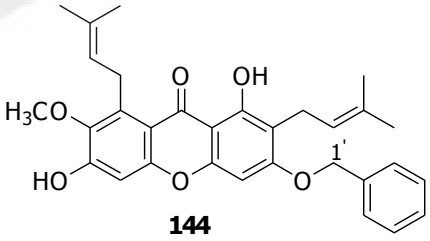

144

Compounds **117** (26.0 mg, 13%) and **144** (48.0 mg, 24%) were synthesized from the *O*-benzylation reaction of **1** by treatment with benzyl bromide in ethanol solution in the presence of mild base potassium carbonate. The ESMS of compound **117** exhibited the $[M+H]^+$ ion at *m/z* 591. The ^{1}H-NMR spectrum of compound **117** showed the presence of new benzylic proton signals at δ_H 5.08 (s, 2H, H-1') and 5.12

(s, 2H, H-1'') as well as aromatic proton signal at δ_H 7.34 (m, 10H). The ^{13}C-NMR spectrum of **117** showed the extra two benzylic carbon at δ_c 70.2 (C-1') and 70.7 (C-1)' indicating that the product was di-*O*-benzylated derivative. A comparison of its NMR and mass data with literature data of 3,6-di-*O*-benzylmangostin indicated that compound **117** was indeed 3,6-di-*O*-benzylmangostin. A literature search revealed that compound **117** has been prepared to evaluate cytotoxicity against MCF-7 and DLD-1 cell lines by Ha and coworkers (Ha; et al. 2009: 830).

Compound **144** was obtained as major product from this reaction. The ^{1}H-NMR spectrum of compound **144** was identical to the spectrum of compound **117** except for the presence of only one benzylic proton signal at δ_H 5.15 (s, 2H, H-1') and a multiplet at δ_H 7.41 (m, 5H) representing one benzyl group. The ^{13}C-NMR spectrum of **144** showed the only one extra benzylic carbon at δ_c 70.3 (C-1') suggesting that it was mono-*O*-benzylated derivative. The position of benzyl group was determined using HMBC. The proton resonating at δ_H 5.15 (s, 2H, H-1') and δ_H 6.37 (s, 1H, H-4) coupled to one of oxygenated quarternary carbon (δ_C 162.5 (C-3)) of the mangostin ring. This implied that the *O*-benzyl group was connected to C-3 on mangostin core. The HR-FABMS of compound **144** at *m/z* 501.2277 was compatible with the molecular formula $C_{31}H_{32}O_6$. The NMR for compound **144** combined with its mass data indicated that **144** was 6-mono-*O*-benzylmangostin.

1.7 Synthesis of 3,6-di-*O*-methylcarboxymangostin (**99**)

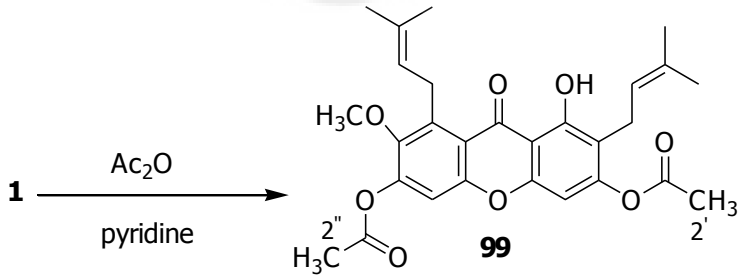

Compound **99** was obtained as a single product (81.0 mg, 68% yield) from acetylation reaction of **1** by treatment with acetic anhydride in pyridine. The ESMS of compound **99** exhibited the $[M+H]^+$ ion at *m/z* 495. The ^{1}H-NMR spectrum of

compound **99** showed two singlet signals assigned to the acetyl methyl proton (δ_H 2.32 (3H, H-2') and 2.37 (3H, H-2")) and the downfield shift of the H-4 and H-5 signals in $CDCl_3$ at δ 6.61 (s, 1H) and 7.10 (s, 1H) when compared with its parent compound **1** (δ_H 6.27 (s, 1H, H-4) and 6.81 (s, 1H, H-5). The only difference in their ^{13}C-NMR spectrum was the presence of the two ester carbonyl at δ_c 168.0 and 168.4. A literature search revealed that compound **99** was previously synthesized by the research group of Gopalakrisnan (Gopalakrisnan; et al. 1997: 519). The comparison of NMR and mass data of **99** with parent **1** and previous report led us assigned compound **99** as 3,6-di-*O*-methylcarboxymangostin.

1.8 Synthesis of 3,6-di-*O*-ethylcarboxymangostin (**145**)

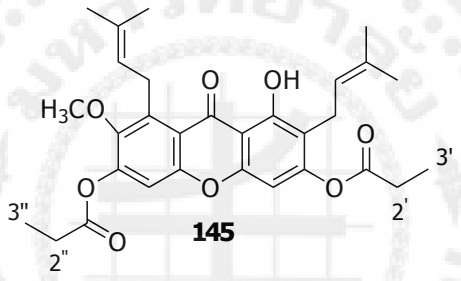

145

Compound **145** was obtained as single product in moderate yield (55 % yield) by the treatment of compound **1** with propionic anhydride in acetone solution in the presence of potassium carbonate. The HR-TOFMS spectrum of compound **145** showed the pseudomolecular ion peak at *m/z* 523.2332 $[M+H]^+$ indicating a molecular formular of $C_{30}H_{35}O_8$. The presence of two propanoates groups were evident from the two triplet signals at δ_H1.27 (3H, *J*= 7.5 Hz, H-3') and 1.30 (3H, *J*= 7.5 Hz, H-3") and from two quartet signals at δ_H 2.61 (2H, *J*= 7.5 Hz, H-2') and 2.66 (2H, *J*= 7.5 Hz, H-2'). In addition, the presence of two propanoate groups was confirmed by using ^{13}C-NMR spectroscopic data. ^{13}C-NMR spectrum of **145** exhibited two ester carbonyl carbons at δ_c 171.5 (C-1') and 171.9 (C-1"). ^{13}C-NMR spectrum of **145** also show the signal of long chain aliphatic carbon of ester group at δ_c 9.00 (C-3' and C-3"), 27.6 (C-2' and C-2"). These spectroscopic data led to conclude that compound **145** was 3,6-di-*O*-ethylcarboxymangostin.

1.9 Synthesis of 3,6-di-*O*-propylcarboxymangostin (**146**)

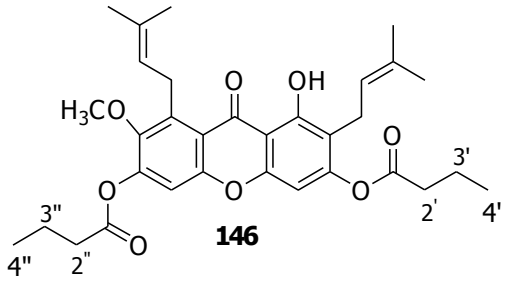

146

Compound **146** was obtained in 70% yield from the treatment of compound **1** with butyric anhydride in acetone solution in the presence of potassium carbonate. The HR-TOFMS of **146** at *m/z* 551.2639 was compatible with the molecular formular $C_{32}H_{39}O_8$. The ^{1}H-NMR spectrum of compound **146** revealed two broad triplet signals at δ_H 2.56 (2H, *J*= 7.2 Hz, H-2') and 2.61 (2H, *J*= 7.5 Hz, H-2") which were assigned as the signals of α -methylene proton of the butanoate. Its ^{1}H-NMR also showed the triplet signals at δ_H 1.04 (3H, *J*= 6.9 Hz, H-4") and multiplet signal at δ_H 1.81 (4H, H-3' and H-3"). The H-4 and H-5 signals appeared at δ_H 6.60 (s, 1H) and 7.09 (s, 1H), a large downfield shift compared with that of α-mangostin **1** (δ_H 6.27 (1H, H-4) and 6.81 (1H, H-5). These downfield shift indicated the presence of ester moiety at the 3- and 6-position. The new quaternary carbon were also observed in ^{13}C-NMR spectrum at δ_c 170.6 and 171.1, which were assigned to ester carbonyl carbons. The NMR data for compound **146** combined with its elemental composition indicated that it was 3,6-di-*O*-propylcarboxymangostin.

1.10 Synthesis of 3,6-di-O-phenylcarboxymangostin (**147**) and 6-mono-O-phenylcarboxymangostin (**148**)

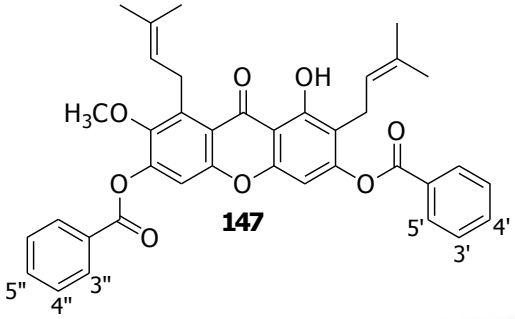

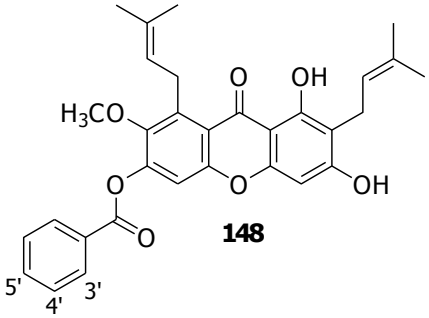

Compounds **147** and **148** were obtained from the treatment of **1** with benzoic anhydride in acetone solution in the presence of potassium carbonate in 39 and 8% yields, respectively. The ESMS spectrum of compound **147** exhibited the $[M+H]^+$ at *m/z* 619. The ^{1}H-NMR spectrum of compound **147** showed the aromatic proton signals at δ_H 7.54 (m, 2H, H-4'), 7.55 (m, 2H, H-4''), 7.68 (m, 2H, H-5', H-5''), 8.23 (m, 4H, H-3', H-3''). The presence of benzoyl moieties at the 3- and 6-position were evident from a downfield shift of H-4 (δ_H 6.78 (s, 1H) and H-5 (δ_H 7.29 (s, 1H) in the ^{1}H-NMR spectrum of compound **147** as compared with that of compound **1** (δ_H 6.27 (1H, H-4) and 6.81 (1H, H-5). ^{13}C-NMR spectrum of **147** also showed the presence of two benzoyl moieties at δ_c 163.9 and 164.2 assigned as carbonyl carbon and δ_c 128.6, 128.8, 128.9, 130.3, 132.3, 133.9 and 134.5 which were assigned to aromatic carbon of benzoyl groups. These spectroscopic data were close enough to conclude that compound **147** was indeed 3,6-di-*O*-phenylcarboxymangostin.

The HR-FABMS spectrum of compound **148** showed the protonated molecular ion peak at *m/z* 515.208. The carbonyl carbon was observed in ^{13}C-NMR spectrum as a quaternary carbon at δ_c 164.2. The ^{13}C-NMR spectrum also showed the presence new aromatic carbon of benzoyl group at δ_c 128.5, 128.8, 130.4 and 134.1 which were assigned as C-2', C-4', C-3' and C-5', respectively. The ^{1}H-NMR spectrum of **148** showed the aromatic proton signals at δ_H 7.56 (br t, 2H, *J*= 7.4 Hz, H-4'), 7.70 (br t, 1H, *J*= 7.3 Hz, H-5'), 8.23 (d, 2H, J= 7.4 Hz, H-3'). The position of the benzoyl group was determined by the analysis of ^{1}H-NMR especially the shifts for singlet signal of H-4 and H-5. The chemical shifts of the H-4 and H-5 of starting mangostin (**1**) displayed at δ_H 6.27 and

6.81, respectively. By comparison of ^{1}H-NMR spectra of compound **148** with these of precursor **1** (Figure 21), H-5 of compound **148** was shifted downfield to δ_H 7.22, while H-4 displayed as singlet signal at ca. δ_H 6.27 indicating that the benzoyl group was connected to mangostin core at C-6 position. The structure characterization of compounds **148** using the spectroscopic data mentioned above concluded that compound **148** was 3,6-di-*O*-phenylcarboxymangostin and 6-mono-*O*-phenylcarboxymangostin, respectively.

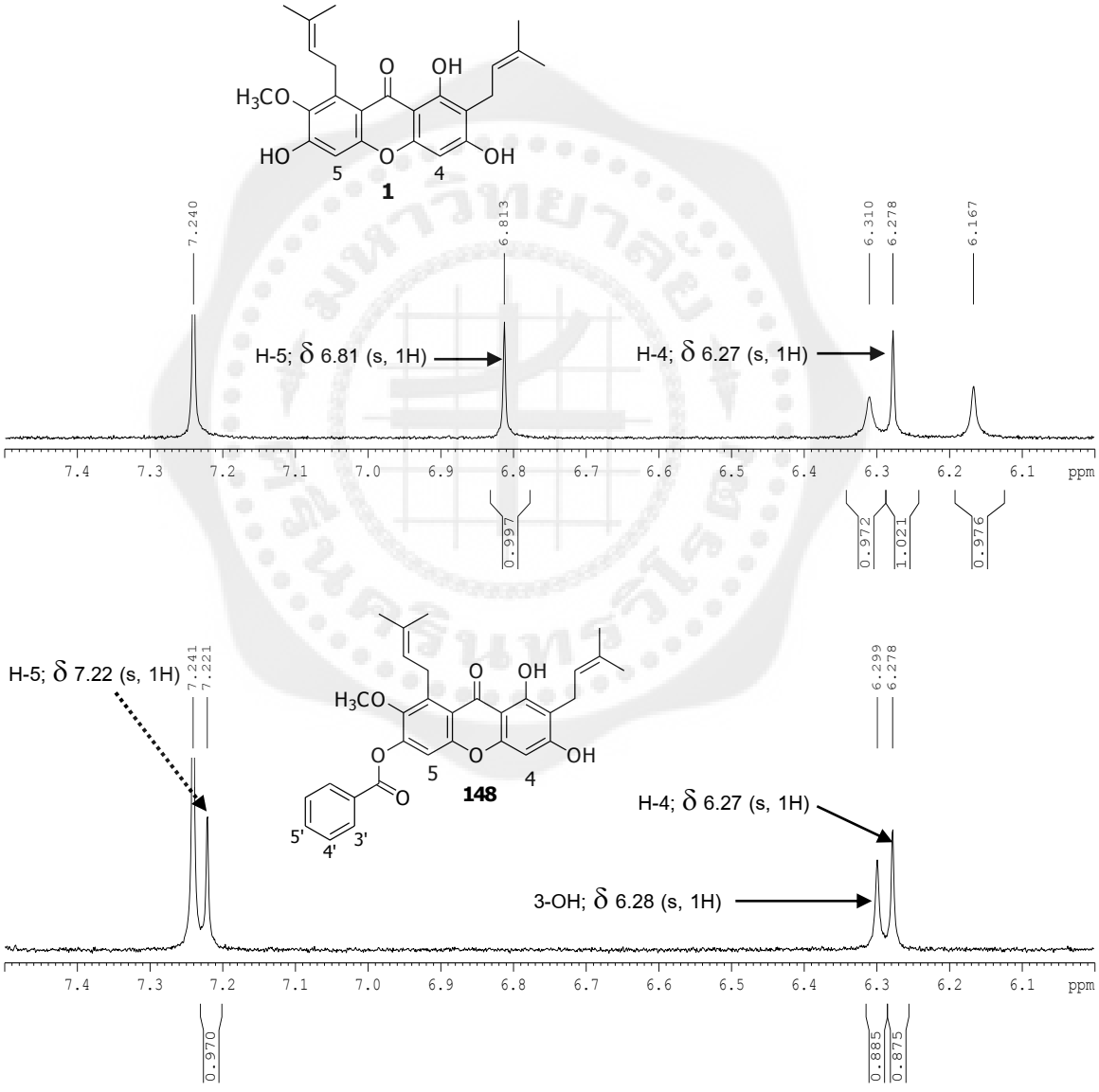

Figure 21 The downfield shift of H-5 in ^{1}H-NMR spectrum (300 MHz, in $CDCl_3$) of **148** compared to that of parent compound **1**

For the synthesis of *O*-alkylated and O-acylated derivatives of mangostin (**1**), the reaction conditions and the results including the percentage yield of the products are summarized in Table 8.

TABLE 8 Reaction conditions and percentage yields of the products obtained from the synthesis of mangostin analogues

Reactions (mole ratio)[a]	Conditions	Isolated yield of di-substituted products	Isolated yield of mono-substituted products
Methylation (1 : 1 : 4)	**1** (152.2 mg, 0.37 mmol), K_2CO_3 (51.7 mg, 0.37 mmol), MeI (200.2 mg, 1.41 mmol), acetone (1 mL), rt, 23 h.	**84** (pale yellow solid, 53.0 mg, 33%)	6-mono-substituted, **140** (pale yellow solid, 61.0 mg, 39%)
Ethylation (1 : excess : 4)	**1** (100.6 mg, 0.24 mmol), 50% KOH (39.7 mg, 0.69 mmol), Et_2SO_4 (125.6 mg, 0.81 mmol), abs. EtOH (1 mL), rt, 4 hours and 30 mins.	**85** (pale yellow solid, 38.0 mg, 24%)	3-mono-substituted, **141** (yellow viscous, 7.0 mg, 6%)
Allylation (1 : 1 : 3)	**1** (100.0 mg, 0.24 mmol), K_2CO_3 (36.6 mg, 0.26 mmol), allyl bromide (88.5 mg, 0.73 mmol), acetone (1 mL), rt, 52 h.	**89** (yellow viscous, 23.0 mg, 19%)	6-mono-substituted, **120** (pale yellow solid, 16.0 mg, 15%)
Bromobutylation (1 : 1 : 2)	**1** (100.6 mg, 0.24 mmol), K_2CO_3 (39.5 mg, 0.28 mmol), 1,4-dibromobutane (106.5 mg, 0.50 mmol), acetone (1 mL), rt, 7 d.	**142** (yellow viscous, 52.0 mg, 31%)	6-mono-substituted, **143** (yellow viscous, 22.0 mg, 16%)
Benzylation (1 : 1.5 : 3.6)	**1** (201.3 mg, 0.49 mmol), K_2CO_3 (96.2 mg, 0.69 mmol), benzyl chloride (228.8 mg, 1.81 mmol), acetone (2 mL), rt, 4 d and 15 h.	**117** (pale yellow solid, 26.0 mg, 13%)	3-mono-substituted, **144** (pale yellow solid, 48.0 mg, 24%)
Acetylation (1 : excess : 3)	**1** (99. mg, 0.24 mmol), dry pyridine (1.0 mL), acetic anhydride (74.6 mg, 0.73 mmol), rt, 24 h.	**99** (pale yellow solid, 81.0 mg, 68%)	-

TABLE 8 (continued)

Reactions (mole ratio)[a]	Conditions	Isolated yield of di-substituted products	Isolated yield of mono-substituted products
Propionylation (1 : excess : 1)	**1** (20.6 mg, 0.05 mmol), K_2CO_3 (98.4 mg, 0.71 mmol), propionic anhydride (6.53 mg, 0.05 mmol), acetone (0.5 mL), rt, 3 h.	**145** (yellow viscous, 14.3 mg, 55%)	-
Butyrylation (1 : 3 : 1)	**1** (100.3 mg, 0.25 mmol), K_2CO_3 (95.7 mg, 0.69 mmol), butyric anhydride (47.5 mg, 0.25 mmol), acetone (1 mL), rt, 4 h.	**146** (pale yellow solid, 95.0 mg, 70%)	-
Benzoylation (1 : excess : 2.8)	**1** (205.1 mg, 0.50 mmol), dry pyridine (1 mL), benzoic anhydride (47.5 mg, 0.25 mmol), acetone (1 mL), rt, 17 h and 30 mins.	**147** (yellow solid, 81.6 mg, 39%)	6-monosubstituted, **148** (yellow solid, 17.0 mg, 8%)

[a] mole **1** : mole base : mole of akylating or acylating agents

From the reaction condition and the product obtained from the *O*-alkylation and *O*-acylation of α-mangostin (**1**) (Table 8) revealed that the di-substituted analogues were the major reaction products in most cases and 1-substituted product was not observed, probably due to the chelation of intramolecular hydrogen bonding of phenolic proton (1-OH) with oxygen ketone carbonyl which led to the difficult in abstraction of H-bonded with the mild base potassium carbonate. The free 3-OH and 6-OH were identical reactive which could be abstracted by potassium carbonate and led to the formation of both 3-mono- and 6-mono- including 3,6-di-*O*-alkyated derivatives. Under the condition employed, the di-substituted and 6-mono-*O*-akylated analogues were obtained whereas the 3-mono-*O*-alkylated derivatives were not observed, this could be due to the 3-OH was affected from steric effect of prenyl group at C-2. For the formation of 3-*O*-alkylated analogues in *O*-ethylation and *O*-benzylation reactions promted us to assume that the formation of both 3-*O*-substituted and 6-*O*-substituted could be occurred at the same time however the only the 3-mono-*O*-alkylated analogues could be isolated after column chromatography under the eluting solvent system employed.

2. Synthesis of tetrahydromangostin (90)

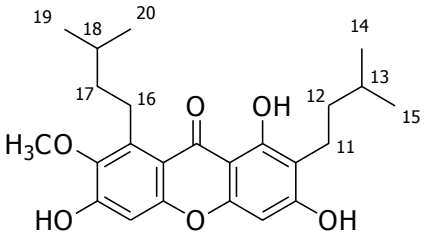

90

Compound **90** was obtained as yellow needles in excellent yield (98%) from catalytic hydrogenation of **1** by using Pd black as catalyst. The complete of hydrogenation was detected by the change of yellow to red color on the TLC after the spray with anisaldehyde-H_2SO_4 reagent. The HR-FABMS of compound **90** at *m/z* 415.2120 $[M+H]^+$ was compatible with the molecular formular $C_{24}H_{31}O_6$. The ^{1}H-NMR of compound **90** revealed the absence of olefinic proton signals at chemical shift in the region of 5.24-5.26 ppm when compared with the parent **1** (Figure 22), which suggested that hydrogenation of alkene moieties had occurred. Its ^{1}H-NMR spectrum exhibited two of broad triplet signals at δ_H 2.63 (2H, *J*= 7.9 Hz) and 3.30 (2H, *J*= 7.9 Hz) assignable to benzylic proton at C-11 and C-16, respectively. The presence of aliphatic signal proton at δ_H 0.95 (d, 6H, *J*= 6.8 Hz, H-14 and H-15), 0.97 (d, 6H, *J*= 6.8 Hz, H-19, H-20), 1.40 (br q, 2H, *J*= 7.9 Hz, H-12), 1.45 (br q, 2H, *J*= 7.9 Hz, H-17), 1.62 (m, 1H, H-13) and 1.73 (m, 1H, H-18) indicated that double bonds of prenyl groups at C-2 and C-8 were hydrogenated. The absence of double bonds of the prenyl side chains were confirmed by using ^{13}C-NMR spectroscopic data. The alkene carbon resonating in region δ_c 122-131 were not observed in the ^{13}C-NMR spectrum of **90** when compared with parent **1**, only aliphatic signals were detected at δ_c 28.2, 28.8, 37.9, 40.2 assigned to C-12, C-13, C-17 and C-18, respectively. The NMR data combined with its elemental composition indicated that compound **90** was tetrahydromangostin. Tetrahydromangostin has been previously synthesized (Iinuma; et al, 1996b: 861), however, its spectroscopic data has not yet been reported.

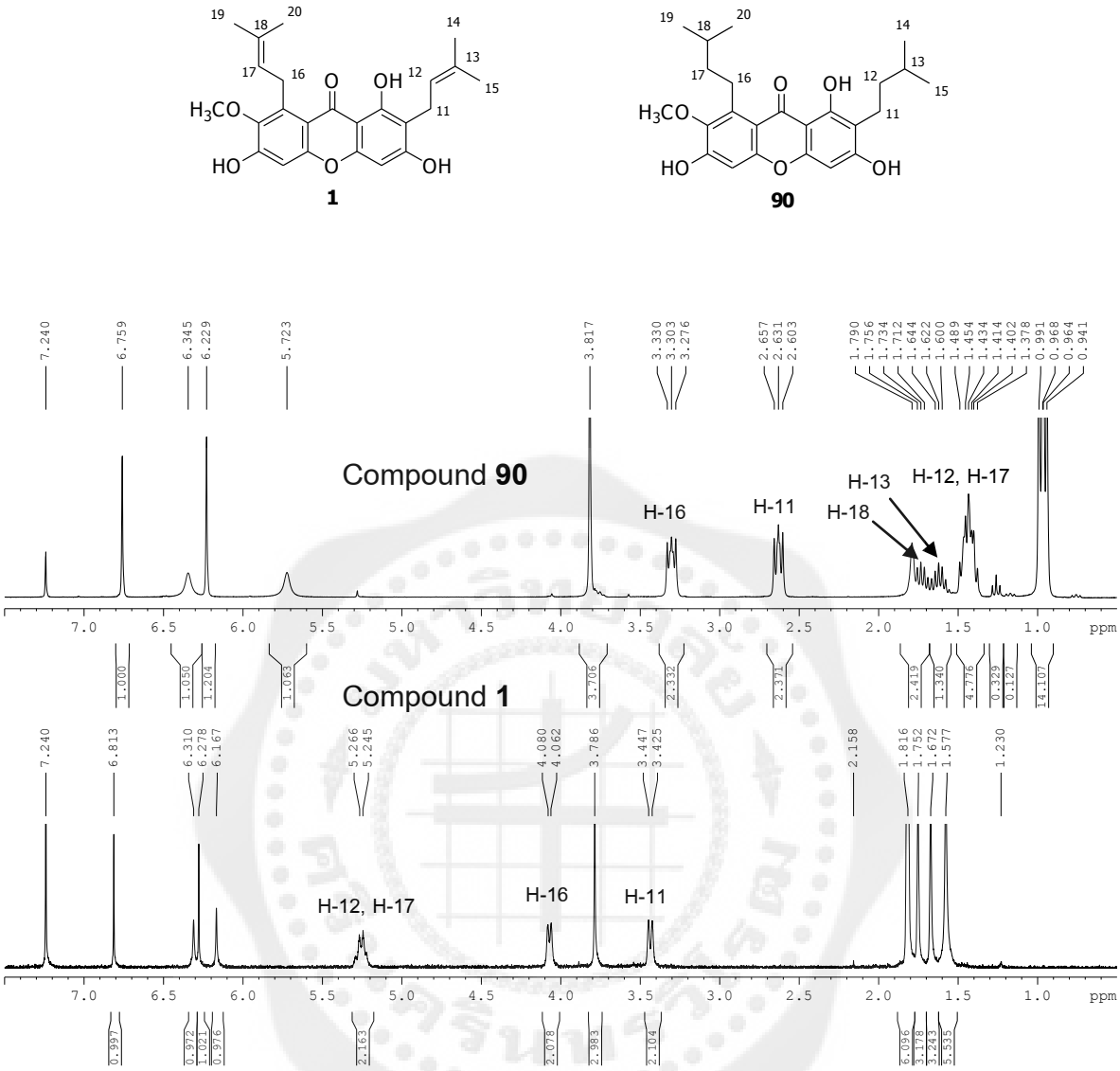

Figure 22 ^{1}H-NMR spectra (300 MHz, in $CDCl_3$) of **90** compared with compound **1**

3. Synthesis of tetrahydromangostin analogues

3.1 Synthesis of 3,6-di-*O*-methyltetrahydromangostin (**149**) and 6-mono-*O*-methyltetrahydromangostin (**150**)

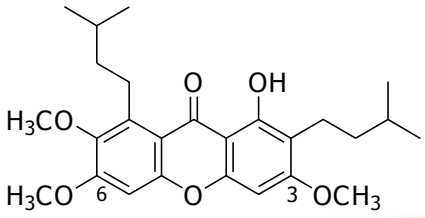

149

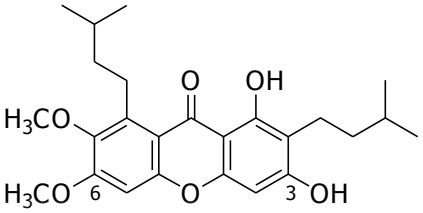

150

Compounds **149** and **150** were obtained in 30% and 40% yields, respectively, from the treatment of compound **90** with methyl iodide in acetone solution in the presence of potassium carbonate. The structures of compound **149** and **150** were characterized by their spectroscopic (^{1}H-NMR, ^{13}C-NMR and MS) data and by compared to the data of parent compound **90**. HR-TOFMS spectrum for compound **149** showed the pseudomolecular ion peak at *m/z* 443.2429 $[M+H]^{+}$ compatible with $C_{26}H_{35}O_6$+H . The ^{1}H-NMR spectrum of **149** (Figure 23a) was identical to that of compound **90** (Figure 23c) except for the presence of signals for two extra singlets at δ_H 3.87 and 3.94, which were assigned as the proton signals of the new methoxyl groups at C-3 and C-6, respectively. The ^{13}C-NMR spectrum of **149** (Figure 24a) revealed the presence of two extra *O*-methyl carbons at δ_c 55.7 and 55.9 which were assigned as 3-OCH_3 and 6-OCH_3, respectively. The spectroscopic data were in agree with the structure of **149**.

The HR-TOFMS of compound **150** showed a pseudomolecular ion $[M-H]^{-}$ at *m/z* 427.2140 corresponding to the molecular formular $C_{25}H_{30}O_6$. The ^{1}H-NMR spectra of **150** (Figure 23b) indicated the presence of one extra sharp singlet at δ_H 3.95 (s, 3H), when compared to compound **90** (Figure 23c) allowed us to assign it as the new methoxyl group on the mangostin core structure. Its ^{13}C-NMR (Figure 24b) also exhibited new *O*-methyl carbon at δ_C 55.9. The methoxy signal at δ_H 3.93 was found to correlate to the oxygenated aromatic carbon in position 6 (δ_C 157.9) in an HMBC experiment. Combining all the information described above we concluded that compound **149** was 6-mono-*O*-methyltetrahydromangostin.

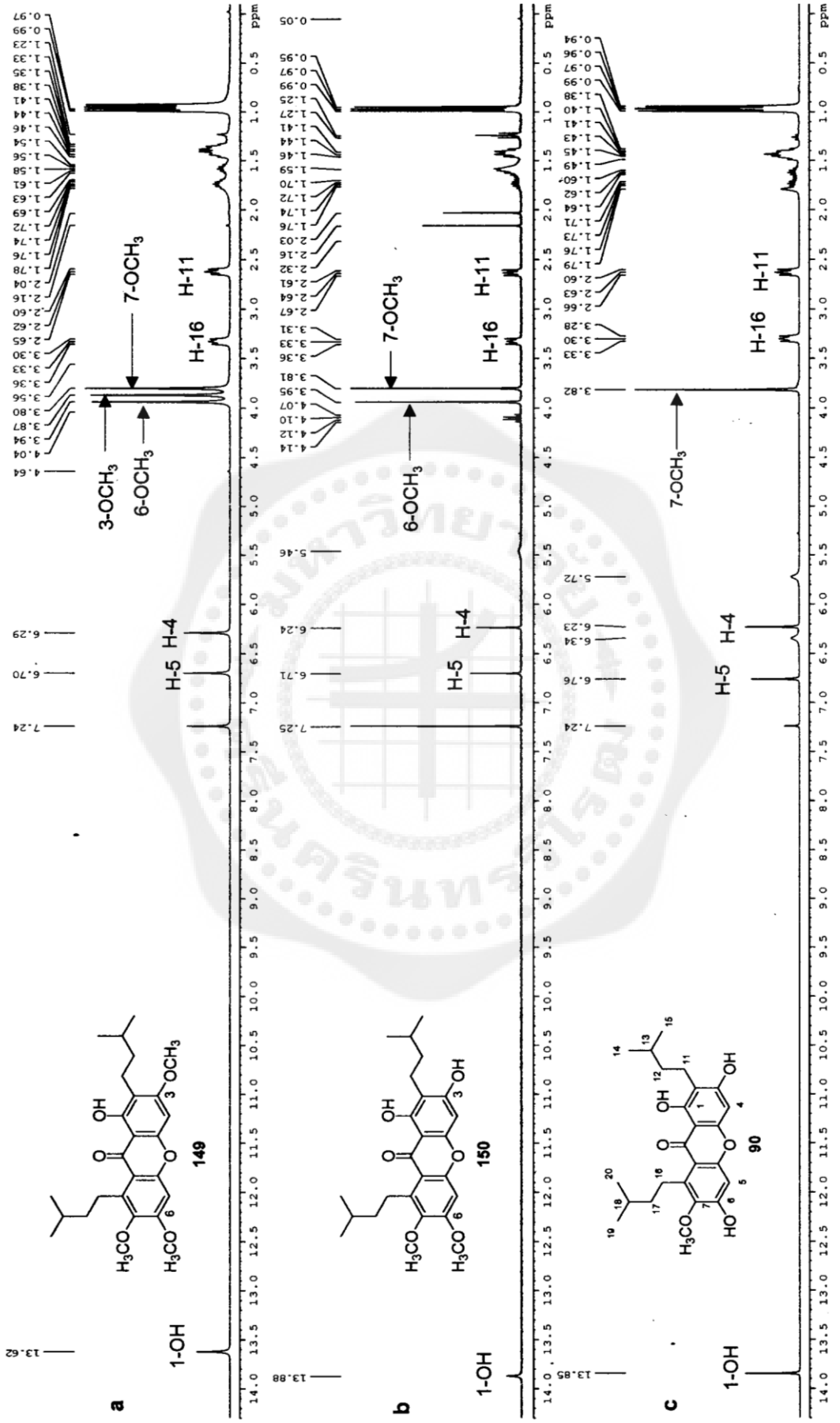

Figure 23a-c ^{1}H-NMR spectra (300 MHz,, $CDCl_3$) of **149** and **150** from methylation reaction compared with starting **90**

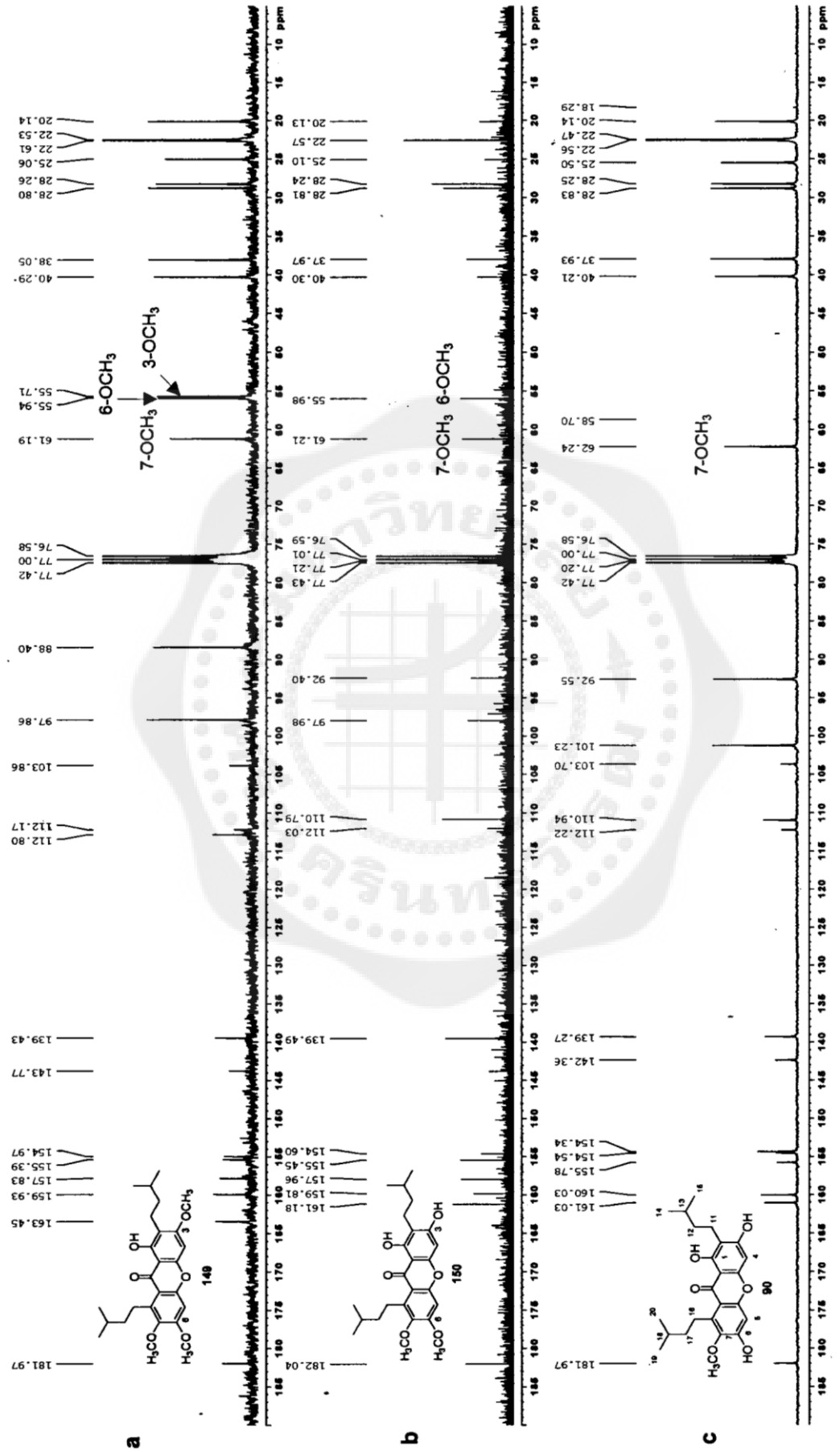

Figure 24a-c ^{13}C-NMR spectra (75 MHz, $CDCl_3$) of **149** and **150** from methylation reaction compared with starting **90**

3.2 Synthesis of 3,6-di-*O*-ethyltetrahydromangostin (**151**) and 6-mono-*O*-ethyltetrahydromangostin (**152**)

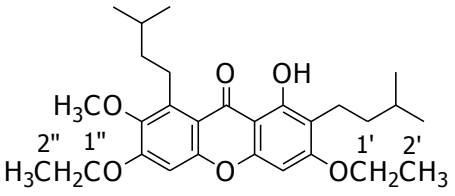

151

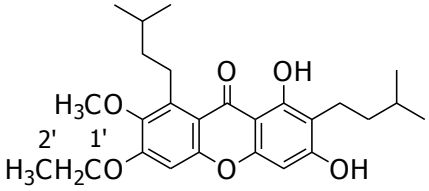

152

Ethylation of **90** by using diethyl sulfate resulted in analogues **151** and **152** in 37% and 55% yields, respectively. The ^{1}H-NMR spectrum of **151** revealed a new two quartets at δ_H 4.04 (2H, *J*= 6.8 Hz, H-1' (δ_c 63.9)) and δ_H 4.12 (2H, *J*= 6.9 Hz, H-1" (δ_c 64.3)) including the extra triplets at δ_H 1.43 (3H, *J*= 6.8 Hz, H-2' (δ_c 14.2)) and δ_H 1.51 (3H, *J*= 6.8 Hz, H-2" (δ_c 14.2)), which suggested that the *O*-ethylation reaction had occurred. HR-FABMS spectrum for compound **151** showed the pseudomolecular ion peak at *m/z* 471.2746 $[M+H]^+$ corresponding to the molecular formular $C_{28}H_{40}O_6$. ^{1}H-NMR data for compound **151** combined with its elemental composition indicated that it was 3,6-di-*O*-ethyltetrahydromangostin.

HR-FABMS spectrum of compound **152** exhibited a pseudomolecular ion $[M+H]^+$ at *m/z* 443.2433 corresponding to the molecular formular $C_{26}H_{36}O_6$. The ^{1}H-NMR of **152** indicated the presence of one quartet at δ_H 4.14 (*J*= 6.9 Hz, H-1') and one triplet at δ_H 1.54 (3H, *J*= 6.9 Hz, H-2'). The quartet signal (δ_H 4.14), which integrated for two protons, indicating that the mangostin ring was mono-substituted. The ^{13}C-NMR spectrum showed extra one methyl and one methylene carbons at δ_c 14.5 (C-2') and 64.4 (C-1'). The proton resonating at δ_H 4.14 and H-5 (δ_H 6.67) displayed co-correlation to same of down field quarternary cabon at δ_C 157.2 (C-6) in HMBC experiment data. The HMBC correlation therefore implies that the ethoxyl group is bonded to a C-6. Thus, compound **152** was confirmed to be 6-mono-*O*-methyltetrahydromangostin.

3.3 Synthesis of 3,6-di-*O*-allyltetrahydromangostin (**153**) and 6-mono-O-allyltetrahydromangostin (**154**)

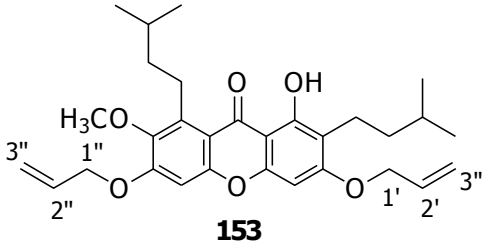

153

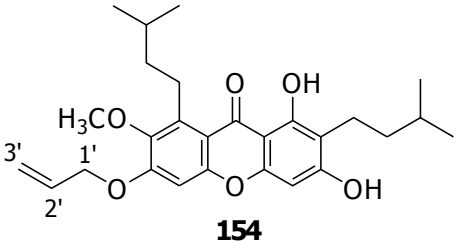

154

Compounds **153** and **154** were obtained in 24% and 59% yields, respectively from the treatment of compound **90** with allyl bromide in acetone solution in the presence of potassium carbonate. HR-TOFMS spectrum for **153** showed the pseudomolecular ion peak at *m/z* 495.2700 $[M+H]^+$. The ^{1}H-NMR spectrum of compound **153** exhibited two of doublet of doublet signals at δ_H 4.58 (*J* = 1.4, 4.8 Hz) and 4.65 (*J*= 1.3, 5.0 Hz) which were integrated of two protons each, assigned to be methylene groups attached to a phenolic oxygen. Its ^{1}H-NMR spectrum also showed the extra olefinic proton at δ_H 5.30 (dd, 1H, *J*= 1.4, 10.5 Hz, H-3$'_{cis}$), 5.34 (dd, 1H, *J*= 1.3, 10.0 Hz, H-3"$_{cis}$), 5.43 (dd, 1H, *J*= 1.4, 14.8 Hz, H-3'$_{trans}$), 5.49 (dd, 1H, *J*= 1.3, 10.0 Hz, H-3"$_{trans}$) and 6.05 (m, 2H, H-2' and H-2"). The NMR data for compound **153** combined with its element composition indicated that it was 3,6-di-*O*-allyltetrahydromangostin.

The molecular mass of **154** was confirmed by HR-TOFMS where a peak was observed at *m/z* 453.2273 $[M-H]^-$, which agrees the calculated value for $C_{27}H_{33}O_6$. The extra signals occurring at δ_H 4.65 (d, 2H, *J*= 4.2 Hz, H-1'), 5.42 (dd, 2H, *J*= 10.7, 16.8 Hz, H-3') and 6.06 (m, 1H, H-2') in its ^{1}H-NMR spectrum were assigned to be the proton of allyl group which was attached to phenolic oxygen. The HMBC experiment revealed long range ^{13}C-^{1}H coupling between the oxygenated quarternary carbon at δ_C 156.7 (C-6) and indicating the location of allyl group in mangostin core. Combining the information described above we concluded that compound **154** was 6-mono-*O*-allyltetrahydromangostin.

3.4 Synthesis of 3,6-di-*O*-(4-bromobutyl)tetrhydromangostin (**155**) and 6-mono-*O*-(4-bromobutyl)tetrhydromangostin (**156**)

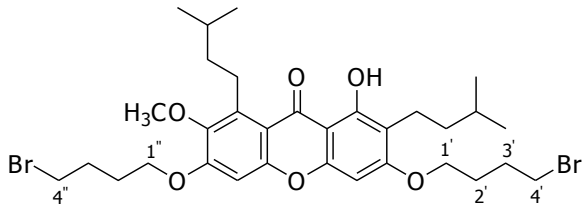

155

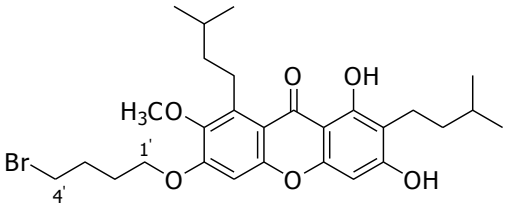

156

Butylation of **90** with 1,4-dibromobutane resulted in analogues **155** and **156** in 21 and 36% yields, respectively. The ^{1}H-NMR data of **155** was identical to that of parent compound **90** except for the presence of four triplet at δ_H 3.49 (3H, *J*= 6.4 Hz, H-4'), 3.51 (3H, *J*= 5.8 Hz, H-4''), 4.08 (2H, *J*= 5.8 Hz, H-1') and 4.10 (2H, *J*= 5.7 Hz, H-1'') and for the presence of multiplet at δ_H 2.01 (2H, H-3''), 2.08 (2H, H-3') and 2.09 (4H, H-2' and H-2''), indicating that compound **155** was disubstituted derivative. Its ^{13}C-NMR spectrum showed two oxygenated methylene carbons at δ_c 67.1 (C-1') and 67.2 (C-1'') and two overlapping brominated methylene carbons at δ_c 33.1. HR-TOFMS spectrum for **155** showed the pseudomolecular ion peak at *m/z* 683.1587 $[M-H]^-$ corresponding to the molecular formular $C_{32}H_{43}Br_2O_6$. The ^{1}H-NMR data for compound **155** combined with its elemental composition indicated that it was 3,6-di-*O*-(4-bromobutyl)tetrahydromangostin.

The HR-TOFMS of compound **156** at *m/z* 549.1847 $[M+H]^+$ was compatible with the molecular formular $C_{28}H_{38}BrO_6$ indicating that it was mono-substituted analogues. Its ^{1}H-NMR data confirmed the presence of only one 4-bromobutyl moiety with one *O*-methylene proton at δ_H 4.10 (br s, 2H, H-1') and one bromomethylene proton at δ_H 3.51 (br t, 2H, *J*= 5.9 Hz, H-4'). The position of 4-bromobutyl group was further confirmed by using HMBC experiment. The HMBC data showed long-range ^{13}C-^{1}H coupling between the methylene proton signal (δ_H 4.10) and a quaternary carbon resonating at δ_C 157.1 (C-6). The ^{1}H-NMR and HMBC data for compound **90** combined with its elemental composition indicated that it was 6-mono-*O*-(4-bromobutyl)tetrahydromangostin.

3.5 Synthesis of 3,6-di-*O*-benzyltetrahydromangostin (**157**) and 6-mono-*O*-benzyltetrahydromangostin (**158**)

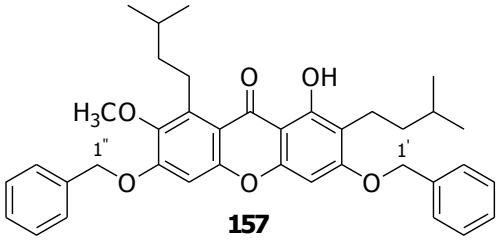

157

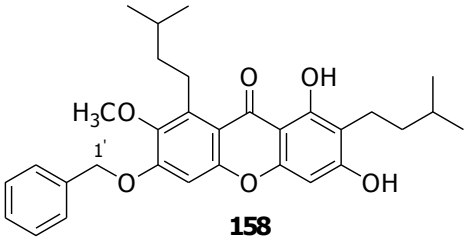

158

Compounds **157** and **158** were obtained in 25 and 42% yields, respectively, from the treatment of compound **90** with benzyl bromide in acetone solution in the presence of potassium carbonate as base. For compound **157**, the addition of benzyl groups are apparent by the appearance the two *O*-benzylic protons and carbons at δ_H 5.13 (2H), δ_c 70.1 and 5.18 (2H), δ_c 70.6 in ^{1}H- and ^{13}C-NMR spectrum. Its ^{1}H-NMR spectrum also exhibited multiplet of aromatic signals at δ_H 7.40, which showed integration for ten protons. HR-TOFMS spectrum for **157** showed the pseudomolecular ion peak at *m/z* 595.3038 $[M+H]^+$ corresponding to the molecular formular $C_{38}H_{43}O_6$ indicating that it was 3,6-di-*O*-benzyltetrahydromangostin.

The molecular mass of **158** was confirmed by HR-TOFMS where a peak was observed at *m/z* 505.2595 $[M+H]^+$, which agrees the calculated value for $C_{31}H_{37}O_6$. The extra signals occurring at δ_H 5.17 (s, 2H, H-1' (δ_c 70.6)) and 7.38 (m, 5H, H-Ph) in ^{1}H-NMR spectrum were assigned to be the proton of benzyl group which was attached to phenolic oxygen. The HMBC experiment revealed long range ^{13}C-^{1}H coupling between the one oxygenated quarternary carbon at δ_C 156.8 (C-6) indicating that the benzyl group was attached at C-6 of mangostin core. Combining all the information described above we concluded that **158** was 6-mono-*O*-benzyltetrahydromangostin.

3.6 Synthesis of 3,6-di-*O*-methylcarboxytetrahydromangostin (**159**)

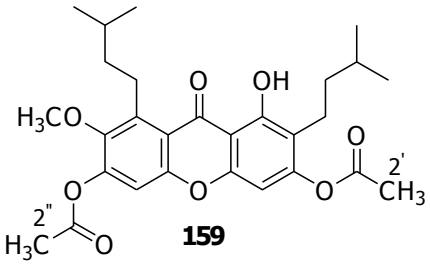

159

Compounds **159** was obtained as a single product (70%) from acetylation reaction of **90** by treatment with acetic anhydride in acetone solution in the presence of potassium carbonate. The structure of **159** was characterized by its spectroscopic (^{1}H-NMR, ^{13}C-NMR and MS) data compared to the data of parent compound **90**. The HR-FABMS of compound **159** exhibited the $[M+H]^{+}$ ion at *m/z* 499.2335, which was compatible with the molecular formular $C_{28}H_{35}O_{8}$. The ^{1}H-NMR spectrum of compound **159** showed two singlet signals at δ_H 2.33 (s, 3H, H-2' (δ_c 20.9)) and 2.37 (s, 3H, H-2" (δ_c 20.9)) assigned to the acetyl methyl proton and the downfield shift of the H-4 and H-5 signals in $CDCl_3$ at δ_H 6.59 (s, 1H) and 7.08 (s, 1H) when compared with the spectrum of its parent compound **90** (δ_H 6.22 (s, 1H, H-4) and 6.75 (s, 1H, H-5). The only difference in their ^{13}C-NMR spectrum was the presence of two ester carbonyl at δ_c 167.9 and 168.5 in **159**. Combining all the spectroscopic data described above we concluded that compound **90** was acetylated to obtain 3,6-di-O-methylcarboxytetrahydromangostin (**159**).

3.7 Synthesis of 3,6-di-*O*-ethylcarboxytetrahydromangostin (**160**)

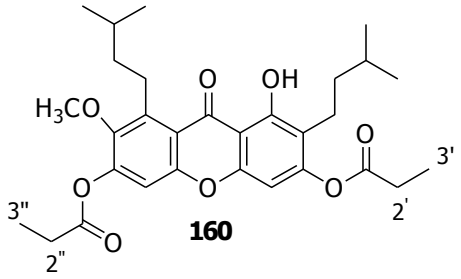

160

Compound **160** was obtained as single product in excellent yield (82%) by the treatment of compound **90** with propionic anhydride in acetone solution in the presence of potassium carbonate. The HR-TOFMS spectrum of compound **160** showed the pseudomolecular ion peak at *m/z* 527.2644 $[M+H]^+$ indicating a molecular formular of $C_{30}H_{39}O_8$. The presence of two propanoate groups were evident from the two triplet signals at δ_H 1.29 (3H, *J*= 7.5 Hz, H-3') and 1.30 (3H, *J*= 7.5 Hz, H-3'') and from two quartet signals at δ_H 2.62 (2H, *J*= 7.5 Hz, H-2') and 2.69 (2H, *J*= 7.5 Hz, H-2''). In addition, the presence of two propanoate groups was confirmed by using ^{13}C-NMR spectroscopic data. ^{13}C-NMR spectrum of **160** exhibited two ester carbonyl carbons at δ_c 171.5 (C-1') and 172.0 (C-1''). ^{13}C-NMR spectrum of **160** also show the signal of long chain ester carbon at δ_c 9.00 (C-3'), 9.1 (C-3''), 27.6 (C-2'), and 27.7 (C-2''). These spectroscopic data were concluded that compound **160** was indeed 3,6-di-*O*-ethylcarboxymangostin.

3.8 Synthesis of 3,6-di-*O*-propyltetrahydromangostin (**161**)

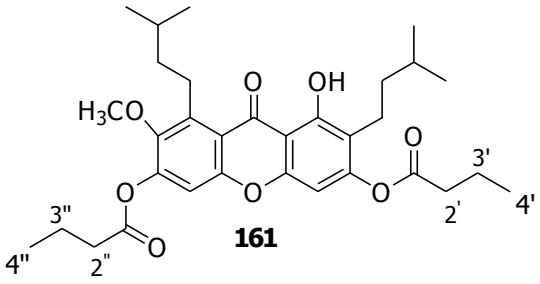

161

Compound **161** was obtained in 97% yield from the treatment of compound **90** with butyric anhydride in acetone solution in the presence of potassium carbonate. The structure of compound **161** was confirmed by spectroscopic (NMR, HR-TOFMS) comparisons with the data of parent compound **90**. The HR-TOFMS of **161** at *m/z* 555.2926 was compatible with the molecular formular $C_{32}H_{44}O_8$. The ^{1}H-NMR spectrum of compound **161** displayed two broad triplet signals at δ_H 2.55 (2H, *J*= 7.7 Hz, H-2') and 2.61 (2H, *J*= 7.3 Hz, H-2") which were assigned as the signals of α -methylene proton of the butanoate. Its ^{1}H-NMR also showed the triplet signals at δ_H 1.05 (3H, *J*= 6.9 Hz, H-4'), 1.06 (3H, *J*= 7.1 Hz, H-4") and multiplet signal at δ_H 1.81 (4H, H-4' and H-4"). The H-4 and H-5 signals appeared as two singlets at δ_H 6.60 and 7.09, which occurred a large downfield shift compared with that of mangostin **90** (δ_H 6.22 (1H, H-4) and 6.75 (1H, H-5). These downfield shift indicated the presence of ester moiety at the 3- and 6-positions.

The new quaternary carbon were also observed in ^{13}C-NMR spectrum at δ_c 170.7 and 171.2, which were assigned to ester carbonyl carbons. The NMR data for compound **161** combined with its elemental composition indicated that it was 3,6-di-*O*-propylcarboxytetrahydromangostin.

3.9 Synthesis of 3,6-di-*O*-phenylcarboxytetrahydromangostin (**162**), 6-mono-*O*-phenylcarboxytetrahydromangostin (**163**) and 3-mono-*O*-phenylcarboxytetrahydromangostin (**164**)

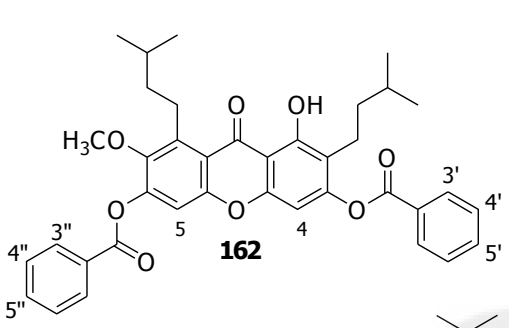

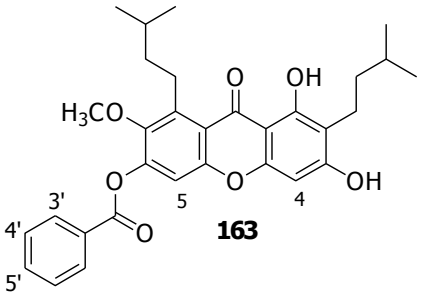

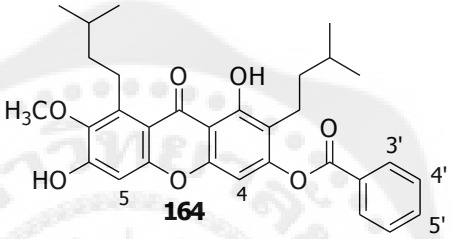

Compounds **162**, **163** and **164** were obtained from the treatment of **90** with benzoic anhydride in acetone solution in the presence of potassium carbonate in 5%, 47% and 13% yields, respectively. The structures of these analogues were confirmed by spectroscopic (NMR, HR-TOFMS) comparisons with the data of parent compound **90**. The HR-TOFMS spectrum of compound **162** exhibited the $[M+H]^+$ at *m/z* 623.2639. The ^{13}C-NMR showed two extra down field quaternary carbon at δ_C 163.8 and 164.3 which assigned as ester carbonyl carbons. The ^{1}H-NMR spectrum of compound **162** showed the aromatic proton signals at δ_H 7.53 (t, 4H, *J*= 7.4 Hz H-4' and H-4"), 7.66 (br t, 1H, *J*= 7.4 Hz, H-5"), 7.67 (br t, 1H, *J*= 7.4 Hz, H-5'), 8.22 (br t, 4H, *J*= 7.4 Hz, H-3', H-3"). The presence of benzoyl moieties at the 3- and 6-position were evident from a downfield shift of H-4 (δ_H 6.76 (s, 1H) and H-5 (δ_H 7.24 (s, 1H) in its ^{1}H-NMR spectrum as compared with that of compound **90** (δ_H 6.22 (1H, H-4) and 6.75 (1H, H-5). The NMR data for compound **162** combined with its elemental composition indicated that it was 3,6-di-*O*-phenylcarboxytetrahydromangostin.

The HR-TOFMS spectrum of compound **163** showed the protonated molecular ion peak at *m/z* 519.2382. The ^{13}C-NMR showed only one extra ester carbonyl carbon at δ_C 164.3 indicating that **163** was mono-benzoylated analogue. The ^{1}H-

NMR spectrum of **163** showed the aromatic proton signals at δ_H 7.55 (t, 2H, *J*= 7.4 Hz, H-4'), 7.69 (t, 1H, *J*= 7.3 Hz, H-5'), and 8.23 (d, 2H, *J*= 7.4 Hz, H-3'). The position of the benzoyl group of the products was determined by the analysis of ^{1}H-NMR especially the shifts for singlet signal of H-4 and H-5. The chemical shifts of the H-4 and H-5 of starting tetrahydromangostin (**90**) displayed at δ_H 6.22 and 6.75, respectively. By comparison of ^{1}H-NMR spectra of compound **163** with these of precursor **90** (Figure 25), a significant shift to downfield to δ_H 7.17 was observed for H-5 of compound **163** indicating that compound **163** was 6-mono-*O*-phenylcarboxytetrahydromangostin.

The HR-TOFMS of **164** at *m/z* 517.2703 $[M-H]^-$ was compatible with the molecular formular $C_{31}H_{39}O_7$. The ^{13}C-NMR showed only one extra ester carbonyl carbon at δ_C 164.5 indicating that **163** was also mono-acylated analogue. The ^{1}H-NMR spectrum of **164** (Figure 25b) revealed aromatic proton signals at δ_H 7.52 (t, 2H, *J*= 7.4 Hz, H-4'), 7.66 (t, 1H, *J*= 7.4 Hz, H-5') and 8.19 (d, 2H, *J*= 7.4 Hz, H-3') indicating that the mangostin core of the benzoylated compound was mono-substituted. The location of benzoyl group of compound **164** was determined by the analysis of ^{1}H-NMR especially the shifts for singlet signal of H-4 and H-5 compared to precursor **90** (δ_H 6.22 (H-4) and 6.75 (H-5). By comparison of ^{1}H-NMR spectra of compound **164** with these of precursor **90**, H-4 of compound **164** showed downfield shift at δ_H 6.71, while H-5 displayed as singlet signal at ca. δ_H 6.79 indicating that compound **164** was the structural isomer of **163** which was 3-mono-*O*-phenylcarboxytetrahydromangostin.

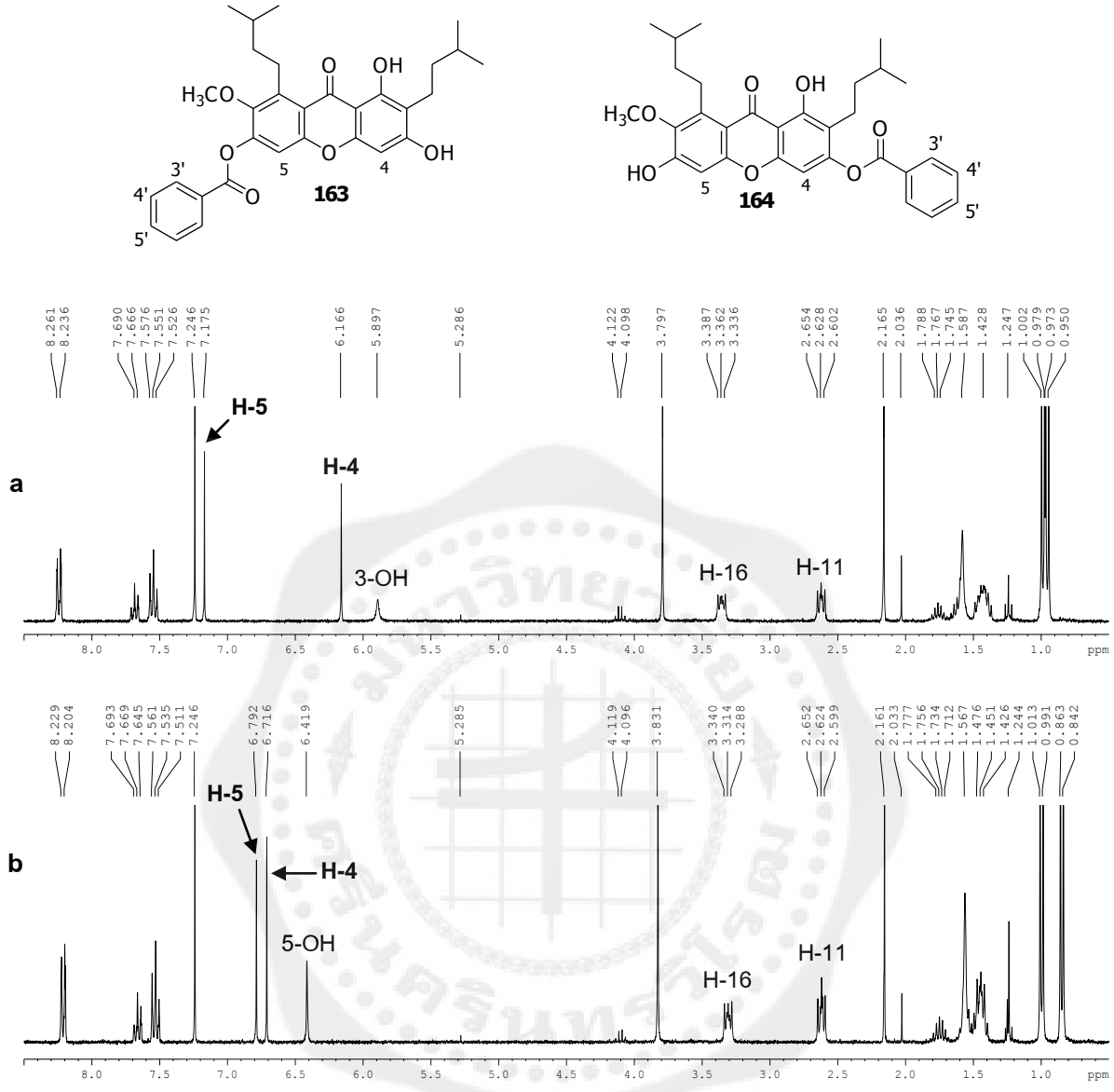

Figure 25a-b The down field shift of H-4 and H-5 in ^{1}H-NMR spectra (300 MHz, $CDCl_3$) of compounds **163** (a) and **164** (b)

For the synthesis of *O*-alkylated and *O*-acylated tetrahydromangostin derivatives, the reaction conditions and the percentage yield of the products are summarized in Table 9 below.

TABLE 9 Reaction conditions and the percentage isolated yields of the products from the synthesis of tetrahydrogenated mangostin derivatives

Reactions (mole ratio)[a]	Conditions	Isolated yield of di-substituted products	Isolated yield of mono-substituted products
Methylation (1 : 1 : 2)	**90** (30.6 mg, 0.07 mmol), K_2CO_3 (11.8 mg, 0.07 mmol), MeI (21.5 mg, 0.15 mmol), acetone, rt, 24 h.	**149** (pale yellow solid, 9.6 mg, 30 %)	6-mono-substituted, **150** (pale yellow solid, 16.0 mg, 40%)
Ethylation (1 : 1 : 1)	**90** (58.3 mg, 0.14 mmol), K_2CO_3 (49.5 mg, 0.14 mmol), Et_2SO_4 (21.5 mg, 0.14 mmol), acetone, rt, 22 h.	**151** (pale yellow solid, 24.8 mg, 37%)	6-mono-substituted, **152** (pale yellow solid, 34.1 mg, 55%)
Allylation (1 : 1 : 1)	**90** (40.6 mg, 0.10 mmol), K_2CO_3 (20.7 mg, 0.15 mmol), allyl bromide (12.0 mg, 0.10 mmol), acetone, rt, 48 h.	**153** (pale yellow solid, 11.6 mg, 24%)	6-mono-substituted, **154** (pale yellow solid, 26.3 mg, 59%)
Bromobutylation (1 : 2 : 2)	**90** (25.8 mg, 0.06 mmol), K_2CO_3 (16.7 mg, 0.12 mmol), 1,4-dibromobutane (25.6 mg, 0.12 mmol), acetone, rt, 24 h.	**155** (pale yellow solid, 8.7 mg, 21%)	6-mono-substituted, **156** (yellow viscous, 12.4 mg, 36%)
Benzylation (1 : 2 : 2)	**90** (38.4 mg, 0.09 mmol), K_2CO_3 (24.8 mg, 0.18 mmol), benzyl bromide (30.7 mg, 0.18 mmol), acetone, rt, 72 h.	**157** (pale yellow solid, 13.9 mg, 25%)	6-monosubstitued, **158** (pale yellow solid, 19.7 mg, 42%)
Acetylation (1 : 1 : 1)	**90** (82.3. mg, 0.19 mmol), K_2CO_3 (31.0 mg, 0.19 mmol), acetic anhydride (19.4 mg, 0.19 mmol), acetone, rt, 18 h.	**159** (pale yellow solid, 69.3 mg, 70%)	-

TABLE 9 (continued)

Reactions (mole ratio)[a]	Conditions	Isolated yield of di-substituted products	Isolated yield of mono-substituted products
Propionylation (1 : 1.5 : 1.5)	**90** (50.7 mg, 0.12 mmol), K_2CO_3 (24.8 mg, 0.18 mmol), propionic anhydride (30.7 mg, 0.18 mmol), acetone, rt, 4 h.	**160** (pale yellow solid, 52.9 mg, 82%)	-
Butyrylation (1 : 2 : 3)	**90** (25.8 mg, 0.07 mmol), K_2CO_3 (19.3 mg, 0.14 mmol), butyric anhydride (47.5 mg, 0.25 mmol), acetone, rt, 30 min.	**161** (pale yellow solid, 32.6 mg, 97%)	-
Benzoylation (1 : 2 : 1)	**90** (60.5 mg, 0.14 mmol), K_2CO_3 (38.6 mg, 0.28 mmol), benzoic anhydride (13.9 mg, 0.14 mmol), acetone, rt, 24 h.	**162** (pale yellow solid, 8.9 mg, 5%)	6-momo-substituted, **163** (pale yellow solid, 21.2 mg, 47%) and 3-mono-substituted, **164** (pale yellow solid, 5.6 mg, 13%)

[a] mole **90** : mole base : mole of alkylating or acylating agents

All synthetic analogues were characterized the chemical structures, the results showed that under condition employed the 6-mono-*O*-alkylated (compounds **150**, **152**, **154**, **156** and **158**) and 3-*O*-di-alkylated analogues (compounds **149**, **151**, **153**, **155** and **157**) were obtained and the 6-mono-*O*-alkyalated compounds were the major reaction products in 34.1 – 59% yields. The 3-mono-O-alkyated analogues was not occurred probably due to the steric hindrance from hydrogenated prenyl side chain at C-2, thus decreasing reactivity of generated phenoxide ion at C-3. For acetylation, propionylation and butyrylation only di acylated products (compounds **159-161**) obtained in 70-97% yields. In benzoylation reaction, di-benzoate **162**, 6-mono-benzoate **163** and 3-mono-benzoate **164** were obtained in 5, 47 and 13% yields, respectively. The results revealed that the addition of hydrogen on to alkene moieties increased the selectivity of acylation of 6-OH led to the formation of 6-mono-*O*-phenylcarboxytetrahydromangostin (**163**) as the major product.

4. Antimycobacterial activity of mangostin and tetrahydromangostin analogues

Followed the Microplate Alamar Blue Assay (MABA), α-mangostin (**1**) and all synthetic mamgostin analogues were tested *in vitro* for their antimycobacterial activity against *M. tuberculosis* H_{37}Ra strain and the results are summarized in Table 10. The first class of mangostin analogues selected for antimycobacterial evaluation was the *O*-alkylated mangostin (**84**, **85**, **89**, **117**, **120** and **140**-**144**) and *O*-acylated mangostin (**99** and **145**-**148**) analogues. The 6-mono-*O*-methylmangostin (**140**, MIC = 6.25 μg/m), 3-mono-*O*-ethylmangostin (**141**, MIC = 6.25 μg/mL) and 6-mono-*O*-(4-bromobutyl) mangostin (**143**, MIC = 12.5 μg/mL) were only as active as, or even much less active than the parent **1** (MIC = 6.25 μg/mL) except the 6-mono-*O*-allylmangostin (**120**, MIC = 3.125 μg/mL) was 2-fold more active than **1**. The di-*O*-alkylated analogues **84**-**85**, **89**, **142** and **117** and 3-mono-*O*-benzylmangostin (**144**) showed complete loss of activity with MIC > 200 μg/mL . The results have indicated that decease in polarity of the mangostin caused deceasing in activity.

We next evaluated the potency of the acylated analogues of mangostin. The results (Table 10) have indicated that the 3,6-di-*O*-phenylcarboxymangostin (**147**) exhibited complete loss of activity whereas 6-mono-*O*-phenylcarboxymangostin (**148**) (MIC = 12.5 μg/mL) showed antimycobacterial activity with 2-fold less active than parent **1**. However, di-*O*-acylated **99** (MIC = 12.5 μg/mL), **145** (MIC = 50 μg/mL) and **146** (MIC = 50 μg/mL) were weakly active. The chemical modification of **1** to the above corresponding ether and ester derivatives did not seem to give promising analogues with enhanced antimycobacterial activity.

We therefore chose to modify the prenyl groups of α -mangostin (**1**). Tetrahydromangostin (**90**), the reduced analogue of **1**, was prepared and assessed for antimycobacterial activity. The assay results indicated that compound **90** (MIC = 1.56 μg/mL) showed 4-fold more active than the parent compound **1**. This observation suggested that the absence of alkene moiety at the both prenyl side chain of the precursor **1** enhanced the antimycobacterial activity. In order to see the influence of hydroxyl groups at C-3 and C-6, the corresponding *O*-alkylated and *O*-acylated analogues of **90** were prepared and their MICs were determined. Di-*O*-alkylated analogues with methyl group (**149**), ethyl group (**151**), allyl group (**153**) and 4-bromobutyl group (**155**) at both hydroxyl groups showed complete loss in activity at the MIC > 200 μg/mL against Mycobacteia

strain tested in this study. However, the 3,6-di-O-benzyletrahydromamgostin (**157**) showed anti-TB activity with MIC value of 12.5 μg/mL. We eventually discovered that the 6-mono-*O*-alkylated analogues **150**, **152** and **154** exhibited the highest activity with the identical MIC 0.78 μ g/mL which was 8-fold more active than the parent **1** (MIC = 6.25 μ g/mL). Comparison of the MICs of the most potent compounds **150**, **152** and **154** with those of the standard drugs, it was evident that these compounds were approximately 3-fold more active than kanamycin sulfate (MIC 2.5 μg/mL) but much less active than isoniazid and rifampin. Compounds **156** and **158** containing higher lipophilicity alkyl chain resulted in decrease in activity. The activity of tetrahydro alkyl ether analogues was sensitive to the nature of lipophilicity of alkyl side chain as from the decreasing activity of compound **156** and **158** is likely attributed to poor cell membrane penetration. Moreover, the activity of ether analogues could be related to the presence of hydroxyl group at C-3 or C-6 as seen from the complete loss of activity of di-*O*-substituted derivatives.

We next evaluated the potency of the *O*-acylated tetrahydro derivatives (Table 10). The results have shown that incorporation of the acyl substituent in compound **90** does not more enhance its antituberculosis activity relative to its un-substituted precursor **90**. The di-*O*-acylated analogues **159** and **160** were approximately 2-fold and 3-fold more active than **1** with MIC 3.13 and 1.56 μ g/mL, respectively. 3,6-Di-*O*-ethylcarboxytetrahydromangostin (**160**) and 3,6-di-*O*-phenyltetrahydromangostin (**162**) did not improve antimycobacterial activity than that of parent compound **1**. The comparison antimycobacterial of di-*O*-acyl with di-*O*-alkyl analogues revealed that the acyl derivatives are still retains moderate to good activity, it is possible that acylated analogues are hydrolyzed of the ester bonds upon uptake into the cells to yield the mono-substituted or non-substituted compounds, which could exhibited anti-TB activity or even these compounds displayed the intrinsic activity. The 6-mono-*O*-phenyltetrahydromangostin (**163**, MIC = 3.125 μg/mL) was 2-fold more active than that of **1** and 4-fold more active than its 3-mono-*O*-phenyl isomer **164** (MIC = 12.5 μ g/mL). The lower activity in 3-*O*-phenyltetrahydromangostin (**164**) is likely due to the less hydrolysable of ester bond to produce active tetrahydromangostin (**90**) than 6-*O*-phenyltetrahydromangostin (**163**) in TB cells. This findings revealed that the number of hydroxyl on the aromatic ring of mangostin, the absence of alkene moiety on prenyl side chain and the nature of the substituents on the oxygen function of the aromatic ring are important for antimycobacterial activity.

TABLE 10 MIC values (μg/mL) of mangostin analogues against *M. tuberculosis*

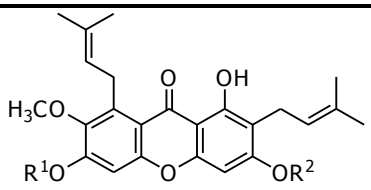

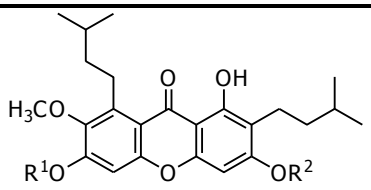

Compounds	R^1	R^2	MIC	Compounds	R^1	R^2	MIC
1	H	H	6.25	**90**	H	H	1.56
84	CH_3	CH_3	inactive	**149**	CH_3	CH_3	inactive
140	CH_3	H	6.25	**150**	CH_3	H	0.78
85	CH_2CH_3	CH_2CH_3	inactive	**151**	CH_2CH_3	CH_2CH_3	inactive
141	H	CH_2CH_3	6.25	**152**	CH_2CH_3	H	0.78
89	$CH_2CH=CH_2$	$CH_2CH=CH_2$	inactive	**153**	$CH_2CH=CH_2$	$CH_2CH=CH_2$	inactive
120	$CH_2CH=CH_2$	H	3.125	**154**	$CH_2CH=CH_2$	H	0.78
142	$(CH_2)_4Br$	$(CH_2)_4Br$	inactive	**155**	$(CH_2)_4Br$	$(CH_2)_4Br$	inactive
143	$(CH_2)_4Br$	H	12.5	**156**	$(CH_2)_4Br$	H	12.5
117	CH_2Ph	CH_2Ph	inactive	**157**	CH_2Ph	CH_2Ph	12.5
144	H	CH_2Ph	inactive	**158**	CH_2Ph	H	6.25
99	$COCH_3$	$COCH_3$	12.5	**159**	$COCH_3$	$COCH_3$	3.13
145	$COCH_2CH_3$	$COCH_2CH_3$	50	**160**	$COCH_2CH_3$	$COCH_2CH_3$	1.56
146	$CO(CH_2)_3CH_3$	$CO(CH_2)_3CH_3$	50	**161**	$CO(CH_2)_3CH_3$	$CO(CH_2)_3CH_3$	25
147	COPh	COPh	inactive	**162**	COPh	COPh	12.5
148	COPh	H	12.5	**163**	COPh	H	3.125
				164	H	COPh	12.5

Inactive at MIC > 200 μg/mL

The obtained antimycobacterial evaluation results revealed that the structural requirements for a mangostin analogues to exhibit antimycobacterial activity were the

presence of free hydroxyl group at C-3 and two saturated bonds of alkyl chains on C-2 and C-8 as well as the presence of lipophilic alkyl chain with appropriate chain length which was attached to the 6-hydroxyl function of the mangostin core (Figure 26).

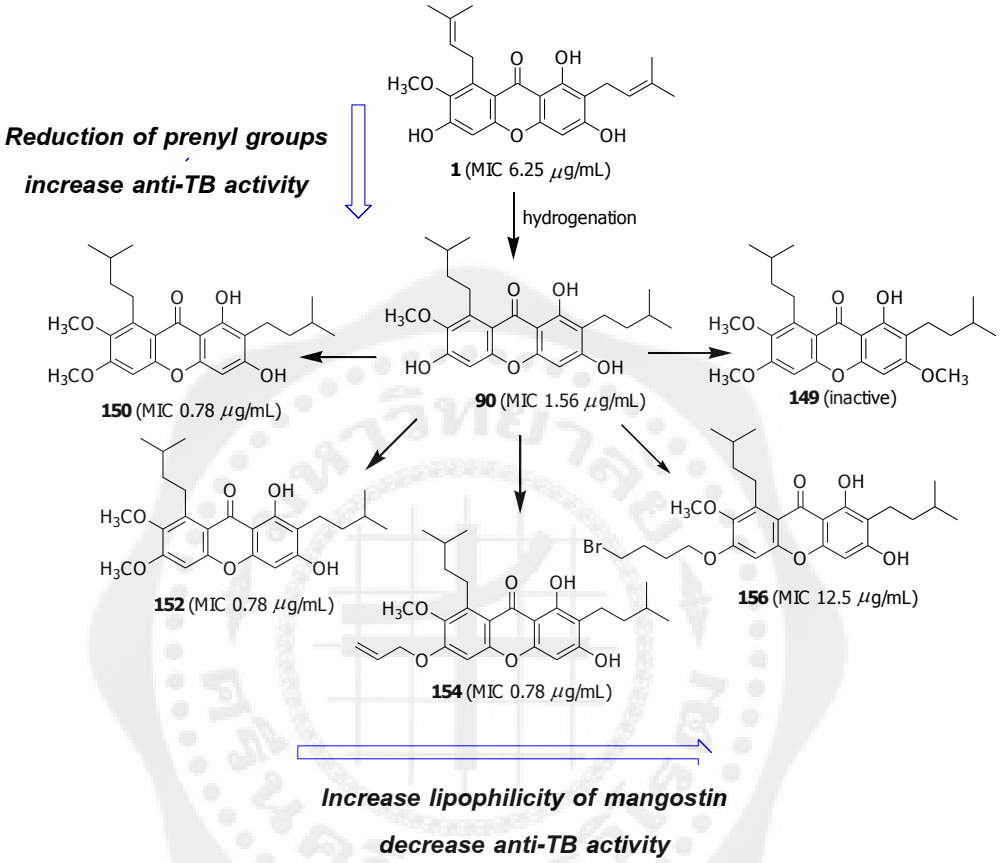

Figure 26 The structure activity relationship (SAR) of mangostin analogues

5. The effect of hydroxyl groups on hydrogenated mangostin core to antimycobacterial activity

We then sought to modify the phenolic functionality of tetrahydromangostin (**90**) in order to assess the importance of the hydroxyl groups for antimycobacterial activity. The inactive compound **149** was chose as starting compound to produce various *O*-methylated analogues of hydrogenated mangostin employing the previous demethylation procedures (Bennet; et al. 1990: 1463).

5.1 Demethylation of **149**

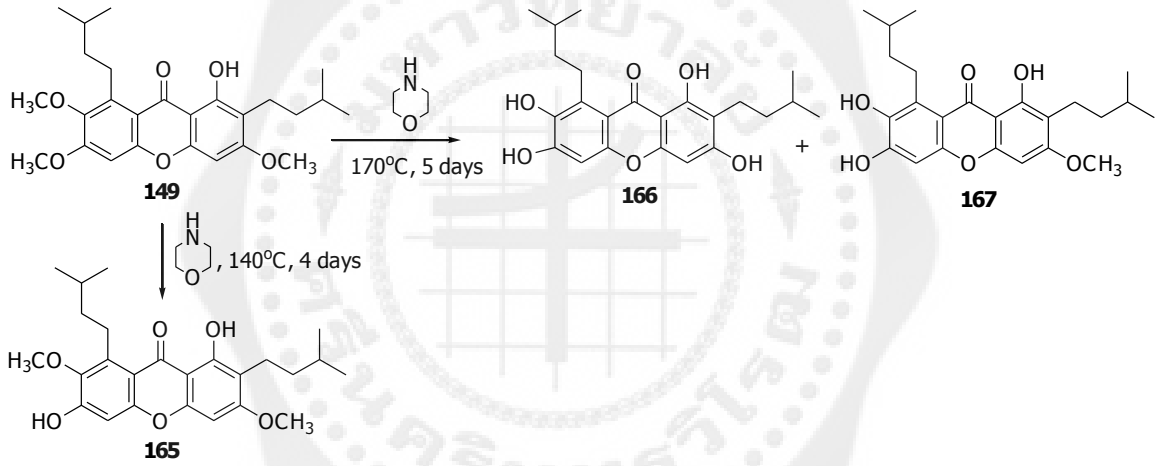

Figure 27 Demethylation of **149** with aqueous morpholine

Treatment of compound **149** (580.0 mg, 1.31 mmol) with aqueous morpholine at 140 ^{o}C for 4 days, gave only 6-*O*-demethylated product **165** in 10% (55.10 mg). The structure of **165** was confirmed by spectroscopic [^{1}H-NMR (Figure 28a), ^{13}C-NMR (Figure 29c) and HR-TOFMS] comparisons with the data of parent compound **149**. The HR-TOFMS spectrum of compound **165** exhibited the [M-H]$^{-}$ at *m/z* 427.2124 corresponding to the molecular formular $C_{25}H_{33}O_6$. The ^{1}H-NMR spectrum of compound **165** (Figure 28a) showed two singlet of methoxyl groups at δ_H 3.82 (3-OCH_3) and 3.87 (7-OCH_3. The HMBC data showed long-range ^{13}C-^{1}H coupling between singlet proton δ_H 3.82 with oxygenated carbon at δ_C 163.6 (C-3) and proton at δ_H 3.87 with oxygenated aromatic

carbon resonating at δ_C 155.0 (C-6) confirming the presence of the methoxyl groups located at C-3 and C-7. The ^{1}H-NMR and HMBC data for compound **165** combined with its elemental composition indicated that **165** was 1,6-dihydroxy-3,7-dimethoxy-2,8-di-(3-methylbutyl)xanthone.

Prolonged treatment of compound **149** with morpholine-water at higher temperature 170^{O}C for 5 days, products **166** and **167** were obtained in 20 and 14% yields, respectively. The ^{1}H-NMR (Figure 28b) and ^{13}C-NMR (Figure 29b) spectra of **166** showed the absence of methoxyl signals at chemical shift in the region δ_H 3.80-3.94 and at δ_c 55.7-61.1 indicating that compound **149** was fully demethylated derivative. HR-TOFMS spectrum for **166** showed the pseudomolecular ion peak at *m/z* 399.1830 $[M-H]^-$ corresponding to the molecular formular $C_{23}H_{27}O_6$. The NMR and mass data indicated that compound **166** was indeed 1,3,6,7-tetrahydroxy-2,8-di-(3-methylbutyl)xanthone.

HR-TOFMS spectrum for **167** showed the pseudomolecular ion peak at *m/z* 413.1972 $[M-H]^-$ with in agreement the calculated values for $C_{24}H_{30}O_6$-H. Compound **167** exhibited one of sharp singlet at δ_H 3.82 (3H) in ^{1}H-NMR spectrum (Figure 28c) which was assigned to be methoxyl proton. The presence of one methoxyl group was also confirmed by ^{13}C-NMR. ^{13}C-NMR of **167** (Figure 29a) exhibited *O*-methoxyl carbon at δ_c 55.6. The HMBC showed correlation of this proton signal (δ_H 3.82) to one oxygenated quaternary carbon at δ_c 163.2 which was assigned as C-3 . Combining all the information described above we concluded that compound **167** was 1,6,7-trihydroxy-3-methoxy-2,8-di-(3-methylbutyl)xanthone.

As observed above, demethylation of the less hindered methoxyl group at C-6 was occurred before the more steric hindered 7-OCH_3 and 3-OCH_3, respectively.

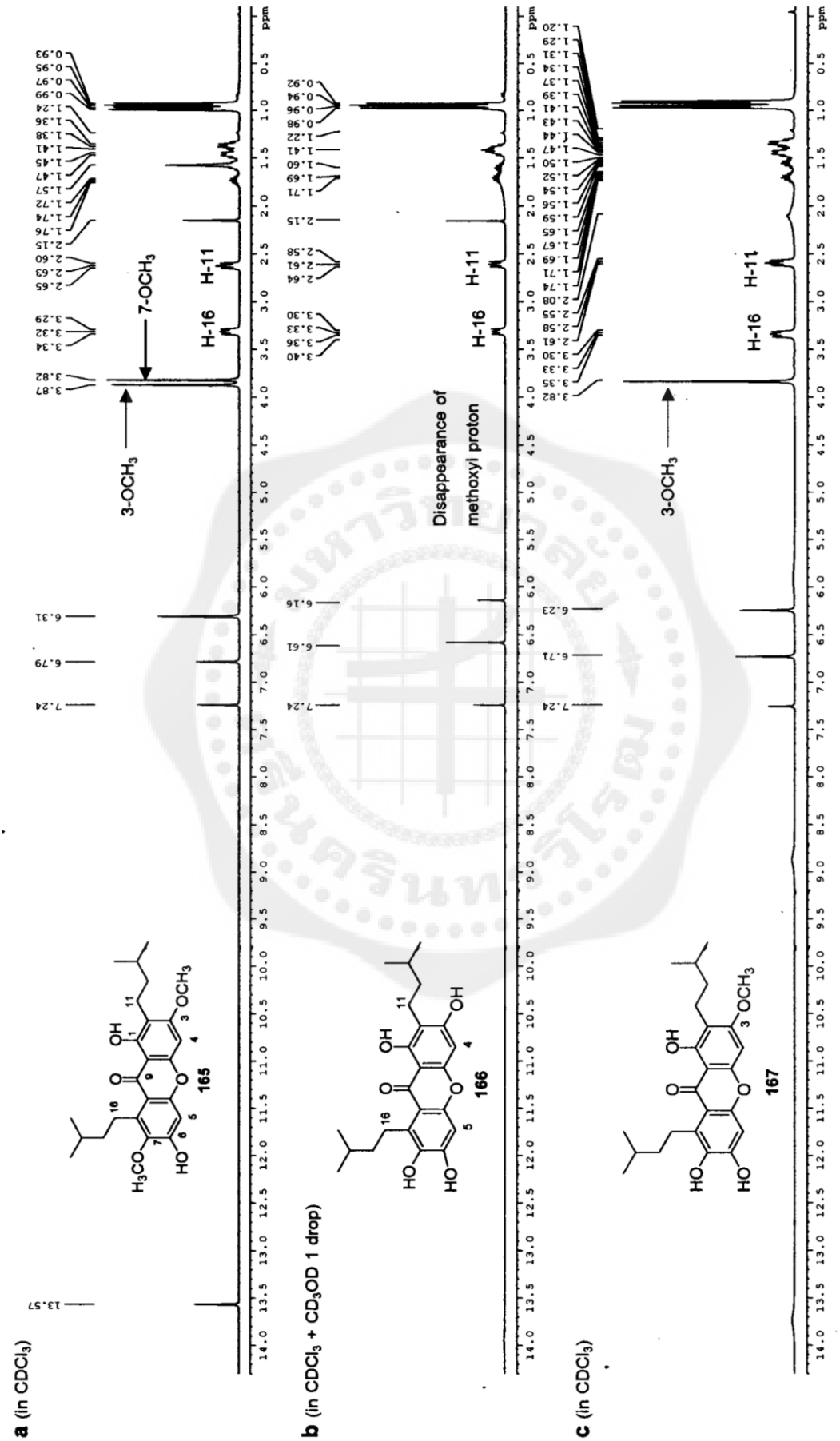

Figure 28a-c ^{1}H-NMR spectra (300 MHz) of the products **165**, **166** and **167** from demethylation reaction of **149**

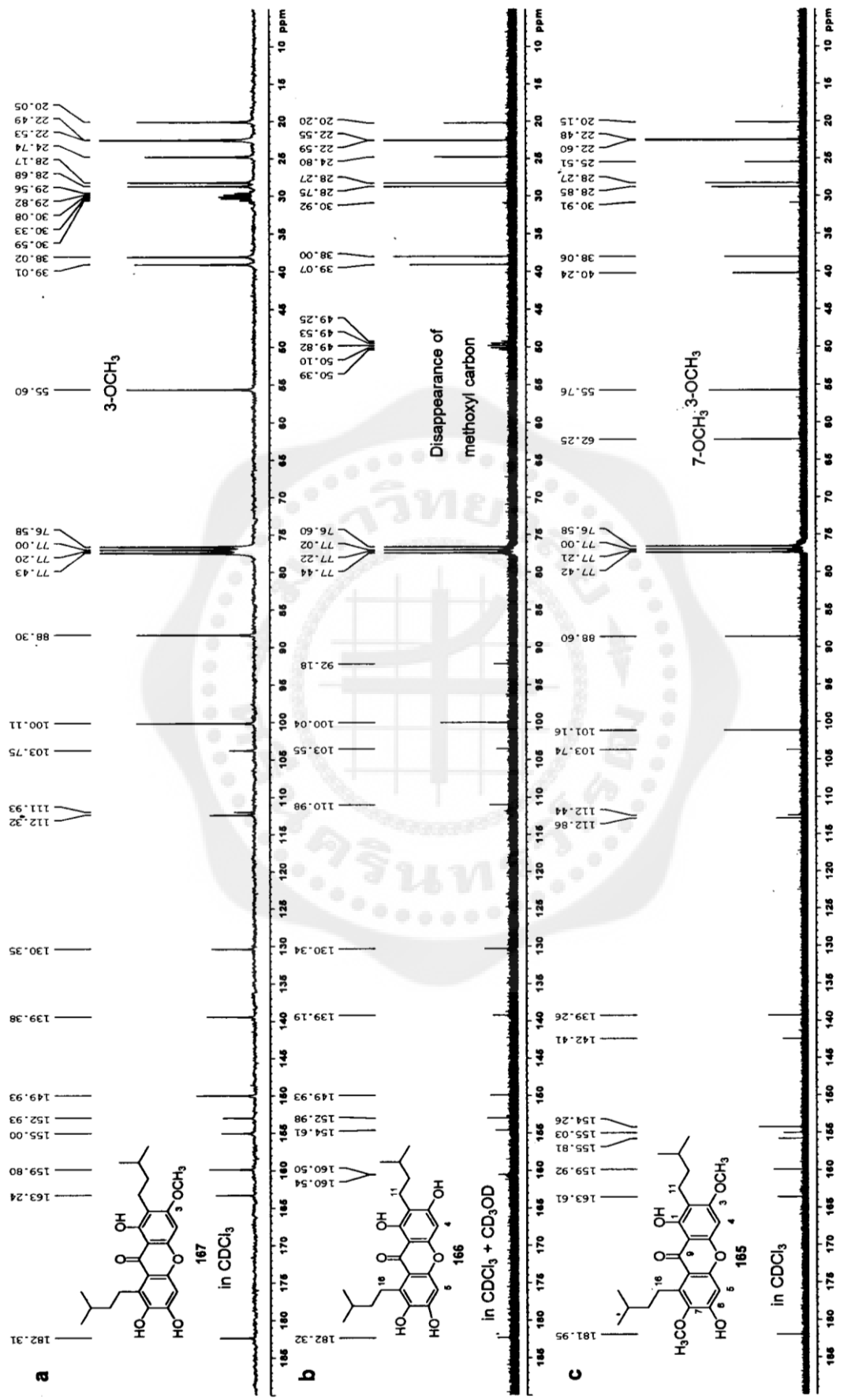

Figure 29 ^{13}C-NMR spectra (75 MHz) of the products **165**, **166** and **167** from demethylation reaction of **149**

5.3 Methylation of **166**

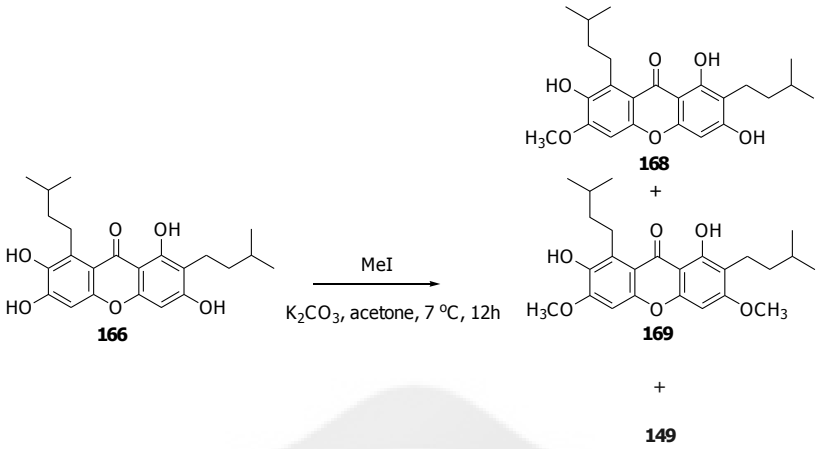

Figure 29 Methylation of **166** to produce new methylated analogues **168** and **169**

Treatment of tetrahydroxylated analogue **166** with iodomethane gave 6-*O*-methylated **168** and 3,6-di-*O*-acylated **169** along with the full methylated analogue **149** in 12, 47 and 12% yields, respectively. The structures of these analogues were confirmed by spectroscopic (NMR, HR-TOFMS) and compared with the data of parent compound **166**. The HR-TOFMS spectrum of compound **168** exhibited the $[M-H]^-$ at *m/z* 413.1961. The ^{13}C-NMR (Figure 31b) and ^{1}H-NMR (Figure 30b) showed one extra methoxyl signal at δ_C 56.2 and δ_H 3.98. The presence of the methoxyl group at C-6 was confirmed by using HMBC experiment. The HMBC data revealed the cross peak of methoxyl proton at δ_H 3.98 with C-6 resonating at δ_C 161.1 indicating that compound **168** was 6-mono-*O*-methylated analogue of **166**.

The ^{1}H-NMR (Figure 30a) and ^{13}C-NMR spectrum (Figure 31a) of **169** showed the presence of two methoxyl groups at δ_H 3.87 (3-OCH_3), δ_C 55.7 (3-OCH_3) and δ_H 3.98 (6-OCH_3) and δ_C 56.2 (6-OCH_3). The HMBC data showed long-range ^{13}C-^{1}H coupling between singlet proton δ_H 3.87 with oxygenated aromatic carbon at δ_C 163.3 (C-3) and proton at δ_H 3.98 with oxygenated quaternary carbon resonating at δ_C 151.2 (C-6). The HR-TOF mass spectrometry data further confirms the structure of **169**, as a molecular ion peak was observed at *m/z* 427.2122 $[M-H]^-$, which was in agreement with the calculated value for $C_{25}H_{31}O_6$. The ^{1}H-NMR, ^{13}C-NMR, HMBC and mass data for compound **169** confirmed that its was 1,7-dihydroxy-3,6-dimehoxy2,8-di-(3-methylbutyl)xanthone.

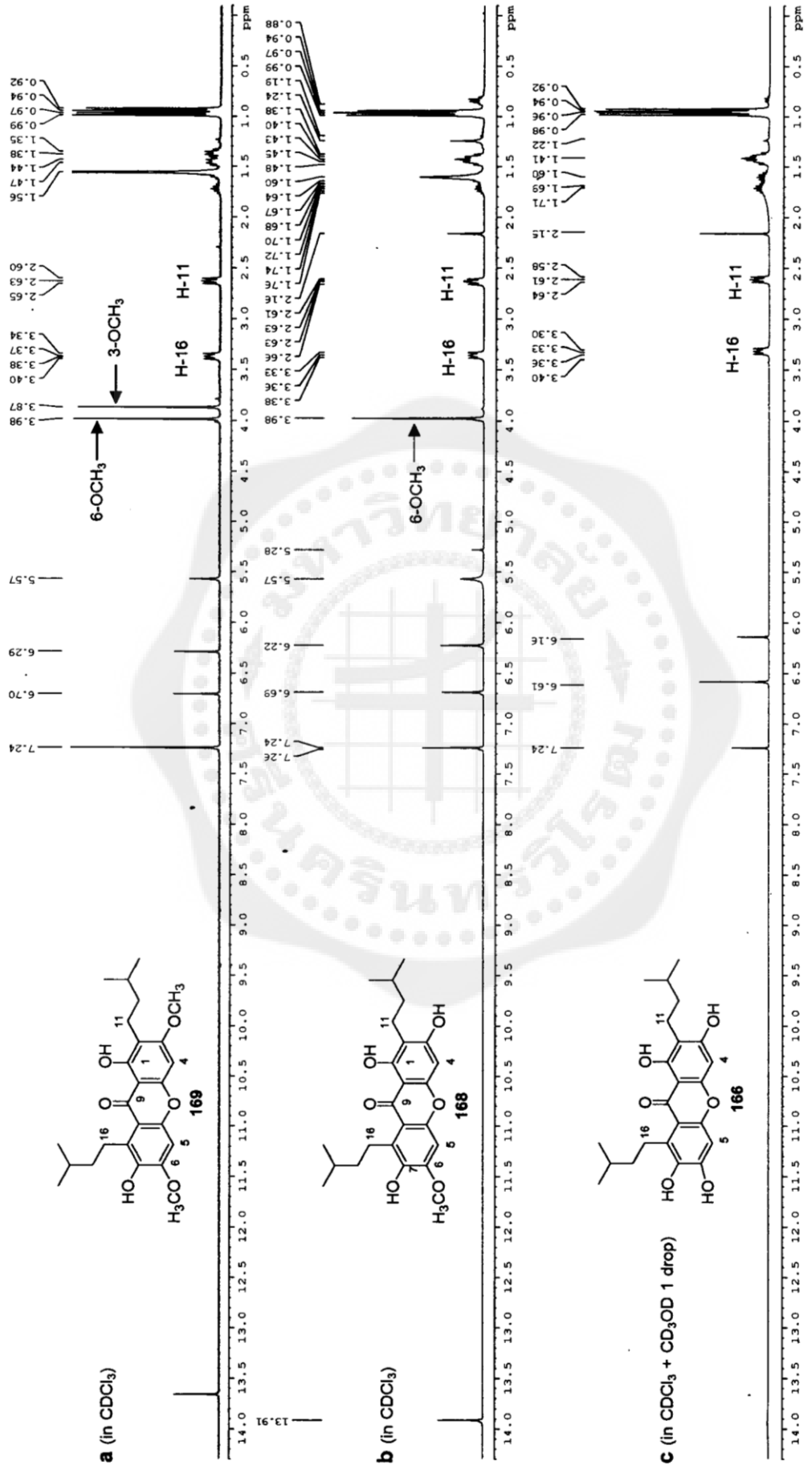

Figure 30 ^{1}H-NMR spectra (300 MHz) of the methylated products **169** and **168** compared with starting **166**

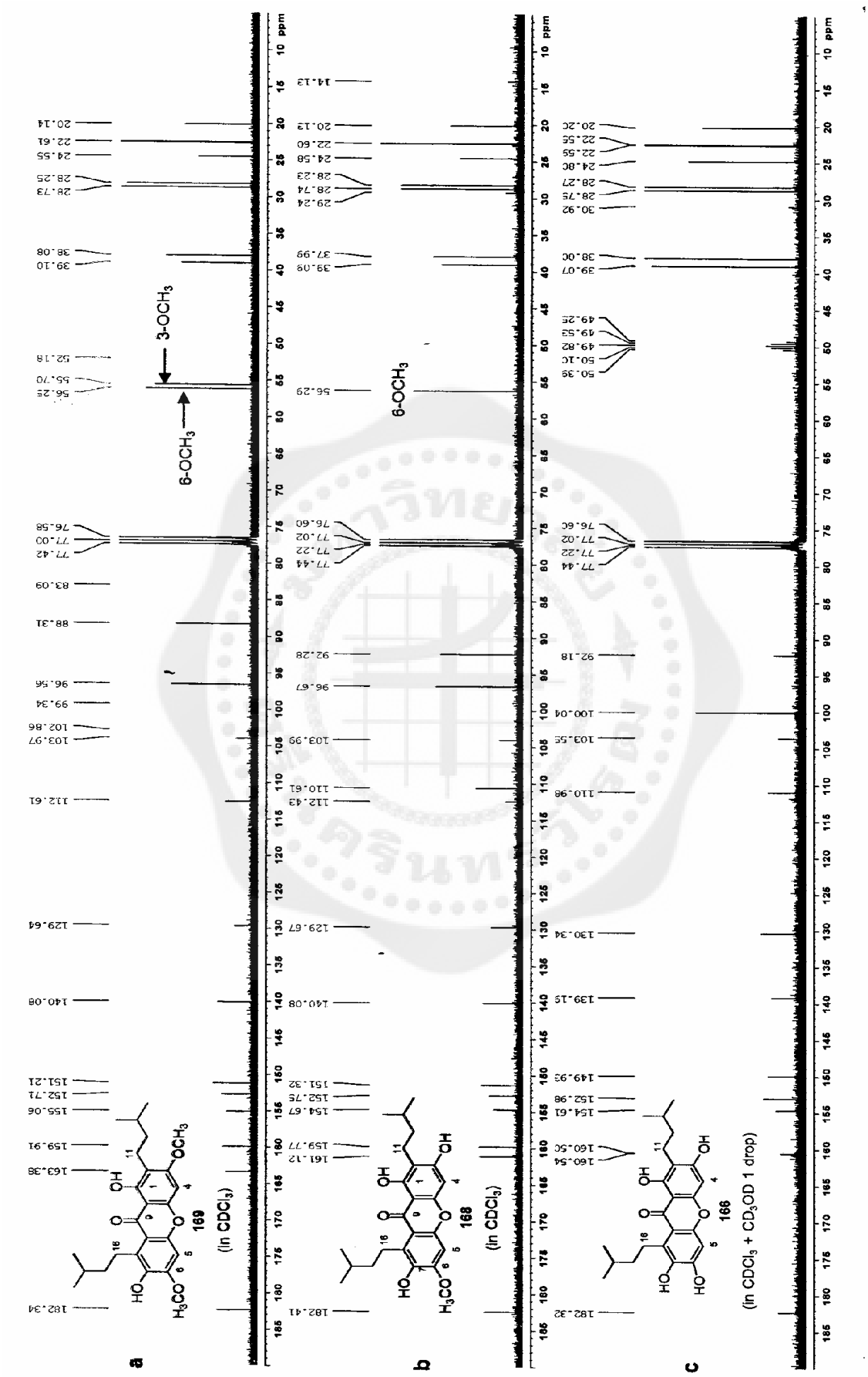

Figure 31 ^{13}C-NMR spectrum (75 MHz) of the methylated products; (a) product **169**; (b) product **168** and (c) starting **166**

5.3 Antimycobacterial activity of mangostin analogues **165-169** compared with the activity of compounds **90**, **149** and **150**

The various *O*-methylated analogues **165-169** were successfully synthesized and evaluated for their antimycobacterial activity against of *M. tuberculosis* $H_{37}Ra$ strain (Table 11).

TABLE 11 Antimycobacterial activity against *M. tuberculosis* of tetrahydomangostin analogues **90**, **149** -**150** and analogues **165-169** (MIC μg/mL)

Compounds	MIC	Compounds	MIC
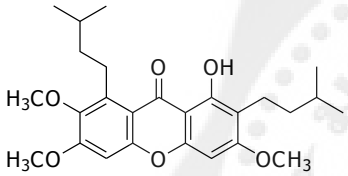 **149**	inactive	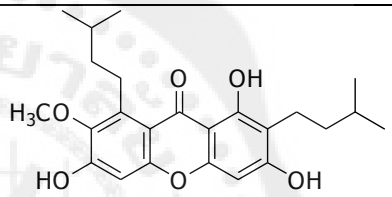 **90**	1.56
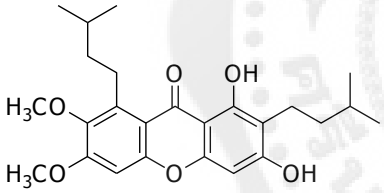 **150**	0.78	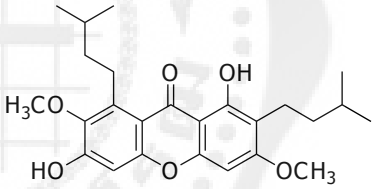 **165**	12.5
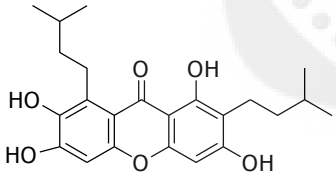 **166**	6.25	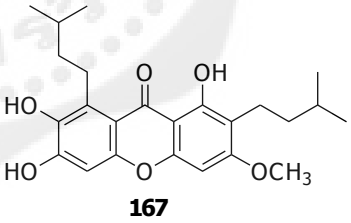 **167**	25
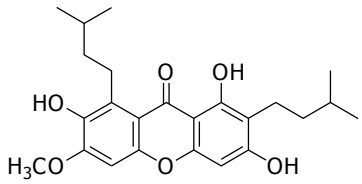 **168**	3.13	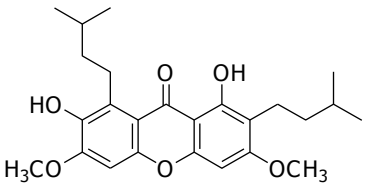 **169**	inactive

1) Inactive at MIC > 200 μg/mL

2) Standard : kanamycin as positive control; MIC = 1.25-2.5 μg/mL, isoniazid MIC = 0.05- 0.1 μg/mL and rifampin MIC = 0.0023-0.0047 μg/mL

The inactive 3,6,7-*O*-trimethylated analogue (**149**) was demethylated to analogue **167** (MIC 25 µg/mL) which showed approximately 8-fold more active than that of starting **149** (MIC > 200 µg/mL) indicating that the hydroxyl groups are necessary to antimycobacterial activity. Among the mono-*O*-methylated analogues (**90**, **167** and **168**), the 7-*O*-methylated analogue **90** was the most active with MIC 1.56 µg/mL suggesting that hydroxyl group at C-3 and C-6 are important to anti-TB activity. For di-*O*-methylated analogues (**150**, **165** and **169**), analogue **169** showed complete loss of activity, assumably due to the absence of 3-OH group or 7-methoxyl group which are crucial for *M. tuberculosis* inhibition whereas analogue **165** which contains two methoxyl groups at C-3 and C-7 was still active (MIC 12.5 µg/mL). Finally, the 6,7-di-*O*-methylated analogue **150** exhibited the highest activity (MIC = 0.78 µg/mL), that is approximately 256-fold more active than the 3,6,7-trimethoxy analogue **149**, indicating that hydroxyl at C-3, methoxyls at C-6 and C-7 are crucial for *M. tuberculosis* inhibition of tetrahydromangostin analogues.

6. Antiviral activity of mangostin analogues

In order to explore the new class of non-nucleoside inhibitors of Herpes simplex virus-1 (HSV-1), α-mangostin (**1**) and some of its analogues which have been evaluated for antimycobacterial activity were further tested for their anti-viral activity against HSV-1. The results are summarized in Table 12.

TABLE 12 IC_{50} values (μg/mL) of mangostin analogues against HSV-1

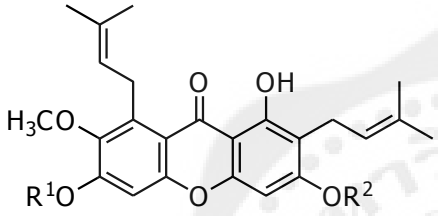

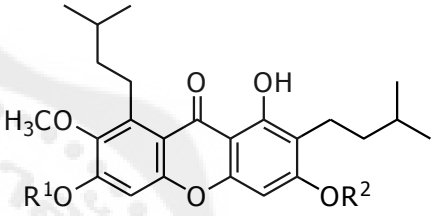

Compounds	R^1	R^2	IC_{50}	Compounds	R^1	R^2	IC_{50}
1	H	H	mod act	**90**	H	H	1.10
84	CH_3	CH_3	inactive	**149**	CH_3	CH_3	mod act
140	CH_3	H	1.39	**150**	CH_3	H	mod act
85	CH_2CH_3	CH_2CH_3	inactive	**151**	CH_2CH_3	CH_2CH_3	weak
141	H	CH_2CH_3	2.30	**152**	CH_2CH_3	H	weak
89	$CH_2CH=CH_2$	$CH_2CH=CH_2$	weak	**153**	$CH_2CH=CH_2$	$CH_2CH=CH_2$	inactive
120	$CH_2CH=CH_2$	H	1.70	**154**	$CH_2CH=CH_2$	H	3.10
142	$(CH_2)_4Br$	$(CH_2)_4Br$	inactive	**155**	$(CH_2)_4Br$	$(CH_2)_4Br$	mod act
143	$(CH_2)_4Br$	H	mod act	**156**	$(CH_2)_4Br$	H	3.30
117	CH_2Ph	CH_2Ph	inactive	**157**	CH_2Ph	CH_2Ph	6.54
144	H	CH_2Ph	3.60	**158**	CH_2Ph	H	5.80
99	$COCH_3$	$COCH_3$	1.50	**159**	$COCH_3$	$COCH_3$	mod act
145	$COCH_2CH_3$	$COCH_2CH_3$	1.60	**160**	$COCH_2CH_3$	$COCH_2CH_3$	weak
146	$CO(CH_2)_3CH_3$	$CO(CH_2)_3CH_3$	7.70	**161**	$CO(CH_2)_3CH_3$	$CO(CH_2)_3CH_3$	inactive
147	COPh	COPh	inactive	**162**	COPh	COPh	nt
148	COPh	H	8.60	**163**	COPh	H	mod act
				164	H	COPh	6.40

1) nt = not tested

2) mod act = moderately active

The antiviral assay revealed that, α -mangostin (**1**) was moderate active compound. Among the *O*-alkylated mangostin derivatives evaluated, 3,6-di-*O*-methylmangostin (**84**), 3,6-di-*O*-ethylmangostin (**85**), 3,6-di-O-(4-bromobutyl)mangostin (**142**) and 3,6-di-O-benzylmangostin (**117**) exhibited complete loss of anti-viral activity whereas 3,6-di-*O*-allylmangostin (**89**) displayed the weak activity. In addition, 6-mono-*O*-methylmangostin (**140**), 3-mono-*O*-ethylmangostin (**141**), 6-mono-*O*-allylmangostin (**120**) and 3-mono-*O*-benzylmangostin (**144**) exhibited strong anti-HSV-1 activity with IC_{50} 1.39, 2.30, 1.70 and 3.60 μg/mL, respectively. Compound **143** exhibited moderately activity against HSV-1. The results indicated that the free hydroxyl groups on mangostin core were crucial for anti-viral activity. For *O*-acylated mangostin analogues, only di-benzoate **147** was inactive whereas di-acetate **99**, di-propionate **145**, di-butanoate **146** and 6-mono-benzoate **148** still retained anti-HSV-1 activity with the IC_{50} 1.5, 1.6, 7.7 and 8.6 μg/mL, respectively. This observation prompted us to assume that the remaining anti-HSV-1 activity of some di-*O*-acylated analogues probably due to the formation of mono-*O*-acylated analogues from hydrolysis of ester that could anti-HSV-1 activity. The hydrogenated analogue **90** (IC_{50}= 1.1 μg/mL) showed more active than that of unsaturated parent **1**. The alkylated and acylated analogues were also evaluated for anti-HSV-1 activity to see the impact of hydroxyl groups and alkene moieties to anti-viral activity of mangostin analogues.

The obtained anti-HSV-1 evaluation of the hydrogenated analogues revealed that some analogues namely, 6-mono-*O*-allyltetrahydomangostin (**154**), 6-mono-*O*-(4-bromobutyl)tetrahydromangostin (**156**), 3,6-di-*O*-benzyltetrahydromangostin (**157**), 6-mono-*O*-benzyltetrahydromangostin (**158**) and 3-mono-*O*-phenylcarboxytetrahydromangostin (**164**), exhibited anti-HSV-1 activity with IC_{50} values of 3.10, 3.30, 6.54, 5.80 and 6.40 μg/mL, respectively. 3,6-Di-*O*-phenylcarboxytetrahydromangostin (**162**) has not been tested for its anti-viral activity. Hydrogenated analogues **149**-**153**, **155**, **159**-**161** and **163** exhibited only moderate, weak or even inactive activity against HSV-1.

The results of the anti-HSV-1 study have shown that mangostin analogues **90**, **99**, **120**, **140-141**, **144**, **145-146**, **148**, **154**, **156-158** and **164** exhibited more potent antiviral activity than that of parent **1** with IC_{50} in the range of 1.10-8.60 μg/mL (Table 12). Among the active compounds, derivatives **90**, **99**, **120** and **145** were more active than standard acyclovir (IC_{50} 2.0 μg/mL) against HSV-1 with IC_{50} 1.10, 1.50, 1.70 and 1.60 μg/mL, respectively. Moreover, these active compounds were considered as a new non-nucleoside anti-HSV-1 agents which have not been reported in the literature. The basis structure activity relationship for anti-HSV-1 activity revealed that the free hydroxyl groups at both C-3 and C-6 on core structure are important for anti-viral activity whereas the impact of double bond on both prenyl side chains remained unclear. The structures of active compounds are shown in Table 13 below.

TABLE 13 IC_{50} values of the active compounds against HSV-1

Compounds	Anti-HSV-1 activity
	IC_{50} (μg/mL)
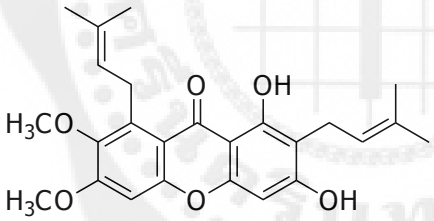 **140**	1.39
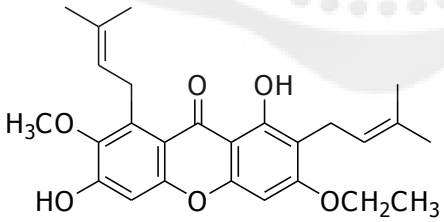 **141**	2.30
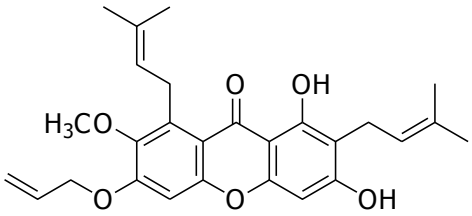 **120**	1.70

TABLE 13 (continued)

Compounds	Anti-HSV-1 activity
	IC_{50} (μ g/mL)
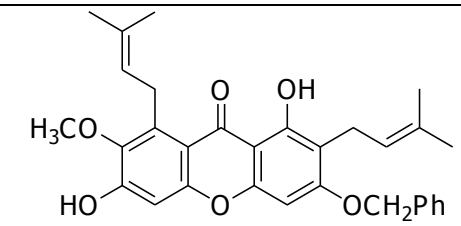 **144**	3.60
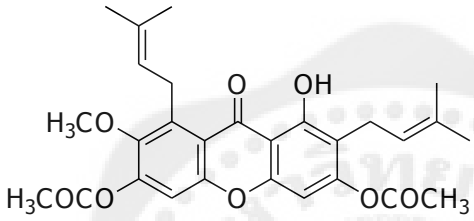 **99**	1.50
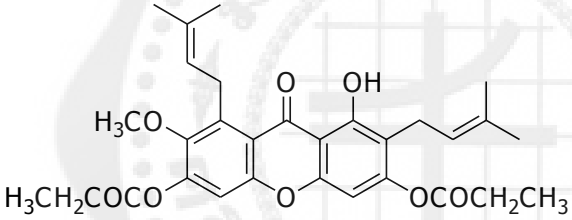 **145**	1.60
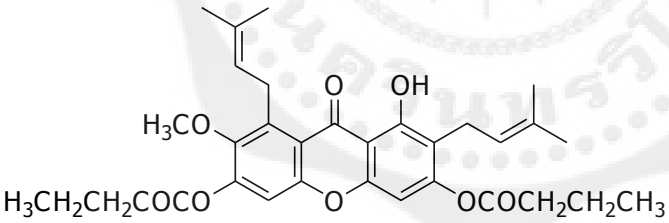 **146**	7.70
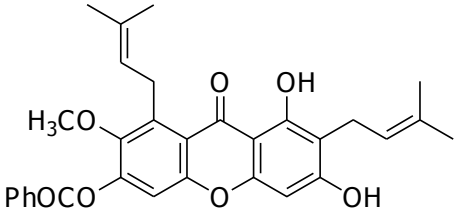 **148**	8.60

TABLE 13 (continued)

Compounds	Anti-HSV-1 activity
	IC_{50} (μ g/mL)
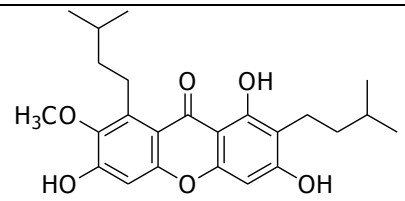 **90**	1.10
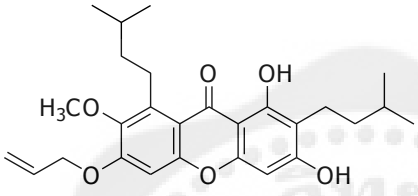 **154**	3.10
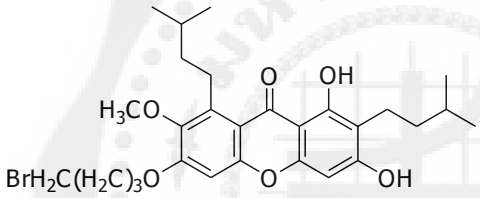 **156**	3.30
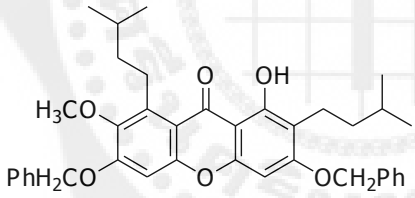 **157**	6.54
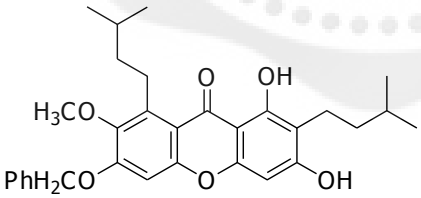 **158**	5.80
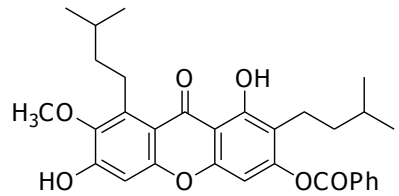 **148**	6.40
Positive drug acyclovir (**75**)	2.0

7. Synthesis of semaxanib (SU-5416, 82)

7.1 Retrosynthetic analysis of SU-5416

The total synthesis of semaxanib (SU-5416, **82**) could be achieved using the disconnection approach shown in Figure 32 below.

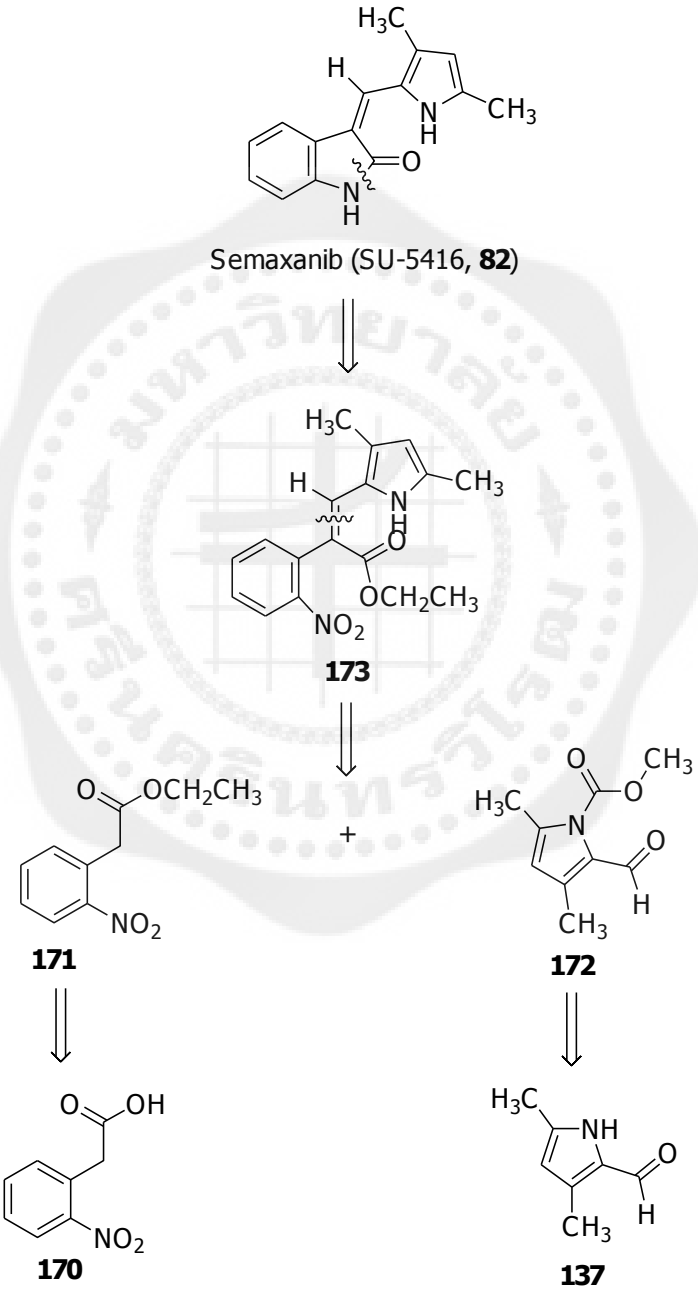

Figure 32 Retrosynthestic analysis of semaxanib **82**

Semaxanib (SU-5416, **82**) could be obtained by nitoreduction of aromatic nitro **173** to aniline which would be cyclized spontaneously. The key intermediate **173** could be prepared from aldol type condensation of ester **171** with the protected pyrrole aldehyde **172**. Ethyl ester **171** could be synthesized from acid catalized esterification of 2-(2-nitrophenyl) acetic acid (**170**) with ethanol. The fragment **172** could be obtained as activated pyrrole aldehyde by treatment of **137** with methyl chloroformate.

7.2 Synthesis of starting ethyl-2-(2-nitrophenyl)acetate (**171**)

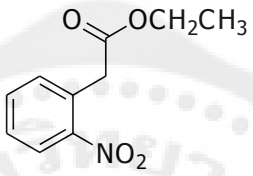

171

Ethyl ester **171** was obtained as white solid (97% yield) by esterification of commercially available ethyl-2-(2-nitrophenyl)acetic acid (**170**) in the presence of catalytic concentrated sulphuric acid. The structure of **171** was confirmed by spectroscopic (NMR, ESMS) and compared with the data of parent **170**. The ESMS of compound **171** exhibited the $[M+H]^+$ ion at *m/z* 210. Its ^{1}H-NMR spectrum of **171** was identical to that of starting **170** except for the presence of two extra signal for methyl proton at δ 1.16 (t, *J*= 7.0 Hz) and methylene proton at δ_H 4.07 (q, *J*= 7.0 Hz) indicating that compound **171** was indeed ethyl-2-(2-nitrophenyl)acetate.

7.3 Synthesis of coupling partner methyl-2-formyl-3,5-dimethyl-1*H*-pyrrole-1-carboxylate (**172**)

Pyrrole carboxaldehyde **137** was quite unreactive. One possible reason for this is that the lone pair of electrons on the pyrrole nitrogen can feed electron density by resonance into the aldehyde carbonyl group thus decreasing its electrophillicity and reactivity. To reduce electron density of aldehyde carbonyl, carbamate protection was selected to increase reactivity of the carbonyl (Handy; et al. 2004: 5057).

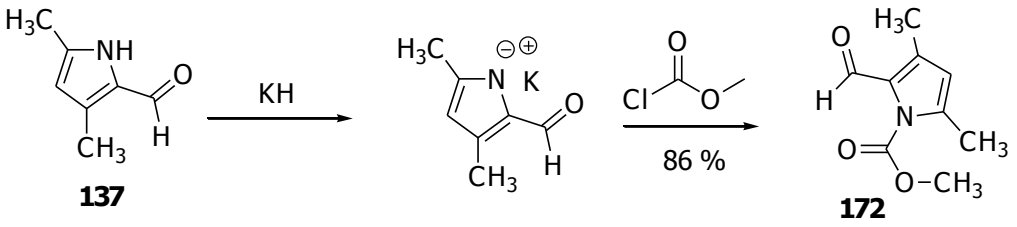

Figure 33 Synthesis of compound **172**

Methyl-2-formyl-3,5-dimethyl-1*H*-pyrrole-1-carboxylate (**172**) was prepared from treatment of **137** with potassium hydride in THF in 0° C followed by adding methyl chloroformate (Figure 33). Compound **172** was obtained in 86% yield after chromatography. The product was fully characterized using spectroscopic data (NMR and mass). The ESMS of compound **172** showed the $[M+H]^+$ ion at *m/z* 182. The ^{1}H-NMR spectrum of **172** showed the new singlet signal at δ_H 4.00 (s, 3H) indicating that the NH-group of the pyrrole was protected as methyl carbamate.

7.4 Aldol-type reaction of compound **171** with aldehyde **172** to produce (*Z*)- ethyl-3-(3,5-dimethyl-1*H*-pyrrol-2-yl)-2-(2-nitrophenyl)acrylate (**173**) and (*E*)-ethyl-3-(3,5-dimethyl-1*H*-pyrrol-2-yl)-2-(2-nitrophenyl)acrylate (**174**)

Ethyl-2-(2-nitrophenyl)acetate **171** was added to a refluxing suspension of potassium carbonate in dry THF containing 18-crown-6 as catalyst. After refluxing the reaction for 3 hours (the reaction became to purple color), the solution of **172** in dry THF was added in one portion, was then stirred under reflux for 24 hours, two major products were observed by TLC. After the reaction was worked up, and purified by column chromatography, two products were obtained as red solid that were desired product (Z)-ethyl-3-(3,5-dimethyl-1*H*-pyrrol-2-yl)-2-(2-nitrophenyl)acrylate (**173**) and undesired product (E)-ethyl-3-(3,5-dimethyl-1*H*-pyrrol-2-yl)-2-(2-nitrophenyl)acrylate (**174**) in 46% and 30% yields, respectively. The mechanism involves an aldol-type condensation and in situ deprotection of the methyl carbamate from the pyrrole nitrogen (Figure 34). According to the proposed mechanism, the benzylic carbanion attacks the carbonyl carbon of the activated aldehyde to form an oxygen anion. This anion then attacks the carbonyl carbon of carbamate protecting group via a 5-membered ring transition state. The pyrrole nitrogen

subsequently abstracts the acidic benzylic hydrogen and elimination reaction ensure to yield the final alkene product with methyl carbonate acting as a leaving group.

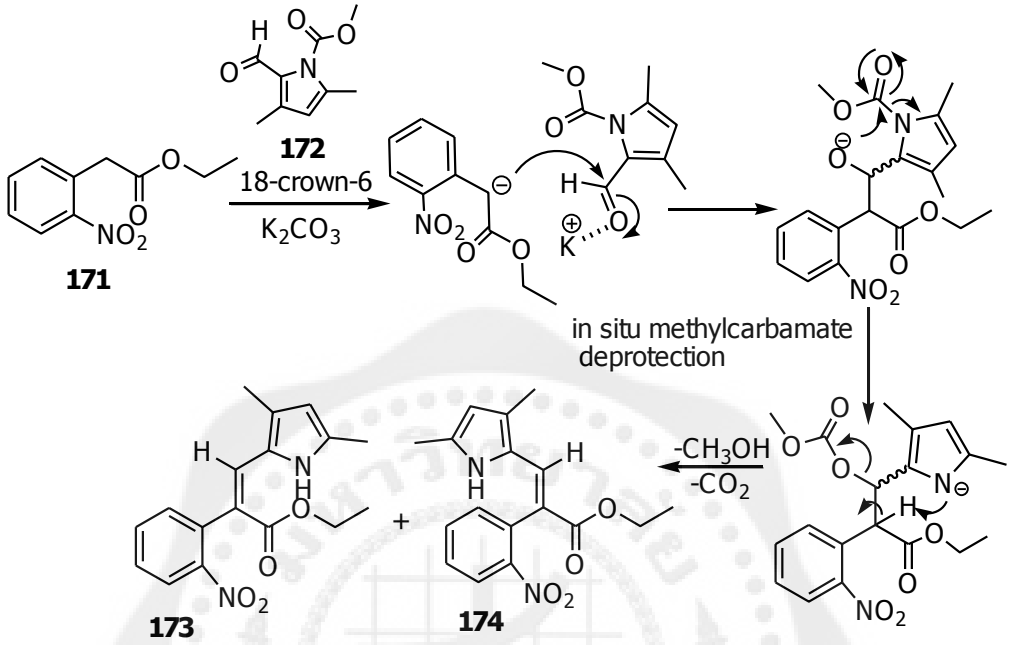

Figure 34 Proposed mechanism for the formation of compound **173** and **174**

In the purification step for a mixture of **173** and **174**, were purified by column chromatography (PET spirit , 2% acetone : PET spirit, 5% acetone: PET spirit, 10% acetone : PET spirit, 15% PET spirit) to obtain the pure products.

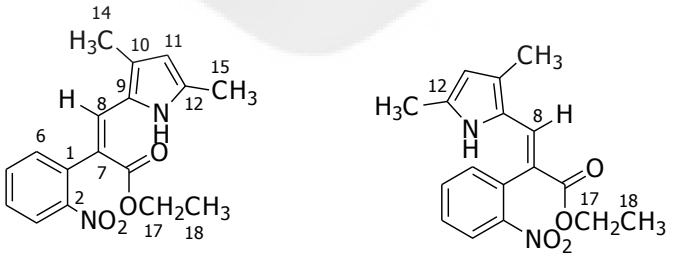

173 **174**

The elucidation of **173** and **174** were substantiated the experimental data obtained from mass spectrometry, NMR and IR spectroscopy. A molecular ion peak at *m/z* 314 of compound **173** was observed on the ESMS spectrum. Compound **174** exhibited a singlet signal at δ_H 6.82 (1H, H-8) in the ^{1}H-NMR spectrum which was assigned to be the vinyl

proton provided from aldol condensation (Figure 35). In addition, ^{1}H-NMR spectrum of **173** showed the broad singlet at δ_H 11.89 (1H, N-H) which belong to the pyrrole proton. The ^{1}H-NMR spectrum also showed the aromatic proton signals at δ_H 8.02 (d, 1H, *J*= 8.0 Hz H-3), 7.62 (t, 2H, *J*= 8.0 Hz, H-4 and H-5), 7.43 (m, 1H, H-6) and 5.90 (s, 1H, H-11) and displayed the signals of ethyl ester group at δ_H 1.13 (t, 3H, *J*= 7.0 Hz, H-18) and 4.12 (q, 2H, *J*= 7.0 Hz, H-17). The NOESY experiment was further used to determine the geometrical isomer of alkene **173**. The sharp singlet at δ_H 6.82 (H-8) showed NOE correlation with H-6 resonating at δ_H 7.43 (m, 1H) (Figure 36) indicating that vinyl proton and the aromatic ring are on the same side of double bond. NOESY experiment revealed that compound **173** was *Z*-alkene. The IR spectrum of **173** showed a prominent broad peak of N-H stretching at 3280 cm^{-1}, the former is characteristic of a hydrogen bonded amine moiety (at wavenumber less than 3300 and broad if H-bonded, Pretsch; et al. 2000:269). The IR data of compound **173** revealed that *Z*-form was stabilized by the intramolecular hydrogen bonding between the oxygen atom of carbonyl and the pyrrole proton (Figure 37).

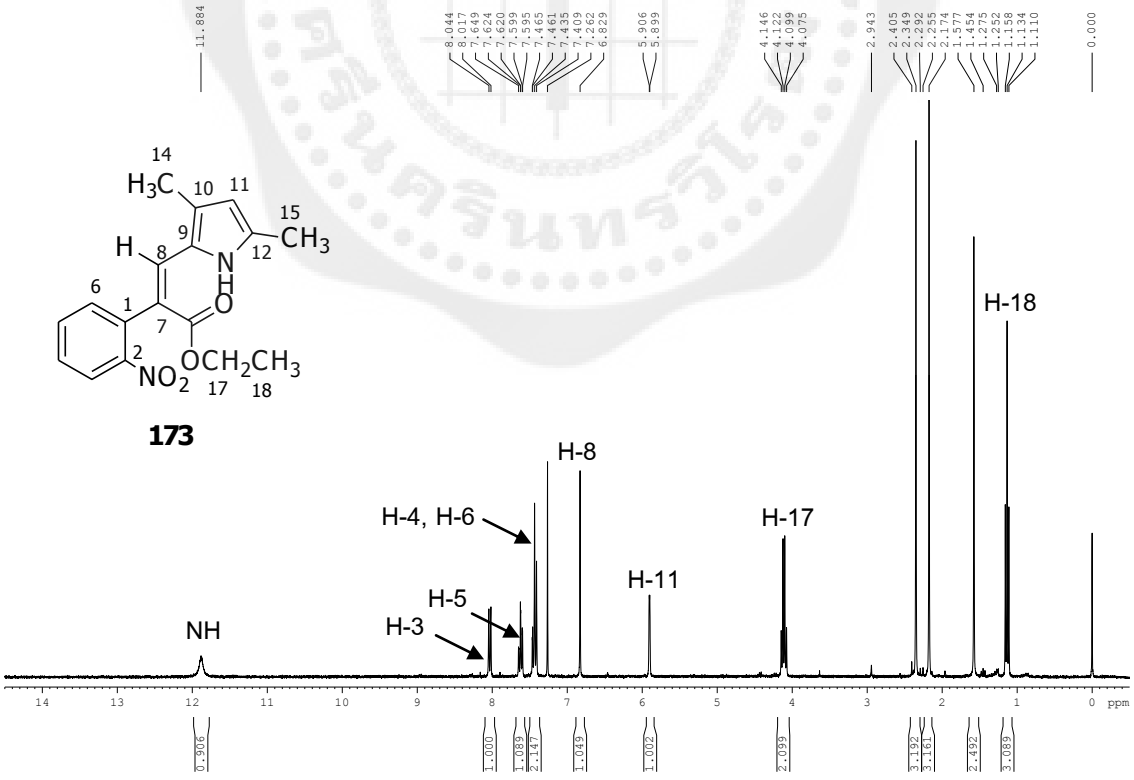

173

Figure 35 ^{1}H-NMR spectrum (300 MHz, $CDCl_3$) of **173**

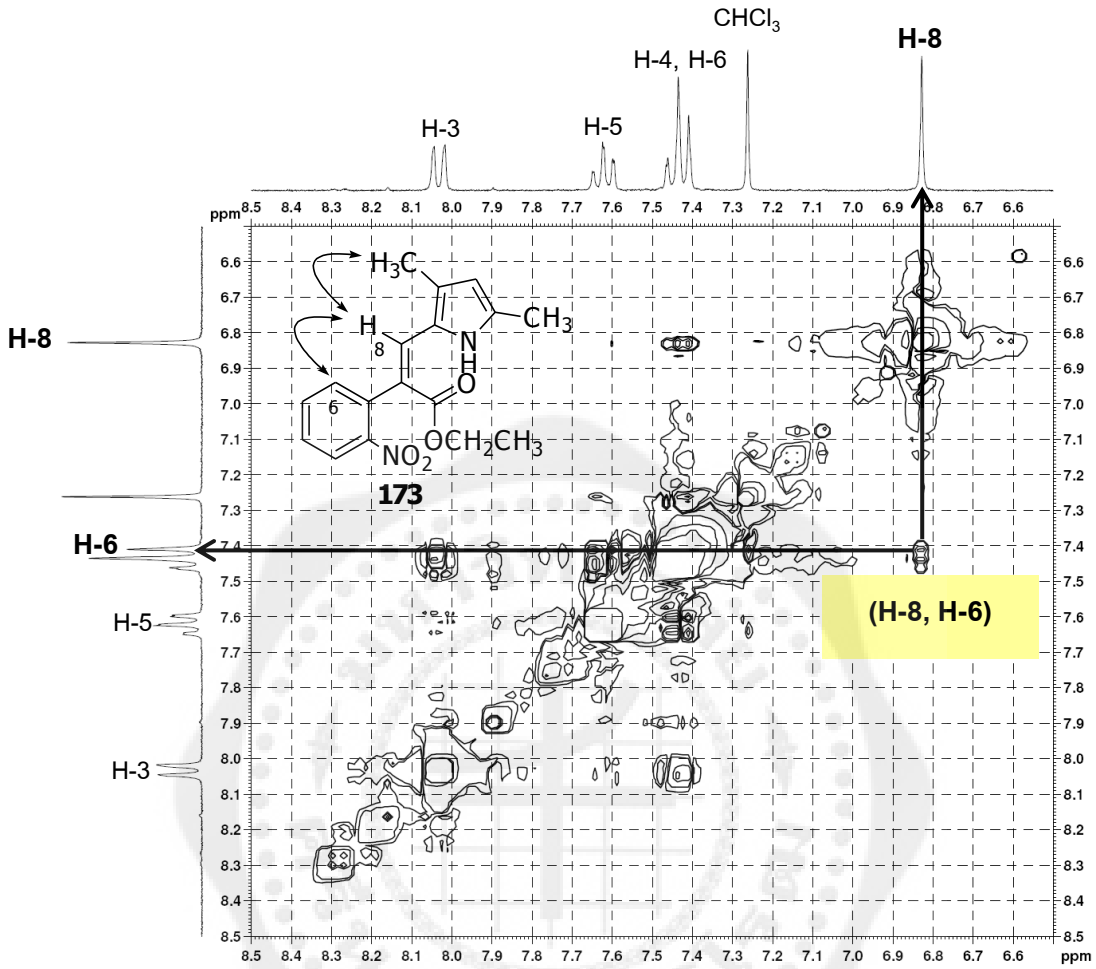

Figure 36 NOE correlation of H-8 and H-6 in NOESY spectrum (300 MHz, $CDCl_3$) of **173**

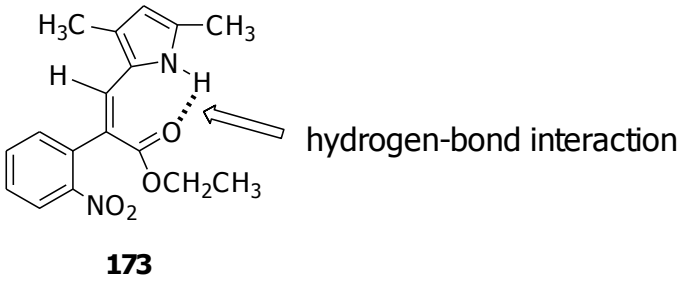

Figure 37 Intramolecular hydrogen bonding (*Z*)-**173**

For the structural elucidation of **174**, was substantiated by using the experimental data obtained from HR-TOFMS, NMR and IR spectrosocopy. A molecular ion peak of *m/z* 315.1237 $[M+H]^+$ was observed on the HR-TOFMS spectrum, which agrees the calculated value for $C_{17}H_{17}N_2O_4$+H. The IR spectrum of **174** showed strong peak of normal N-H stretching at 3420 cm^{-1}, which gave the evidence of non-intramolecular hydrogen bond. The ^{1}H-NMR spectrum (Figure 38) exhibited the aromatic proton signals at δ_H 8.19 (d, 1H, *J*= 7.5 Hz H-3), 7.67 (t, 2H, *J*= 7.5 Hz, H-6), 7.59 (t, 1H, *J*= 7.5 Hz, H-5), 7.49 (t, 1H, *J*= 7.5 Hz, H-4) and 5.47 (s, 1H, H-11). In addition, compound **174** exhibited a singlet signal at δ_H 7.75 (1H, H-8) and broad singlet at δ_H 6.80 (1H, N-H) in the ^{1}H-NMR spectrum which were assigned to be vinyl proton provided from aldol condensation and pyrrole proton, respectively. Compound **174** displayed triplet signal at δ_H 1.19 (3H, *J*= 7.0 Hz) which was assigned as methyl group of ethyl ester.

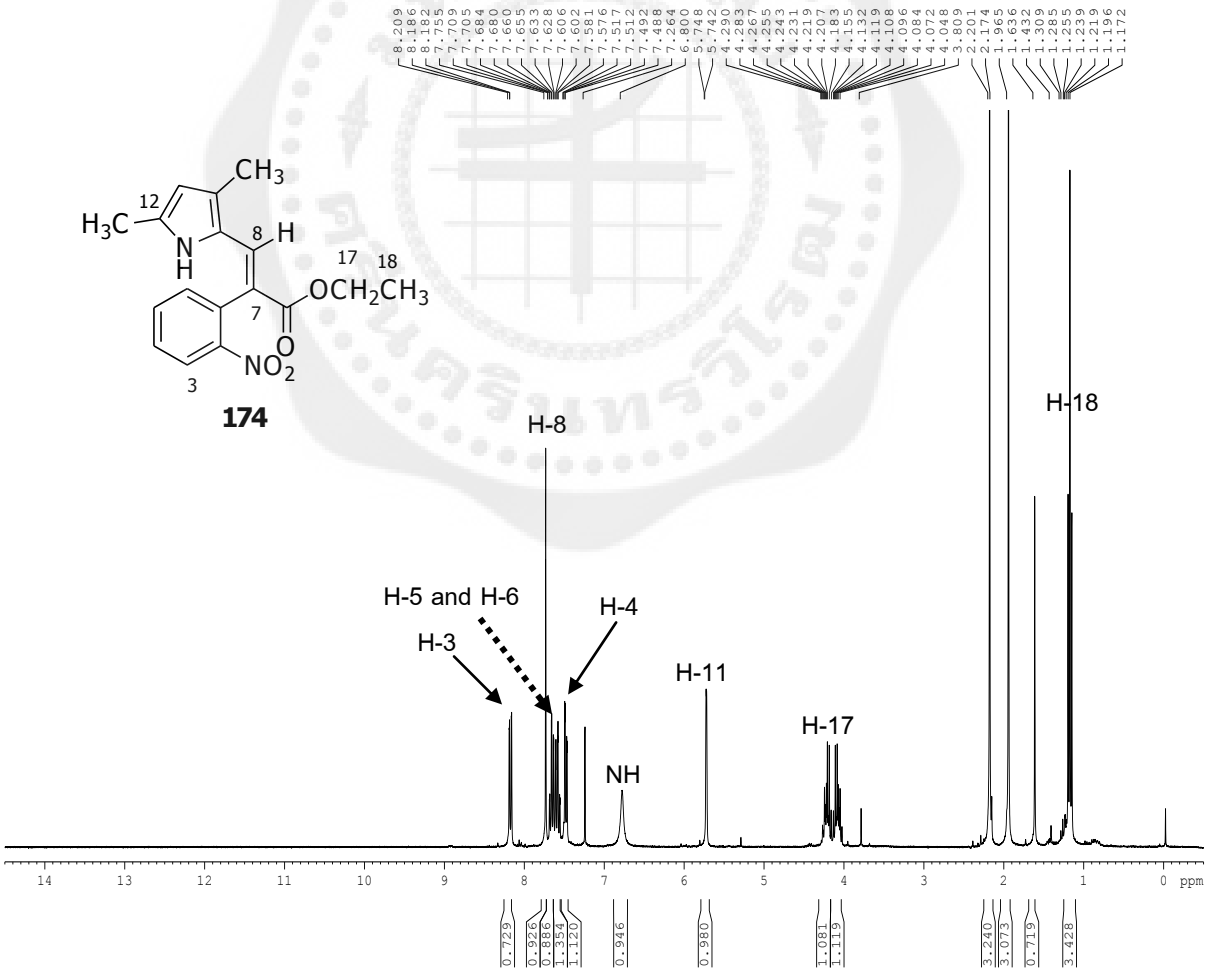

Figure 38 ^{1}H-NMR spectrum (300 MHz, $CDCl_3$) of (*E*)-**174**

The NOESY spectrum of **174** showed weak correlation between aromatic H-6 and pyrrole proton indicating that pyrrole and aromatic ring are on the same side of double bond. The spectroscopic (NOESY) and mass analysis confirmed that compound **174** was geometrical isomer of compound **173** which was *E*-form. Interestingly, in the ^{1}H-NMR spectrum of **174**, two methylene protons were not equivalent and appeared as two of quartet of doublet resonating at δ_H 4.10 (*J*= 4.0, 7.0 Hz) and 4.23 (*J*= 4.0, 7.0 Hz) with integration one proton each. This observation is attributed to the diastereotropic relationship of methylene proton due to the atropisomerism. The formation of atropisomers of compound **174** was showed in figure 39.

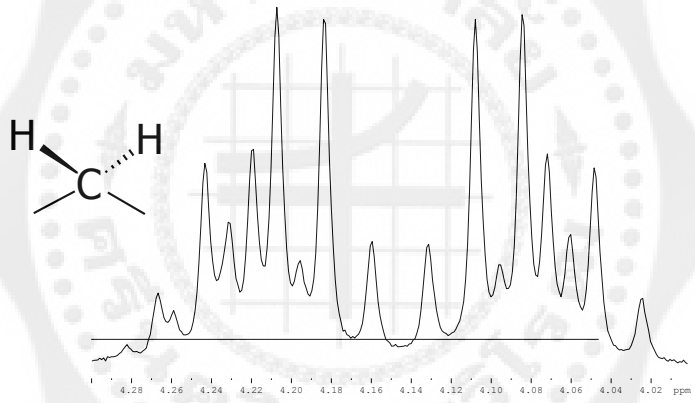

non equivalent CH_2 in ^{1}H NMR spectrum

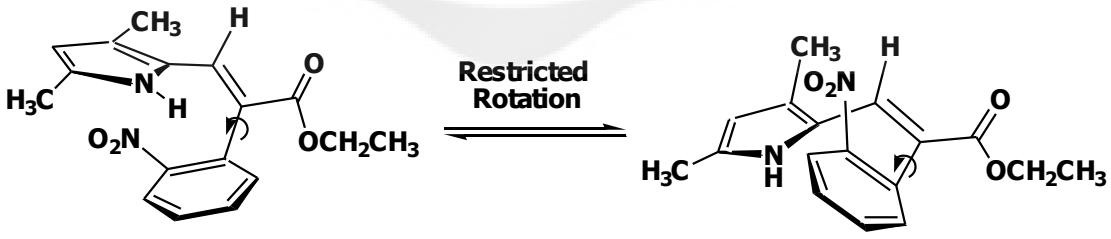

Figure 39 The signal of non-equivalent methylene proton in ^{1}H-NMR spectrum and the proposed atropisomerism of (*E*)-**174**

The atropisomerism of compound **174** could be occurred probably due to nitro group can not freely pass by the pyrrole ring together with the restricted rotation creates an axis or chirality thus two atropisomers are formed. The formation atropisomerism gave rise to separate signals of methylene proton in the ^{1}H-NMR spectrum of **174**.

7.5 Acid catalized isomerisation of (*E*)-**174**

It is known that (*Z*)- or (*E*)- alkenes could be converted to another isomer under various conditions such as acid, base, thermal induced, and light induced (Clayden; elt al. 2001: 326). Undesired product **174** was treated with various acids such as H_2SO_4, HCl and *p*-toluene sulfonic acid (*p*-TsOH) to produce (Z)-alkene ethyl ester **173**. The results revealed that the treatment of **174** with H_2SO_4 occurred the *E*-*Z* isomerism faster than the use of HCl and *p*-TsOH as catalyst and gave **173** in 58% yield along with recovered **174** in 17% after chromatography (Figure 40).

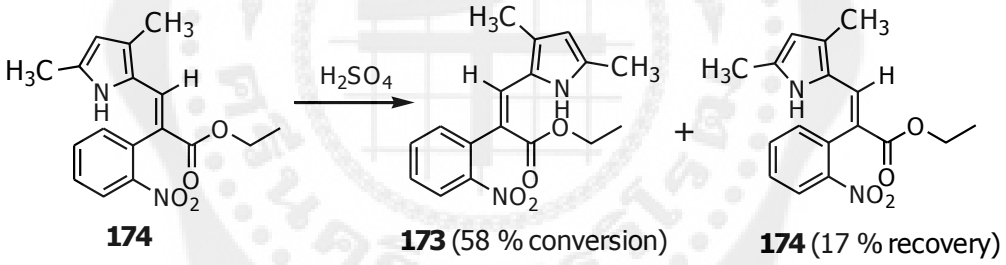

Figure 40 Acid catalized isomerisation of (*E*)-**174**

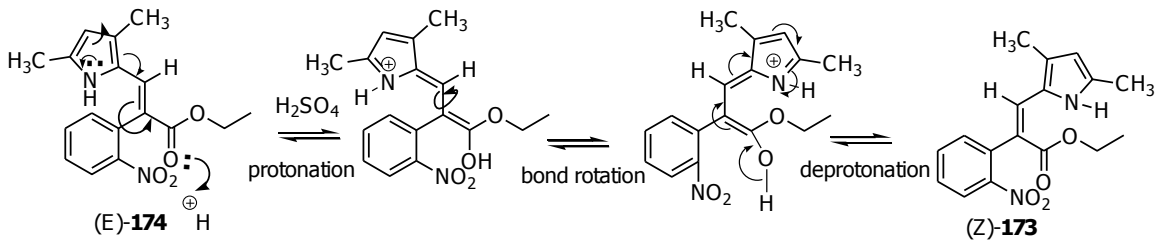

Figure 41 The equilibrium between (*E*)-**174** and (*Z*)-**173** under acidic condition

The isomerisation of **174** in to **173** in acidic condition was occurred, probably due to the oxygen carbonyl was protonated with acid to generate pyrrolium cation followed by single bond rotation led to the (*E*)- and (*Z*)- isomerism in the equilibrium. The proposed mechanism is showed in figure 41.

7.6 Reductive cyclisation of desired (*Z*)-**173** to produce semaxanib (SU-5416, **82**)

Regarding the successfully reduce aromatic nitro compound **173** in to SU-5416 via cyclisation and elimination with Fe^{0} (Anthony; et al. 2007: 1-56, Figure 42), reduction of **173** with different reducing agent was conducted. We decided to reduce compound **173** with using other alternative reducing conditions which were H_2/Pd-C, $NaBH_4$/Pd-C and $HCOONH_4$/Pd-C including using Fe^{0}/CH_3COOH. The results were summarized in Table 14.

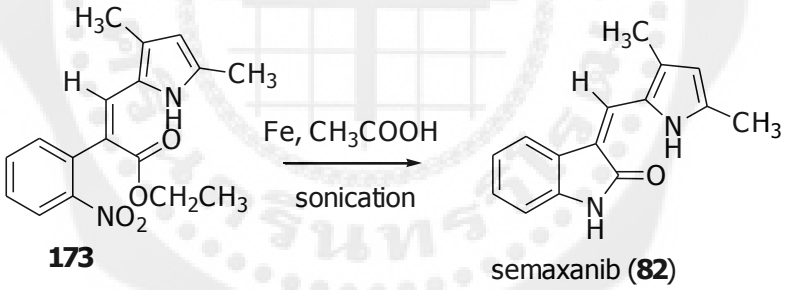

173 semaxanib (**82**)

Figure 42 Reduction of **173** to produce of semaxanib (**82**)

TABLE 14 Reduction conditions to produce SU-5416 (**82**)

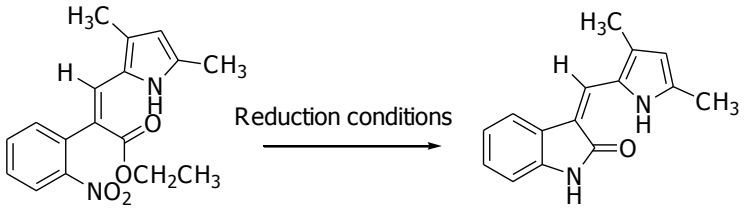

173 semaxanib (**82**)

Method	Reduction condition	SU5416 (82) (%)	Side products (%)
1	$HCOONH_4$/ 10% Pd-C	NR	-
2	Fe(0)/CH_3COOH	81%	-
3	$NaBH_4$/10% Pd-C/MeOH-H_2O	72%	-
4	H_2/10% Pd-C	36%	Decomposed

NR = no reaction occurred

In all reduction conditions, the use of Fe-zero valent and $NaBH_4$ which could potentially be used for the synthesis of **82** whereas the catalytic hydrogen transfer reduction by using ammonium formate (Method 1) could not provide **82**. In addition, catalytic hydrogenation of aromatic nitro **173** gave **82** only 36% along with decomposed yellow product. The structure of **82** was fully characterized by NMR (^1H, ^{13}C and NOESY) spectroscopy and electrospray mass spectrometry (ESMS). The molecular mass of **82** was confirmed by ESMS where a peak was observed at m/z 238 $[M+H]^+$ which corresponded with molecular mass of **82**. The ^{13}C-NMR spectrum showed 15 signals corresponding to the 15 expected signals. The signal at δ_c169 was characteristic of a conjugated carbonyl moiety. In addition, the ^{13}C-NMR spectrum of the product showed the absence of nitro aromatic carbon signal at δ_c148.5 compared with starting **173** indicating that nitro group was transformed into the new functional group. The confirmation of the formation of SU-5416 (**82**) from reductive cyclisation of compound **173** were the absence of the ethyl ester signal in ^1H-NMR spectrum (DMSO-d_6) of **82** and the appearance of two new broad singlet at the down field region at δ_H 13.34 and 10.78 with integration one proton

each which were assigned to be hydrogen bonded pyrrole proton (H-14) and oxindole proton (H-1), respectively. The configuration of **82** was determined using NOE analysis. The NOESY spectrum of **82** demonstrated that alkene proton (H-9) showed correlation with benzene proton (H-5) indicating that the alkene proton was located in the same face with benzene ring. This observation concluded that the exoclyclic double bond of **82** was existed as *Z*-configuration. Further confirmation of the presence of intramolecular hydrogen bonding was the appearance the broad band observed at the wave number 3170 cm^{-1} in the IR spectrum, which is characteristic of secondary amine group, specifically hydrogen-bonded amine.

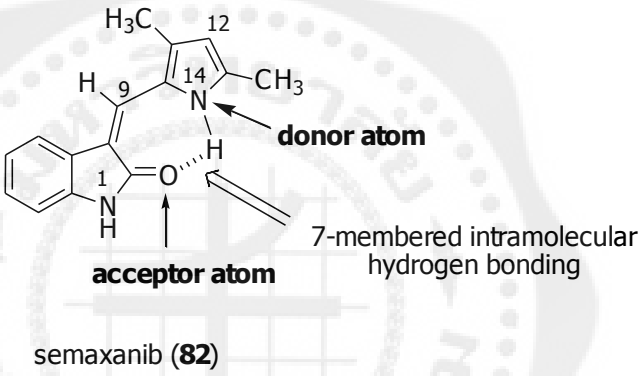

Figure 43 Intramolecular hydrogen bonding of semaxanib (**82**)

This observation suggested that the *Z*-form of **82** was stabilized by intramolecular H-bond. This H-bond is more stabilized due to the conjugated double bonds occurring between the donor (N-atom of pyrrole group) and acceptor atom (oxygen atom of carbonyl group of oxindole ring) (Figure 43). This effect is referred to as "resonane-assisted hydrogen bonding" (Bertolasi; et al. 1991: 4917).

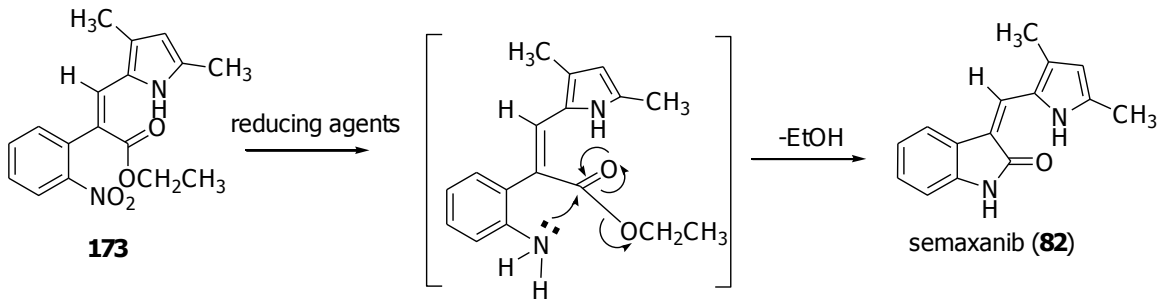

173

Figure 44 Reductive cyclisation of **173** to produce **82** (semaxanib)

The proposed mechanism (Figure 44) involves reduction of nitro group to the aniline followed by a spontaneous cyclisation and fragmentation reaction releasing compound **82** and ethanol. The free electron pair of the emerging NH_2 group attacks the carbonyl carbon leading to the cyclisation to an indoline derivative and release of the ethanol leaving group. The generated structure **82** is the angiogenesis inhibitor SU-5416. The successful formation of SU-5416 (**82**) from **173** by reduction provides new strategy for synthesis of the potent angiogenic inhibitor **82**.

CHAPTER 5
CONCLUSION

1. Structural modifications of mangostin with enhanced antimycobacterial and antiviral activities

1.1 Synthesis of α-mangostin (**1**) analogues

α-Mangostin (**1**) has successfully modified as various *O*-alkylated, *O*-acylated and hydrogenated derivatives by using *O*-alkyaltion, *O*-acylation as well as catalytic hydrogenation reactions. Among these synthetic compounds, analogues **84** and **140** have been reported as naturally occurring oxygenated xanthones (Panthong: et al. 2006: 999). and compounds **85**, **89**-**90**, **99** and **117** were found to be known synthetic analogues of mangostin (Gopalakrisnan; et al. 1997: 519). In addition, compounds **165**-**169** were also synthesized as a new series of demethylated tetrahydromangostin analogues from demethylation or methylation reaction.

1.2 Antimycobacterial activity of synthetic mangostin analogues

α -Mangostin (**1**) and its synthetic analogues have been tested for antimycobacterial activity against *M. tuberculosis* strain H_{37}Ra. The results showed that a number of synthetic analogues exhibited more potent activity than that of parent α-mangostin (**1**). In this studies revealed that tetrahydromangostin analogues were the most active of analogues, with 6-mono-*O*-akylated **150**, **152** and **154** being the most active compounds at the same MIC 0.78 μg/mL. Structure of these compounds are given in Figure 45 below.

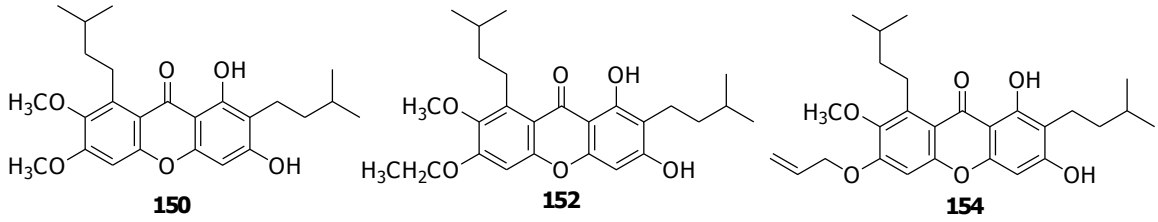

Figure 45 Structures of the most active compounds against *M. tuberculosis*

The structure activity relationship showed that the structural requirements for a mangostin analogues to exhibit antimycobacterial activity were the presence of free hydroxyl group at C-3 and two saturated alkyl chains on C-2 and C-8 as well as the presence of appropriated lipophilic alkyl chain attacked on 6-OH.

1.3 Antiviral activity of synthetic mangostin analogues

Anti-viral assay against HSV-1 of mangostin analogues revealed that compounds **90**, **99**, **120**, **140-141**, **144-146**, **148**, **154**, **156-158** and **164** were more active than that of parent **1** with IC_{50} in the range of 1.10-8.60 μg/mL. Among active analogues, only compounds **90**, **99**, **120** and **145** showed more anti-HSV-1 activity than positive acyclovir (IC_{50} 2.0 μg/mL) with IC_{50} 1.10, 1.50, 1.70 and 1.60 μg/mL, respectively. In addition, all active compounds were considered as interesting promising lead compounds of the new class of non-nucleoside anti-HSV-1.

2. New synthetic strategy for angiogenesis inhibitor, semaxanib (SU-5416, 82)

Semaxanib (SU-5416, **82**) concerning potent of angiogenic inhibitor is of great importance due to its known and potential to inhibition the formation of new blood vessels of tumour cells as well as its synthetic usefulness in the synthesis of other indoline-2-one anti-angionenesis compounds. Hence, to develop new and efficient synthesis leading to **82** is a field of interest. In this study, there was one target intermediate **173**, the synthetic strategies of that involved the Aldol condensation. The target product semaxanib (**82**) was successfully synthesized in moderate over all yield from easily available materials through four new steps with relatively high to moderate yields (Figure 46).

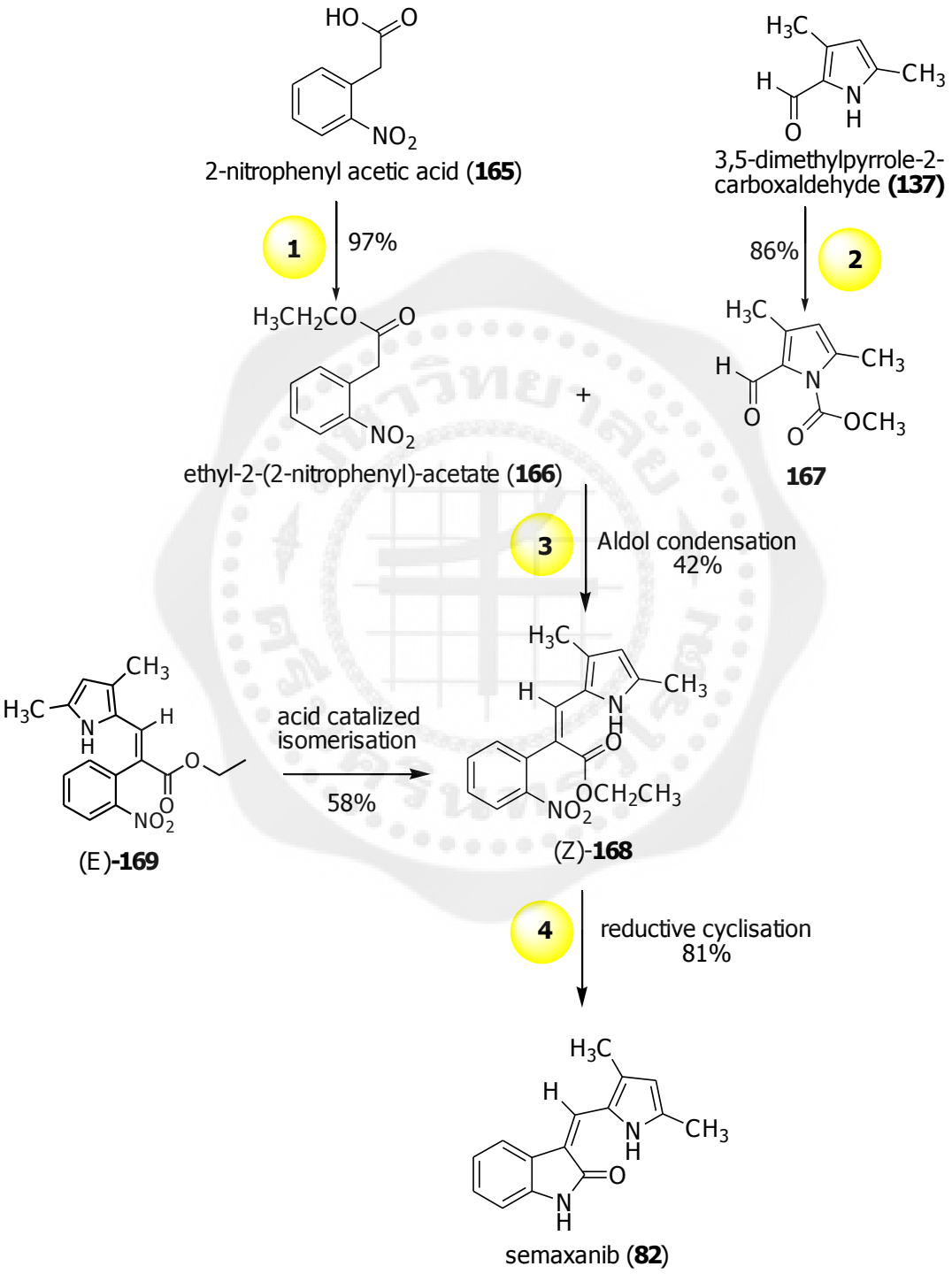

Figure 46 The summarized new strategy for synthesis of semaxanib (SU-5416, **82**)

REFERENCES

REFERENCES

Antony, G.; & Kelso, J.M. (2007). *Dual action anti-tumour prodruds activated by hyproxia*. Dissertation, Bs. C. (Medicinal chemistry). Australia: University of Wollongong.

Azebaze, A.G.B.; et al. (2006). Prenylated xanthone derivatives with antiplasmodial activity from *Allanblackia monticola*. *Chemical & Pharmaceutical Bulletin*. 54(1): 111-113.

Bacon, T.H.; et al. (2003). Herpes simplex virus resistance to acyclovir and penciclovir after two decade of antiviral therapy. *Clinical Microbiology Review*. 16(1): 114-128.

Balasubramanian, K.; & Rajagopalan, K. (1988). Novel xanthones from *Garcinia mangostana*, structures of BR-xanthone-B. *Phytochemistry*. 27: 1552-1554.

Bennett, G.J.; & Lee, H-H. (1989). Xanthones from Guttiferae. *Phytochemistry*. 28: 967-998.

Bennett, G.J.; Lee, H-H.; & Lee L-P. (1990). Synthesis of minor xanthones from *Garcinia mangostana*. *Journal of Natural Products*. 53(6): 1463-1470.

Bergers, G.; & Benjamin, L.E. (2003). Tumorigenesis and angiogenic switch. *Natures Review Cancer*. 3(6): 401-410.

Boonnak, N.; et al. (2009). Anti-*Pseudomonas aeruginosa* xanthones from the resin and green fruits of *Cratoxylum cochinchinese*. *Tetrahedron*. 65: 3003-3013.

Brennan, P.J. (2003). Structure, function, and biogenesis of the cell wall of *Mycobacterium tuberculosis*. *Tuberculosis*. 83: 91-97.

Chayavichitsilp, P.; et al. (2009). "Herpes simplex". *Pediatrics in Review*. 30(4): 119–129.

Chen, L-G.; Yang, L-L.; & Wang, C-C. (2008). Anti-inflammatory activity of mangostins from *Garcinia mangostana*. *Food & Chemical Toxicology*. 46: 688-693.

Chen, S-X.; Wan, M.; & Loh, B-N. (1996). Active constituents against HIV-1 protease from *Garcinia mangotana. Planta Medica*. 62: 381-382.

Clayden, J.; et al. editors. (2001). *Organic chemistry*. United States: Oxford University. p. 326-327.

Cole, S.T.; et al. (1998). Deciphering the biology of *Mycobacterium tuberculosis* from the complete genome sequence. *Nature*. 393 (6685): 537-544.

Dickerson, F.B.; et al. (2003). "Infection with herpes simplex virus type 1 is associated with cognitive deficits in bipolar disorder". *Biological Psychiatry*. 55 (6): 588–593.

Duan, Y-H.; et al. (2010). Bioactive xanthones from the stems of *Cratoxylum formosum* ssp. *pruniflorum*. *Journal of Natural Products*. 73(7): 1283-1287.

Dye, C. (2009). Doomsday postponed? preventing and reversing epidemics of drug-resistant tuberculosis. *Nature Reviews Microbiology*. 7(1): 282-287.

Ernkvist, M. (2008). *Controlling angiogenesis-functional studies of angiogenesis*. Dissertation, Ph. D. Sweden: Department of Oncology-Pathology Karolinska Institutet.

Fong, T.A.T.; et al. (1999). SU5416 is a potent and selective inhibitor of the vascular endothelial growth factor receptor (Flk-1/KDR) that inhibits tyrosine kinase catalysis, tumor vascularization, and growth of multiple tumor types. *Cancer Research*. 59: 99-106.

Fukuyama, Y.; et al. (1998). Prenylated xanthones from *Garcinia subelliptica*. *Phytochemistry*. 30(10): 3433-3436.

Gamble, A.B.; et al. (2007). Aryl nitro reduction with iron powder or stannous chloride under ultrasonic irradiation. *Synthetic Comunications*. 37: 2777-2786.

Gopalakrishnan, G.; Banumathi, B.; & Suresh, G. (1997). Evaluation of the antifungal activity of natural xanthones from *Garcinia mangostana* and their synthetic derivative. *Journal of Natural Products*. 60: 519-524.

Ha, L.D.; et al. (2009). Cytotoxic geranylated xanthones and *O*-alkylated derivatives of α-mangostin. *Chemical & Pharmaceutical Bulletin*. 57(8): 830-834.

Hamada, M.; et al. (2003). Biological activities of α-mangostin derivatives against acidic sphingomyelinase. *Bioorganic & Medicinal Chemistry Letters*. 13: 3151-3153.

Hanahan, D.; & Weinberg, R.A. (2000). The hallmarks of cancer. *Cell*. 100: 57-70.

Handy, S.T.; et al. (2004). Protection of poorly nucleophilic pyrroles. *Tetrahedron Letter*. 45: 5057-5060.

Iikubo, K.; et al. (2002). The fist direct synthesis of α-mangostin, a potent inhibitor of the acidic sphingomyelinase. *Tetrahedron Letters*. 43: 291-293.

Iinuma, M.; et al. (1996a). Five new xanthones from *Garcinia dulcis*. *Journal of Natural Products*. 59: 472-475.

----------. (1996b). Antibacterial activity of xanthones from Guttiferaeous plants against Methicillin-resistant *Staphylococcus aureus*. *Journal of Pharmaceutical and Pharmacology*. 48: 861-865.

Joy, P.P.; et al. (1998). *Medicinal plants*. India: Kerala Agricultural University.

Jung, H-A.; et al. (2006). Antioxidant xanthones from the pericarp of *Garcinia mangostana* (Mangosteen). *Journal of Agricultural and Food Chemistry*. 54(6): 2077-2082.

Kaomongkolgit, R.; Jamdee, K.; & Chaisomboon, N. (2009). Antifungal activity of alpha-mangostin against *Candida albicans. Journal of Oral Science*. 51(3): 401-406.

Laphookhiew, S.; et al. (2006). Cytotoxic and antimalarial prenylated xanthones from *Cratoxylum cochinchinense* [abstract]. *Chemical & Pharmaceutical Buletin*. 54(5): 745-747.

Litz, J.; et al. (2004). The multi-targeted kinase inhibitor SU5416 inhibits small cell lung cancer growth and angiogenesis, in part by blocking Kit-mediated VEGF expression. *Lung Cancer*. 46(3): 283-291.

Loo, A.E.K.; & Huang, D. (2007). Assay-guided fractionation study of α -amylase inhibitors from *Garcinia mangostana* pericarp. *Journal of Agricultural & Food Chemistry*. 55: 9805-9810.

Lubkoll, J.; et al. (2010). Tendem Horner-Wadsworth-Emmons/Heck procedures for the preparation of 3-alkenyl-oxindoles: the synthesis of semaxanib and GW441756. *Tetrahedron*. 66: 6606-6612.

Mahabusarakam, W.; et al. (2006). Prenylated xanthones as potential antiplasmodial substances. *Planta Medica*. 72: 912-916.

Mahabusarakam, W.; & Wiriyachitra, P. (1987). Chemical constituents of *Garcinia mangostana*. *Journal of Natural Products*. 50(3): 474-478.

Matsumoto, K.; et al. (2003). Induction of apoptosis by xanthones from mangosteen in human leukemia cell lines. *Journal of Natural Products*. 66(8): 1124-1127.

----------. (2004). Preferential target is mitochondria in α-mangostin-induced apoptosis in human leukemia HL60 cells. *Bioorganic & Medicinal Chemistry*. 12: 5799-5806.

Mologni, L. (2006). Inhibition of RET tyrosine kinase by SU5416. *Journal of Molecular Endocrinology*. 37: 199-212.

Nazre, M.; Clyde, M.M.; & Latiff, A. (2007). Phytogenetic relationships of locally cultivated Garcinia species with some wild relatives. *Malasian Applied Biology*. 36(1): 31-40.

Nishiyama, Y.; et al. (2009). Synthetic studies of mangostin derivatives with an inhibitory activity on PDGF-induced human aortic smooth cells proliferation. *Heterocycles*. 77(2): 759-765.

Obolskiy, D.; et al. (2009). *Garcinia mangostana* L.: a phytochemical and pharmacological review. *Phytotherapy Research*. 23(8): 1047-65.

Olsson, A-K.; et al. (2006). VEGF receptor signalling-in control of vascular function. *Reviews*. 7: 359-371.

Pai, B.R.; Natarajan, S.; & Suguna, H. (1979). Synthesis and pharmacology of mangostin-3,6-di-glucoside. *Journal of Natural Products*. 42(4): 361-365.

Panthong, K.; et al. (2006). Tetraoxygenated xanthones from the fruits of *Garcinia cowa*. *Phytochemistry*. 67: 999-1004.

Perers, V.; Nagem, T.J.; & Oliveira, F.F.D. (2000). Tetraoxygenated naturally occuring xanthones. *Phytochemistry*. 55: 683-710.

Riscoe, M.; Kelly, J.X.; & Winter, R. (2005). Xanthones as antimalarial agents: discovery, mode of action, optimization. *Current Medicinal Chemistry*. 12(21): 2539-2549.

Rosenthallab. (2011). *Schematic representation of VEGF family ligands and their receptors*. Retrieved February 23, 2011, from http://www.rosenthallab.com/gallery/list php?pageNum_rsDisplay=14&totalRows_rsDisplay=76.

Sakami, Y.; et al. (2005). Antibacterial activity of α-mangostin against vancomycin resistant *Enterococci* (VRE) and synergism with antibiotics. *Phytomedicine*. 12: 203-208.

School of Bioscience. (2011). *Cell wall biosynthesis and assembly in Mycobacterium tuberculosis*. University of Birmingham. Retrieved February 23, 2011, from http://bioscience-people.bham.ac.uk/About/staff_profiles_research.asp?ID=119.

Sridhar, S.S.; & Shepherd, F.A. (2003). Targeting angiogenesis: a review of angiogenesis inhibitors in the treatment of lung cancer. *Lung Cancer*. 42: 581-591.

Suksamrarn, S.; et al. (2006). Cytotoxic prenylated xanthones from the young fruit of *Garcinia mangostana*. *Chemical & Pharmaceutical Buletin.* 54(3): 301-305.

----------. (2003). Antimycobacterial activity of prenylated xanthones from the fruits of *Garcinia mangostana. Chemical & Pharmaceutical Bulletin*. 51(7): 857-59.

----------. (2002). Xanthones from the green fruit halls of *Garcinia mangostana*. *Journal of Natural product*. 65(5): 761-63.

Sultalbawa, M.U.S. (1980). Xanthonoids of tropical plants. *Tetrahedron*. 36: 1465-506.

Sun, L.; et al. (1998). Synthesis and biologicalevaluatio of 3-substituted indolin-2-ones: a novel class of tyrosine kinase inhibitors that exhibit selectivity toward particular receptor tyrosine kinases. *Journal of Medicinal Chemistry*. 41: 2588-603.

Tomioka, H. (2006). Current status of some antituberculosis drugs and the development of new antituberculous agents with special reference to their *in vitro* and *in vivo* antimicrobial activities. *Current Pharmaceutical Design*. 12: 4047-4070.

Tortora, G.; Melisi, D.; & Ciardiello, F. (2004). Angiogenesis: A target for cancer therapy. *Pharmaceutical Design*. 10(1): 11-26.

Wikivisual. (2011). *Virus*. Wikipedia. Retrieved February 23, 2011, from http://en. wikivisual.com/index.php/Virus.

Winter, R.W.; Riscoe, M.K.; & Hinrichs, D.J, Inventors. Xanthones analogs for treating infectious diseases and complexation of heme and porphyrins. US patent 2002/0055644 A1. 2002 May 9.

Yates, P.; & Stout, G.H. (1958). The structure of mangostin. *Journal of American Chemical Society*. 80(7): 1961-1970.

GLOSSARY

LIST OF ABBREVIATIONS AND SYMBOLS

α	=	Alpha
β	=	Beta
CDCl3	=	Deuterated chloroform
^{o}C	=	Degree Celsius
^{13}C-NMR	=	Carbon-13 Nuclear Magnetic Resonance
cm	=	Centimeter
cm^{-1}	=	Reciprocal centimeter (unit of wave number)
δ	=	Chemical shift (for NMR data)
DIBAL	=	Diisobutylaluminium hydride
ESMS	=	Electrospray ionization Mass Spectrometry
ETH	=	Ethambutol
EtOAc	=	Ethyl acetate
EC	=	Endotherial cells
ECM	=	Extracellular matrix
FABMS	=	Fast Atom Bombardment Mass Spectrometry
g	=	Gram
h	=	Hour
^{1}H-NMR	=	Poton Nuclear Magnetic Resonance
HMBC	=	^{1}H-Detected Heteronuclear Multiple Bond Coherence
HRTOFMS	=	High Resolution Time of Flight Mass Spectrometry
HSV-1	=	Herpes Simplex Virus type 1
HSV-2	=	Herpes Simplex Virus type 2
Hz	=	Hertz
IC_{50}	=	50% Inhibitory Concentration
INH	=	Isoniazid
IR	=	Infrared
i.p.	=	Intraperitonial injection
J	=	Coupling constant
KBr	=	Potassium bromide
kg	=	Kilogram
L	=	Liter

LIST OF ABBREVIATIONS AND SYMBOLS (continued)

MeOH	=	Methanol
MFC	=	Minimum fungicidal concentration
MIC	=	Minimum Inhibitory Concentration
$[M+H]^+$	=	Protonated molecular ion
mg	=	Miligram
m/z	=	Mass to charge ratio
μ	=	Micro
$NaBH_4$	=	Sodium borohydride
NMR	=	Nuclear Magnetic Resonance Spectroscopy
NOESY	=	Nuclear Overhauser Effect Spectroscopy
ν_{max}	=	Wave number at maximal absorbtion
OH	=	Hydroxyl group
Pd	=	Paladium
p-TsOH	=	*para*-Toluene sulfonic acid
RIF	=	Rifampin
SDR	=	Single drug resistance
TB	=	Tuberculosis
TBS	=	*tert*-Butyldimethylsilyl
VEGF	=	Vascular endothelial growth factor

CURRICULUM VITAE

CURRICULUM VITAE

Name : Pichit Sudta

Date of Birth : July 29, 1981

Place of Birth : Roi-Ed

Address : 59/8 Tumbol Boopanphan, Suwannaphum District, Roi-Ed

Education Background :

2003	Bachelor of Science in Chemistry Srinakharinwirot University, Bangkok, Thailand
2007	Master of Science in Chemistry Srinakharinwirot University, Bangkok, Thailand

Scholarships :

2005-2007	Research assistantship
2007-2010	The Royal Golden Jubilee Ph. D. Program scholarship

Work Experience :

2010	Research Fellow School of Chemistry, University of Wollongong, NSW, Australia

Award :

Outstanding poster presentation award, Pure and Applied Chemistry International Conference 2011. Miracle Grand Hotal, Thailand, January, 2011.

Publications :

1. Suphavanich K, Maitarad P, Hannongbua S, **Sudta P**, Suksamrarn S, Tantirungrotchai Y, Limtrakul J. CoMFA and CoMSIA studies on a new series of xanthone derivatives against oral human epidermoid carcinoma (KB) cancer cell line. *Monatsh Chem*., (Monatshefte fur Chemie/Chemical Monthly). 2009. 140: 273-280; DOI 10.1007/s00706-008-0014-5.

Patents :

1. Suksamrarn S, **Sudta P**, Kunchanawatta S, Ratananukul P, Suksamrarn A. (2007). Xanthones with antimycobacterial activity. *Thai Patent Application*, No. 0701003620, 20 July 2007.

2. Suksamrarn S, **Sudta P**, Jiarwapi P, Jaratrungtawee A, Ratananukul P, Suksamrarn A. Xanthones with antiherpes simplex type 1 activity. *Thai Patent Application*, No. 0901004650, 16 October 2009.

3. Suksamrarn S, **Sudta P**, Ratananukul P, Suksamrarn A. Xanthone analogues with antiherpes simplex type 1 activity. *Thai Petty Patent Application*, No. 0903001233, 16 October 2009.

Poster presentations :

1. Phanasant K, Maitarad P, **Sudta P**, Suksamrarn S, Tantirungrotchai Y, Limtrakul J. CoMFA and CoMSIA studies on xanthone derivatives against anti oral human epidermoid carcinoma (KB) cancer cell. International Conference on Modeling in Chemical and Biological Engineering Sciences. The Rama Garden Hotel, Bangkok Thailand, October 25 – 27, 2006. Poster number 14 CBES-06-00147.

2. Suphavanich K, Maitarad P, **Sudta P**, Suksamrarn S, Tantirungrotchai Y. CoMFA and CoMSIA studies on xanthone derivatives against breast (BC-1) cancer cell line. Pure and Applied Chemistry International Conference 2008 . Sofitel Centara Grand Bangkok, Thailand, January, 2008. Poster number S4-PO-16.

3. **Sudta P**, Jiaravapi P, Kunchanawatta C. Suksamrarn A, Suksamrarn S. Antimycobacterial activity of α–mangostin derivatives against *Mycobacterium tuberculosis*. Pure and Applied Chemistry International Conference 2011. Miracle Grand Hotal, Thailand, January, 2011. Poster number OM_O0063.